

# **Analysis of the effect of atorvastatin on the virulence of Fungal Pathogens**



A thesis submitted to the National University of Ireland, Maynooth for  
the degree of Doctor of Philosophy by

Ahmad Bashir Ajdidi MSc

**Supervisor**

Prof. Kevin Kavanagh,  
Medical Mycology Unit,  
Dept. of Biology,  
Maynooth University,  
Co. Kildare.

**Head of Department**

Prof. Paul Moynagh,  
Dept. of Biology,  
Maynooth University,  
Co. Kildare.

**October 2019**

## **Declaration**

This Thesis has not been submitted in whole or in part to this or any other university for any degree and is original work of the author except where otherwise stated.

Signed: \_\_\_\_\_

Date: \_\_\_\_\_

To the memory of my father

Bashir Ajdidi

## Acknowledgments

I would like to sincerely thank my supervisor **Prof. Kevin Kavanagh** for the unlimited support, suggestions, comments, advice, and encouragement provided during the course of this work. I have really appreciated all of your time and help over the years.

I also would like to thank all the **team in biology research group** in Biology department, and the **technical staff**, especially for help in all my experimental work.

Also, I would like to thank my friends, **Gerard Sheehan**, for his help in proteomic experiments and data analyses and **Fathi Abukrees** for helping and unblemished moral support and also my colleagues and friends in medical mycology lab for their invaluable help and encouragement.

Sincere thanks to my **Mum**, my **brothers**, and my **sisters** for giving me so much unconditionally and for their and support when I needed them.

I would like to thank **Ghada** my wife, my kids, **Farah**, **Renad**, **Ainoor** and **Omar** for their patients, sacrifices and inspirations during the period of my study.

Finally, I gratefully acknowledge the financial support from **the Ministry of Higher Education and Scientific Research of Libya**.

## **Publications**

### **Publications from thesis**

- Ajdidi, A., Sheehan, G., Abu Elteen, K., Kavanagh, K., 2019. Assessment of the *in vitro* and *in vivo* activity of atorvastatin against *Candida albicans*. *Journal of medical microbiology* jmm001065.
- Ajdidi, A., Sheehan, G., Kavanagh, K., 2020. Exposure of *Aspergillus fumigatus* to Atorvastatin Leads to Altered Membrane Permeability and Induction of an Oxidative Stress Response. *Journal of Fungi* 6, 42.

### **Poster presentation**

- An analysis of the role of Statins in reducing the virulence of *Candida albicans* Microbiology society annual conference 2019 (8-11 April, Belfast, UK).
- An analysis of the role of Statins in reducing the virulence of *Candida* Poster presentation: Research day Jun 5<sup>th</sup>, 2018. Maynooth university.
- Analysis of the effect of atorvastatin on the growth of *Aspergillus fumigatus*. Poster presentation: Research day Jun 5<sup>th</sup>, 2018. Maynooth university.

### **Publication from other work**

- Izzat, S., Rachid, S., **Ajdidi, A.**, El-Nakady, Y.A., Liu, X.-X., Ye, B.-C., Müller, R., 2020. The ROK like protein of *Myxococcus xanthus* DK1622 acts as a pleiotropic transcriptional regulator for secondary metabolism. *Journal of Biotechnology* 311, 25–34.

# Table of Contents

Acknowledgments.....	iii
Publications.....	iv
Poster presentation.....	iv
Publication from other work.....	iv
List of figures.....	ix
List of abbreviations.....	xxiii
Chapter 1.....	1
1 Introduction.....	2
1.1 Fungal pathogens of humans.....	2
1.2 Responses of Host to Fungal infections.....	3
1.3 Types of Fungal Human Pathogens.....	4
1.4 <i>C. albicans</i> .....	5
1.5 <i>Aspergillus fumigatus</i> .....	14
1.6 Antifungal drugs.....	20
1.7 Statins.....	24
1.8 Insects as a model for human pathogens.....	27
1.9 <i>Galleria</i> as an <i>in vivo</i> model.....	29
1.10 Overall objective:.....	31
Chapter 2.....	32
2 Material and method.....	33
2.1 Strains used in this work.....	33
2.2 Culture conditions.....	34
2.3 General laboratory practice and sterilization procedures.....	36
2.4 Preparation of Atorvastatin.....	37
2.6 Effect of atorvastatin on the viability of <i>C. albicans</i> .....	37
2.7 Fluorescence microscopy of fungal cells.....	38
2.8 Determination of Adherence ability of <i>C albicans</i> .....	38
2.9 Analysis of susceptibility of <i>C. albicans</i> to <i>Trichoderma</i> lysing enzyme preparation. ....	39

2.10	Ergosterol extraction and quantification .....	39
2.11	Determination of amino acid leakage .....	41
2.12	Bradford assay and protein quantification .....	42
2.13	Assessment of Catalase activity of cells .....	43
2.14	<i>Galleria mellonella</i> viability assay .....	43
2.15	Determination of fungal load in <i>G. mellonella</i> larvae .....	43
2.16	Determination of fungicidal activity of hemocytes .....	44
2.17	Analysis of the effect of atorvastatin on the growth of <i>A. fumigatus</i> .....	44
2.18	RP-HPLC Gliotoxin.....	44
2.19	Quantification of atorvastatin administered <i>G. mellonella</i> larvae by using HPLC .....	47
2.20	Whole cell protein extraction from the fungal cells.....	48
2.21	Solutions and buffers used for 1D and 2D SDS-PAGE.....	49
2.22	Preparation of SDS–PAGE mini-gels.....	52
2.23	In gel trypsin digestion and bioinformatics analysis of LC/MS results.....	54
2.24	Protein methodology for shotgun label free proteomics.....	55
2.25	<i>G. mellonella</i> larval storage and experimental conditions.....	62
2.26	Extraction of haemocytes from <i>G. mellonella</i> larvae .....	64
2.27	Haemocyte mediated killing using <i>C. albicans</i> as a target.....	65
2.28	Extraction of <i>G. mellonella</i> haemolymph.....	65
2.29	Statistical analysis of data.....	66
2.30	Data Availability.....	66
Chapter 3.....		67
3.1	Introduction.....	68
3.2	Susceptibility assay.....	69
3.3	Analysis of the effect of atorvastatin on the growth of <i>Escherichia coli</i> or <i>Staphylococcus aureus</i> .....	75
3.4	Effect of atorvastatin on the viability of <i>C. albicans</i> .....	77
3.4	Ergosterol extraction and quantification.....	78
3.5	Determination of Amino acid Leakage.....	79
3.6	Assessment of protein release.....	80

3.7	Fluorescence microscopy of atorvastatin treated <i>C. albicans</i> .....	80
3.8	Adherence assay of <i>C. albicans</i> .....	81
3.9	Analysis of susceptibility of <i>C. albicans</i> to cell wall lysing enzyme .....	82
3.10	Assessment of Catalase activity .....	83
3.11	Assessment of toxicity and <i>in vivo</i> antifungal efficacy of atorvastatin .....	84
3.12	Proteomic analysis of the effect of atorvastatin on <i>C. albicans</i> .....	85
3.14	Discussion.....	109
Chapter 4.....		114
4.1	Introduction.....	115
4.2	Analysis of atorvastatin effect on growth of <i>A. fumigatus</i> on solid medium.....	116
4.3	Susceptibility assay.....	118
4.4	Effect of atorvastatin with amphotericin B on biomass of <i>A. fumigatus</i> .....	122
4.5	Fluorescence microscopy.....	124
4.6	Ergosterol extraction and quantification.....	125
4.7	Atorvastatin induces leakage from <i>A. fumigatus</i> .....	126
4.8	Effect of atorvastatin and atorvastatin in combination with amphotericin B on Gliotoxin release of <i>A. fumigatus</i> .....	128
4.9	Label-free proteomic analysis of response of <i>A. fumigatus</i> to atorvastatin .....	130
4.10	Effect of statin on <i>Galleria</i> infected with <i>A. fumigatus</i> .....	142
4.11	Discussion.....	143
Chapter 5.....		148
5.1	Introduction.....	149
5.2	Effect of atorvastatin on <i>C. albicans</i> infected <i>G. mellonella</i> .....	152
5.3	Quantification of atorvastatin of injected <i>G. mellonella</i> larvae by using HPLC	154
5.4	Determination of fungal load in <i>G. mellonella</i> larvae .....	155
5.5	Determination of haemocyte density .....	156
5.6	Determination of response of atorvastatin treated <i>C. albicans</i> cell to haemocytes. .....	157
5.7	Label-free Proteomic analysis of response of <i>G. mellonella</i> to atorvastatin .....	159
5.7.2	Administration of atorvastatin to <i>G. mellonella</i> larvae by force feeding .....	163
	Discussion.....	168



Chapter 6.....	171
General discussion.....	171
Chapter 7.....	179
References.....	179

## List of figures

<b>Figure 1. 1:</b> Adhesion (A), invasion (B), biofilm formation (C), dimorphism (D), switching (E) and fitness traits (F) (Mayer <i>et al.</i> , 2013). .....	12
<b>Figure 1. 2:</b> Images of <i>A. fumigatus</i> showing hyphae, conidiophore and conidia. (Image of <i>A. fumigatus</i> from Alunos online). .....	14
<b>Figure 1. 3:</b> Gliotoxin structure.....	20
<b>Figure 1. 4:</b> Mechanism of action of antifungal agents. ( <a href="https://microbiologyinfo.com">https://microbiologyinfo.com</a> ).....	21
<b>Figure 1. 5:</b> The prevalent sterol found in human cells is cholesterol however the prevalent sterol found in fungi is ergosterol making ergosterol a good target for antifungal drug development. .	21
<b>Figure 1. 6:</b> Mechanism of action of anti-hypercholesteremia (statins). Statins prevent cholesterol biosynthesis by inhibiting the conversion of HMG-CoA to mevalonic acid.....	26
<b>Figure 1.7:</b> Insects used as models for human pathogens. (A) <i>Drosophila melanogaster</i> ; (B) <i>anduca sexta</i> ; (C) <i>Galleria mellonella</i> and (D) <i>Bombyx mori</i> (Kemp and Massey, 2007).....	29
<b>Figure 2.1:</b> Standard curve of ergosterol which was generated using samples of known concentrations (mg/ml). .....	40
<b>Figure 2.2:</b> Standard curve of aspartic acid which was generated using samples of known concentrations. ....	41

**Figure 2.3:** Standard curve of glutamic acid which was generated using samples of known concentrations. .... 42

**Figure 2. 4:** Detection of gliotoxin by RP-HPLC. Gliotoxin detection was performed at 254 nm with a retention time of approximately 17.1 minutes. Image shows gliotoxin detection of 1µg/10µl. .... 46

**Figure 2.5:** Standard curve of gliotoxin reference. .... 46

**Figure 2.6:** Detection of atorvastatin by RP-HPLC. atorvastatin detection was performed at 254 nm with a retention time of approximately 21.9 minutes. Image shows atorvastatin detection of 1mg/10ml. .... 47

**Figure 2.7:** A standard curve of peak value versus atorvastatin concentration was constructed using different concentrations of atorvastatin standards (mg/ml)..... 48

**Figure 2.8:** Image shows the C-18 spin placed in a 1.5 ml microcentrifuge tubes..... 60

**Figure 2.9:** Larvae were stored in 9 cm petri-dishes with 0.45 mm Whatmann filter paper inserted on the lids and some wood shavings..... 62

**Figure 2.10:** Administration of a solution to *G. mellonella* via (A) intra-haemocoel injection through the last left pro leg and (B) force feeding..... 63

**Figure 2.11:** Isolated of hemolymph from larvae. .... 64

**Figure 3.1:** Effect of atorvastatin on growth of *C. albicans*. *C. albicans* (initial concentration 10<sup>4</sup> cells per well) was exposed to atorvastatin (0.75 µg/ml – 195 µg/ml) in YEPD. Growth (%) was calculated by comparing atorvastatin treated *C. albicans* to control cells after 24 h growth (\*; p < 0.05, \*\*; p < 0.01 \*\*\*; p < 0.001). .... 70

<b>Figure 3.2A:</b> The percentage growth of <i>C. albicans</i> exposed to a serial dilution of Amphotericin B and (0.012 - 6.25 µg/ml) in presence atorvastatin (12 µg/ml).....	72
<b>Figure 3.2B:</b> The percentage growth of <i>C. albicans</i> exposed to a serial dilution of caspofungin (0.014 – 3.75 µg/ml) and in presence atorvastatin (12 µg/ml).....	73
<b>Figure 3.2C:</b> The percentage growth of <i>C. albicans</i> in the presence of a serial dilution of miconazole (0.97 – 250 µg/ml) and in presence atorvastatin (12 µg/ml).....	74
<b>Figure 3.2D:</b> The percentage growth of <i>C. albicans</i> exposed to a serial dilution of % DMSO (0.097 – 25%) in presence atorvastatin (12 µg/ml).....	75
<b>Figure 3.3 (A) and (B):</b> Effect of atorvastatin on growth of <i>E. coli</i> and <i>S. aureus</i> respectively. Bacterial cells (initial concentration $1.5 \times 10^6$ per well) exposed to atorvastatin (0.75 µg/ml – 195 µg/ml) in nutrient broth. No inhibition of growth was observed due to atorvastatin treatment by comparing atorvastatin treated bacterial cell to control cells after 24 h. ....	76
<b>Figure 3.4:</b> Effect of atorvastatin (6, 12, and 24 µg/ml) on viability of <i>C. albicans</i> at different time points (2, 4 and 24 h), (*; $p < 0.05$ , **; $p < 0.01$ ). ....	77
<b>Figure 3.5:</b> Atorvastatin exposure reduced the ergosterol content of <i>C. albicans</i> . Ergosterol quantification was performed using a Gas Chromatograph with a flame ionization detector and a chrompack capillary column. Ergosterol standards were used to calibrate the instrument. Ergosterol content was expressed in terms of mg/ml (*; $p < 0.05$ ). ....	78
<b>Figure 3.6:</b> Effect of atorvastatin on release of amino acids from <i>C. albicans</i> . The effect of atorvastatin (12 µg/ml) on <i>C. albicans</i> amino acid release was determined by ninhydrin	

colorimetric assay. Atorvastatin treatment resulted in increased amino acid release relative to control cells (\*; p < 0.05, \*\*; p < 0.01 \*\*\*; p < 0.001). ..... 79

**Figure 3.7:** Effect of atorvastatin on protein release from *C. albicans*. The effect of atorvastatin (12 µg/ml) on *C. albicans* protein release was determined by Bradford protein assay. Atorvastatin treatment resulted in increased protein release relative to control cells (\*; p < 0.05, \*\*; p < 0.01 \*\*\*; p < 0.001). ..... 80

**Figure 3.8:** Calcofluor staining of *C. albicans* following exposure to atorvastatin, (Magnification x 400). *C. albicans* cells were exposed to atorvastatin (6, 12 and 24 µg/ml) for 24 hr, stained with Calcofluor white and visualized with an Olympus BX51 fluorescence microscope. Increased fluorescence indicated an increase in the chitin content of cells. .... 81

**Figure 3.9:** The adherence ability of *C. albicans* following exposure to atorvastatin (12 µg/ml), (\*\*; p < 0.01). ..... 82

**Figure 3.10:** Enzyme susceptibility assay of *C. albicans* of exposed to 10 mg/ml of *Trichoderma* lysing enzyme. Differences in the % growth statistically non-significant (p > 0.05). ..... 83

**Figure 3.11:** Catalase activity of *C. albicans* protein exposed to 17 mM H<sub>2</sub>O<sub>2</sub> for 20 minutes. Differences in the levels of catalase activity were deemed statistically significant at (\*\*; p < 0.01). ..... 84

**Figure 3.12:** Effect of atorvastatin on viability of *G. mellonella* larvae infected with *C. albicans*. Larvae injected with atorvastatin (4.55 or 9.09 mg/kg) displayed no decrease in survival. Larvae were inoculated with *C. albicans* (1 × 10<sup>6</sup> /larva) and followed up 30 mins later with atorvastatin (4.55 or 9.09 mg/kg) and survival was monitored over 144 h. Atorvastatin (4.55 or 9.09 mg/kg) treatment enhanced larval survival relative to non-treated larvae. .... 85

<b>Figure 3.13:</b> Visualization by 1 D SDS-BAGE of released proteins from <i>C. albicans</i> following exposure to atorvastatin 12 µg/ml. Yeasts were exposed to atorvastatin released proteins were precipitated and separated by SDS-PAGE.....	86
<b>Figure 3.14:</b> Analysis of protein leakage from a control and atorvastatin (12 µg/ml) treated <i>C. albicans</i> cells by 2D-IEF/PAGE analysis.....	88
<b>Figure 3.15:</b> Shotgun proteomics of responses of <i>C. albicans</i> to atorvastatin (12 µg/ml) after 24 h at 30 °C. Principal component analysis of control and atorvastatin treated <i>C. albicans</i> for 24 h showing a clear distinction between control and treatment. ....	91
<b>Figure 3.16:</b> Shotgun proteomics of responses of <i>C. albicans</i> to atorvastatin (12 µg/ml) after 24 h at 30 °C. Two-way unsupervised hierarchical clustering of the median protein expression values of all statistically significant differentially abundant proteins from <i>C. albicans</i> control (C1, C3, C4) and atorvastatin treated (T1, T2, T4) <i>C. albicans</i> .....	91
<b>Figure 3.17:</b> Shotgun proteomics of responses of <i>C. albicans</i> to atorvastatin (12 µg/ml) after 24 h at 30 °C. Volcano plot showing the distribution of quantified proteins according to p value ( $-\log_{10}$ p-value) and fold change ( $\log_2$ mean LFQ intensity difference). Proteins above the horizontal line are considered statistically significant (p value < 0.05) and those to the right and left of the vertical lines indicate relative fold changes $\pm 1.5$ .....	92
<b>Figure 3.18:</b> Volcano plot showing the distribution of quantified ergosterol biosynthesis related proteins (blue) according to p value ( $-\log_{10}$ p-value) and fold change ( $\log_2$ mean LFQ intensity difference). Proteins above the horizontal line are considered statistically significant (p value < 0.05) and those to the right and left of the vertical lines indicate relative fold changes $\pm 1.5$ . ....	94

**Figure 3.19:** Kegg analysis of proteins changed in abundance in the steroid biosynthesis pathway in *C. albicans*. Proteins which are colored black are differentially abundant in *C. albicans* treated with atorvastatin (12 µg/ml)..... 96

**Figure 3.20:** Interaction network analysis of up regulated proteins in atorvastatin (12 µg/ml) treated *C albicans*. Protein interaction information was obtained from the STRING database using gene lists extracted for statistically significant differentially abundant (SSDA) proteins of increased abundance in treated *C albicans*. Statistically enriched KEGG and Gene Ontology (GO) terms were examined to identify pathways and processes enriched within each set of proteins. .... 97

**Figure 3.21:** Bar chart showing changes to number of proteins involved in various enzyme classes at level 3 ontology. Proteins were assigned groups based on involvement in enzyme classes for control and atorvastatin treated. Closed bar: control, open bar: treated. .... 105

**Figure 3.22:** Bar chart showing changes to number of proteins involved in various biological processes at level 3 ontology. Proteins were assigned groups based on involvement in biological processes for control and atorvastatin treated. Closed bar: control, open bar: treated. .... 106

**Figure 3.23:** Bar chart showing changes to number of proteins given various molecular functions at level 3 ontology. Proteins were assigned groups based on involvement in molecular function for control and atorvastatin (12 µg/ml) treated *C. albicans*. Closed bar: control, open bar: treated. .... 107

**Figure 3.24:** Bar chart showing changes to number of proteins in various cellular components at level 3 ontology. Proteins were assigned groups based on involvement in cellular components in the total proteome for control and treated. Closed bar: control, open bar: treated. .... 108

**Figure 4.1:** Growth surface area of *A. fumigatus* on Malt agar plate supplemented with different concentrations of atorvastatin (1.5, 3 and 6 µg/ml) (A). A bar chart of growth area per square centimeter of *A. fumigatus* vs time (48, 72 and 96 h) (B) (\*\*\*; p < 0.001)..... 117

**Figure 4.2:** Effect of atorvastatin on growth of *A. fumigatus*. *A. fumigatus* (initial concentration 10<sup>6</sup>/ml) was exposed to atorvastatin SAB culture medium. Growth (%) was calculated by comparing atorvastatin treated *A. fumigatus* to control cells after 48 h growth (\*\*; p < 0.01 \*\*\*; p < 0.001)..... 118

**Figure 4.3A:** The percentage growth of *A. fumigatus* exposed to a serial dilution of Amphotericin B (6.25 µg/ml) stock solution in presence atorvastatin (3 µg/ml). ..... 119

**Figure 4.3B:** The percentage growth of *A. fumigatus* exposed to a serial dilution of caspofungin (3.75 µg/ml) stock solution and in presence atorvastatin (3 µg/ml). ..... 120

**Figure 4. 3C:** The percentage growth of *A. fumigatus* exposed to a serial dilution of miconazole (250 µg/ml) stock solution and in presence atorvastatin (3 µg/ml). ..... 121

**Figure 4.3D:** The percentage growth of *A. fumigatus* exposed to a serial dilution of DMSO (25 %) stock solution and in presence atorvastatin (3 µg/ml). ..... 122

**Figure 4.4 A and B:** The biomass of *A. fumigatus* exposed to atorvastatin (1.5 and 6 µg/ml). *A. fumigatus* was grown in SAB culture medium at 37<sup>0</sup>C. Biomass was calculated by comparing atorvastatin treated *A. fumigatus* to control cells after 72 h growth (\*\*; p < 0.01 \*\*\*; p < 0.01). Morphological difference of *A. fumigatus* cultures that supplemented with atorvastatin (3 µg/ml) (B). ..... 123



**Figure 4.5:** Calcofluor staining of *A. fumigatus* following exposure to atorvastatin. (Magnification x 400). *A. fumigatus* cells were exposed to atorvastatin (3 µg/ml) for 24 hr., stained with Calcofluor white and visualized with an Olympus BX51 fluorescence microscope. .... 124

**Figure 4.6:** Atorvastatin (3 µg/ml) exposure reduced the ergosterol content of *A. fumigatus*. Ergosterol quantification was performed using a Gas Chromatograph with a flame ionization detector and a chrompack capillary column. Ergosterol standards were used to calibrate the instrument. Ergosterol content was expressed in terms of mg/ml (\*\*; p < 0.01). .... 125

**Figure 4.7:** Effect of atorvastatin on release of amino acids from *A. fumigatus*. The effect of atorvastatin (3 µg/ml) on *A. fumigatus* amino acid release was determined by ninhydrin colorimetric assay. Atorvastatin treatment resulted in increased amino acid release relative to control cells (\*; p < 0.05, \*\*; p < 0.01 \*\*\*; p < 0.001). .... 127

**Figure 4.8:** Effect of atorvastatin on release of protein from *A. fumigatus*. The effect of atorvastatin (3 µg/ml) on *A. fumigatus* protein release was determined by Bradford protein assay. Atorvastatin treatment resulted in increased protein release relative to control cells (\*; p < 0.05, \*\*; p < 0.01). .... 128

**Figure 4. 9:** Atorvastatin (3 µg/ml) exposure increased the gliotoxin release from *A. fumigatus*. Gliotoxin quantification was performed using a HPLC. The gliotoxin standards were used to calibrate the instrument. Gliotoxin content was expressed in terms of ng/ml (\*; p < 0.01\*\*; p < 0.01). .... 129

**Figure 4.10:** Atorvastatin and atorvastatin in combination with amphotericin B exposure increased the gliotoxin release from *A. fumigatus*. Gliotoxin quantification was performed using a HPLC. The gliotoxin standards were used to calibrate the instrument. Gliotoxin content was expressed in terms of ng/ml (\*; p < 0.01\*\*; p < 0.01)..... 130

**Figure 4.11:** Principal component analysis of control and atorvastatin treated *A. fumigatus* for 24 h showing a clear distinction between control and treatment. .... 131

**Figure 4.12:** Two-way unsupervised hierarchical clustering (B) of the median protein expression values of all statistically significant differentially abundant proteins from *A. fumigatus* control (C1, C3, C4) and atorvastatin treated (T5, T7, T8) *A. fumigatus*. .... 132

**Figure 4.13:** Volcano plot showing the distribution of quantified proteins according to p value ( $-\log_{10}$  p-value) and fold change ( $\log_2$  mean LFQ intensity difference). Proteins above the horizontal line are considered statistically significant (p value < 0.05) and those to the right and left of the vertical lines indicate relative fold changes  $\pm 1.5$ . .... 133

**Figure 4.14:** Interaction network analysis of up regulated proteins in atorvastatin (3 $\mu$ g/ml) treated *A. fumigatus*. Protein interaction information was obtained from the STRING database using gene lists extracted for statistically significant differentially abundant (SSDA) proteins of increased abundance in treated *A. fumigatus*. Statistically enriched KEGG and Gene Ontology (GO) terms were examined to identify pathways and processes enriched within each set of proteins. .... 136

**Figure 4.15:** Bar chart showing changes to number of proteins involved in enzyme classes at level 3 ontology. Proteins were assigned groups based on involvement in biological processes for control and atorvastatin treated. Open bar: control, closed bar: treated. .... 138

**Figure 4.16:** Bar chart showing changes to number of proteins involved in various biological processes at level 3 ontology. Proteins were assigned groups based on involvement in biological processes for control and atorvastatin treated. Open bar: control, closed bar: treated. .... 139

**Figure 4.17:** Bar chart showing changes to number of proteins in various cellular components at level 3 ontology. Proteins were assigned groups based on involvement in cellular components in the total proteome for control and treated. .... 140

**Figure 4.18:** Bar chart showing changes to number of proteins given various molecular functions at level 3 ontology. Proteins were assigned groups based on involvement in molecular function for control and atorvastatin (3µg/ml) treated *A. fumigatus*. Open bar: control, closed bar: treated. .... 141

**Figure 4.19:** Effect of atorvastatin on viability of *G. mellonella* larvae infected with *A. fumigatus*. Larvae administered a dose of with atorvastatin (9.09 mg/kg) displayed no decrease in survival. Larvae were inoculated with *A. fumigatus* ( $1 \times 10^6$ /larva) and followed up 30 mins, 2 h, or 4 h later with atorvastatin (9.09 mg/kg). Atorvastatin treatment enhanced larval survival relative to non-treated larvae. .... 142

**Figure 5.1A:** Effect of atorvastatin on viability of *G. mellonella* larvae infected with *C. albicans*. Viability was monitored over 96 h. Larvae injected with atorvastatin (12 µg/ml) treated *C. albicans* culture displayed decrease in ability to kill *G. mellonella* larvae. Atorvastatin treatment enhanced larval survival relative to non-treated larvae. (\*\*\*,  $p < 0.0001$ ). .... 153

**Figure 5.1B:** Effect atorvastatin on *G. mellonella* larvae infected with *C. albicans* and extent of melanisation over 48 hours. Group 1 (10 larvae) negative control were injected with 20µl PBS, group 2 (10 larvae) positive control were injected with 20µl *C. albicans* cells ( $5 \times 10^5$ ) and group 3 (10 larvae) were injected with *C. albicans* cells ( $5 \times 10^5$ ) and atorvastatin (12 µg/ml). .... 153

**Figure 5.2:** *G. mellonella* inoculated by intra-hemocoel injection with atorvastatin (5 and 10 mg/ml). Atorvastatin quantification was performed using a HPLC. The standards atorvastatin was used to calibrate the instrument. (\*\*\*: P<0.001). ..... 155

**Figure 5.3:** Determination of fungal load in *G. mellonella* larvae. Survival of larvae and fluctuations in fungal cell density in *C. albicans* infected larvae. All values are the mean ± SE of three independent replicates. (\*\*\*;p< 0.001). ..... 156

**Figure 5.4:** The effect of atorvastatin on hemocytes densities of *G. mellonella* larvae. Larvae were inoculated by intra-hemocoel injection with different concentration of atorvastatin (25, 50, 100, and 200 ug/ml) and were incubated at 30 °C for 24 hours. Changes in haemocyte density in response to Atorvastatin. (\*; p < 0.05). ..... 157

**Figure 5.5:** Response of atorvastatin (12µg/ml) treated *C. albicans* cell to hemocytes at different time points (0, 20, 40, 60 and 80 minutes). Results displayed that the percent of colony count were decreased by time. (\*: p< 0.05). ..... 158

**Figure 5.6:** Principal component analysis of control *G. mellonella* larvae and intra haemocoel atorvastatin injected *G. mellonella* larvae for 24 hours showing a clear distinction between control and treatment. .... 160

**Figure 5.7:** Two-way unsupervised hierarchical clustering of the median protein expression values of all statistically significant differentially abundant proteins from *G. mellonella* control (5, 7 and 8) and intra haemocoel atorvastatin injected *G. mellonella* larvae (17, 18 and 20). ..... 161

**Figure 5.8:** Volcano plot showing the distribution of quantified proteins according to p value (–log<sub>10</sub> p-value) and fold change (log<sub>2</sub> mean LFQ intensity difference). Proteins above the

horizontal line are considered statistically significant (p value < 0.05) and those to the right and left of the vertical lines indicate relative fold changes  $\pm 1.3$ . ..... 162

**Figure 5.9:** Principal component analysis of control *G. mellonella* larvae and force fed atorvastatin injected *G. mellonella* larvae for 24 hours showing a clear distinction between control and treatment. .... 164

**Figure 5.10:** Two-way unsupervised hierarchical clustering of the median protein expression values of all statistically significant differentially abundant proteins from *G. mellonella* control (9, 11 and 12) and force fed atorvastatin injected *G. mellonella* larvae (13, 15 and 16). ..... 165

**Figure 5.11:** Volcano plot showing the distribution of quantified proteins according to p value ( $-\log_{10}$  p-value) and fold change ( $\log_2$  mean LFQ intensity difference). Proteins above the horizontal line are considered statistically significant (p value < 0.05) and those to the right and left of the vertical lines indicate relative fold changes  $\pm 1.3$ . 166

## List of tables

- Table 3.1:** Identities of proteins observed to be altered in intensity following 1-D electrophoresis of samples from *C. albicans* cells in response to atorvastatin 12 µg/ml. Bands were excised, trypsin digested and analysed using LC-MS..... 87
- Table 3.2:** Two Dimensional SDS-PAGE analysis list of identified proteins, using LC-MS, leaking from the *C. albicans* when the culture was exposed atorvastatin (12 µg/ml)..... 89
- Table 3.3:** List of identified ergosterol related proteins, using label-free proteomics leaking from the *C. albicans* when the culture was exposed atorvastatin (12 µg/ml)..... 95
- Table 3.4:** Relative fold changes of proteins increased in abundance of atorvastatin (12 µg/ml) treated *C. albicans* and the number of matched peptides, sequence coverage, and overall intensity. Only proteins that had more than two matched peptides and were found to be differentially expressed at a level greater than  $\pm 1.5$ -fold were considered to be in significantly variable abundances between control and treated..... 98
- Table 3.5:** Relative fold changes of proteins decreased in abundance of atorvastatin (12 µg ml) treated *C. albicans* and the number of matched peptides, sequence coverage, and overall intensity. Only proteins that had more than two matched peptides and were found to be differentially expressed at a level greater than  $\pm 1.5$ -fold were considered to be in significantly variable abundances between control and treated..... 101
- Table 4.1:** Relative fold changes of proteins increased in abundance in atorvastatin (3 µg/ml) treated *A. fumigatus* and the number of matched peptides, sequence coverage, and overall intensity. Only proteins that had more than two matched peptides and were found to be differentially

expressed at a level greater than +1.5-fold were considered to be in significantly variable abundances between control and treated..... 134

**Table 4.2:** Relative fold changes of proteins decreased in abundance of atorvastatin (3 µg/ml) treated *A. fumigatus* and the number of matched peptides, sequence coverage, and overall intensity. Only proteins that had more than two matched peptides and were found to be differentially expressed at a level greater than -1.5-fold were considered to be in significantly variable abundances between control and treated..... 135

**Table 5.1:** Relative fold changes of proteins increased in abundance of intra haemocoel atorvastatin injected *G. mellonella* larvae and the number of matched peptides, sequence coverage, and overall intensity. Proteins had more than two matched peptides and were found to be differentially expressed at a level greater than ± 1.5-fold were considered to be in significantly variable abundances between control and treated larvae..... 163

**Table 5.2:** Relative fold changes of proteins increased in abundance of atorvastatin force fed *G. mellonella* larvae and the number of matched peptides, sequence coverage, and overall intensity. Proteins had more than two matched peptides and were found to be differentially expressed at a level greater than ± 1.5-fold were considered to be in significantly variable abundances between control and treated larvae..... 166

**Table 5.3:** Relative fold changes of proteins increased in abundance of atorvastatin force fed *G. mellonella* larvae and the number of matched peptides, sequence coverage, and overall intensity. Proteins had more than two matched peptides and were found to be differentially expressed at a level greater than ± 1.5-fold were considered to be in significantly variable abundances between control and treated larvae..... 167

## List of abbreviations

Ator	Atorvastatin
BECs	Buccal Epithelial cells
ACN	Acetonitrile
AMP	Anti-microbial Peptide
ADP	Adenosine diphosphate
ATP	Adenosine triphosphate
BP	Biological process
BSA	Bovine serum albumin
Cat	Catalase
°C	Degrees centigrade
CC	Cellular component
cm	Centimeter
DMSO	Dimethyl sulfoxide
DNA	Deoxyribonucleic acid
DTT	Dithiothreitol
ERG	Ergosterol
EST	Expressed sequence tag
EDTA	Ethylene diamine tetra acetic acid
g	gram
<i>g</i>	G-force
GO	Gene ontology
h	Hour



HMG-CoA	3 hydroxy-3-methylglutaryl-CoA
HMGR	3-hydroxy-3-methylglutaryl-CoA reductase
HPLC	High performance liquid chromatography
IAA	Iodoacetamide
LDL	Low-Density Lipoproteins
kDa	Kilodaltons
kg	Kilogram
LC/MS	Liquid chromatography mass spectrometry
LFQ	Label free quantification
M	Molar
MF	molecular Function
mg	Milligram
μg	Microgram
min	minute
μl	microliter
mM	Millimolar
NADPH	Nicotinamide adenine dinucleotide phosphate
NB	Nutrient Broth
OD	Optical Density
PBS	Phosphate buffered saline
P	value Probability
pH	Potential of hydrogen
pI	Isoelectric point

ROS	Reactive oxygen species
SSDA	Statistically Significant Differentially Abundant
TEMED	N,N,N',N'-Tetramethylethylenedimine
TFA	Trifluoroacetic acid
U	Unit
V	Volts
v/v	volume per volume
w/v	weight per volume
YEPD	Yeast extract-peptone-D-glucose

## Abstract

Fungal pathogens of humans cause harmful infections and can cause diverse diseases in humans which range from superficial skin infections to life-threatening diseases. The opportunistic pathogen *Candida albicans* causes a wide range of diseases primarily in immunocompromised individuals. *Aspergillus fumigatus* is a serious cause of disease in immune deficient patients or in those with pulmonary disease (e.g. cystic fibrosis (CF), asthma), and is the second most common opportunistic fungal pathogen of humans. *Galleria mellonella* larvae are an ideal model of infection to quickly and easily evaluate the virulence of a range of human fungal pathogens. Atorvastatin is a member of the statin drug family which are the main therapeutic agents used to decrease high serum cholesterol levels by inhibiting HMG-CoA reductase enzyme. HMG-CoA is an enzyme that is responsible for the production of farnesyl diphosphate which is the precursor for the production of cholesterol in humans and ergosterol in fungi. The aim of the work presented here was to analyse the antifungal activity of a widely prescribed statin (atorvastatin) and assess the effect of atorvastatin on the virulence of *C. albicans* and *A. fumigatus*. The study also investigated the effect of atorvastatin on *G. mellonella* larvae. The results obtained demonstrated that atorvastatin has anti-fungal activity and it reduced growth and viability of *C. albicans* and *A. fumigatus*. Exposure of *C. albicans* and *A. fumigatus* to this drug leads to the release of protein, amino acids and a reduction in ergosterol synthesis, and increased gliotoxin release in *A. fumigatus*. Proteomic analysis revealed increased abundance of proteins associated with an oxidative stress response, ergosterol biosynthesis and secondary metabolites. Atorvastatin can be used to inhibit the growth of *C. albicans* and *A. fumigatus* in *G. mellonella* larvae. Atorvastatin was shown to be non-toxic to *G. mellonella* larvae and not to induce an immune response when administered to

larvae. The results presented in this thesis indicate that atorvastatin is non-toxic and capable of inhibiting the growth and virulence of *C. albicans* and *A. fumigatus*.

# **Chapter 1**

## **Introduction**

# 1 Introduction

## 1.1 Fungal pathogens of humans

Fungal pathogens of humans cause harmful infections and thus, are considered to be hidden killers (Brown *et al.*, 2012). It has been found that each year these fungal pathogens kill more than 1.5 million people and affect over a billion people all around the world. However, they are still a neglected topic by public health authorities even though most deaths from fungal diseases are avoidable (Bongomin *et al.*, 2017). Fungi can cause diverse diseases in humans which range from superficial skin infections to life-threatening diseases causing damage to internal organs. Such fungal species include dermatophytes, *Cryptococcus* species, *Candida* and many more (Richardson, 1991, Brown *et al.*, 2012). Fungi causing superficial skin diseases are common and can be treated easily but invasive infections caused by fungi tend to possess decreased incidence rate and thus, could be life-threatening especially for patients who are diagnosed with AIDS, or any autoimmune disorder (Jain *et al.*, 2010). Such patients are known as immunocompromised and due to their lower immunity they tend to be more vulnerable to such fungal species than healthy individuals (Vargas and Joly, 2002). It has also been determined that the patients who receive chemotherapy for treating cancers and those who undergo transplantation of organs such as kidney could also develop fatal diseases on exposure to certain fungi (Richardson, 2005). Advanced medicine has extensively enhanced the number of immunosuppressed patients who are likely to be more vulnerable to invasive fungal pathogens (Pfaller and Diekema, 2007). Nevertheless, very few researchers have studied the invasiveness of fungal pathogens in humans while most of the researchers have extensively provided information about other microbial pathogens including viruses and bacteria. Moreover, enhanced development in the field of

medicine has slowed down due to new diagnostic techniques and more potent antifungal drugs (Wong *et al.*, 2014).

## **1.2 Responses of Host to Fungal infections**

*Aspergillus fumigatus*, *Cryptococcus neoformans* and *Candida albicans* are the three most significant fungal pathogens which cause diseases in human. Primarily, such pathogens are found to infect immunocompromised patients as a consequence of intervention therapies which include cancer, organ transplant and leukemia or because of immunodeficiency such as HIV and neutropenia (Pfaller and Diekema, 2004). This reflects the significance of the defensive property of the individual's immune system in managing and impeding invasive infections. Furthermore, it has been observed that in healthy individuals, such fungal pathogens begin to connect with the mucosal surfaces of organs ultimately leading to the colonization and commensalism (Boddy, 2016). However, within the immunocompromised patients, such pathogens are found to cause severe infections in the superficial surfaces and could be distributed throughout that causing lethal infections (*de Melo et al.*, 2017). In order to counteract such fungal pathogens, the host uses an extensive interactive network of chemical signals, cells and proteins disseminated in tissues and blood, which together give rise to adaptive and innate immunity (Cavaliere *et al.*, 2018). Invasive diseases caused by of filamentous fungi, for example, *Aspergillus* species produce important mortality and morbidity in patients, who are immune compromised with malignancies of haematology, transplants of hematopoietic stem cell recipients and patients with the disease of chronic granulomatous (Barnes and Marr, 2007, (Richardson, 2005). Fungi can cause infections and affect the host immune mechanism due to the expression of various proteins and genes linked with their pathogenesis, known as virulence factors (Latgé, 2001). Production of virulence factors within aspergilli occurs during their growth in host naturally, these virulence factors defend

aspergilli in adverse conditions and increase the spread of *Aspergillus* infection in human tissue (Ben-Ami *et al.*, 2010).

### **1.3 Types of Fungal Human Pathogens**

Based on the type of infections caused by each fungus, fungal pathogens of human are categorized as follows;

#### **1.3.1 Systemic infections**

Infections or diseases which prevail deep in the tissues including nervous system and essential body organs could be chronic and fatal at the same time. The fungal pathogens causing systemic infections tend to enter the human body via open wounds on skin. The fungus is then transmitted throughout the human body either through respiratory system or blood circulation causing more lethal infections in the internal organs. Such types of fungi are named as saprotrophic fungi which grow in the soil (Shoham *et al.*, 2019).

#### **1.3.2 Intermediate infections**

Intermediate infections prevail under the skin and remain confined. The prevalence of intermediate infections is, however, lower than other types. It is intermediate between systemic and superficial infections (Cornely *et al.*, 2017).

#### **1.3.3 Superficial infections**

These infections occur when fungi attach either to the skin or appendages including hair and nails. These types of fungal pathogens are named as dermatophytes and cause infections such as athlete's foot, ringworms and jock-itch (Reddy, 2017).



#### 1.4 *C. albicans*

The polymorphic fungus *C. albicans* is a member of the normal human microbiome. In most individuals, *C. albicans* resides as a lifelong, harmless commensal (Mayer et al., 2013). However, it is an opportunistic pathogen for some immunologically weak and immunocompromised people (Kim and Sudbery, 2011). Several species of *Candida* also form candidiasis which is a condition in which the fungus grows in an individual. It is also observed in patients with HIV because the condition gives the tendency to grow pathogens, which often form infections (Höfs et al., 2016). *C. albicans* biofilm formation initiates with the adhesion of the yeast to the substrate surface, followed by cell proliferation, intensive hyphae production and an increase in the extracellular matrix (Ribeiro et al., 2017). It is commonly associated with biofilms and can be implanted in clinical devices alongside human tissues (Ramage et al., 2006). The increased incidence of infection caused by *Candida* species is mainly due to the increase of the AIDS epidemic, an increasingly aged population, higher numbers of immunocompromised patients and the more widespread use of indwelling medical devices (YeSudhaSon and Mohanra, 2015). *C. albicans* is the commonest serious fungal pathogen of humans, variously reported as causing between 250 000 and 400 000 deaths per annum worldwide as well as extensive morbidity of around 100 million episodes of recurrent vaginitis (da Silva Dantas et al., 2016). Candidemia is *Candida* bloodstream infection, also called candidiasis, it is the most common form of invasive candidiasis (Kullberg and Arendrup, 2015). In the United States, candidemia is one of the most common causes of bloodstream infections in hospitalized patients (Wisplinghoff et al., 2004), and it often results in long hospital stays and death. It is also responsible for high medical costs (Morgan et al., 2005). Conventional antifungal therapy relies upon the use of polyene, azole or echinocandin drugs but

the delivery of appropriate therapy is often problematic due to the appearance of resistance and the inherent toxicity of some antifungal therapies (Scorzoni *et al.*, 2017).

#### **1.4.1 Diseases Caused by *C. albicans***

*C. albicans* is the most common type of fungal infection in the human body. The most common type of infections and diseases caused by *C. albicans* includes urinary tract infection, genital yeast infection, oral thrush, and mucocutaneous candidiasis which can be identified by focusing on the symptoms of diseases and infections (Vila *et al.*, 2017). Other diseases with increased *Candida* infections include HIV for which chemotherapies and steroid medications must be taken by the individual facing infection or disease. The immune system of an individual can be weakened by illness, stress or some other medications. When an immune system of an organism weakens then *Candida* turns into an aggressive pathogen which causes fungal infections within the body.

#### **1.4.2 Mechanism of action and virulence of *C. albicans***

*C. albicans* can cross the host's protective barriers and colonize virtually every internal organ causing life-threatening conditions (Johnson *et al.*, 2013). *C. albicans* penetrates and infects the immunocompromised patient by various processes that lead to infection. The fungal cells adhere to the surface of epithelial cells in the oral cavity and followed by biofilm formation across it then penetrates into the epithelial cells. Once inside the hyphae continues its way through the epithelial cells until it gets to the bloodstream. Once in the bloodstream, the fungus can be easily disseminated throughout the body and then the fungus can use virulence factors to start growth

inside the body. Virulence factors are traits and adaptations that allow *C. albicans* to prosper within the human body (Odds, 1994).

### **1.4.3 Adherence**

Virulence factors are the ones that are recognized by various examples of pathogens coming from several species like *C. albicans*, *A. fumigatus* and others. Interactions of the human fungal pathogen with the host tissues are key factors in the pathogenesis of mycoses. According to the concept that adherence of microorganisms is a prerequisite for initiation of the infection and disease (Fig 1.1A), many studies have sought to identify the fungal adhesins and their respective receptors (Tronchin *et al.*, 2008). In order for *C. albicans* to infect and spread throughout an immunocompromised individual, it must be able to adhere to the surface of epithelial cells (usually in the oral cavity) so it can develop in order to penetrate the cells and disseminate throughout the body (Henriques *et al.*, 2006, Modrzewska and Kurnatowski, 2015). *C. albicans* possesses an extensive repertoire of virulence factors that allow successful colonization and dissemination in the host (Mayer *et al.*, 2013) and these include the ability to adhere to host tissue and produce a range of enzymes (e.g. secreted aspartyl proteinase, phospholipase, Naglik *et al.*, 2003). A similar process of purging epithelial cells of fungal cells occurs in the urinary tract and vagina, leading to a similar adhesion process (Fisher *et al.*, 2011). Yeast adherence to buccal cells was highest and the lowest using urinary tract cells, while vaginal epithelium was intermediate (Sandin *et al.*, 1987). *C. albicans* possess a set of unique proteins that allow it to mediate the adhesion process to epithelial cells more successfully (Garcia *et al.*, 2011). The mechanisms of adherence incorporating adhesins such as ligand-receptor on the yeast cell surface. The well-studied gene family agglutinin like sequence (ALS). The genes that encode the ALS family of proteins encode glycoposphatidylinositol (GPI)-linked glycoproteins that are used to interact with the epithelial

cells to adhere to them. The ALS3 is particularly important and encodes eight glycosylphosphatidylinositol (GPI) cell-surface proteins that are responsible for binding amino acids and sugar on an abiotic surface (Cotter and Kavanagh 2000). The most important of the eight ALS proteins encoded is Als-3, as it is upregulated during adhesion of *C. albicans* to oral epithelial cells (Murciano *et al.*, 2012). Another adhesion protein is Hwp1, which is hyphae associated GPI-linked protein that acts as a substrate to the mammalian transglutaminases, covalently linking *C. albicans* to the host cells (Staab *et al.*, 1999).

#### **1.4.4 Invasion**

It has been observed that *C. albicans* invades epithelial cells (Fig 1.1B) by two mechanisms which include induced endocytosis and active penetration (Maza *et al.*, 2017). The pathogen does not rely on active penetration of host cellular mechanism or machinery however it depends upon recognition of the cytoskeleton of host. The first action of *C. albicans* is to reach the deep tissues by breaking the epithelial barrier (Naglik *et al.*, 2011). The interaction of *C. albicans* is important for having commensal growth of the organism along with fungal pathogenicity and host defense. In the process of invasion, especially during induced endocytosis, the organism expresses invasins. These invasions are in the form of specialized proteins that allows the organism to bind to the host cell. These proteins help the organism to engulf the host, while the dead hyphae take up the host cell (Cassone, 2015). The invasins have been identified in the process of induced endocytosis: Als-3 and Ssa-1. Ssa-1 is a cell surface expressed protein which is part of the heat shock family 70 (Hsp70). Both Als-3 and Ssa-1 bind to E-cadherin and are believed to induce endocytosis through a calthrin dependent pathway. Macro-pinocytosis has been mentioned as a potential influencer as

well in induced endocytosis of *C. albicans* (Phan *et al.*, 2007). By comparing the two processes, it has been observed that active penetration is completely opposite of induced endocytosis because active penetration is not passive while induced endocytosis is a passive process. Active penetration is also driven by fungal adhesion and physical force.

#### **1.4.5 Thigmotropism**

Thigmotropism is a directional growth movement that occurs as a mechanosensory response to a touch stimulus. Thigmotropism (Fig 1.1B) is involved in the dissemination of hyphae between layers of cells and specific directional growth. The weakest area on the cell membrane can be sensed through thigmotropism and so the hyphae can penetrate and invade the host cell (Davise *et al* 1999; Kumamoto; 2008). It allows *C. albicans* to initiate an appropriate response to the surface it has attached to whereby attachment to a biotic surface results in invasion and by contact attachment to an abiotic surface results in biofilm formation (Mayer *et al*; 2013).

#### **1.4.6 Biofilm formation**

The majority of infections caused by *C. albicans* are associated with biofilm formation (Fig 1.1C) in which the target is an abiotic surface or host cells (Brunke *et al.*, 2016), which is significant for the *C. albicans* to develop and infect the host. Biofilms are mainly the colonies of the organism which are encased in extracellular matrix. The growth occurs in a few stages which include adherence to host cells, expansion of yeast cells, progression of film, and diffusion of *C. albicans* cells to a new biofilm (Ribeiro *et al.*, 2017). A positive relation between cell surface hydrophobicity and biofilm formation has been expounded (Li *et al.*, 2003). This may be mediated by cell surface proteins which are encoded by members of the ALS family of adhesin-producing

genes and EAP1 (Green *et al.*, 2004). The populations of *C. albicans* cells were determined microscopically in the formation of biofilm. *Candida* yeast and germ tubes were attached to the mucosal surface and consisted of a mixture of closely associated yeast and hyphae surrounded by an extracellular matrix (Harriott *et al.*, 2010). The hyphal structure was demonstrated to be an essential component for providing the structural integrity and development of characteristic multilayered biofilm (Mayer *et al.*, 2013). One feature of biofilms formed by *C. albicans* is the mixture of different morphological forms. Morphological biofilm is a heterogeneous component containing a mixture of yeast, hyphae and pseudohyphae forms (Hawser and Douglas, 1994). Efflux pumps present in the biofilm are actively pumping out any drug that may come into contact with the biofilm and these pumps appear to be found in the biofilm in large quantities (Mukherjee *et al.*, 2003). Biofilms in *C. albicans* have been reported on most medical devices and frequently occur on catheters, dentures, voice prosthetics implants and artificial joints (Ramage *et al.*, 2006). Recent evidence suggests that biofilms also form on the mucosal surfaces of the mouth and vagina. Biofilms of *C. albicans* form when single cells attach and grow on the surface to form microcolonies, which then produce 3-D structure complex that merge together hyphae and an exopolymer matrix (Chandra *et al.*, 2001).

#### **1.4.7 Polymorphism and switching**

Polymorphism and switching are the ability of an organism to take many forms (Fig 1.1D and 1.1E). It has been observed that *C. albicans* is a polymorphic organism that changes its form and goes through many morphological transitions between hyphal form, pseudohyphal form, and yeast (Neville *et al.*, 2015). The polymorphism of the organism means that it can grow in several forms

clinically. There also a different immune response that should be present in the human body because *C. albicans* has various forms and it grows so there should be different immune responses for different phases of *C. albicans*. Hyphae can actively penetrate host tissue allowing them to invade the bloodstream and avoid host immune cells such as macrophage (Calderon and Fonzi, 2001). It is the ability to switch from budding yeast to hyphae that is important for virulence. The yeast form can become engulfed by macrophages however it is differentiating into a hyphal form and penetrates the macrophages cell membrane allowing escape from the macrophage (Saville *et al.*, 2003, Lorenz *et al.*, 2004). It also grows in other forms rather than yeast, pseudohyphae, and hyphae which include opaque and white cells which form into chlamydospores (da Silva Dantas *et al.*, 2016). White and opaque cells differ in virulence, mating ability, pheromone production and competency in evading host defence system. white cells have a key role in internal infection such as systemic bloodstream infection whereas opaque colonies are more prevalent in skin infections, produces essential for initiation of mating and are more resistant to host neutrophil (Kvaal *et al.*, 1999; Kolotila and Diamond, 1990).

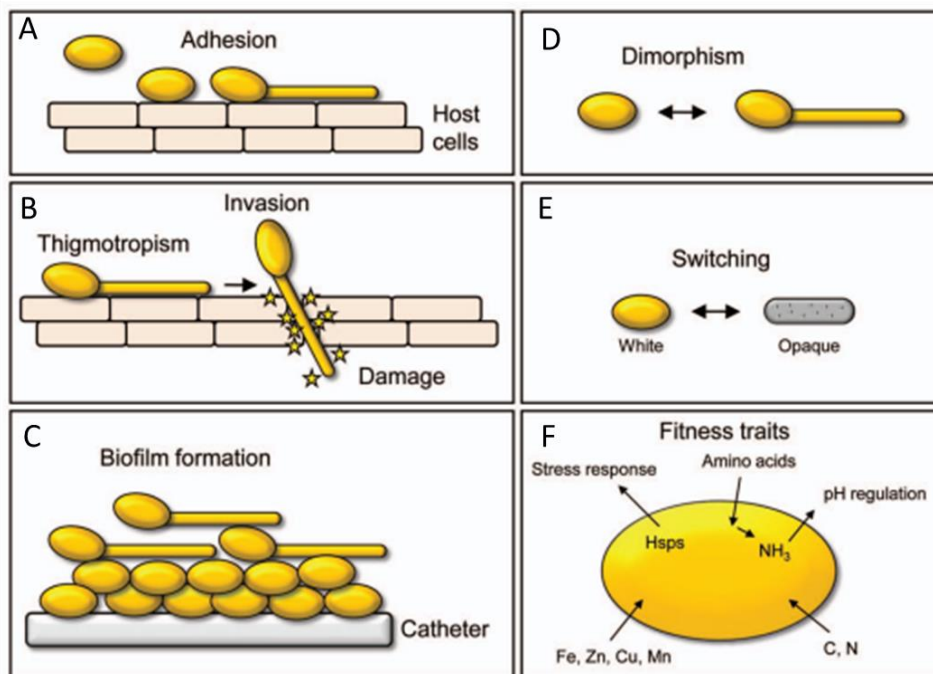


**Figure 1.1:** Adhesion (A), invasion (B), biofilm formation (C), dimorphism (D), switching (E) and fitness traits (F) (*Candida albicans* pathogenicity mechanisms Mayer *et al.*, 2013).

### 1.4.8 pH and environmental adaptation

There is an extreme impact of the environment on fungal and bacterial growth. The most important thing which is under consideration while focusing on environmental adaptation includes the pH (Fig 1.1F) in which the organism grows (Höfs *et al.*, 2016). *C. albicans* colonizes and infects anatomical sites of different pH range, including the oral, gastro-intestinal tracts and the vaginal cavity (Davis, 2003) which can cause severe stress to *C. albicans*. In order to overcome this, *C. albicans* can alter itself in order to adapt to the changing pH environment (Davis, 2009). *C. albicans* senses and changes itself to the pH of the environment, in addition, it can also dictate its extracellular environment. It does this by alkalinizing the surrounding environment, which is nutrient-starved, thereby inducing hyphae formation (Mayer *et al.*, 2012). It has been observed



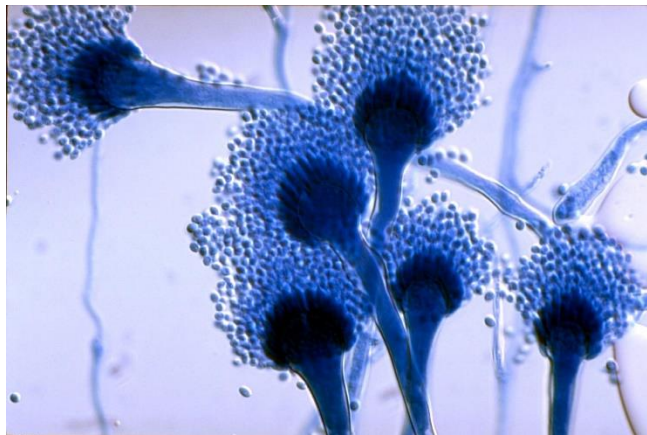
that the acidic pH results in structural loss of an organism, and the outer fibrillar layer reduces in size due to acidic pH. Also, acidic pH disrupts the architecture of the structure of an organism. The organism requires ambient pH in vaginal mucosa, stomach and GI tract for colonizing (Davis, 2003). The development in acidic environments include cell wall modifying which results in improved chitin and  $\beta$ -glucan exposure at the cell wall periphery (Sherrington *et al.*, 2017).

#### **1.4.9 Signaling Pathways**

Signaling pathways are the molecules that act in a group to control the cell functions such as cell death or cell division. For having the responses in the motion of *C. albicans*, signaling pathways are necessary. These are used in MAP kinase pathways that are responsible for sensing environmental changes and transducing the signals detected from the cell surface to the interior of the cell by sequential protein activation. Activated MAP kinases kinases phosphorylate MAP kinases kinases, which in turn phosphorylate MAP kinases (Navarro-Garcia *et al.*, 2001). The MAP kinase usually translocates to the nucleus where activation of different transcription factors leads to changes in gene expression and/or protein activity, which results in turn in the triggering of specific cellular responses required for adaptation (Gustin *et al.*, 1998, (Lengeler *et al.*, 2000). In all this molecular interplay, the cell wall has a major role both as a sensor and a protector of the living cell. MAP kinase pathways later broken into three which are known as Mck 1 pathways which activates an oxidative stress response acting along with maintaining the cell integrity, Hog1 which is responsible for thermal, oxidative and osmotic stress and Cek 1 which is the final pathway for signaling that involves adaptation to thermal stress and maintenance of filamentation (Sellam *et al.*, 2019).

### 1.5 *Aspergillus fumigatus*

*Aspergillus* is a species of fungus that lives in soil, plant matter, and household dust. Among the species of *Aspergillus* that are pathogenic towards humans, the most pathogenic, and the primary causative agent of aspergillus related infections is *A. fumigatus* (Morgan *et al.*, 2005). It can also produce airborne spores called conidia (Fig 1.2). People can inhale many of these conidia on a daily basis. In a healthy individual, the immune system eliminates them from the body without a problem. However, it is a serious cause of disease in immunocompromised patients or in those with pulmonary disease (e.g. cystic fibrosis (CF), asthma) and conidia can quickly germinate and grow in the lung. By increasing in the population of immunocompromised patients *A. fumigatus* has become the second most common opportunistic fungal pathogen of humans (Netea *et al.*, 2003).



---

**Figure 1.2:** Images of *A. fumigatus* showing hyphae, conidiophore and conidia. (<https://alunosonline.uol.com.br/biologia/aspergilose-pulmonar.html>)

### **1.5.1 *A. fumigatus* and the Environment**

Mostly *A. fumigatus* is isolated from a range of substrates in the environment. *A. fumigatus* continues to grow at 37 °C with pH 3.7-7.6 optimally, it can be isolated when soil and decaying vegetation range between 12 and 65 °C with the ranges of pH between 2.1 to 8.8 (Kwon-Chung and Sugui, 2013). *A. fumigatus*, like an effective recycler in nature, has adaptable metabolisms which fulfill its nutritional need in various environments. Self-heating heaps of compost are the key environmental site for *A. fumigatus* because of its evident thermo-tolerance. *A. fumigatus* forms small hydrophobic conidia, the head of these conidia forms large numbers of green-grey spores with a diameter of 2 to 3 µm makes them float in the environment. *Aspergillus* conidia is found to be 1 to 100 in concentrations that can pass through the clearance mechanism of mucocilliary while breathing. Thus, it penetrates the alveoli of lungs (Paulussen *et al.*, 2017).

### **1.5.2 Diseases caused by *A. fumigatus***

#### **1.5.2.1 Aspergillosis**

Aspergillosis is linked with vast range of disease (Frisvad and Larsen, 2016). Infections related to aspergillosis are generally observed in individuals with altered immune mechanism, host elements are as crucial as the virulence factors of fungus. Virulence factors serve a key role in the particular pathogenesis caused by *Aspergillus* species, the immune status of the host also serves a major role in increasing the fungal virulence factor production in the host (Bodey and Vartivarian, 1989) (Tracy *et al.*, 2016). Different physical components are also causing pathogenicity, for example,

the capability of fungus to multiply in minute size of conidia, pH of the tissues of the host and at optimum temperature (Kwon-Chung and Sugui, 2013).

### **1.5.2.2 Invasive Aspergillosis**

Invasive Aspergillosis is a kind of pulmonary aspergillosis that can be found in patients with weak immune function. It is the most serious kind of aspergillosis that happens once the infection spreads quickly from human lungs to skin, heart, kidneys, and brain (Sugui et al., 2015). Invasive aspergillosis happens in individuals who have weak immune systems because of the chemotherapy for cancer, any disease related to immune system or bone marrow transplantation. Invasive aspergillosis can be fatal if left untreated. The signs and symptoms of invasive aspergillosis are based on the organs that are affected, generally, they include, eye symptoms, skin lesions, headaches, chills and fever, breathlessness, joint or chest pain and hemoptysis (Bruder Nascimento *et al.*, 2016). There are various forms of aspergillosis involving pulmonary aspergillosis, pulmonary invasive aspergillosis and aspergilloma, notwithstanding the availability of new antifungal agents, the morbidity rate due to invasive aspergillosis has increased steadily (Blyth *et al.*, 2007).

### **1.5.2.3 Allergic Broncho-Pulmonary Aspergillosis (ABPA)**

ABPA is a hypersensitive response to the species of *Aspergillus* (usually *A. fumigatus*) which happens in patients who have cystic fibrosis or asthma. Immune reactions to the antigens of *Aspergillus* cause airway blockage and if it is left untreated, pulmonary fibrosis or bronchiectasis can occur. Signs and symptoms include asthma with productive cough, sometimes anorexia and fever (Sugui *et al.*, 2015). Diagnosis depends upon imaging tests and history that can be confirmed by checking IgE levels and *Aspergillus* skin testing, specific *A. fumigatus* antibodies, circulating

precipitins. It is treated with corticosteroids, but patients with the condition of the refractory disease are treated by itraconazole (Frisvad and Larsen, 2016).

### **1.5.3 *A. fumigatus* and virulence factors**

Pathogenicity of *A. fumigatus* is dependent upon various factors of the host (immune status) and virulence factors of the pathogen. According to Raksha and Urhekar, (2017) the virulence factors that have been recognized for various *A. fumigatus* include, adhesins, pigments, hydrolytic enzymes for example proteases, ribonucleases, phospholipases, restrictocin; catalases, superoxide-dismutases, mycotoxins and low-molecular-weight non-protein metabolites. Blatzer and Latge, (2017) argue that, gliotoxin the main mycotoxin, is among the strong virulence factors, caused by *A. terreus* and *A. fumigatus* isolates in the samples of patient, although, the formation of aflatoxins are mainly observed in the cases of *A. flavus*. It is noted that mycotoxins are able to serve a key role in increasing pathogenesis of aspergillus invasiveness (Bruder Nascimento *et al.*, 2016). It is also noted that gliotoxin is formed *in vivo* in animal tissues infected and affected by *A. fumigatus* as well as it was previously present in patients' serum with intrusive aspergillosis (Woo *et al.*, 2017). According to Bruder Nascimento *et al.*, (2016) virulence factors are considered to be extremely significant in examining any pathogen which assists in differentiating between species which are pathogenic and non-pathogenic. The occurrence of virulence factors within aspergilli isolates might provide the invasiveness signals of species from *Aspergillus* (Paulussen *et al.*, 2017). With respect to the alterations in virulence factors formed by different species of *Aspergillus*, it can be observed that phospholipase, proteinase, haemolysin, and biofilm formation are most significant virulence factors (Ghorbel *et al.*, 2019). *A. fumigatus* can produce a biofilm *in*

*vitro* on PS and bronchial epithelial cells with typical characteristics. (Seidler *et al.*, 2008). A variety of host components are also activated during aspergillosis which enhance the *in vivo* colonization and biofilm formation by *A. fumigatus*, like serum components, fetuin A, has been recently reported to accelerate the growth of *A. fumigatus* and facilitate the formation of a thick biofilm (Toyotome *et al.*, 2012). It is necessary analysis and understanding of *A. fumigatus* biofilms is necessary to devise newer and better antifungal targets for treating complex *A. fumigatus* biofilm-associated diseases (Kaur and Singh, 2014).

#### **1.5.4 Mycotoxins**

Mycotoxins are the toxic compounds that are formed by specific kinds of molds which can form mycotoxins on several food items like spices, dried fruits, cereals, and nuts. The growth of mold can happen before or after harvesting, on the food itself in humid, damp and warm conditions or during storage. Some molds can produce more than one mycotoxin and some mycotoxins are produced by more than one fungal species (Zain, 2011). Contamination by mycotoxins in human food and animal feed is a significant worldwide problem because mycotoxins are naturally occurring toxic substances (Charoenpornsook and Kavisarasai, 2006). Mycotoxins are secondary metabolites produced by fungi, and they can cause mycotoxicosis (diseases and death) in humans and animals (Liew and Mohd-Redzwan, 2018). *A. fumigatus*, an important human pathogen, produces several mycotoxins including gliotoxin (Hof and Kupfahl, 2009).

### 1.5.5 Gliotoxin

Gliotoxin (Fig. 1.3) is considered to be a significant virulence factor of *A. fumigatus*. It has immunosuppressive characteristics which might suppress and lead to apoptosis in specific immune cells, including thymocytes, neutrophils, macrophages, eosinophils, and granulocytes (Hof and Kupfahl, 2009). Particularly, neutrophils exposed to gliotoxin produce reduced “reactive oxygen species (ROS)” and finish less phagocytic activities and also gliotoxin is considered to interfere with the activation of T-cells (Orciuolo *et al.*, 2007). Furthermore, gliotoxin serves as a farnesyl transferase inhibitor which inhibits the activity of chymotrypsin of 20S proteasome non-competitively (Paulussen *et al.*, 2017). *In vivo* gliotoxin shows anti-inflammatory activity (McDougall, 1969). This was explored as an anti-fungal, anti-viral and antibiotic agent (Aljofan *et al.*, 2009). Gliotoxin inactivates several enzymes which include glutaredoxin, nuclear factor-  $\kappa$ B and NADPH oxidase. Nuclear factor-  $\kappa$ B inhibition leads to prevent the release of cytokine and inflammatory reaction induction (Pahl *et al.*, 1996). The immunosuppressive characteristics of gliotoxin are due to bridge of disulfide bond in its structure (Trown and Bilello, 1972). There are interactions between the molecules of sulfur which creates thiol groups and bridge of disulfide contained in the residues of cysteine, gliotoxin serves by obstructing the residues of thiol in the cell-membrane (Kwon-Chung and Sugui, 2009). Also, gliotoxin activates the Bcl-2 family member known as Bak to mediate apoptosis (Nguyen *et al.*, 2014). Then, the activated Bak allows the ROS release, which produces pores in mitochondrial membrane, such pores enable the cytochrome C release that stimulates the cell apoptosis (Pardo *et al.*, 2006).

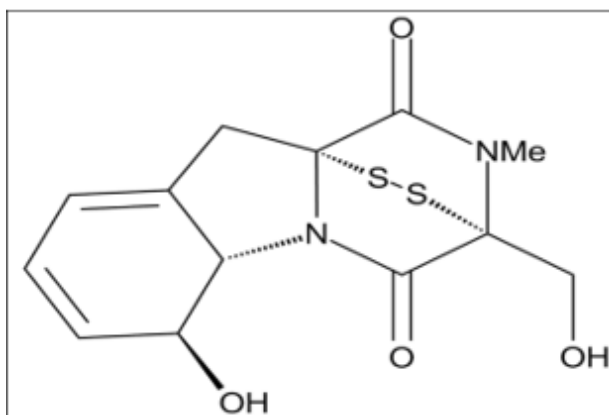


**Figure 1. 3:** Gliotoxin structure. (<https://www.apexbt.com/gliotoxin.html>).

## 1.6 Antifungal drugs

An antifungal agent is a drug that selectively eliminates fungal pathogens from a host with minimal toxicity to the host. An antifungal medication, also known as an antimycotic medication, is a pharmaceutical fungicide or fungistatic used to treat and prevent mycosis such as athlete's foot, ringworm, candidiasis (thrush), serious systemic infections such as cryptococcal meningitis, and others. The major groups of antifungals are the polyenes, the azoles, and the echinocandin; these groups are distinguished primarily by chemical structure and mechanism of action. The main mode of action of azole and polyene antifungal agents is the damage of the cell membrane (Fig. 1.4). Sterols are one of the main constituents of the cell membrane and are important in maintaining appropriate membrane fluidity and rigidity, and hence, the proper function of the cell membrane. Antifungals take advantage of little differences between fungi and humans in the biosynthesis of sterols. For most fungi, the predominant membrane sterol is ergosterol (Fig. 1.5). Because human cell membranes use cholesterol, instead of ergosterol, antifungal drugs that target ergosterol synthesis are selectively toxic.



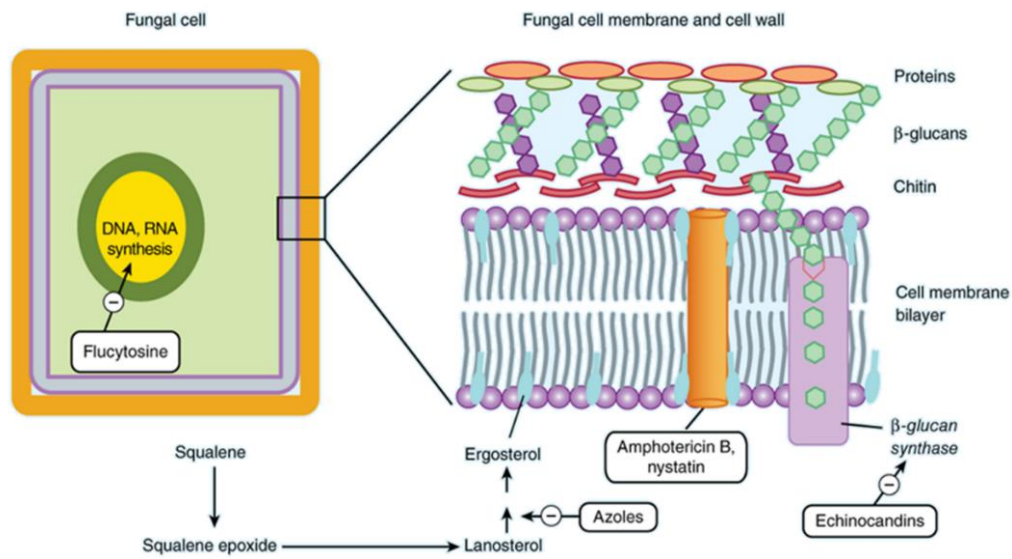


**Figure 1. 4:** Mechanism of action of antifungal agents. Basic and clinical pharmacology, 13e Bertram G. Katzung, Anthony J. Trevor.

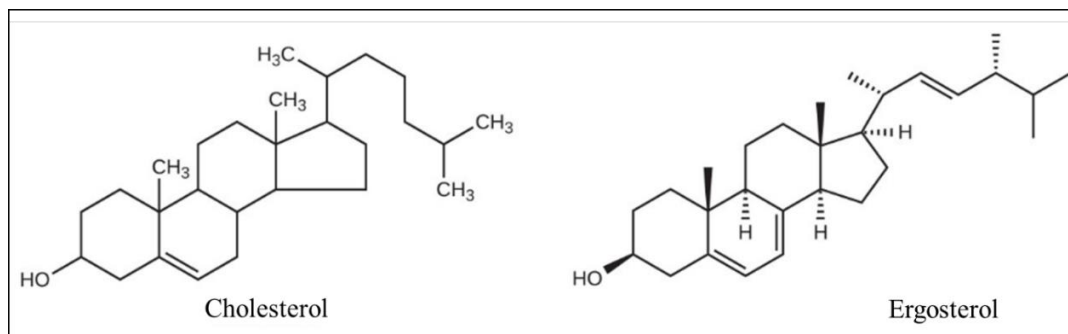


**Figure 1. 5:** The prevalent sterol found in human cells is cholesterol however the prevalent sterol found in fungi is ergosterol making ergosterol a good target for antifungal drug development. (<https://courses.lumenlearning.com/cuny-kbcc-microbiologyhd/chapter/mechanisms-of-other-antimicrobial-drugs/>)

### 1.6.1 Azoles

Azoles are the largest class of clinically used antifungal drugs that act mainly by rupturing the cell membrane by inhibiting the action of lanosterol 14-  $\alpha$ -demethylase enzyme, the enzyme involved in the biosynthesis of ergosterol (Odds *et al.*, 2003). This damages the membrane structure and disrupts many functions of fungal membrane leading to inhibition of fungal growth (Diaz-Guerra *et al.*, 2003). Ergosterol is the largest sterol component of the fungal cell membrane, and has structural differences from human cholesterol, so azoles do not cross react with host cell. The azole family includes imidazoles (miconazole, econazole, clotrimazole, and ketoconazole), triazoles (fluconazole, itraconazole) and the largest agent voriconazole (second generation, synthetic triazole derivative of fluconazole) and posaconazole (hydrated analogue of itraconazole). Many azoles are effective both for topical use as well as for the treatment and prophylaxes of invasive fungal infection (Utz, 1980).

### 1.6.2 Polyenes

Polyenes are typically obtained from some species of *Streptomyces* bacteria (Fjervik and Zotchev, 2005). Polyenes bind to the ergosterol in the fungal cell membrane, which creates hydrophilic pores in the cell membrane (Gray *et al.*, 2012). Consequently, the cellular permeability is altered and leads to leakage of cytosolic component and, therefore, death (Gray *et al.*, 2012). One of the most effective drugs against pathogenic fungi is the polyene amphotericin B (Reeves *et al.*, 2004). Amphotericin B's mechanism of action relies upon the creation of apertures in the fungal cell membrane, altering the permeability of the cell and resulting in release of the contents of the cell. Amphotericin B has a broad spectrum of action and remains the drug of choice for many forms of

deep fungal infection. The Amphotericin B molecules face inwards, creating a pore of about 0.1-0.4 nm wide, allowing cellular contents to pour out, and hydrogen ions to invade the cell, raising the acidity of the cytoplasm (Reeves *et al.*, 2004). The other member of polyene is nystatin, used for the topical treatment of oral, oesophageal, gastrointestinal, genital, and cutaneous forms of candidiasis (Cirillo *et al.*, 1964).

### **1.6.3 Echinocandins**

Echinocandins are a class of antifungal drugs that target the fungal cell wall. These agents are large lipopeptide molecules that are inhibitors of  $\beta$ -(1,3)-glucan synthesis, an action that damages fungal cell walls, which lyse easily by osmotic pressure (Denning, 2003). The echinocandins family includes caspofungin, micafungin and anidulafungin. Caspofungin is used in the treatment of acute invasive candidiasis and as a rescue treatment for invasive aspergillosis (Denning *et al.*, 2002).

### **1.6.4 Antifungal resistance**

Antifungal agents treat fungal infections by killing or stopping the growth of pathogenic fungi in the body. Fungi, like bacteria, can develop antibiotic resistance. Antifungal resistance occurs when fungi no longer respond to antifungal agents. Only three types of antifungal drugs currently exist, so antifungal resistance can severely limit treatment options. Common antifungal therapy depends on the use of polyene, azole or echinocandin drugs but the delivery of appropriate therapy is often problematic due to the presence of resistance and the inherent toxicity of some antifungal therapies (Scorzoni *et al.*, 2017). Some types of fungi, like *Candida auris*, can become resistant to all three drug types (Ostrowsky *et al.*, 2020). (Alexander *et al.*, 2013) demonstrated that the *Candida*

isolates with acquired resistance to azoles and echinocandins have been reported more frequently. *C. glabrata* isolates showed no underlying mutations for both echinocandin and azole resistance (Spettel *et al.*, 2019). Aldardeer *et al.*, (2020)) showed that the rise in *C. parapsilosis* resistance to fluconazole is alarming. The continuing problems associated with existing antifungal therapies (e.g. toxicity, drug resistance) offer the possibility of employing an active, non-toxic therapy such as atorvastatin to supplement existing therapies (Galgóczy, 2011; Nyilasi *et al.*, 2010)

## 1.7 Statins

Statins are the main therapeutic agents used to decrease high serum cholesterol levels and are among the most widely prescribed drugs currently on the market (Macreadie *et al.*, 2006). Angiographic studies have demonstrated that these compounds reduce the progression and may induce the regression of atherosclerosis (Vaughan *et al.*, 2000). They competitively inhibit 3-hydroxy-3-methylglutaryl-CoA (HMG-CoA) reductase by competitively binding to its binding sites (Qiu *et al.*, 1991). HMG-CoA is an enzyme that catalyses the conversion of HMG-CoA to mevalonate, which leads to the production of farnesyl diphosphate (Macreadie *et al.*, 2006). Farnesyl diphosphate is the precursor for the production of cholesterol in humans or ergosterol in plants and eukaryotic microorganisms (Macreadie *et al.* 2006). If the statin-binding site of fungal HMG-CoA reductase is like that of human HMG-CoA reductase, it might be expected that statins or their derivatives could also be used to inhibit the growth of fungal pathogens through inhibition of ergosterol synthesis. Statins have *in vitro* activities against several human pathogenic fungi, including *Candida spp.*, *Cryptococcus neoformans*, and *Zygomycetes* (Chamilos *et al.*, 2006).

Some of the statins are obtained after fungal fermentation; lovastatin, pravastatin and simvastatin, others by synthesis: fluvastatin, atorvastatin, and cerivastatin (Camelia Stancu and Sima, 2001).

### **1.7.1 Statins mechanism of action**

Hypercholesterolemia (high levels of cholesterol), is considered a significant risk factor in coronary artery disease. About two-thirds of total body cholesterol is an endogenous synthesis (Kriaa *et al.*, 2019), thus the possibility of controlling represents an effective way of lowering plasma cholesterol level (Manzoni and Rollini 2001). Statins (Fig 1.6) selectively inhibit hydroxymethyl glutaryl-coenzyme A (HMG-CoA) reductase, the first enzyme in cholesterol biosynthesis pathway. The mechanism used by statins to reduce the cholesterol level in the human body revolves around the increased uptake and degradation of low-density lipoproteins, also known as LDL cholesterol (Bellosta *et al.*, 2000). The liver plays a central role in lipid metabolism, serving as the center for lipoprotein uptake, formation, and export to the circulation (Corey and Cohen, 2015). Statins target the hepatocytes and inhibit the catalyzing of HMG-CoA reductase by not only out-competing HMG-CoA reductase for the active sites, but also by altering the enzyme on formation upon binding to the active site. This prevents HMG-CoA reductase from acquiring the correct structure necessary to successfully produce cholesterol, making statins very effective and specific (Corsini *et al.*, 1999). The inhibition of HMG-CoA then induces the activation of a protease that blocks the sterol regulatory element binding proteins (SREBPs) from moving to the endoplasmic reticulum to the nucleus. This increases the gene expression of LDL receptors, leading to an increase in the number of LDL receptors being produced. Therefore, the reduction

of LDL in hepatocytes leads to the increase of hepatic LDL receptors, which in turn reduces the amount of LDL within the circulating blood (Sehayek *et al.*, 1994).

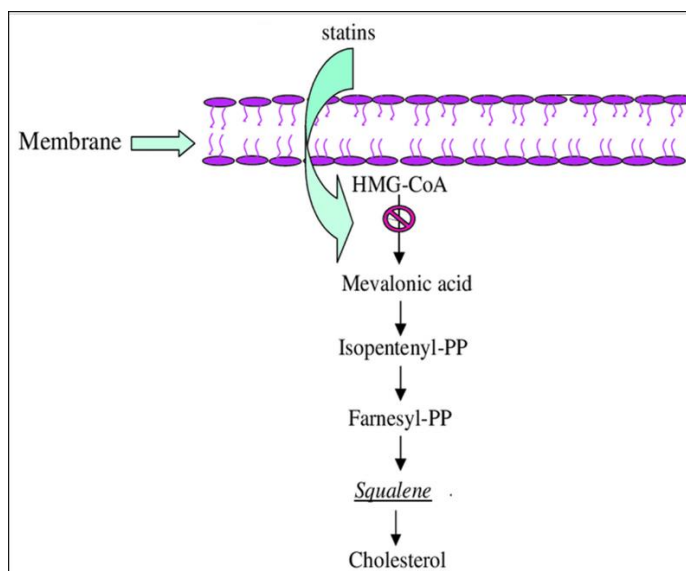


**Figure 1. 6:** Mechanism of action of anti-hypercholesteremia (statins). Statins prevent cholesterol biosynthesis by inhibiting the conversion of HMG-CoA to mevalonic acid.

### 1.7.2 Statins Prospect as Antifungals

The fungal equivalent of cholesterol is ergosterol, which is a main component of the cell membrane in both *C. albicans* and *A. fumigatus*, and just like cholesterol, it depends on the production of farnesyl diphosphate (Dhar *et al.*, 2013). The target of statins is the precursors of cholesterol, in particular, farnesyl diphosphate. The induced inhibition of farnesyl diphosphate has wider modulations than just reducing cholesterol in the human body. Statins are well-known inhibitors of 3-hydroxy-3-methylglutaryl-CoA reductase (HMGR), the key enzyme of the cholesterol

synthesis pathway (Maciejak *et al.*, 2013). It could, therefore, be supposed that if statins could inhibit cholesterol, they could inhibit the production of ergosterol (Macreadie *et al.*, 2006a). Ergosterol, a 5,7-diene oxysterol, is the most abundant sterol in the fungal cell membrane, where it regulates permeability and fluidity (Manzoni and Rollini, 2002). Because of its crucial functions, unique structural properties, and particular biosynthetic steps, ergosterol is the target of the majority of clinically available antifungals. The mode of action of most anti-fungal drugs is to target and interact with ergosterol in the fungal cell (Ghannoum and Rice, 1999). Any product that can prevent the production of ergosterol would therefore be an invaluable member of the anti-fungal family and could be used in combination with all the other drugs, as well as potentially on its own (Brilhante *et al.*, 2015). Some previous studies have shown that statins do have an effect as antifungal drugs. Macreadie *et al.*, (2006), showed that *A. fumigatus* and some species of *Candida* show a reduced level of growth once treated with statins. The lower level of growth could be due to the fact that the fungi were grown in the presence of statin, leading to a lower level of ergosterol (Macreadie *et al.*, 2006a). Another study (Qiao *et al.*, 2007) confirmed these results, suggested that statins have an inhibitory effect on ergosterol in *A. fumigatus*.

## **1.8 Insects as a model for human pathogens**

The vertebrate innate immune system has strong structural and functional similarities to the insect immune system (Kavanagh and Reeves, 2004, Renwick *et al.*, 2007). As a result of these conserved similarities a wide range of insects have been employed to study the virulence of bacterial and fungal pathogens and give results that are comparable with those obtained using

vertebrates (e.g., mice) (Lemaitre and Hoffmann, 2007, Ben-Ami, 2011). In recent times more interest in in-vivo insect models has come about with the global increase in antibiotic and antifungal resistance as a result of more immunocompromised individuals who are susceptible to mostly commensal pathogenic organisms that include *Candida*, *Aspergillus*, and *Cryptococcus* species (Romani, 2004). Both mammalian and insect models are susceptible to similar pathogens and share common infection pathologies (Kemp and Massey, 2007). The insect screening model provides an innovative way to simultaneously examine the mechanisms of microbial pathogenicity and the activity of potential drug agents without the drawbacks of mammalian models. This has led to a variety of insect host models being established for such purposes. These include the well characterised fruit fly *Drosophila melanogaster* (Lemaitre *et al.*, 1996), wax moth *Galleria mellonella* (Kavanagh and Reeves, 2004) and the silkworm *Bombyx mori* (Hamamoto *et al.*, 2004) (Fig 1.7).



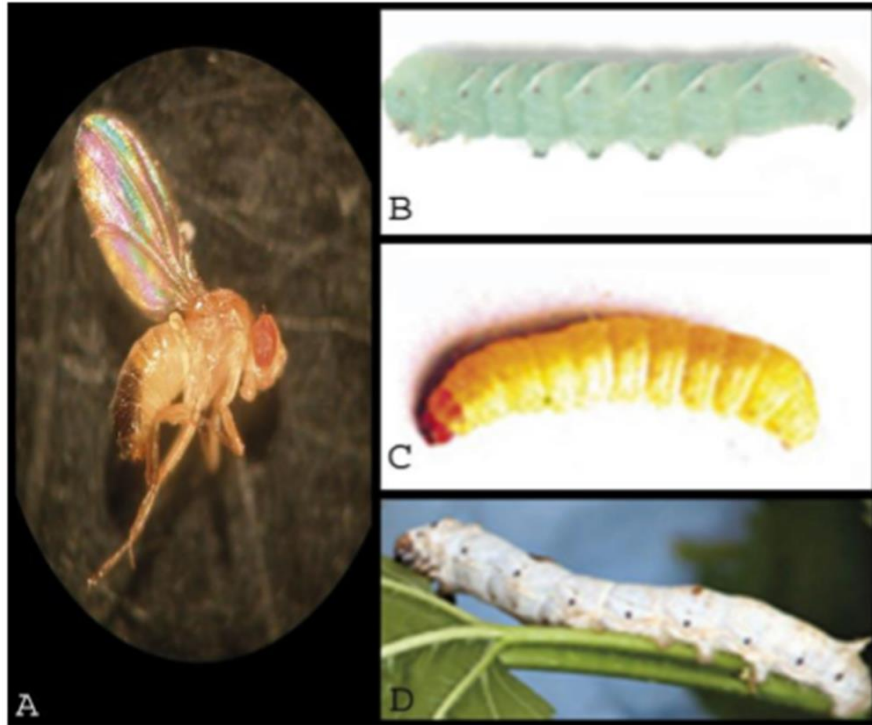


**Fig. 1.7:** Insects used as models for human pathogens. (A) *Drosophila melanogaster*; (B) *Manduca sexta*; (C) *Galleria mellonella* and (D) *Bombyx mori* (Kemp and Massey, 2007)

### 1.9 *Galleria* as an *in vivo* model

The greater wax moth or honeycomb moth, *Galleria mellonella*, has become important in many different lines of research (Abidalla, 2018). *G. mellonella* is found throughout the world. *G. mellonella* larvae (range between 1.5 - 2.5 cm) enable an easy means of inoculation with specific amounts of drug or pathogen via the pro-leg making *G. mellonella* more amenable to drug pharmacodynamics studies (Kavanagh and Fallon, 2010). *G. mellonella* larvae have been considered as a viable alternative to other models of infection since they are cheap and require no specialist equipment (Kay *et al.*, 2019). In addition to their importance in apiculture, wax moth

larvae are widely used as model organisms for studies in insect physiology and human with pathogens (Browne and Kavanagh, 2013). *G. mellonella* larvae were used to assess the virulence of *C. albicans* and to investigate the virulence of pathogenic and non-pathogenic yeast species (Cotter *et al.*, 2000). Pathogen virulence and antimicrobial efficacy testing of agents can be analysed by using a number of parameters in *G. mellonella* including the degree of melanisation in response to a pathogen, larval death, alterations in fungal burden, changes in haemocyte densities and changes in antimicrobial peptide expression (Bergin *et al.*, 2003). Brennan *et al.*, (2002) established a positive correlation between the virulence of *C. albicans* mutants in *G. mellonella* larvae and in *BalbC* mice and a strong correlation was also established between the virulence of *A. fumigatus* mutants in larvae and mice (Slater *et al.*, 2011). *G. mellonella* has several innate immune similarities to mammals they lack many defined organ systems preventing the full study of fungal dissemination and antifungal therapy which is possible in mammals (Kavanagh and Fallon, 2010). *G. mellonella* larvae have also been utilised for assessing the *in vivo* activity of amphotericin B, flucytosine and fluconazole following challenge with *C. neoformans* (Mylonakis *et al.*, 2005) and to evaluate the antifungal properties of novel silver-based compounds (Rowan *et al.*, 2009). *G. mellonella* larvae are now utilized as an infection model for *Cryptococcus neoformans* (Mylonakis *et al.*, 2005) and (London *et al.*, 2006) identified that a number of virulence-related genes important in *C. neoformans* mammalian infections were also involved in infection of *G. mellonella*.

### 1.10 Overall objective:

- Establish the antifungal activity of a widely prescribed statin (Atorvastatin).
- Assess the effect of atorvastatin on the virulence of *C. albicans* and *A. fumigatus*.
- Analyse the proteomic responses of *C. albicans* and *A. fumigatus* to atorvastatin exposure.
- Study the effect of atorvastatin on *G. mellonella* larvae and analyse the proteomic responses to atorvastatin exposure.

## **Chapter 2**

# **Materials and Methods**

## **2 Material and method**

### **2.1 Strains used in this work**

#### **2.1.1 *Candida albicans* strain**

A single colony of *C. albicans* (MEN) (serotype B, wild type originally isolated from an eye infection by Dr. D. Kerridge, Cambridge, UK) was transferred to sterile YEPD broth (section 2.2.1) using a sterile inoculating loop. The flask was re-plugged with cotton wool and incubated at 30 °C at 200 x *g* overnight.

#### **2.1.2 *Aspergillus fumigatus* strain**

*A. fumigatus* ATCC 26933, (American Type Culture Collection, Maryland, USA) was used in this work. Stocks of *A. fumigatus* were maintained on malt extract agar (MEA) (Oxoid Ltd Basingstoke, UK) (section 2.2.3) at 37 °C and sub-cultured every 4 weeks. Culture was grown in different types of media for susceptibility assay, see section 2.2.4 and 2.2.5.

#### **2.1.3 Bacterial strains (*S. aureus* and *E. coli*)**

*S. aureus* and *E. coli* (Clinical isolates) were obtained from St James Hospital, Dublin and were transferred aseptically using a sterile loop from a single colony grown on nutrient agar to nutrient broth (Oxoid Ltd., Basingstoke, UK) (section 2.2.8) and grown overnight at 37 °C and 100 x *g* to the early stationary phase.

## **2.2 Culture conditions**

### **2.2.1 YEPD [Yeast Extract peptone D-glucose] broth / agar**

YEPD broth was made by dissolving glucose (2% w/v), yeast extract (1% w/v), and bacteriological peptone (2% w/v) in deionized water and autoclaving at 121<sup>0</sup>C for 15 minutes. For solid media preparation 2% (w/v) agar was added and autoclaved as described. In some cases, antibiotic erythromycin (1 mg/ml) was added to the hand warm agar prior to pouring to control bacterial contamination in determining fungal load in *Galleria mellonella* larvae. This was prepared by dissolving 0.1g erythromycin in 1 ml of deionized (di) H<sub>2</sub>O and transferring the erythromycin solution into the hand warm agar solution 100 ml. Once in the agar solution the plates were spread as normal and stored at 4 <sup>0</sup>C in the dark. All erythromycin supplemented plates were used within 3 days.

### **2.2.2 *C. albicans* liquid culture and cell harvest**

A colony of *C. albicans* (MEN) was aseptically transferred to sterile YEPD broth using a sterile inoculating loop. The flask was re-plugged with cotton wool and incubated at 30 <sup>0</sup>C at 100 x g overnight. To get a suspension of *C. albicans* cells, 50 ml culture was transferred to a sterile 50 ml tube and centrifuged at 500 x g for 5 minutes. The cellular pellet was washed twice in sterile PBS and the final cell concentration in a 10 ml volume of sterile PBS was ascertained by Haemocytometer.

### **2.2.3 Malt Extract Agar (MEA)**

Malt extract agar was prepared by adding 50 grams of MEA per liter of deionized water, mixing and autoclaving at 121 °C for 15 minutes. Agar was poured into petri-dish once it was hand hot.

### **2.2.4 Sabouroud dextrose liquid medium**

Sabouroud dextrose powder (30 gram) was dissolved in one litre of distilled water, mixed well, and sterilized by autoclaving at 121 °C for 15 minutes.

### **2.2.5 Czapek-Dox broth**

Czapek-Dox broth powder (35 gram) was dissolved in one litre of deionized water, mixed well, and sterilized by autoclaving at 121 °C for 15 minutes

### **2.2.6 Nutrient broth (NB)**

NB (13 gram) powder was dissolved in 1 liter of distilled water. This was mixed well and sterilized by autoclaving at 121 °C for 15 minutes.

### **2.2.7 *A. fumigatus* culture and cell harvest**

Stocks of *A. fumigatus* conidia were grown and maintained on Malt Extract Agar (Oxoid Ltd Basingstoke UK) at 37 °C in a thermally controlled incubator for 4 to 5 days. Sterile medium was inoculated in a sterile laminar flow hood and *A. fumigatus* conidial inoculations of  $5 \times 10^7$  per 100 ml culture were used. Conidia of *A. fumigatus* were harvested in a safety cabinet Class II. 10 ml PBS-T [0.1% (v/v) Tween 80] was used to wash the plates. Conidia were harvested by centrifugation at (2,056 x g) for 5 minutes at room temperature on a Beckmann GS-6 bench centrifuge. The supernatant was removed, and the conidial pellet was washed twice in sterile PBS

to remove excess Tween 80 and re-suspended in sterile PBS. The concentration of conidia in the suspension was determined by counting with a Haemocytometer.

## **2.3 General laboratory practice and sterilization procedures**

### **2.3.1 Chemicals and reagents**

All reagents were of the highest purity and were purchased from Sigma Aldrich Ltd, Somerset, U.K unless otherwise stated.

### **2.3.2 Sterilization procedures**

All growth culture media were sterilized by autoclaving before use at 121<sup>0</sup>C and 15 lb/sq.in for 15 minutes. Any liquid unsuitable for autoclaving was filter-sterilized using a pore size 0.45 and 0.2 µm (Sarstedt, Nümbrecht, Germany). All used liquid and solid cultures were autoclaved prior to disposal. Laboratory equipment such as micro-centrifuge tubes and pipette tips were kept in a sealed container and sterilized by autoclaving at 121<sup>0</sup>C for 15 minutes prior to use. Semi-solid agar media were allowed to cool until hand hot, (approximately 45-55°C) and poured under sterile conditions using 9 cm petri-dishes. All work with *A. fumigatus* was carried out using a class II safety cabinet.

### **2.3.3 Phosphate buffered saline (PBS)**

One PBS (NaCl 8.0 g/l, KCl 0.2 g/l, Na<sub>2</sub>HPO<sub>4</sub> 1.15 g/l, KH<sub>2</sub>PO<sub>4</sub> 0.5 g/l, pH 7.3) tablet (Oxoid Ltd Basingstoke UK) was dissolved in 100ml deionised water and autoclaved at 121<sup>0</sup>C for 15 minutes. PBS was made fresh as required and stored at room temperature.



## 2.4 Preparation of Atorvastatin

Atorvastatin (20 mg Film-Coated Rowex Ltd) tablets were ground to a powder using a pestel and mortar and dissolved in sterile PBS with agitation. The solution was filtered sterilised using 0.45 µm and 0.02 µm pore filters (Sarstedt, Nümbrecht, Germany).

## 2.5 Susceptibility of fungal cells to increasing concentrations of atorvastatin

*C. albicans* was grown to stationary phase in YEPD and cells were counted on a haemocytometer and diluted to a cell density of  $1 \times 10^6$  cells/ml. In the case of *A. fumigatus* conidia were harvested in a safety cabinet and a cell suspension was prepared in SAB liquid media. Cells were counted on a haemocytometer and were diluted to a cell density of  $1 \times 10^5$  cells/ml. Using 96 well plates (Costar, New York, USA) and a multi-channel pipette, 200µl of the media was placed into each well of the first row, this was the control media; growth media (100µl) was placed in each well of the other 11 rows. The atorvastatin solution (100µl) was placed in each well of row 12 and then serially diluted (50:50) as far as row 3. Once the drug gradient had been established cells (100µl) were added to each well. *C. albicans* plates were incubated at 30 °C for 24 h and *A. fumigatus* plates were incubated at 37 °C for 48 h. Growth was quantified by reading on an absorbance plate reader (Synergy HT, Bio-Tek) at 600 nm.

## 2.6 Effect of atorvastatin on the viability of *C. albicans*

*C. albicans* cells were incubated in 10 ml PBS supplemented with different concentrations of atorvastatin for different time points at 30 °C. An aliquot was removed, serially diluted, and 100µl of diluted sample was spread onto YEPD agar plates. Resulting colonies were enumerated and expressed as % survival relative to the control.

## **2.7 Analysis of atorvastatin effect on growth of *A. fumigatus* on solid medium**

Malt extract agar was prepared and poured into petri-dish once it was hand hot, different concentrations of atorvastatin (1.5, 3, 6  $\mu$ l) were added to the hand warm agar prior to pouring. *A. fumigatus* ( $5 \times 10^6$ ) was inoculated on the center of the plate, incubated at 37 °C for 48, 72 and 96 h).

## **2.8 Fluorescence microscopy of fungal cells**

Cells were grown in the presence of a different concentration of atorvastatin for 24 and 72 h for *C. albicans* and *A. fumigatus* respectively, harvested, washed in PBS and stained with Calcofluor white (Sigma) for 15 min at 16 °C on a glass slide. Cells were washed twice (PBS) and a cover slide was placed on top. Cells were viewed with an Olympus BX51 fluorescence microscope at magnification x 400.

## **2.9 Determination of Adherence ability of *C albicans***

The adherence of *C. albicans* to buccal epithelial cells (BECs) was analysed as described (Murphy and Kavanagh, 2001). A culture of *C. albicans* was grown in the presence or absence of atorvastatin for 24 h. Cells were counted using a haemocytometer and cells were harvested, washed with PBS and re-suspended in 1ml of PBS. Human buccal epithelial cells (BECs) were collected from healthy volunteers using sterile tongue depressors by gently scraping the inside of the cheek. The BECs ( $5 \times 10^5$ ) were washed in PBS (500 x g, 5 minutes) and resuspended in 1ml PBS. The final solutions of yeast and BECs (1ml each) were mixed together gently to give a ratio of yeast to

BECs of 50:1 and placed in an incubator at 30 °C for 2 h. The mixture was then filtered through a polycarbonate mesh with a pore size of 20µm and washed with 10ml of PBS. The yeast/BEC suspension was smeared onto a clean glass slide and allowed to air dry overnight. The cells were heat fixed by passing the slide through the flame of a Bunsen burner a few times. The slides were flooded with 1% (w/v) crystal violet and washed with distilled water and allowed dry. The number of yeast cells adhering to BECs was counted using a light microscope (HP), and the average number adhering per BEC was calculated.

#### **2.10 Analysis of susceptibility of *C. albicans* to *Trichoderma* lysing enzyme preparation.**

Five ml of 24 h *C. albicans* culture were taken, inoculated in 50ml YEPD ( $1 \times 10^7$ ) and incubated at 30 °C for 3- 4 h. Cells were harvested, washed with sterile PBS and centrifuged. *C. albicans* cells were resuspended in MB buffer (0.5 M KCl, 0.1 M NaCl and 0.1 M acetic acid) at PH 5.5. *Trichoderma* lysing enzyme (SIGMA) was added to the cell suspension. 100 µl of the sample were taken at different time points (0, 20, 40, 60 and 80 min.), diluted with sterile distilled water (1:10000) 100 µl was taken, spread on YEPD plate and incubated at 30 °C for 24 h to count the colonies.

#### **2.11 Ergosterol extraction and quantification**

The method of Arthington-Skaggs *et al.* (1999) was used to extract the sterols with slight modifications. One-gram dry weight of each sample was washed twice with sterile PBS and resuspended in 3 ml of a solution containing 20% (w/v) KOH (Sigma) and 60% (v/v) ethanol. Samples were placed in a heated (85 to 90 °C) shaking water bath for 2 h. N-heptane (2 ml) was added to the solution and vortexed for 10 seconds. The top aqueous layer containing ergosterol

was separated by centrifugation for 5 min at 3000 xg and collected. Different concentrations of ergosterol standard were prepared to produce a standard curve (Fig 2.1). Ergosterol quantification was performed using a Gas Chromatograph (Hewlett Packard 5890 series II) with a flame ionization detector and a chrompack capillary column (Chrompack International BV, Middleburg, The Netherlands). The carrier gas was N<sub>2</sub>, and the injector and detector temperatures were set at 320 °C. Ergosterol standards were used to calibrate the instrument.

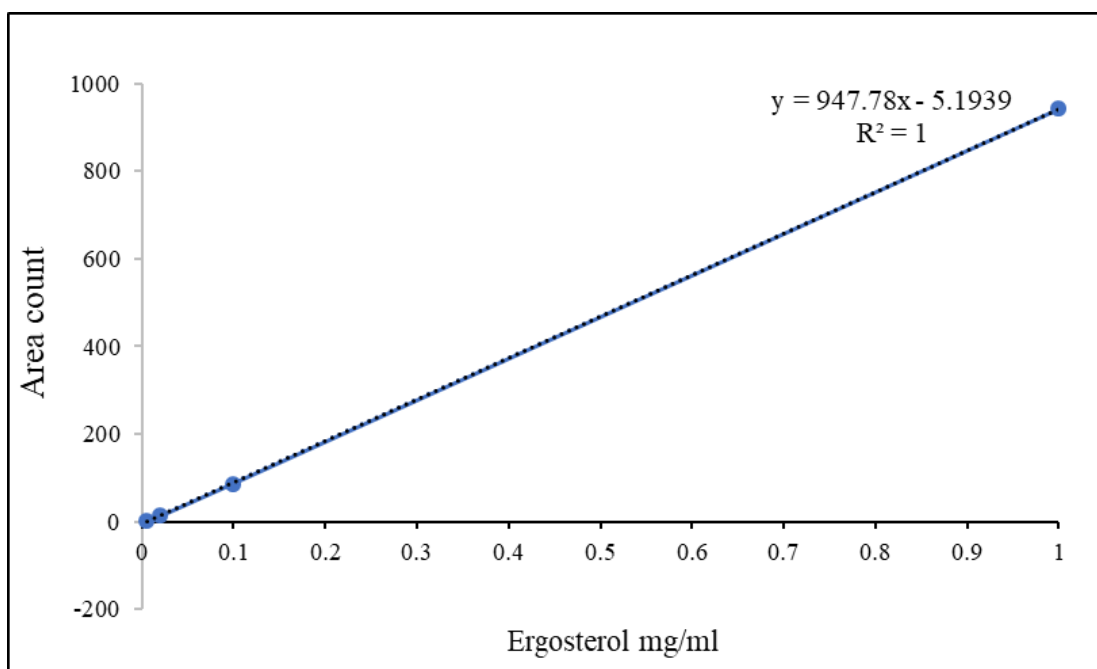


**Figure 2.1:** Standard curve of ergosterol which was generated using samples of known concentrations (mg/ml).

## 2.12 Determination of amino acid leakage

Amino acid leakage from cells exposed to atorvastatin for 0 to 4 h was determined using the ninhydrin colorimetric method and expressed in terms of aspartic acid and glutamic acid. Standard curves were produced using different concentrations of aspartic acid and glutamic acid (Fig. 2.2 and Fig 2.3). Ninhydrin (Sigma-Aldrich) was dissolved in ethanol to give a final concentration of 0.35% (w/v) and 250 $\mu$ l was added to each sample (1 ml) and heated to 95  $^{\circ}$ C for 4 min followed by cooling on ice. The absorbance at 600 nm was recorded on a spectrophotometer (Beckman DU 640 Spectrophotometer).

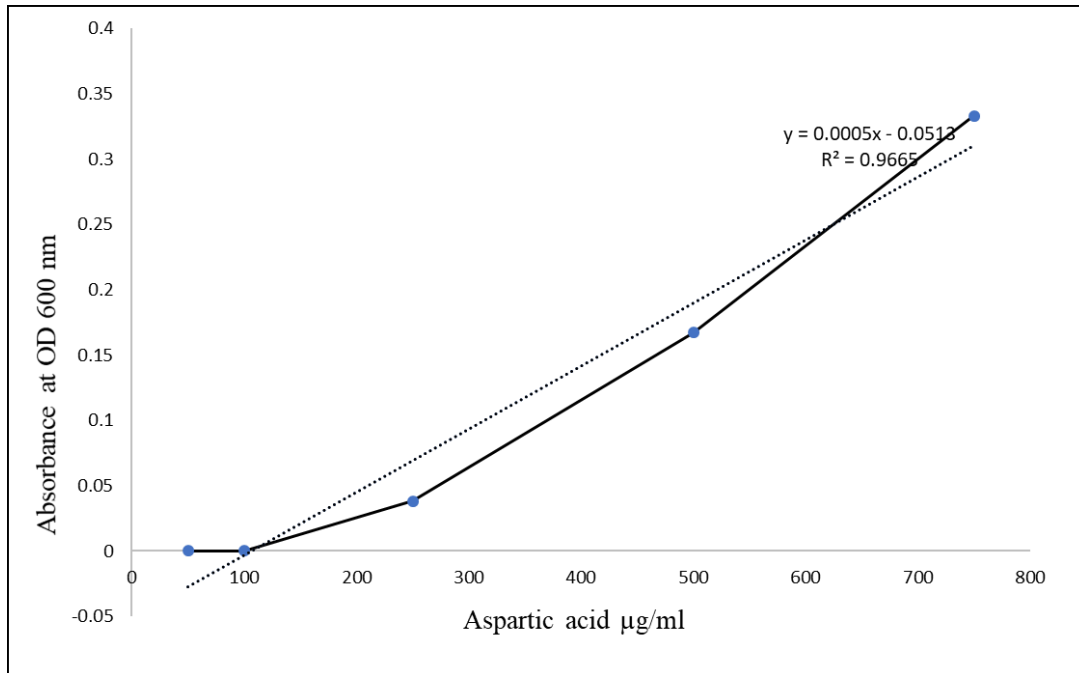


**Figure 2.2:** Standard curve of aspartic acid which was generated using samples of known concentrations.

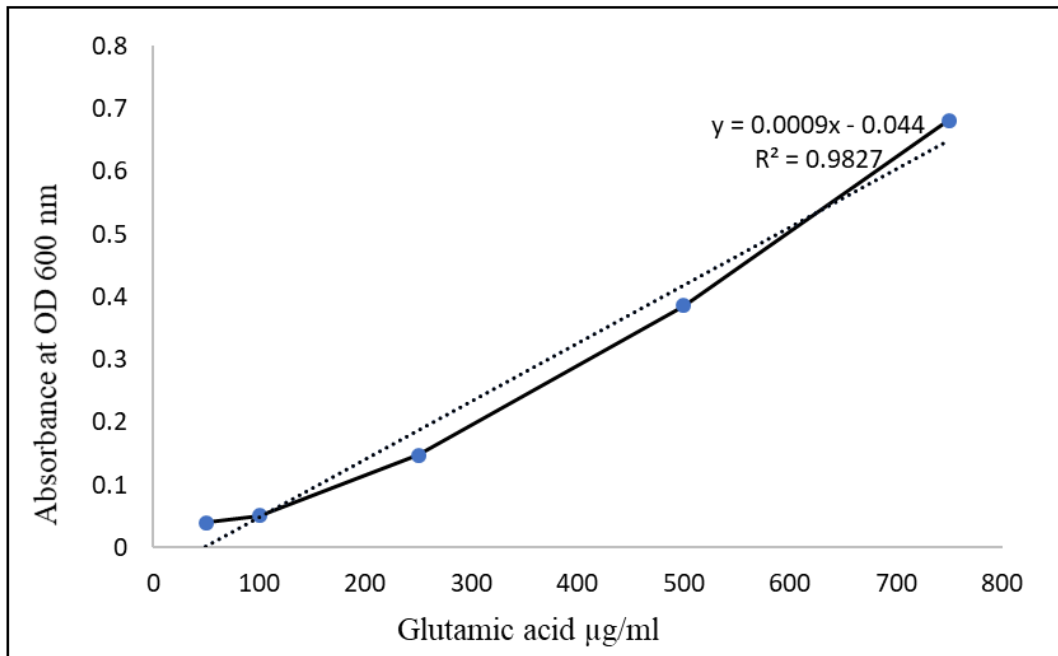


**Figure 2.3:** Standard curve of glutamic acid which was generated using samples of known concentrations.

### 2.13 Bradford assay and protein quantification

*C albicans* protein samples were diluted in sterile PBS. Biorad Bradford protein assay reagent was diluted in ddH<sub>2</sub>O (ratio 1:5). Twenty microliters of sample were placed in a 1 ml cuvette. To this 980µl of diluted Biorad Bradford protein assay reagent was added. The cuvettes were inverted to mix the contents and then allowed to incubate for 5 minutes at room temperature before being read in a microcentrifuge tube Bio-photometer. The quantity of protein was based on the OD600 readings.

#### **2.14 Assessment of Catalase activity of cells**

Catalase activity was measured as described (Rowan *et al.*, 2009) with slight modifications. Protein was extracted from cells as described (section 2.17). Protein extract was added to 1.8 ml of 17 mM H<sub>2</sub>O<sub>2</sub> and left at room temperature for 15 minutes. The suspension was centrifuged at 10,000 x g (Eppendorf centrifuge 5417R) for 1 minute to stop the reaction. The supernatant was removed and placed in a clean quartz cuvette. The absorbance at 240 nm was obtained on a Beckman DU640 spectrophotometer. A blank consisted of 17 mM H<sub>2</sub>O<sub>2</sub>.

#### **2.15 *Galleria mellonella* viability assay**

Liquid cultures of *C. albicans* were grown to exponential phase. The cells were counted using a hemocytometer and 5 x 10<sup>7</sup> cells were harvested. These cells were washed twice using PBS and re-suspended in 1ml of PBS. Culture were diluted to 5 x 10<sup>7</sup>/ml. Thirty *G. mellonella* larvae, with no black spots on their backs (0.02-0.026gm) were selected and placed into three Petri dishes with some wood shavings. Ten larvae were injected with 20µl of the cultures (1 x 10<sup>6</sup>/ml) into the last left pro-leg of the *Galleria*, under sterile working conditions using insulin syringe, 10 were injected with 20µl of the treated culture and the other 10 larvae were injected with 20µl of the PBS (blank). The larvae were incubated overnight at 30 °C. Mortality was assessed by visual inspection and lack of movement when gently probed.

#### **2.16 Determination of fungal load in *G. mellonella* larvae**

Three larvae inoculated with *C. albicans* were homogenized using a pestle and mortar in 3 ml of sterile PBS. This was serially diluted with PBS, and 100 µl aliquots of the resulting dilutions were plated on YEPD plates containing erythromycin (1 mg/ml) to prevent bacterial overgrowth.

These plates were incubated at 30 °C for 48 h. The fungal load was calculated as the yeast cell density per larva and was based on the number of colonies that grew at specific dilutions.

### **2.17 Determination of fungicidal activity of hemocytes**

Larvae were inoculated with 20 µg of atorvastatin and incubated for 0, 20, 40, 60 and 80 minutes (n = 10). Hemocytes were extracted from larvae and incubated at a density of 1x10<sup>6</sup>/ml at 30 °C in PBS in a thermally controlled stirring chamber. Cell free hemolymph opsonized *C. albicans* (2x10<sup>6</sup> cells) were added and killing was measured as described previously (Sheehan and Kavanagh, 2018) by diluting and plating yeast cell suspensions onto YEPD agar plates. Plates were incubated and the resulting number of colonies enumerated. Results were calculated as the mean (± S.D.) from at least three experiments with colony counts performed in triplicate for each sample and expressed as a percentage of the original number at time zero.

### **2.18 Analysis of the effect of atorvastatin on the growth of *A. fumigatus***

SAB culture medium (50 ml) was inoculated initially with 1x10<sup>5</sup> *A. fumigatus* conidia/ml. Four different concentrations of atorvastatin plus control were used in this experiment. Cultures were incubated at 37 °C on a rotary incubator, samples were taken every 72 h, filtered using miracloth, and wet hyphae mass was measured (wet weight).

### **2.19 RP-HPLC Gliotoxin**

Reversed phase HPLC is the most commonly used form of HPLC. Different compounds have different retention times. For a particular compound, the retention time will vary depending on the



pressure used, the nature of the stationary phase, the exact composition of the solvent and the temperature of the column. In this work RP-HPLC was employed to quantify gliotoxin concentrations in *A. fumigatus* culture supernatants.

### **2.19.1 Buffer used in (RP-HPLC)**

#### **Buffer A.**

(1 L) HPLC grade water was placed in a darkened Duran bottle. 0.1% (v/v) Trifluoroacetic acid was added and mixed thoroughly. This was made fresh on the day.

#### **Buffer B.**

HPLC grade acetonitrile (1 L) was placed in a clear Duran bottle. Trifluoroacetic acid 0.1% (v/v) was added to the bottle and contents of the bottle were mixed thoroughly. This was made fresh on the day.

### **2.19.2 *A. fumigatus* gliotoxin extraction and quantification**

Seventy-two h *A. fumigatus* cultures were harvested by filtration using mira-cloth. Chloroform (20 ml) was added to the same volume of supernatant for each filtrate sample and the solution was mixed continually for 2 h. The chloroform was collected and evaporated to dryness in a rotary evaporator. Dried extracts were dissolved in 500 µl methanol (Fisher chemical) and stored at -20 °C until assayed. Gliotoxin was determined by reversed phase-HPLC (Agilent 1200 Series). The mobile phase was acetonitrile (Fisher Chemical), 0.1% (v/v) trifluoroacetic acid (Sigma-Aldrich) and deionized-distilled water. Gliotoxin extract (20 µl) was injected onto a C18 Hewlett Packard column. Gliotoxin concentrations (50, 100 and 200 ng/ml) were dissolved in methanol (Sigma-Aldrich) to create a standard curve of peak area versus gliotoxin concentration was constructed (Fig 2.4).

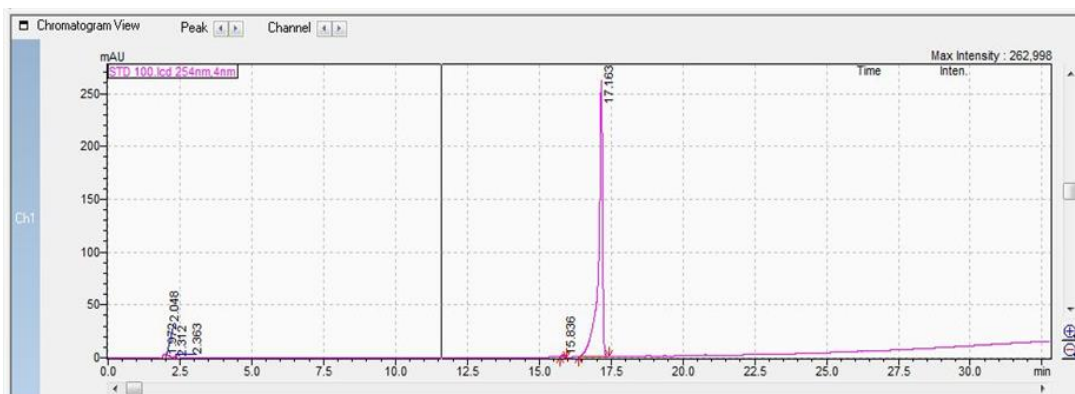


**Figure 2.4:** Detection of gliotoxin by RP-HPLC. Gliotoxin detection was performed at 254 nm with a retention time of approximately 17.1 minutes. Image shows gliotoxin detection of 1 $\mu$ g/10 $\mu$ l.

### 2.19.3 Preparation of extracts for detection of gliotoxin by reversed phase HPLC

A standard curve of peak value versus gliotoxin concentration (Fig 2.5) was constructed using different concentrations of gliotoxin standards ( $\mu$ g/10 $\mu$ l).

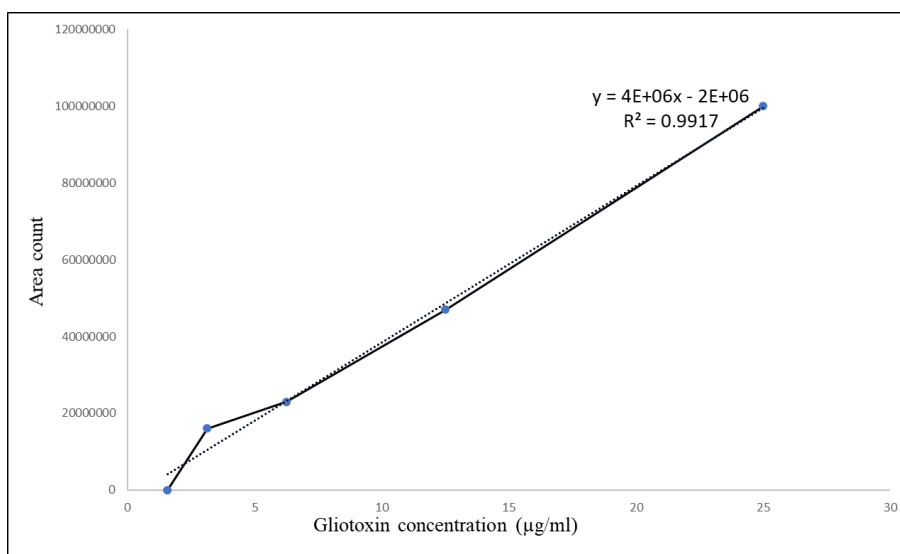


**Figure 2.5:** Standard curve of gliotoxin reference.

## 2.20 Quantification of atorvastatin administered to *G. mellonella* larvae by HPLC

Atorvastatin was determined by reversed phase-HPLC (Agilent 1200 Series). The mobile phase was acetonitrile (Fisher Chemical), 0.1% (v/v) trifluoroacetic acid (Sigma-Aldrich) and deionized-distilled water. Atorvastatin extract (20  $\mu$ l) was injected onto a C18 Hewlett Packard column. Atorvastatin concentrations (1, 10 and 100 ng/ml) were dissolved in methanol (Sigma-Aldrich) to create a standard curve of peak area versus atorvastatin concentration was constructed (Fig 2.6). A standard curve of peak value versus atorvastatin concentration (Fig 2.7) was constructed using different concentrations of atorvastatin standards (mg/10ml).

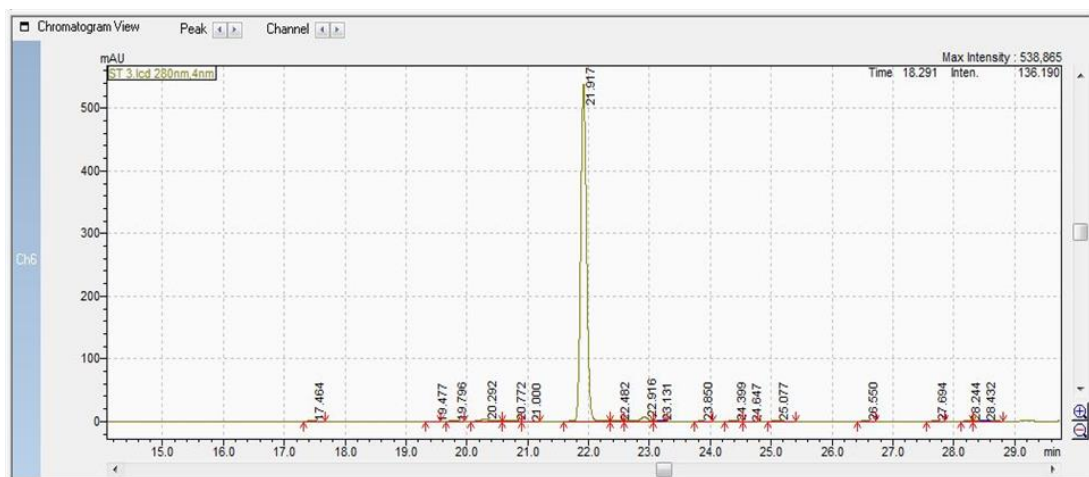


**Figure 2.6:** Detection of atorvastatin by RP-HPLC. Atorvastatin detection was performed at 254 nm with a retention time of approximately 21.9 minutes. Image shows atorvastatin detection of 1mg/10ml.

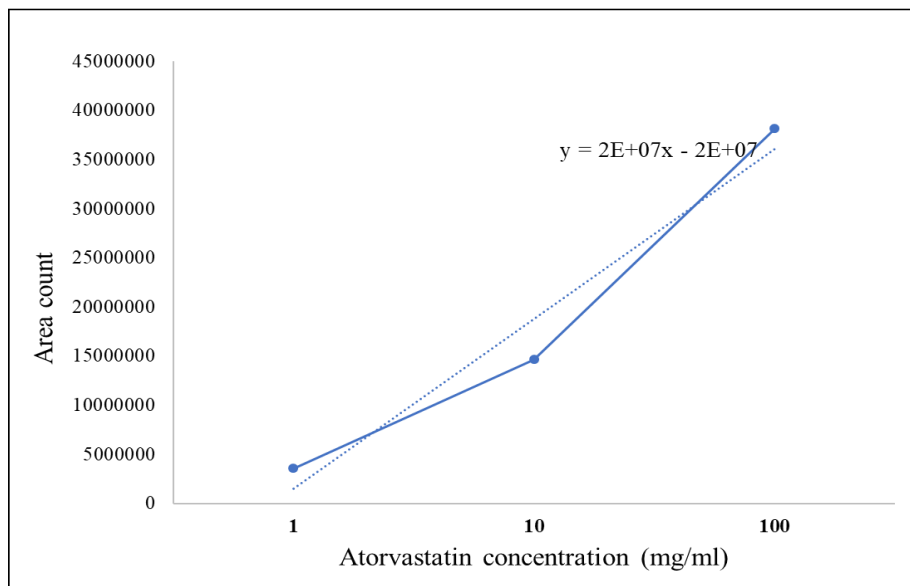


**Figure 2.7:** A standard curve of peak value versus atorvastatin concentration was constructed using different concentrations of atorvastatin standards (mg/ml).

## 2.21 Whole cell protein extraction from the fungal cells

### 2.21.1 Whole cell protein extraction from *C albicans*

A culture of *C. albicans* was grown to stationary phase in YEPD broth for 24 h at 30 °C in an orbital incubator. A cell suspension was centrifuged at 8000 x g for 10 min, washed twice with PBS. Four ml of lysis buffer (6M urea, 2M thiourea, 0.1M Tris-HCL) and supplemented with protease inhibitors (aprotinin, pepstatin,A, TLCK, leupeptin) 1 µl/1ml of buffer was added to one gm of cell pellet and mix until a viscous liquid consistency was obtained. The viscous liquid was sonicated at 50% power, cycle 3 for 15 second. This was repeated three times with the sample

being cooled on ice between each sonication. Protein supernatant were obtained by centrifugation (10,000 x g 4 °C for 15 min) and pellet was discarded.

### **2.21.2 Whole cell protein extraction from *A. fumigatus***

A culture of *A. fumigatus* was grown in SAB liquid culture media for 72 h at 37 °C in an orbital incubator. A 100 ml volume of the culture medium was filtered through 2 layers of Mira-cloth and squeezed to dry. Hyphae were left 5 minutes to dry on filter paper. A certain weight of mycelia mass was added to 50 ml falcon tube and Snap frozen in liquid nitrogen to break-up by agitation. Mycelium (1 gram) was ground to a fine powder using mortar and pestle with liquid nitrogen followed by the addition of four ml of protein extraction buffer [0.4 M NaCl, 10mM Tris HCl, 2 mM EDTA] supplemented with aprotinin, pepstatin, TLCK, leupeptin (1µl/1ml) and ground until a viscous liquid consistency was attained. The suspension was sonicated using sonication probe (Bandelin sonopulse, Bandelin electronic, Berlin) at 50% power, cycle 3 for 15 second. This was repeated three times with the sample being cooled on ice between each sonication. Protein supernatant were obtained by centrifugation (10,000 x g 4 °C fore 15 min) and pellet was discarded.

### **2.22 Solutions and buffers used for 1D and 2D SDS-PAGE**

#### **Coomassie Blue Stain Solution:**

Brilliant Blue R    2 g  
Methanol            450 ml  
Acetic acid         100 ml

Made to 1 L with distilled water

#### **Coomassie De-stain Solution:**

Acetic acid 100 ml

Methanol 200 ml

And 700 ml of distilled were added

### **IEF Equilibration (Reducing) Buffer**

30% (v/v) Glycerol (150 ml)

2% (w/v) SDS (10 g)

6M Urea (180.1 g)

50mM Tris HCl (3.94 g)

Up to 500 ml distilled water, pH adjusted at 6.8, Aliquoted into 20ml (in 50 ml falcon tubes) and stored at -20 °C. When using, add 2% DTT (0.4 g), for reducing (2.5% IAA (0.5 g) + few grains of Bromophenol Blue) for alkylation.

### **IEF Buffer**

8 M Urea (48 g)

1% (v/v) Triton X100 (1 ml)

4% (w/v) Chaps (4 g)

10 mM Tris HCl (0.158 g)

2 M Thiourea (15.22 g)

Made up to 100 mls of sterile distilled water Aliquot into 2 ml samples and stored at -20 °C When using, add 65 mM DTT (0.2 g) and 0.8% (v/v) Ampholytes (2 µl)

### **Running Buffer 10X = Electrode Buffer**

Trizma base 30 g

Glycine 144 g

SDS (sodium lauryl sulphate) 10 g

Made to 1 L with distilled water, pH should be 8.9, stored at room temp and 1:10 Dilution in distilled water = 1X

**1% Agarose (for sealing strips):**

1 g Agarose 100 ml

10X Running Buffer

Few grains of Bromophenol Blue

Heat until boiling and sets when cool.

**200 mM EDTA Solution:**

EDTA (14.89 g)

Made to 200ml with Distilled water, pH at 7.2

**5X Sample Buffer for 1-D SDS-PAGE.**

SDS 2.0 g

DTT 1.54 g

2 ml of [0.2 % (w/v) Bromophenol blue (0.1 g) + 50% (w/v) Sucrose (25 g) made to 50 ml H<sub>2</sub>O]

3 M Tris HCl (pH 6.7)

2.1 ml 200 mM EDTA (pH 7)

0.5 ml Add deionized water- make up to 20 ml

Aliquoted to 500 microliters. Stored at -20 °C

**Tris-HCl 1.5 M**

Tris – HCl (1.5 M) was prepared by dissolving 11.8 g Trizma Base (Tris Base) in 50 ml deionised water and adjusted to pH 8.9. Following pH adjustment 1.5 M Tris – HCl was filter sterilised through a 0.22 µM cellulose filter (Millipore) and stored at 4°C.

**Tris – HCl 0.5 M**

0.5 M Tris-HCl was prepared by dissolving 3.94 g Trizma Base in 50 mls deionised water and adjusted to pH 6.8. Following pH adjustment 0.5 M Tris– HCl was filter sterilised through a 0.22  $\mu$ M filter (Millipore) and stored at 4°C.

#### **Ammonium Persulphate (APS) 10%**

APS (10% w/v) was prepared by adding 0.05 g APS into 0.5 ml of deionized water and vortexing to dissolve completely. APS (10% w/v) was prepared fresh every day and kept on ice when not in use.

#### **Sodium Dodecyl Sulphate (SDS) 10% w/v**

Sodium Dodecyl Sulphate (SDS), (10% w/v) was prepared by adding 10 g SDS to 100 mls of deionized water and left to stir until all SDS had been solubilized. The solution was stored at room temperature after filtration through a 0.22  $\mu$ M filter.

### **2.23 Preparation of SDS–PAGE mini-gels**

All glass plates were washed in warm soapy water and cleaned thoroughly with 70% ethanol prior to use in SDS–PAGE mini-gels, (Mini-Protean II gel casting apparatus). A 12.5% acrylamide gel was normally used in experimental procedure. The separating gel separates the proteins from each other depending on size therefore aiding visualization. All gels were used within 24 h of setting and were allowed to polymerize for at least one h prior to being loaded. Solution component of separating gel 12.50%, 1.5 M Tris-HCl 3 ml, deionized water 3.8 ml, 30% Acrylamide 5 ml 10% v/v SDS 120  $\mu$ l, 10% v/v APS 75  $\mu$ l, TEMED 3  $\mu$ l. These volumes were sufficient to make 3 mini-gels.



### **2.23.1 Loading and voltages of 1-D SDS-PAGE**

Protein was extracted from a sample (grown with and without atorvastatin) using method described in section 2.17.1. Bradford method was used to calculate the concentration of protein see (2.11) and equal concentrations were loaded into the wells of separating gel and run at 50 Volts for 10 minutes followed by 80 Volts for 120 minutes on (Bio-Rad, CA, USA). Gels were stained with Coomassie Blue solution for 5 h and destained with Coomassie destaining solution for 8 h.

### **2.23.2 Preparation and analysis of 2-D SDS-PAGE**

Protein was extracted from a sample as mentioned before. Using the Bradford method, a solution of 100 µg/ml protein was prepared and then precipitated by adding three times the volume of ice-cold acetone and incubated overnight at -20 °C. The precipitated protein was collected by centrifugation (12,400 x g) for 30 minutes at 4 °C (Eppendorf centrifuge 5417R). The acetone was removed, and the pellet was allowed to air dry. The dried precipitated protein was resuspended in 250 µl IEF buffer (see 2.18.4) with 0.8% (v/v) IPG buffer, pH 3-10 (G.E. Healthcare BioSciences AB, Uppsala, Sweden;) and few grains of bromophenol blue. The solution was applied to a 13 cm Immobiline™ DryStrip pH 3-10 (G.E. Healthcare) and iso-electric focusing was performed on an Ettan IPGphor II (Amersham Biosciences, NJ, USA) system using the following program.

1. Step and Hold 50 Volts 12 h
2. Step and Hold 250 Volts 15 minutes
3. Gradient 8000 Volts 5 h
4. Step and Hold 8000 Volts 8 h.

Following IEF IPG strips were frozen at -80°C or were transferred to equilibration. Strips were initially equilibrated in 5 ml reducing equilibration buffer for 15 minutes. Strips were transferred to the 5 ml alkylation buffer for 15 minutes. Following equilibration, strips were rinsed in 1X electrode running buffer. Strips were placed on top of SDS-

PAGE gels and sealed with 1% w/v agarose sealing solution. The top of the gel was sealed with molten cooled sealing solution and allowed to set. The second dimension of protein separation was achieved by placing the gels in ProteanXi-II vertical electrophoresis cells as per manufacturer's instructions. The inner chamber was filled to the top with 5X electrode running buffer while the outer chamber was filled with 2X running buffer. Gels were initially electrophoresed for 1 h at 50 volts and at 80 volts for the remaining time. Gels were monitored regularly to assess the level of electrophoresis and were transferred to a staining dish of Coomassie Blue solution and destained with destaining solution, until the blue background was removed.

#### **2.24 In gel trypsin digestion and bioinformatics analysis of LC/MS results.**

The method of Shevchenko *et al.*, (2006) was used in processing of bands and spots for LC-MS analysis with slight modifications. LC/MS grade acetonitrile 100 % (v/v) was used to wash tubes and pipette tips. Following this 30-minute incubation period 500 $\mu$ l of acetonitrile was added for 10 minutes shaking at room temperature. Samples were centrifuged at 20,000 x g for 10 minutes and the supernatant was removed. Gel pieces were placed in 40  $\mu$ l of 1:1 ammonium bicarbonate (100 mM): acetonitrile (100 % (v/v) and incubated with occasional vortexing for one h. The supernatant was removed and 40  $\mu$ l of 100% (v/v) acetonitrile was placed over gel pieces and incubated until gel became white and shriveled. Acetonitrile was removed and gel pieces were covered with 500  $\mu$ l 50mM ammonium bicarbonate for 5 minutes. An equal volume of 100% (v/v) acetonitrile was added and the pieces were incubated for a further 15 minutes. Supernatant was removed and pieces were again covered with acetonitrile until gel became white and shrunk. Trypsin (20  $\mu$ g-Promega) was reconstituted in 100  $\mu$ l of reconstitution buffer (10 mM ammonium bicarbonate containing 10% acetonitrile). This was aliquoted into 10 x10  $\mu$ L aliquots and to each

of these 500  $\mu$ l of 50 mM Ammonium Bicarbonate was added. The trypsin solution (50  $\mu$ l) was added to each gel piece. This was incubated at 4°C for 1 h and at 37°C overnight. For peptide recovery samples were centrifuged at 20,000xg for 10 minutes and supernatant was transferred to a fresh 1.5ml tube. Extraction buffer (1:2 5% formic acid (v/v): acetonitrile) was added to the gel pieces (50  $\mu$ l) and incubated at 37°C for further 15 minutes. Samples were centrifuged at 20,000 xg for 10 minutes and added to the supernatant. Extracts were dried in a vacuum centrifuge overnight. Dried peptides were resuspended in 20  $\mu$ l of 0.1% formic acid and sonicated for 2 minutes. Samples were filter sterilized and supernatants were added to mass spectroscopy vials (Agilent Technologies, USA). Samples were analysed on a 6340 Ion Trap LC/MS spectrometer (Agilent Technologies) using BSA as external reference standards. Resulting data were analysed using the mascot search engine, ([www.matrixscience.com](http://www.matrixscience.com)). The mass error tolerance was 1 Da allowing for a maximum of no more than 2 missed cleavages. Verification of protein sequences was confirmed by blasting the protein sequence on the Uniprot, ([www.uniprot.org](http://www.uniprot.org)), and NCBI, ([www.ncbi.nlm.nih.gov](http://www.ncbi.nlm.nih.gov)), databases. Identified proteins are listed by their GI number as accessed through [www.ncbi.nlm.nih.gov](http://www.ncbi.nlm.nih.gov).

## **2.25 Protein methodology for shotgun label free proteomics**

### **2.25.1 Acetone precipitation of protein samples**

Acetone precipitation was used to concentrate protein from a dilute sample and also to purify protein samples. The required volume of protein was calculated following Biorad Bradford assay quantification (section 2.11). The correct protein volume was aliquoted into a fresh pre-chilled microcentrifuge tube and 100% ice cold acetone was added to the tube at a volumetric ratio of 1:3

(sample: acetone). Protein was left at -20°C overnight and then precipitated at 13,000 x g for 10 minutes to pellet protein. All protein pellets were placed upside down to air dry for 5 mins following removal of acetone.

### **2.25.2 In solution digest protocol for overnight peptide digestion for label free proteomics.**

The list of buffers used for the in-solution digestion of proteins in preparation for label free proteomics are presented below. Buffers were made fresh daily. Protease Max (Promega) was used in order for the trypsin (Promega) to digest the protein when using urea and thiourea. All water was deionised and was taken fresh before use from the deionised water dispenser.

- **Sample Resuspension Buffer (pH to 8.0)**

7.2g Urea, 2M Thiourea, 0.1M Tris-HCL in 20mls diH<sub>2</sub>O

- **200mM Ammonium Bicarbonate (AmBic) solution**

0.394g Ammonium bicarbonate in 25ml water

- **50mM AmBic**

2.5ml 200mM AmBic in 7.5ml water

- **0.5M Dithiothreitol (DTT)**

0.077g DTT in 1ml 50mM AmBic

- **0.55M Iodoacetamide (IAA) (Protect from light)**

0.102g IAA in 1ml 50mM AmBic

- **ProteaseMax solution (1mg/100µl)**

1mg ProteaseMax TM Surfactant Trypsin Enhancer (Promega) in 100µl 50mM AmBic

- **Trypsin solution (0.5µg/µl)**

20µg Sequence grade modified trypsin (Promega) in 40µl trypsin reconstitution buffer (Promega).

Following overnight acetone precipitation, the protein samples were centrifuged at 13000 x g for 10 minutes and allowed to air dry. Pellets were resuspended in 25µl of sample resuspension buffer. To aid in pellet resuspension samples were placed in a sonication bath for 5 minutes and vortexed for approximately 30 seconds. Protein enumeration was carried out using a Qubit fluorometer, and the Qubit protein assay kit (Thermo scientific). Protein concentrations for each sample determined by the qubit protein assay were later used to quantify the samples to (1µg µl<sup>-1</sup>) just before they were loaded onto the Q-exactive. One hundred and five microliters of 50mM ammonium bicarbonate was added to the samples. Following the addition of 1µl of 0.5M DTT samples were incubated at 56 °C for 20 minutes. Samples were allowed cool to room temperature. The samples were alkylated by the addition of 2.7µl 0.55M IAA and incubated at room temperature in the dark for 15 minutes. One microliter of ProteaseMax solution and trypsin solution were added to the samples. The samples were wrapped in tinfoil, incubated for 24 h at 37 °C in an orbital shaker.

### **2.25.3 Sample clean-up prior to loading on Q-Exactive MS.**

The list of buffers used for the sample clean-up for use on Q-exactive using C18 spin columns (Thermo Scientific) are listed below. Buffers were made fresh directly before use. All water was deionised and was taken fresh before use from the deionised dispenser. The C18 columns are designed to trap only 30µg of protein and so is the final step of re-quantification before loading on the Q-exactive OrbiTrap. Care was taken to ensure the resin did not reach any flow through.

- **Sample buffer (2% TFA, 20% Acetonitrile)**

200µL Acetonitrile, 20µl TFA in 780µl diH<sub>2</sub>O

- **Equilibration Buffer (0.5% TFA, 5% Acetonitrile)**

25µl TFA, 250µl Acetonitrile in 4.3ml diH<sub>2</sub>O

- **Wash buffer (Same as equilibration buffer)**

- **Elution buffer (70% Acetonitrile, 30% water)**

700µL Acetonitrile in 300µl diH<sub>2</sub>O

- **Activation buffer (50% Acetonitrile, 50% water)**

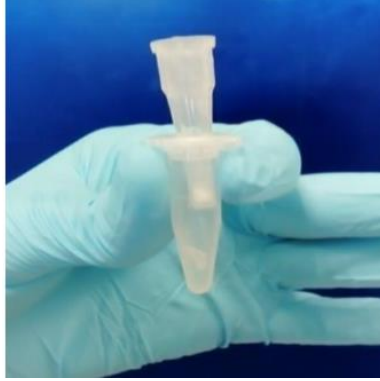
5ml Acetonitrile in 5ml diH<sub>2</sub>O

- **Loading buffer (0.05% TFA, 2% Acetonitrile)**

Taken straight from the Q-exactive buffer reservoirs.

Digested protein samples were briefly centrifuged in a microfuge to collect any condensate, straight from the 37 °C incubator following overnight peptide digestion. TFA to a concentration of 0.75% of the total volume of sample was added (approximately 0.75µl), vortexed briefly, and incubated at room temperature for 5 minutes. Samples were centrifuged at 13000 x g for 10 minutes to remove any debris that may have formed overnight, and the supernatant transferred to a fresh tube. Samples were mixed at a ratio of 3 parts sample:1part sample buffer. Pierce™ C-18

spin columns (Thermo scientific) were tapped briefly to settle the resin, and the protective caps were removed from either end. Holes were pierced in the lid of sterile microcentrifuge tubes to place C-18 spin columns into (Fig. 2.8). Resin was activated using 200 $\mu$ l of activation buffer, added to the top of the resin, and centrifuged at 1500 x *g* for 1 minute. Flow through was discarded and the process repeated. Equilibration buffer (200 $\mu$ L) was added to the column, spun for one-minute 1500 x *g* and the flow through discarded, and repeated once more. Samples were loaded to the top of the resin in the C18 column, and a fresh receiver tube placed underneath. Tubes were spun at 1500 x *g* for 1 minute, flow-through collected, and placed back onto the resin. This was repeated three times to ensure complete peptide binding to the C18 resin. C18 columns were placed in a fresh receiver microcentrifuge tube, and 200 $\mu$ l of wash buffer added. This was then spun at 1500 x *g* for one minute, flow through discarded, and the process repeated a total of three times to remove containments such as urea and ammonium bicarbonate. Column was placed over a fresh receiver tube, this time with the lid open and no hole pierced through the lid, and 20 $\mu$ l of elution buffer added to the top of the resin bed. The tubes were spun at 1500 x *g* for 1 minute, and the flow-through untouched. This was repeated a total of three times to obtain a final volume of 60 $\mu$ l in the receiver microcentrifuge tube. This was now the cleaned peptide sample. Samples were dried down in a SpeedyVac and stored at 20 $\mu$ l until running on the Q-exactive.



---

**Figure 2.8:** Image shows the C-18 spin placed in a 1.5 ml microcentrifuge tubes.

#### **2.25.4 Preparation of sample prior to loading on Q-Exactive mass spectrometer**

The protein concentration of each sample (from Qubit protein assay) was used to determine the concentration of sample loading buffer needed to achieve peptide resuspension at a concentration of (1  $\mu\text{g}/\mu\text{l}$ ). The samples were vortexed for 30 seconds and placed in a water bath for sonication for 5 minutes. Following resuspension of the peptide pellet, samples were spun at 13000 x g for 5 minutes at room temperature to pellet any insoluble material, and 30 $\mu\text{l}$  of the supernatant transferred to vials (VWR).

#### **2.25.5 Parameters for running samples on Q-Exactive mass spectrometer**

One microliter of peptide suspension was eluted onto the Q-Exactive, a high-resolution accurate mass spectrometer connected to a Dionex Ultimate 3000 (RSLCnano) chromatography system. Peptides were separated by an increasing acetonitrile gradient on a Biobasic C18 Picofrit<sup>TM</sup> column (100 mm length, 75 mm ID), using a 180 minutes reverse phase gradient at a flow rate of



250 ml /min. All data were acquired with the mass spectrometer operating in automatic data dependent switching mode. A high-resolution MS scan (300-2000 Dalton) was performed using the Orbitrap to select the 15 most intense ions prior to MS/MS.

#### **2.25.6 Parameters for analysing quantitative results and statistical analysis**

Protein identification from the MS/MS data was performed using the Andromeda search engine in MaxQuant (version 1.2.2.5; <http://maxquant.org/>) to correlate the data against a database for *G. mellonella* (Galleria\_6\_frame\_database), depending on the experiment. A combined database for the two organisms (*Drosophila melanogaster* and *Bombyx mori*) was also used. The following search parameters were used: first search peptide tolerance of 20 ppm, second search peptide tolerance 4.5ppm with cysteine carbamidomethylation as a fixed modification and N-acetylation of protein and oxidation of methionine as variable modifications and a maximum of 2 missed cleavage sites allowed. False Discovery Rates (FDR) were set to 1% for both peptides and proteins and the FDR was estimated following searches against a target-decoy database. Peptides with minimum length of seven amino acid length were considered for identification and proteins were only considered identified when more than one unique peptide for each protein was observed. Results processing, statistical analyses and graphics generation were conducted using Perseus v. 1.5.0.31. Label free quantification (LFQ) intensities were log<sub>2</sub> -transformed and ANOVA of significance and t-tests between the proteomes of control and treated larvae was performed using a p value of 0.05 and significance was determined using FDR correction (BenjaminiHochberg). Proteins that had non-existent values (indicative of absence or very low abundance in a sample) were included in the study only when they were completely absent from one group and present in at least three of the four replicates in the second group (referred to as qualitatively differentially

abundant proteins). The Blast2GO suite of software tools was utilized to assign gene ontology terms (GO terms) relating to biological processes (BP), molecular function (MF) and cellular component (CC). Enzyme commission (EC) numbers and Kyoto Encyclopedia of Genes and Genomes (KEGG) pathway mapping was performed as part of the Blast2GO annotation pipeline.

## **2.26 *G. mellonella* larval storage and experimental conditions**

### **2.26.1 *G. mellonella* storage and food**

Sixth instar larvae of the greater wax moth *G. mellonella* (Lepidoptera: Pyralidae, the Greater Wax Moth) (Mealworm Company, Sheffield, England) were purchased and stored in wood shavings (Fig 2.9) in the dark at 15°C to prevent pupation (Cotter *et al.*, 2000); (Hornsey and Wareham, 2011). Larvae weighed  $0.22 \pm 0.03$ g and were excluded if there was evidence of localised melanisation or infection.



---

**Figure 2.9:** Larvae were stored in 9 cm petri-dishes with 0.45 mm Whatmann filter paper inserted on the lids and some wood shavings.

### 2.26.2 Inoculation of *G. mellonella* larvae

Larvae were injected through the last left pro-leg, with a Myjector U-100 insulin syringe, (Terumo Europe N.V., 3001 Leuven, Belgium), while applying mild pressure to the insect to allow the opening of pro-legs (Fig 2.10A). In order to administer compounds by the feeding route, a blunted Myjector syringe was gently inserted into the mouth of larvae to force-feed 20 $\mu$ l of each solution (Mukherjee *et al.* 2013) (Fig. 2.10B).

The larvae were kept in 9cm petri-dishes with 0.45 mm Whatmann filter paper inserted on the lids and some wood shavings for all experiments. Great care was taken with each injection to maintain a high accuracy of drug or pathogen delivery. All *in vivo* assays were performed on three separate occasions using a group size of 10 larvae per dish (unless stated otherwise) and average results were calculated. For viability studies larvae were injected with sterile PBS as a control for the injection of larvae.

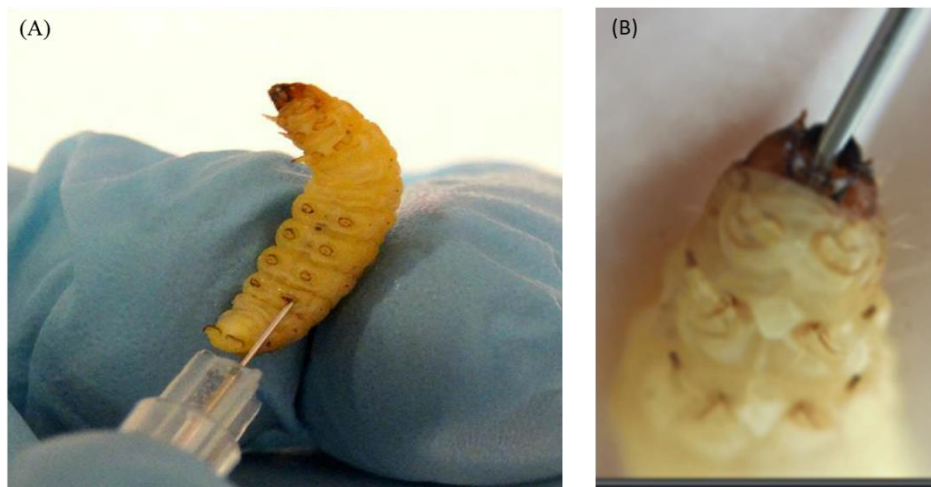


**Figure 2.10:** Administration of a solution to *G. mellonella* via (A) intra-haemocoel injection through the last left pro leg and (B) force feeding.

## 2.27 Extraction of haemocytes from *G. mellonella* larvae

Larvae were pierced through the head with a sterile 23G needle and haemolymph was squeezed through the head region Fig (2.11) into a pre-chilled microcentrifuge tube. Haemocytes were pelleted by centrifugation at 500 x g for 5 minutes and washed in PBS to remove any excess haemolymph. Following a further centrifugation step at 500 x g for 5 minutes, the remaining supernatant was removed, and the pelleted cells were resuspended gently in 1 ml of PBS (supplemented with 0.37% 2-mercaptoethanol).

Hemocyte density was determined by bleeding 5 larvae (two drops hemolymph (40  $\mu$ l) / larva) into a pre-chilled micro-centrifuge tube to prevent melanization. The collected hemolymph was diluted in PBS supplemented with 0.37% (v/v) mercaptoethanol and cell density was assessed with a hemocytometer and expressed as hemocytes per ml of hemolymph. Experiments were performed on three independent occasions and the means  $\pm$  SE. were determined.



---

**Figure 2.11:** Isolated of hemolymph from larvae.

## 2.28 Haemocyte mediated killing using *C. albicans* as a target

*G. mellonella* larvae were administered atorvastatin and incubated at 30 °C for 24 h. Ten larvae were bled into 10 ml of cold PBS. The haemocytes were pelleted by centrifugation at 500 x g. Cell free haemolymph was poured into a separate container and left on ice. The pelleted haemocytes were washed in 10ml of cold sterile PBS, resuspended in 1 ml of PBS and adjusted to  $1 \times 10^5$  cells/ml. *C. albicans* were grown up to the stationary phase in YEPD broth. The cell suspension was transferred to a sterile 50 ml universal and centrifuged at 1500 x g. The pellet of *C. albicans* cells was washed in sterile PBS, resuspended in 40ml of PBS, enumerated and adjusted to  $2 \times 10^5$  cell/ml. The *C. albicans* cells were transferred into the container with the cell free haemolymph to allow for the opsonization of the cells. The solution of cell free haemolymph and *C. albicans* cells were incubated for 30 mins at 30 °C. The opsonized *C. albicans* cells were pelleted by centrifugation at 1500 x g and resuspended in 1 ml of PBS. Haemocytes ( $1 \times 10^5$  cells/ml) were mixed with opsonised *C. albicans* cells ( $2 \times 10^5$  cells/ml) in a ratio of 1:2 in a stirred chamber at 30 °C (Bergin *et al.*, 2005). Aliquots were removed at t = 0, 20, 40, 60 and 80 minutes and serially diluted (1/100) in ice cold minimal essential medium to quench phagocytosis, prior to plating on YEPD agar plates to ascertain fungal viability. The percentage reduction in yeast cell viability was calculated based on viability of control which was defined as 100% as t = 0.

## 2.29 Extraction of *G. mellonella* haemolymph

Haemolymph was extracted from *G. mellonella* larvae by piercing and bleeding through the anterior end with a sterile 23G needle (Section 2.5.1) and haemolymph was squeezed into a pre-chilled microcentrifuge tube containing a few grains of N-phenylthiourea to prevent melanisation.

A 1/10 dilution in cold PBS was carried out using a pipette tip with the tip cut off to enable uptake of the viscous haemolymph. Haemocytes were pelleted by centrifugation at 1500 x g for 5mins and the protein supernatant was transferred to a fresh pre-chilled microcentrifuge tube and stored at -20 °C. For protein enumeration and quantification, a further 1/10 dilution of the protein supernatant was carried out (1/100 of the original). Protein was then quantified using the Bradford assay as mentioned in section 2.11 and adjusted 100µg.

### **2.30 Statistical analysis of data**

All experiments were performed on three independent occasions and results are expressed as the mean ± SE. Statistical significance in growth assay, viability assay, ergosterol quantification and leakage experiments was assessed by t-test. Larval survival was assessed by Kaplan-Meier log rank. All statistical analysis was performed using GraphPad Prism. Differences were considered significant at  $p \leq 0.05$ .

### **2.31 Data Availability**

The MS proteomics data and MaxQuant search output files have been deposited to the ProteomeXchange Consortium (Côté *et al.*, 2012) via the PRIDE partner repository with the dataset identifier *Candida albicans* PXD013365, *Aspergillus fumigatus* PXD015254 and *Galleria mellonella* PXD016067.

## **Chapter 3**

**Assessment of *in vitro* and *in vivo* anti-*Candida* activity  
of atorvastatin.**

### 3.1 Introduction

The yeast *Candida albicans* is a member of the normal human microbiome. In most individuals, *C. albicans* resides as a lifelong, harmless commensal (Mayer *et al.*, 2013). Although, it is an opportunistic pathogen for some immunologically weak and immunocompromised people (Kim and Sudbery, 2011). *C. albicans* induces a wide range of superficial and life-threatening systemic infections in susceptible patients (Mayer *et al.*, 2013). The yeast *C. albicans* has a range of virulence factors that allow successful colonization and dissemination in the host and these involve the adhesion of the yeast to the host tissue, followed by cell proliferation, production of a range of enzymes, biofilm formation and altered phenotype to overcome the host's immune response (Naglik *et al.*, 2003, (Calderone and Fonzi, 2001). Common antifungal therapy depends on the use of polyene, azole or echinocandin drugs but the delivery of appropriate therapy is often problematic due to the presence of resistance and the inherent toxicity of some antifungal therapies (Scorzoni *et al.*, 2017). Statins (e.g. atorvastatin, lovastatin, pravastatin, simvastatin) are one of the most widely prescribed medications and lower cholesterol levels in blood (Nyilasi *et al.*, 2010 (Galgóczy, 2011). They competitively inhibit 3 hydroxy-3-methylglutaryl-CoA (HMG-CoA) reductase by competitively binding to its binding sites (Istvan, 2002). HMG-CoA is an enzyme that catalyses the conversion of HGM-CoA to mevalonate, which leads to the production of farnesyl diphosphate (Macreadie *et al.*, 2006b). Farnesyl diphosphate is the precursor for the production of cholesterol in humans or ergosterol in plants and eukaryotic microorganisms (Macreadie *et al.*, 2006b). Fungal HMG-CoA reductases are also inhibited by statins which results in a reduction in the ergosterol content and an inhibition of fungal growth (Nyilasi *et al.*, 2010b). Statins inhibit the growth of a wide range of medically important fungi (e.g. *Aspergillus fumigatus*, *Candida albicans*), but not *Candida krusei*, (Galgóczy, 2011) and supplementation of statin-



containing growth medium with ergosterol lead to recovery of growth indicating that statins specifically inhibit the mevalonate pathway (Macreadie et al., 2006b). Prolonged exposure of cells of *Candida glabrata* to statins lead to an increase in the percentage of *petite* (respiratory deficient) mutations in the population suggesting that statins may also affect the integrity of mitochondrial DNA (Westermeyer and Macreadie, 2007). Patients on statin therapy display fewer fungal infections (Sun and Singh, 2009) thus suggesting that statins may be capable of inhibiting the growth of fungi *in vivo* and so may represent a novel, non-toxic antifungal treatment option (Donnino et al., 2009; Spanakis et al., 2010). Statins have *in vitro* activities against several human pathogenic fungi, including *Candida spp.*, *Cryptococcus neoformans*, and *Zygomycetes* (Chamilos et al., 2006). In addition, administration of statins to patients with severe sepsis (Dobesh et al., 2009) or bacteremia (Kruger, 2006) resulted in increased survival possibly due to a reduction in inflammatory responses (Weitz-Schmidt, 2002). The aim of the work presented here was to characterise the effect of atorvastatin on *C. albicans* and establish its *in vitro* and *in vivo* antifungal activity using *Galleria mellonella* larvae.

## **3.2 Susceptibility assay**

### **3.2.1 Determination of susceptibility of *C. albicans* to atorvastatin**

A susceptibility assay was applied to test the sensitivity of *C. albicans* against the compound. A serial dilution was constructed on the 96-well plate so that the growth of the yeast in different drug concentrations can be accurately determined. This test was set up in accordance with procedures described in section 2.5 and the concentrations of atorvastatin was 0.75 µg/ml – 195 µg/ml. The percentage growth of *C. albicans* in the presence of atorvastatin was then calculated and is

illustrated in (Fig. 3.1). The results revealed that a dose of 96  $\mu\text{g/ml}$  reduced growth by  $74.6 \pm 0.3$  % at 24 h ( $p < 0.0001$ ). Concentrations of 12 and 24  $\mu\text{g/ml}$  reduced growth by  $11.9 \pm 1.1\%$  and  $21.8 \pm 0.5$  % ( $p < 0.05$ ) respectively at 24 h.

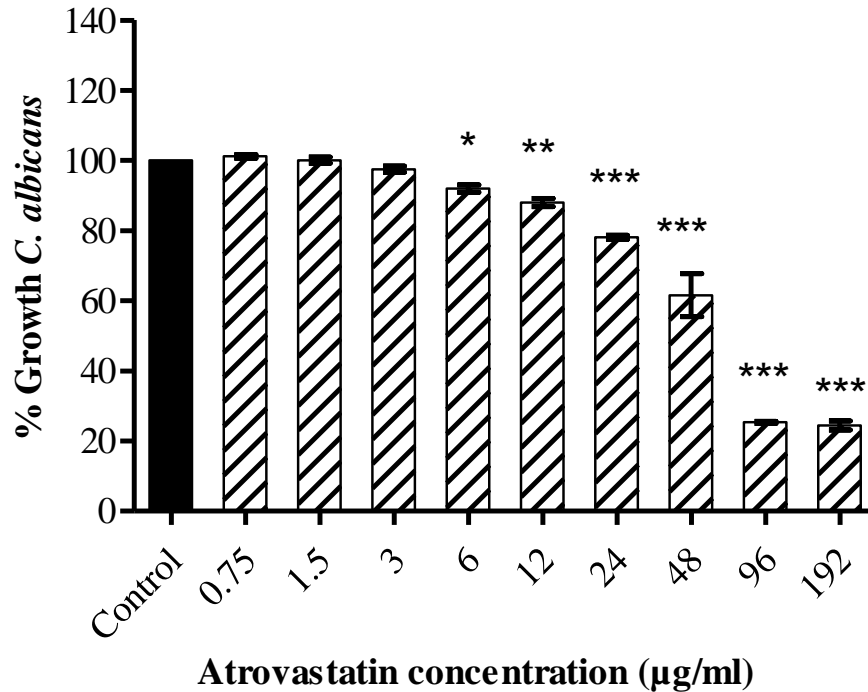


**Figure 3.1:** Effect of atorvastatin on growth of *C. albicans*. *C. albicans* (initial concentration  $10^4$  cells per well) was exposed to atorvastatin (0.75  $\mu\text{g/ml}$  – 192  $\mu\text{g/ml}$ ) in YEPD. Growth (%) was calculated by comparing atorvastatin treated *C. albicans* to control cells after 24 h growth (\*;  $p < 0.05$ , \*\*;  $p < 0.01$  \*\*\*;  $p < 0.001$ ).

### **3.2.2 Susceptibility assay of *C. albicans* to a combination of antifungal drugs and atorvastatin.**

Susceptibility assays were carried out on *C. albicans* to test the sensitivity of the yeast to amphotericin B (highest concentration = 6.25 µg/ml), caspofungin (3.75 µg/ml), miconazole (250 µg/ml) or DMSO (25%) stock solutions (Fig 3.2 A, B, C and D) both singly and in combination with, atorvastatin (12 µg/ml) in accordance with the protocol set out in method (2.5). The results of these tests showed a slight increase in the percentage growth of *C. albicans* when the atorvastatin was combined with amphotericin B, but not miconazole, caspofungin or DMSO.

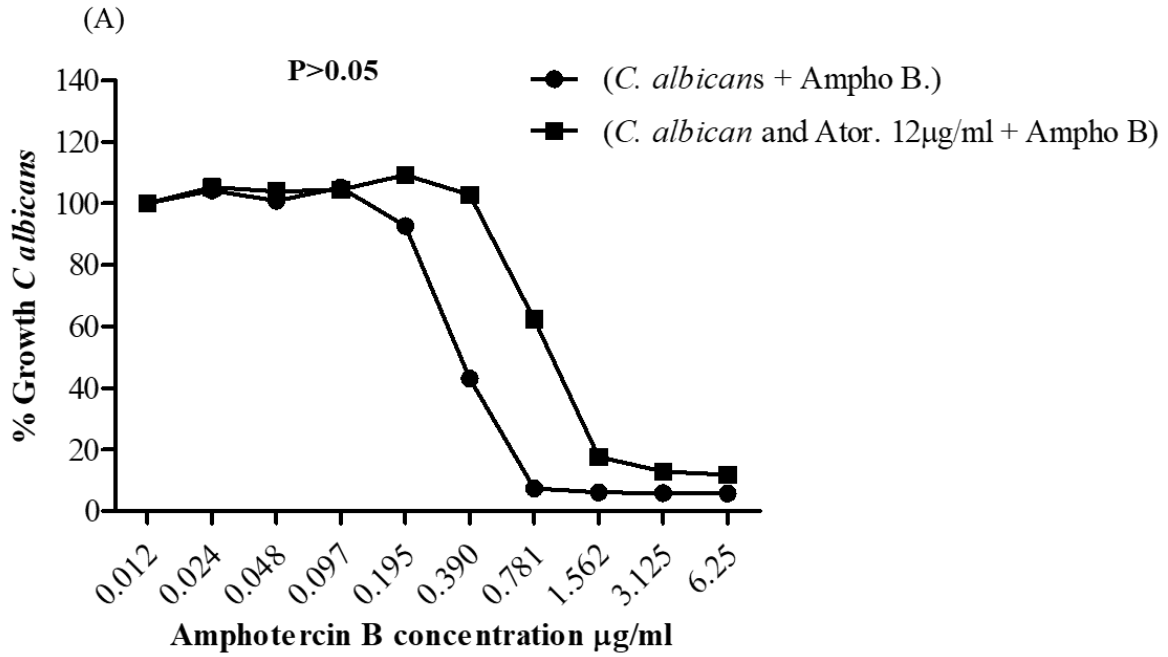


**Figure 3. 2A:** The percentage growth of *C. albicans* exposed to a serial dilution of Amphotericin B and (0.012 - 6.25 µg/ml) in presence atorvastatin (12 µg/ml).

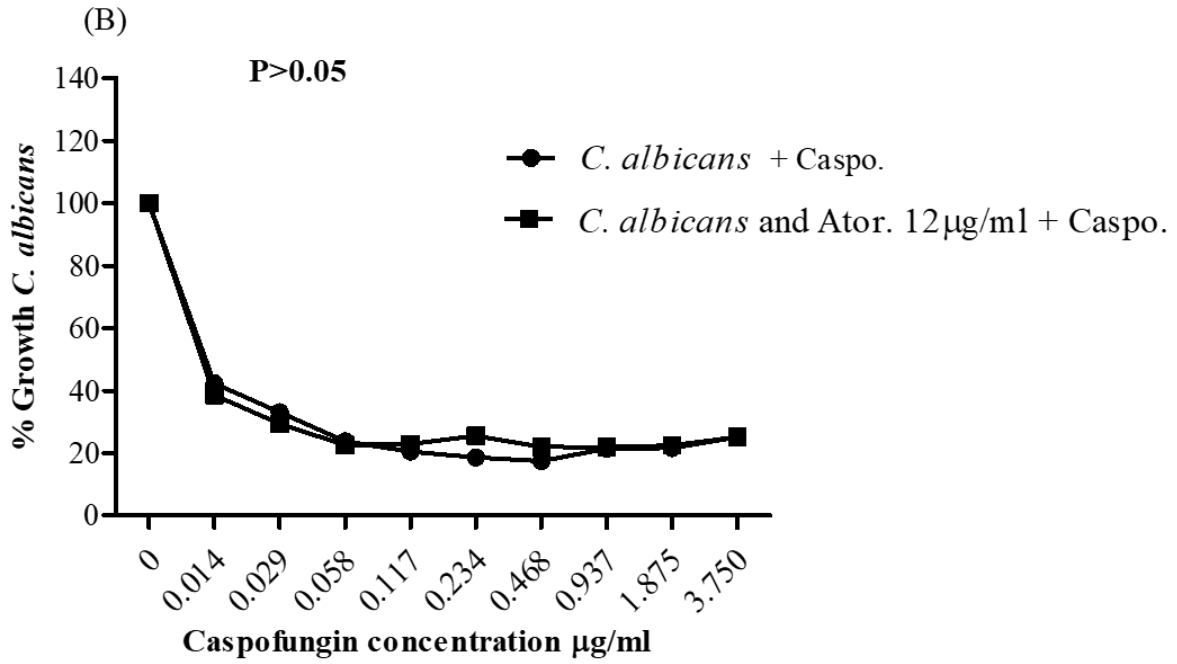


**Figure 3. 2B:** The percentage growth of *C. albicans* exposed to a serial dilution of caspofungin (0.014 – 3.75 µg/ml) and in presence atorvastatin (12 µg/ml)

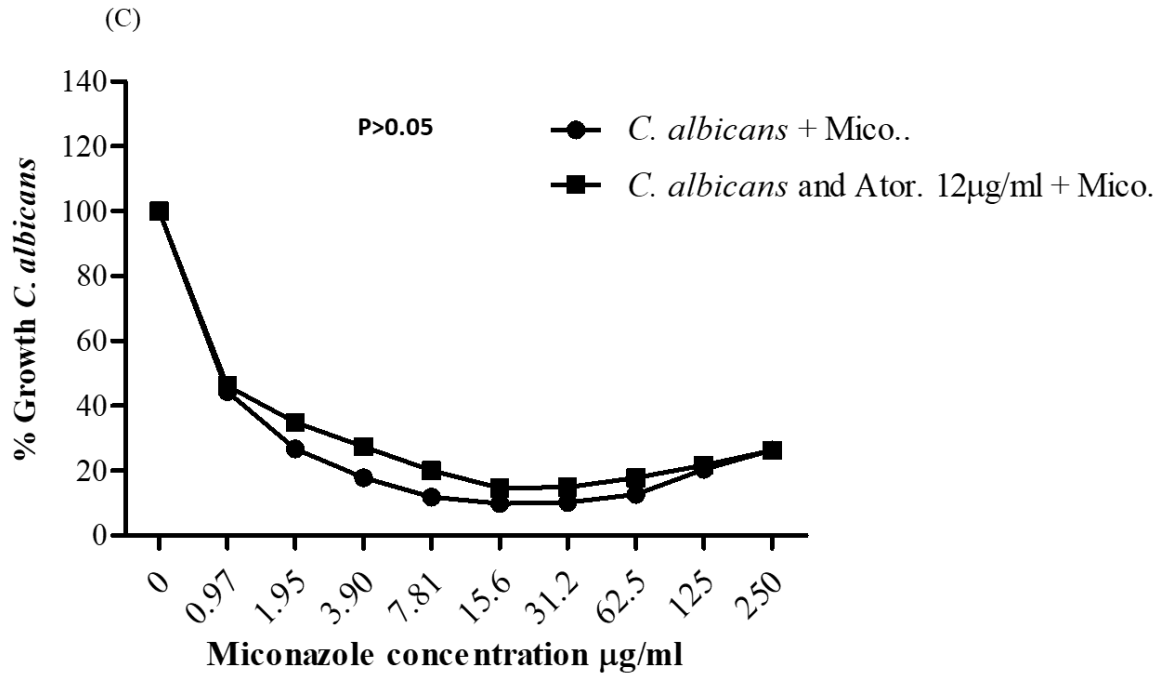


**Figure 3.2C:** The percentage growth of *C. albicans* in the presence of a serial dilution of miconazole (0.97 – 250 µg/ml) and in presence atorvastatin (12 µg/ml).

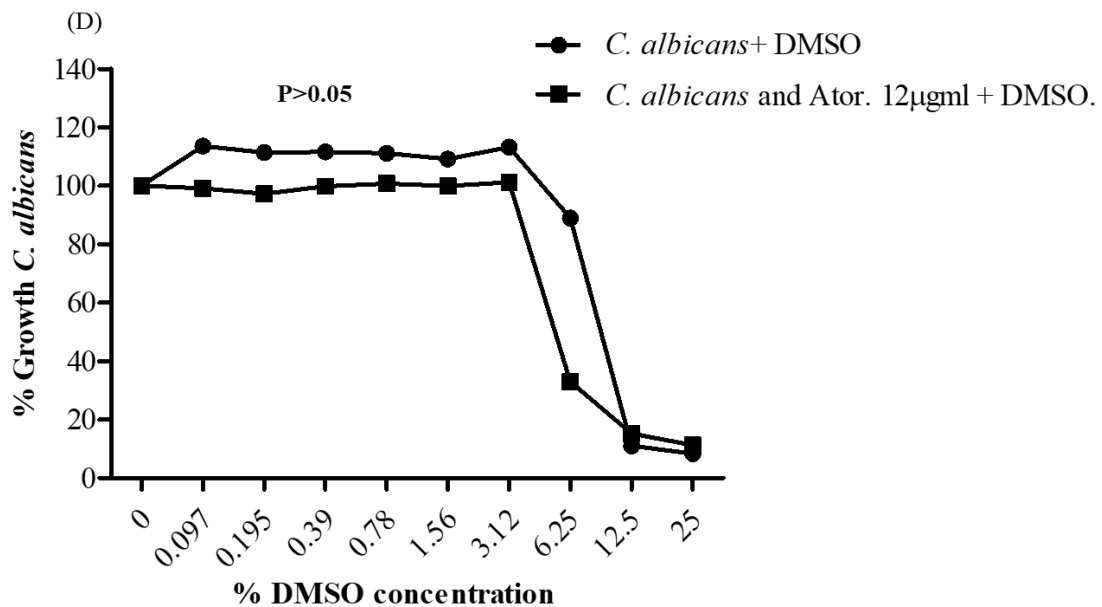


**Figure 3. 2D:** The percentage growth of *C. albicans* exposed to a serial dilution of % DMSO (0.097 – 25%) in presence atorvastatin (12 µg/ml)

### 3.3 Analysis of the effect of atorvastatin on the growth of *Escherichia coli* or *Staphylococcus aureus*.

The impact of atorvastatin on *E. coli* and *S. aureus* growth was evaluated. The results showed that atorvastatin has no activity against *S. aureus* and *E. coli* (Fig. 3.3 A and B).

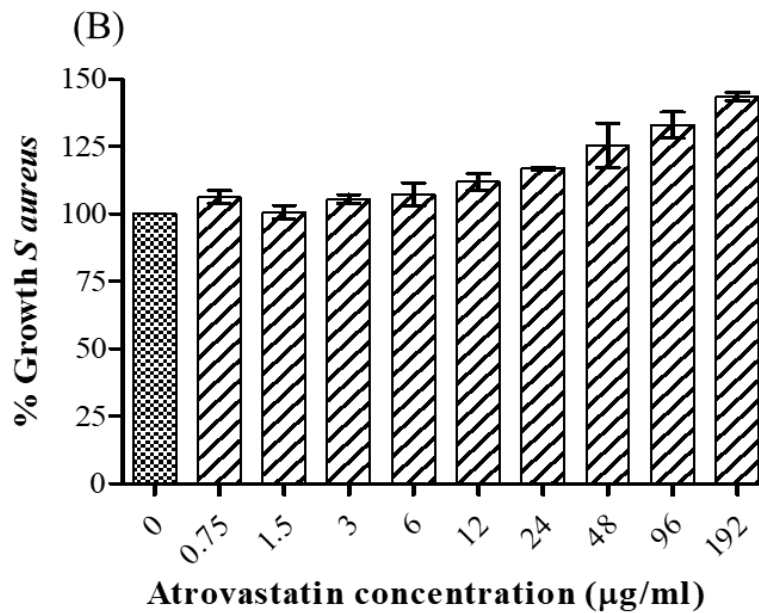
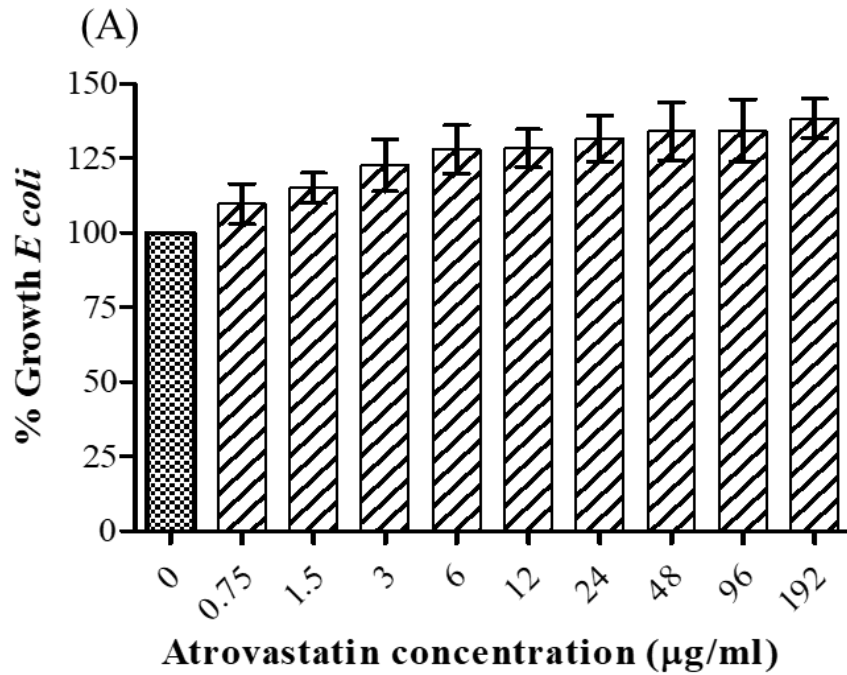


**Figure 3.3 A and B:** Effect of atorvastatin on growth of *E. coli* and *S. aureus* respectively. Bacterial cells (initial concentration  $1.5 \times 10^6$  per well) exposed to atorvastatin (0.75 µg/ml – 192 µg/ml) in nutrient broth. No inhibition of growth was observed due to atorvastatin treatment by comparing atorvastatin treated bacterial cell to control cells after 24 h.



### 3.4 Effect of atorvastatin on the viability of *C. albicans*

The effect of atorvastatin on the viability of *C. albicans* was also assessed and the results revealed a small fungicidal effect (Fig 3.4). Exposure of cells to 24  $\mu\text{g/ml}$  atorvastatin reduced viability by  $19 \pm 1.6 \%$  at 4 h and by  $22.5 \pm 0.9 \%$  at 24 h.

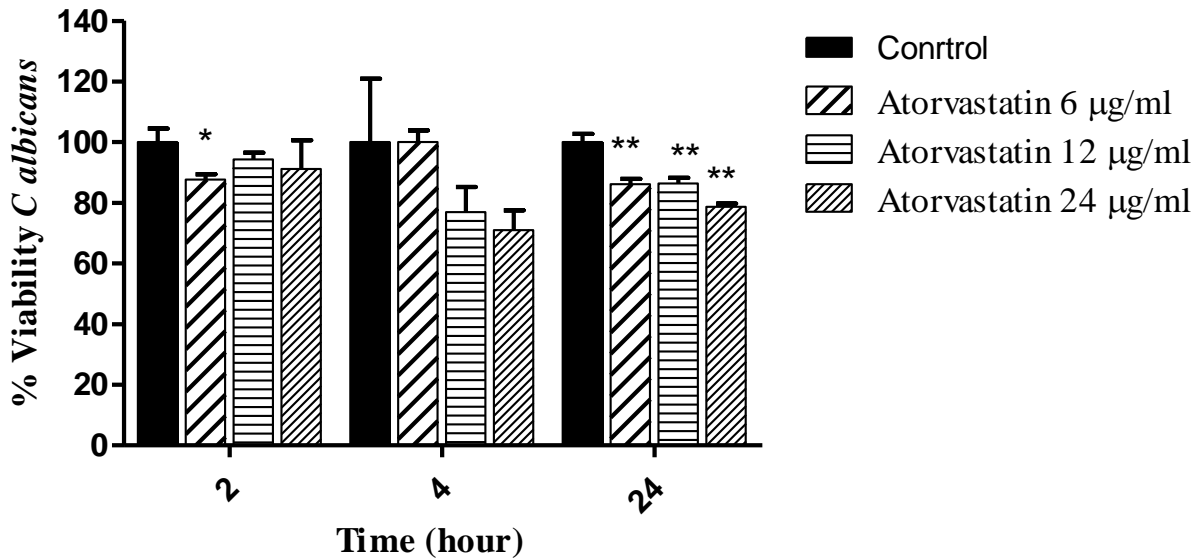


**Figure 3.4:** Effect of atorvastatin (6, 12, and 24  $\mu\text{g/ml}$ ) on viability of *C. albicans* at different time points (2, 4 and 24 h), (\*;  $p < 0.05$ , \*\*;  $p < 0.01$ ).

### 3.4 Ergosterol extraction and quantification.

Exposure of *C. albicans* to atorvastatin (12 µg/ml) for 24 h lead to a reduction in the ergosterol content of cells (control =  $0.063 \pm 0.008$  µg/ml and treatment =  $0.027 \pm 0.003$  µg/ml ( $p = 0.04$ ) (Fig 3.5).

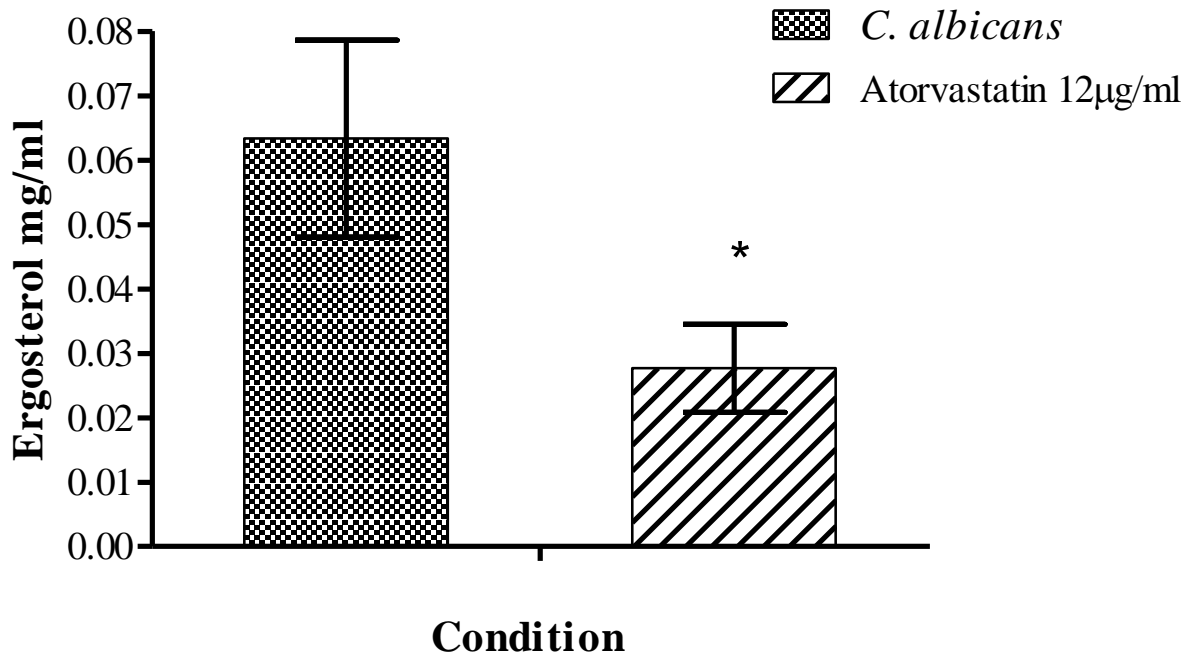


**Figure 3.5:** Atorvastatin exposure reduced the ergosterol content of *C. albicans*. Ergosterol quantification was performed using a Gas Chromatograph with a flame ionization detector and a chrompack capillary column. Ergosterol standards were used to calibrate the instrument. Ergosterol content was expressed in terms of mg/ml (\*;  $p < 0.05$ ).

### 3.5 Determination of Amino acid Leakage

Exposure of cells to atorvastatin (12  $\mu\text{g/ml}$ ) for up to 4 hr lead to an increase in amino acid (Fig 3.6) leakage from cells. Exposure to atorvastatin for 2 h lead to an amino acid concentration of  $1.97 \pm 0.09 \mu\text{g/ml}$  and  $1.78 \pm 0.1 \mu\text{g/ml}$  amino acids at 4 h.

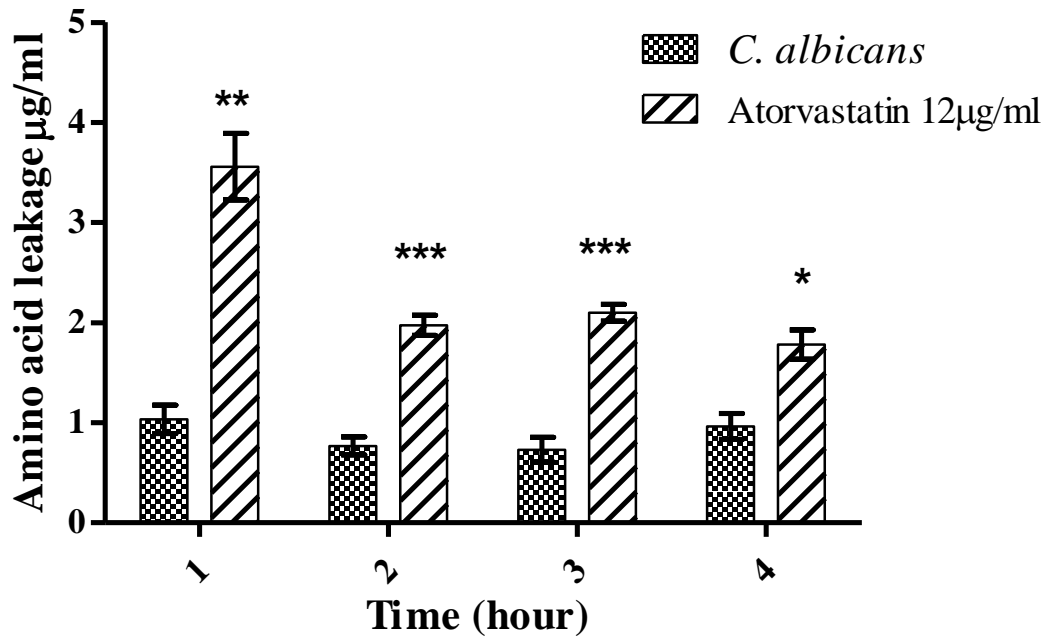


**Figure 3.6:** Effect of atorvastatin on release of amino acids from *C. albicans*. The effect of atorvastatin (12  $\mu\text{g/ml}$ ) on *C. albicans* amino acid release was determined by ninhydrin colorimetric assay. Atorvastatin treatment resulted in increased amino acid release relative to control cells (\*;  $p < 0.05$ , \*\*;  $p < 0.01$  \*\*\*;  $p < 0.001$ ).

### 3.6 Assessment of protein release

Exposure of cells to atorvastatin (12  $\mu\text{g/ml}$ ) for up to 4-h lead to an increase in protein leakage from cells (Fig. 3.7). Protein release at 2 and 4 h was  $147.7 \pm 10.8$  and  $132.7 \pm 18.1$   $\mu\text{g/ml}$ , control was  $57.3 \pm 6.2$  and  $35.67 \pm 4.6$   $\mu\text{g/ml}$  respectively ( $p < 0.05$ ).

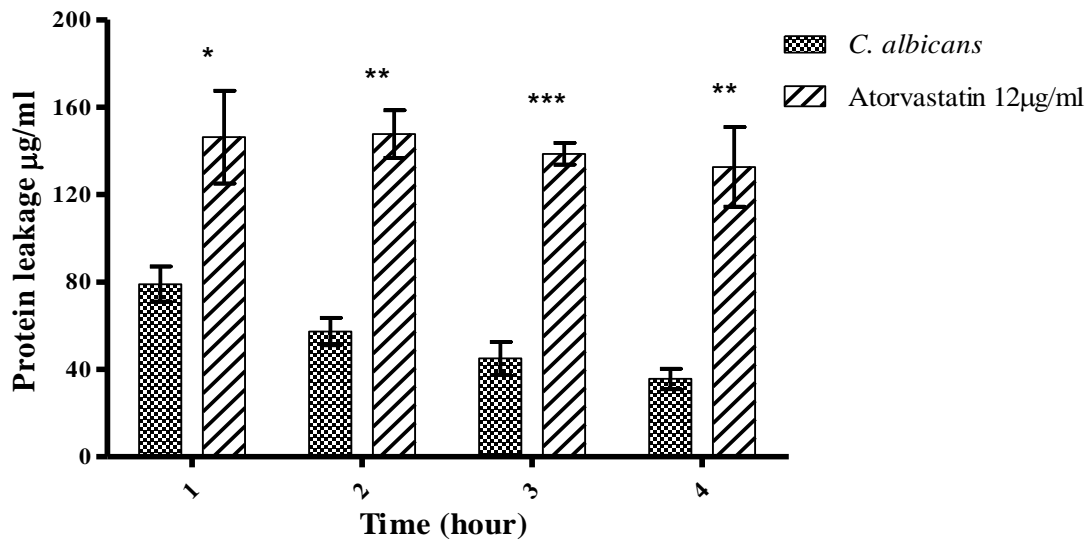
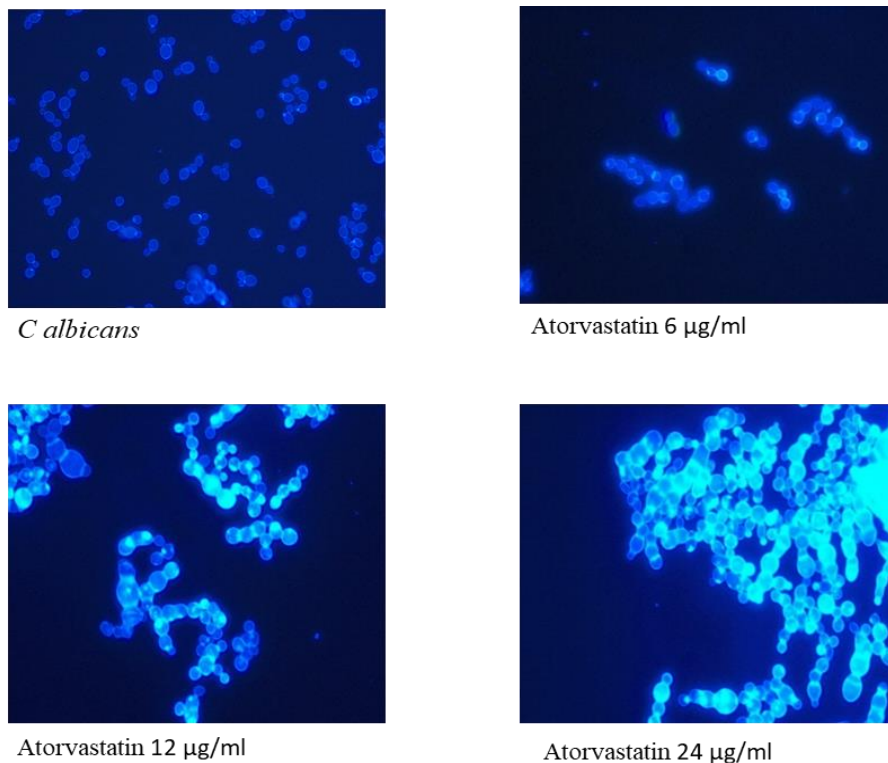


**Figure 3.7:** Effect of atorvastatin on protein release from *C. albicans*. The effect of atorvastatin (12  $\mu\text{g/ml}$ ) on *C. albicans* protein release was determined by Bradford protein assay. Atorvastatin treatment resulted in increased protein release relative to control cells (\*;  $p < 0.05$ , \*\*;  $p < 0.01$  \*\*\*;  $p < 0.001$ ).

### 3.7 Fluorescence microscopy of atorvastatin treated *C. albicans*

Altered membrane permeability could lead to distortions in the fungal cell wall. Staining cells with calcofluor following exposure to atorvastatin revealed increased fluorescence indicating an

increase in the chitin content of cells. Atorvastatin treated cells also appeared larger and demonstrated incomplete cell separation (Fig. 3.8).



---

**Figure 3.8:** Calcofluor staining of *C. albicans* following exposure to atorvastatin, (Magnification x 400). *C. albicans* cells were exposed to atorvastatin (6, 12 and 24 µg/ml) for 24 h, stained with Calcofluor white and visualized with an Olympus BX51 fluorescence microscope. Increased fluorescence indicated an increase in the chitin content of cells.

### 3.8 Adherence assay of *C. albicans*

Atorvastatin treated cells demonstrated a reduced ability to adhere to exfoliated buccal epithelial cells indicating a possible disruption to the surface of the yeast cell (Fig. 3.9). Control cells showed  $5.55 \pm 0.6$  yeast cells adhering per BEC while cells exposed to atorvastatin showed  $3.02 \pm 0.5$  adhering per BEC ( $p = 0.009$ ).

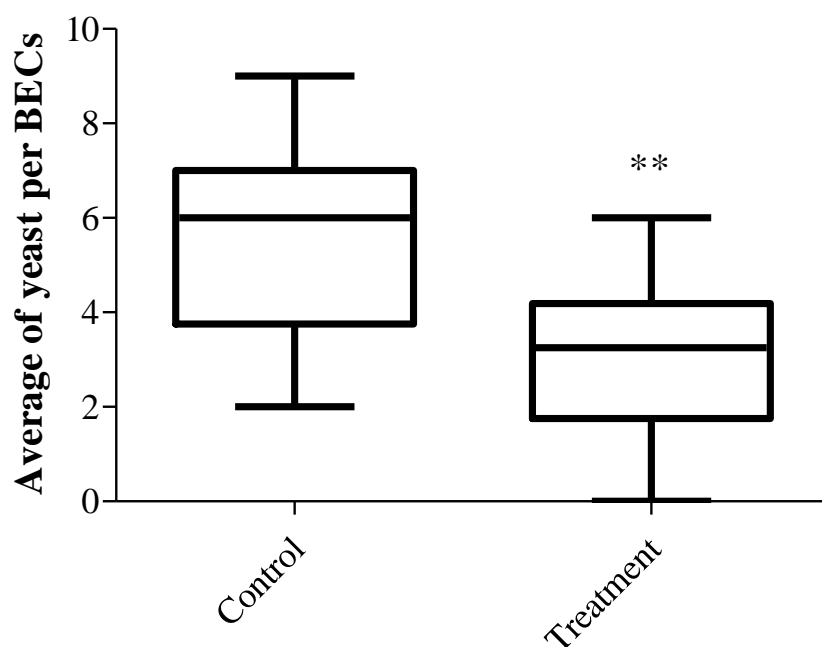


**Figure 3.9:** The adherence ability of *C. albicans* following exposure to atorvastatin (12  $\mu$ g/ml), (\*\*;  $p < 0.01$ ).

### 3.9 Analysis of susceptibility of *C. albicans* to cell wall lysing enzyme

Fig. 3.10 shows the % of colony of *C. albicans* control and atorvastatin (12  $\mu$ g/ml) treated cultures exposed to Trichoderma lysing enzyme (10 mg/ml) (SIGMA). There were no significant changes in colony growth of the atorvastatin treated culture compared to control. This result indicates that no major alteration in the cell wall susceptibility to degradation.

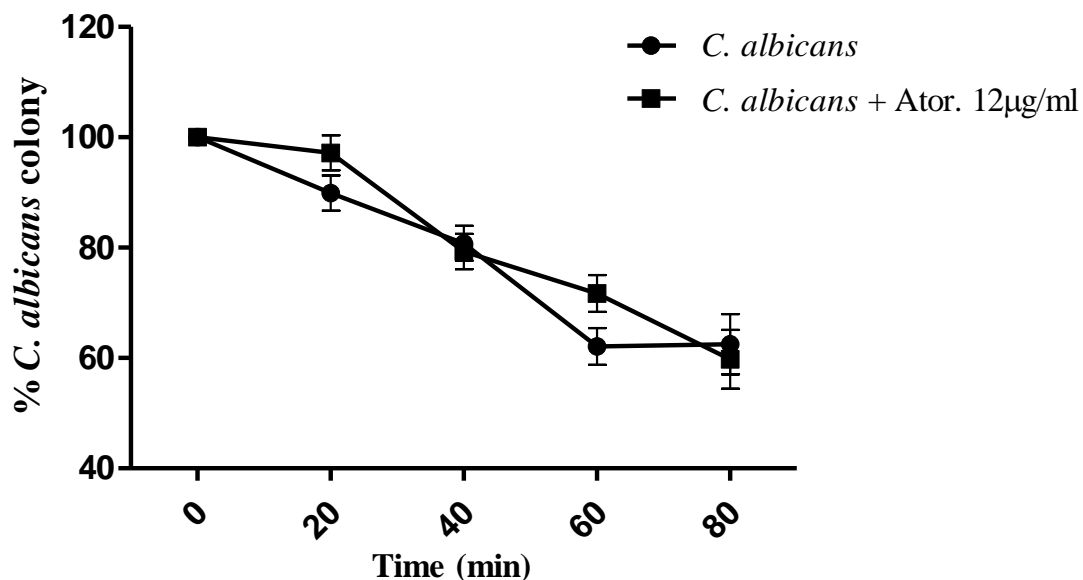


**Figure 3.10:** Enzyme susceptibility assay of *C. albicans* of exposed to 10 mg/ml of *Trichoderma* lysing enzyme. Differences in the % growth statistically non-significant ( $p > 0.05$ ).

### 3.10 Assessment of Catalase activity

In the work presented here, determination of the activity of catalase (CAT) was performed on *C. albicans* cells and atorvastatin (6, 12 and 24 µg/ml) treated *C. albicans* cells which had been exposed to 17 mM hydrogen peroxide for 30 min. Total (CAT) activity increased to  $0.6 \pm 0.04$  % and to  $0.66 \pm 0.0$  % at atorvastatin concentration (6 µg/ml) and (12 µg/ml) respectively compared to the control (*C. albicans*)  $0.272 \pm 0.02$  % when cells were exposed to 17 mM hydrogen peroxide for 30 min (Fig. 3.11).

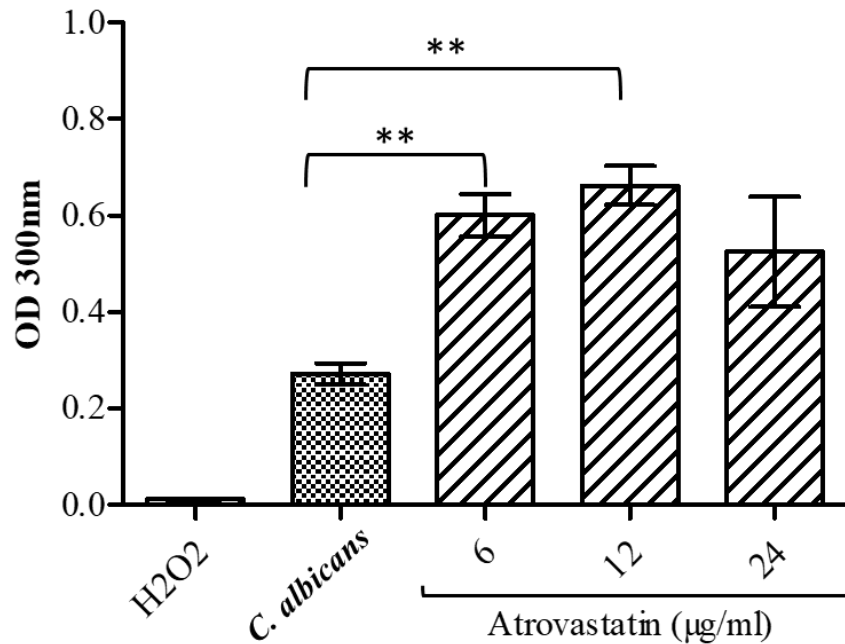


**Figure 3.11:** Catalase activity of *C. albicans* protein exposed to 17 mM H<sub>2</sub>O<sub>2</sub> for 20 minutes. Differences in the levels of catalase activity were deemed statistically significant at (\*\*;  $p < 0.01$ ).

### 3.11 Assessment of toxicity and *in vivo* antifungal efficacy of atorvastatin

Administration of doses of atorvastatin (4.55 or 9.09 mg/kg) to *G. mellonella* larvae by intra haemocoel injection resulted in no adverse effect over 144 h (Fig 3.12). Larvae infected with *C. albicans* were subsequently administered a dose of atorvastatin (4.55 or 9.09 mg/kg) 30 minutes post-infection. The results indicate increased survival in those larvae given a dose of atorvastatin (4.55 or 9.09 mg/kg). Larvae infected with *C. albicans* showed a survival of  $76.8 \pm 3.5\%$  at 72 h and  $18.1 \pm 4.2\%$  at 144 h. In contrast those larvae administered a dose of atorvastatin 9.09 mg/kg displayed a survival rate of  $94.3 \pm 1.96\%$  at 72 h and  $60 \pm 6.4\%$  at 144 h ( $p < 0.05$ ).



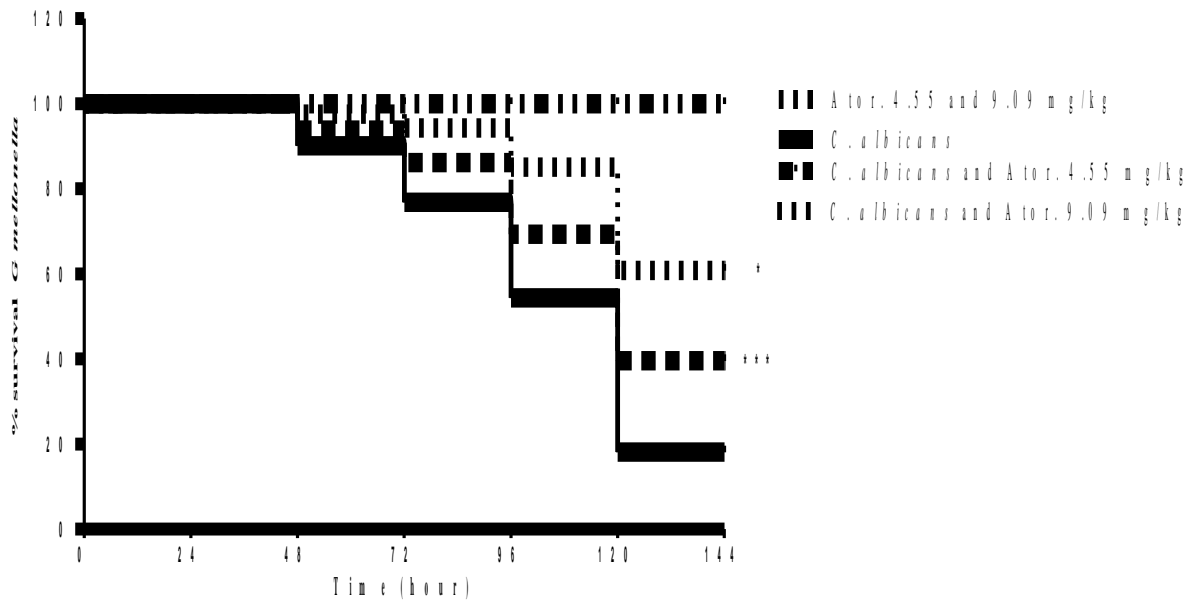


**Figure 3.12:** Effect of atorvastatin on viability of *G. mellonella* larvae infected with *C. albicans*. Larvae injected with atorvastatin (4.55 or 9.09 mg/kg) displayed no decrease in survival. Larvae were inoculated with *C. albicans* ( $1 \times 10^6$  /larva) and followed up 30 mins later with atorvastatin (4.55 or 9.09 mg/kg) and incubated at 30 °C. Survival was monitored over 144 h. Atorvastatin (4.55 or 9.09 mg/kg) treatment enhanced larval survival relative to non-treated larvae.

### 3.12 Proteomic analysis of the effect of atorvastatin on *C. albicans*

#### 3.12.1 One-dimensional SDS-PAGE analysis of released protein

In order to ascertain whether atorvastatin induced the release of proteins from *C. albicans*, cells were suspended in PBS, exposed to atorvastatin (12 µg/ml) for 24 h and the released constituents were precipitated as described in section 2.17.1. The proteins that were released from *C. albicans* cells by 24 h were collected and placed on ice with protease inhibitors (see 2.17.1). Proteins were

resolved on a 1-D SDS PAGE gel and stained with colloidal Coomassie blue (Fig. 3.13). It was evident that several proteins were released from the control cells during the 24 h of incubation period. When cells were exposed to atorvastatin 12  $\mu\text{g/ml}$ , increased release of protein was evident when compared to the control. There was a significant difference in the abundance of band 1 (hsp72-like protein), 2 (heat shock protein SSA2), 3 (elongation factor 3), 4 (glycogen/starch/alpha-glucan phosphorylase), 5 (hexokinase), 6 (enolase, partial), 7 (fructose-bisphosphate aldolase), 8 (Malate dehydrogenase), 9 (enolase, partial), and 10 (peptidylprolyl isomerase) (Table 3.1).

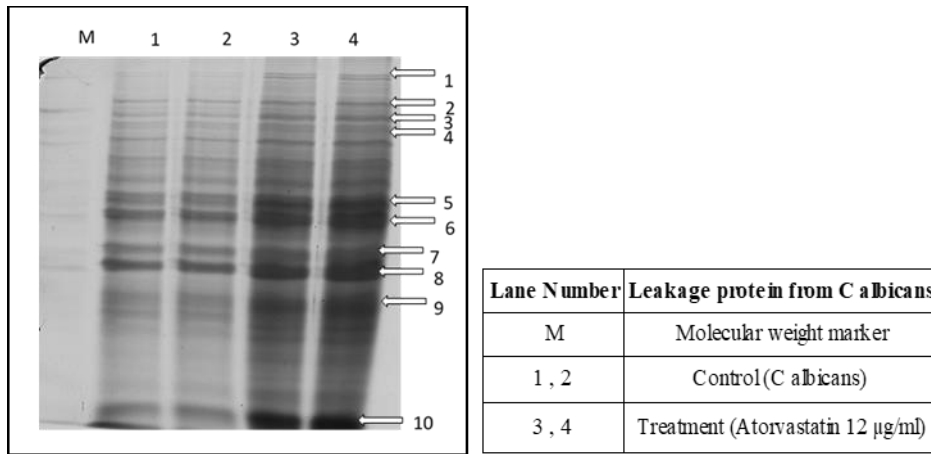


**Figure 3.13** Visualization by 1 D SDS-PAGE of released proteins from *C. albicans* following exposure to atorvastatin 12  $\mu\text{g/ml}$ . Yeasts were exposed to atorvastatin released proteins were precipitated and separated by SDS-PAGE.

**Table 3.1:** Identities of proteins observed to be altered in intensity following 1-D electrophoresis of samples from *C. albicans* cells in response to atorvastatin 12 µg/ml. Bands were excised, trypsin digested and analysed using LC-MS.

Band	Protein	Accession no.	Score	Coverage	pI	Organism	Estimated molecular mass
1	hsp72-like protein	KGU36014.1	1358	36%	4.96	<i>C.albicans P75063</i>	70545
2	heat shock protein SSA2	EEQ42742.1	646	19%	4.96	<i>C. albicans WO-1</i>	70199
3	elongation factor 3	CAA77567.1	403	7%	5.52	<i>C. albicans</i>	117483
4	glycogen/starch/alpha-glucan phosphorylase	KGR03307.1	341	8%	5.66	<i>C. albicans P57072</i>	102993
5	hexokinase	KGU01242.1	577	22%	5.5	<i>C. albicans P87</i>	53835
6	enolase, partial	AHB86321.1	2120	64%	5.54	<i>C. albicans</i>	47071
7	fructose-bisphosphate aldolase	XP_722690.1	889	40%	5.69	<i>C. albicans SC5314</i>	39362
8	Malate dehydrogenase	EMG48348.1	395	20%	6.1	<i>C. maltosa Xu316</i>	34910
9	enolase, partial	AHB86321.1	1018	36%	5.54	<i>C. albicans</i>	47071
10	peptidylprolyl isomerase	XP_721313.1	401	37%	7.74	<i>C. albicans SC5314</i>	17678

### 3.12.2 Effect of atorvastatin on the protein leakage from *C albicans* as assessed by

#### Two Dimensional SDS-PAGE analysis

Two-dimensional SDS-PAGE was employed in order to further separate the released proteins and thus facilitate their identification by LC-MS. Cells were exposed to atorvastatin (12 µg/ml) for 24 h and the released proteins were collected, separated by 2-D electrophoresis and stained with colloidal Coomassie blue (2.18.1). It is obvious that atorvastatin induced the release of a number of proteins and a change in spot intensity was observed as shown in (Fig. 3.14). Selected spots were excised, washed, trypsin digested and analyzed on LC-MS as described previously (section 2.20). Fourteen peptide spots were successfully identified. The spot intensity changed following the treatment of cells with atorvastatin. There was a significant increase in the abundance of some spots such as spot 2 (enolase, partial), 5 (alcohol dehydrogenase 1), 6 (malate dehydrogenase, NAD-dependent) 7 (phosphoglycerate mutase), 8 (fructose-bisphosphate aldolase), 9 (UDP-N-

acetylglucosamine pyrophosphorylase) and 11 (peptidylprolyl isomerase) (Table 3.2). A number of proteins 1 (adenosine kinase), 4 (malate dehydrogenase1), 13 (phosphoglycerate kinase) showed decrease in abundance when *C. albicans* cells were exposed to (12 µg/ml) atorvastatin for 24 h (Table 3.3).

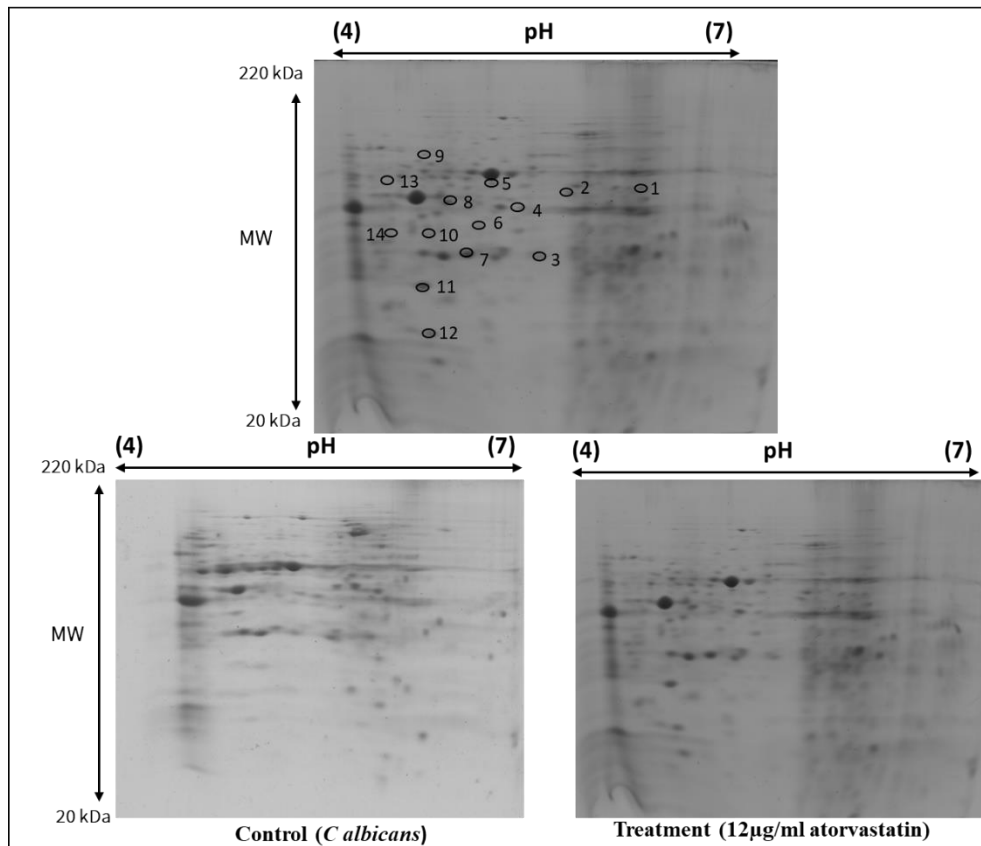


**Figure 3.14:** Analysis of protein leakage from a control and atorvastatin (12 µg/ml) treated *C. albicans* cells by 2D-IEF/PAGE analysis.

**Table 3.2:** Two Dimensional SDS-PAGE analysis list of identified proteins, using LC-MS, leaking from the *C. albicans* when the culture was exposed atorvastatin (12 µg/ml).

Spot no.	Protein name	Accession no.	Organism	Score	Coverage	Fold change
1	adenosine kinase	KGR05046.1	<i>C. albicans P57072</i>	597	28%	-1.9
2	enolase, partial	AHB86321.1	<i>C. Albicans</i>	837	31%	1.4
3	hypothetical protein MG7_03415	KGU26040.1	<i>C. albicans P34048</i>	244	25%	-1.9
4	malate dehydrogenase	EEQ43187.1	<i>C. Albicans wo-1</i>	1043	52%	-2
5	Alcohol dehydrogenase 1	P43067.1	<i>C albican</i>	393	34%	10.7
6	malate dehydrogenase, NAD-dependent	KGQ86444.1	<i>C. albicans P94015</i>	542	46%	2
7	Phosphoglycerate mutase	EMG50907.1	<i>C. maltosa Xu316</i>	215	15%	1.7
8	fructose-bisphosphate aldolase	XP_722690.1	<i>Candida albicans SC5314</i>	265	15%	2.1
9	UDP-N-acetylglucosamine pyrophosphorylase	KGQ85212.1	<i>C. Albicans P94015</i>	588	22%	2.1
10	hypothetical protein MGO_03165	KHC35483.1	<i>C. albicans P76055</i>	87	4%	1.7
11	peptidylprolyl isomerase	XP_721313.1	<i>C albicans SC5314</i>	319	24%	2.7
12	54S ribosomal protein L16	XP_009227451.1	<i>Gaeumannomyces tritici R3-111a-1</i>	78	4%	1.7
13	phosphoglycerate kinase	XP_711323.1	<i>Candida albicans SC5314</i>	224	10%	- 4.4
14	hypothetical protein	KGR06433.1	<i>C. albicans P57072</i>	247	12%	7.3

The 2D-PAGE gel approach is subject to the restrictions imposed by the gel method, which include limited dynamic range, difficulty handling hydrophobic proteins, and difficulty detecting proteins with extreme molecular weights and *pI* values (Zhu *et al.*, 2009). And after the results that we got from 2D-PAGE we decided to identify protein by using label-free quantification (commonly abbreviated to LFQ) of shotgun proteomics. LFQ techniques allow us to analyse many samples in a single experiment and are normally used in the screening and discovery phases of projects. The rapid development of label-free quantitative proteomic techniques has provided fast and low-cost measurement of protein expression levels in complex biological samples.

### 3.12.3 Label-free proteomics of response of *C. albicans* to atorvastatin

Comparative analysis of differential protein abundance in atorvastatin treated *C. albicans* was performed using label-free proteomics. A principal component analysis (PCA) was performed on all filtered proteins and identified distinct proteomic differences between the control and statin

treated samples (Fig. 3.15). The heat maps also show major differences in the relative abundance of proteins in the control and atorvastatin treated cells (Fig 3.16). In total 1575 proteins with two or more peptides were identified and 465 proteins were determined to be differentially abundant (ANOVA,  $p < 0.05$ ) with a fold change of  $>1.5$ . Of this, 231 were found in higher abundance in the atorvastatin treated cells and 234 were present in lower abundance in the treated cells. A total of 74 proteins were present in all three control samples and absent in all three treated samples, and a further 57 were present in each replicate of the atorvastatin treatment and absent in all three control samples. The volcano plot (Fig. 3.17) shows the relative increase or decrease in abundance of proteins in the atorvastatin treated cells compared to the control cells. A variety of proteins were increased in abundance in atorvastatin treated cells (Table 3.4) and these included squalene monooxygenase ERG1 (4.52 fold), lanosterol synthase (3.30 fold), 3-keto-steroid reductase (2.78 fold), lanosterol 14- $\alpha$  demethylase (2.57 fold) and acetyl-CoA C-acetyltransferase (2.23 fold). A number of proteins were decreased in abundance in the treated cells (Table 3.5) and included Hsp12p (-6.33 fold), small heat shock protein 21 (-6.26 fold), yeast-form wall Protein1 (-5.68 fold), Wh11p (-4.93 fold), Acyl-CoA desaturase (-4.88 fold) and heat shock protein SSA1 (-4.40 fold).

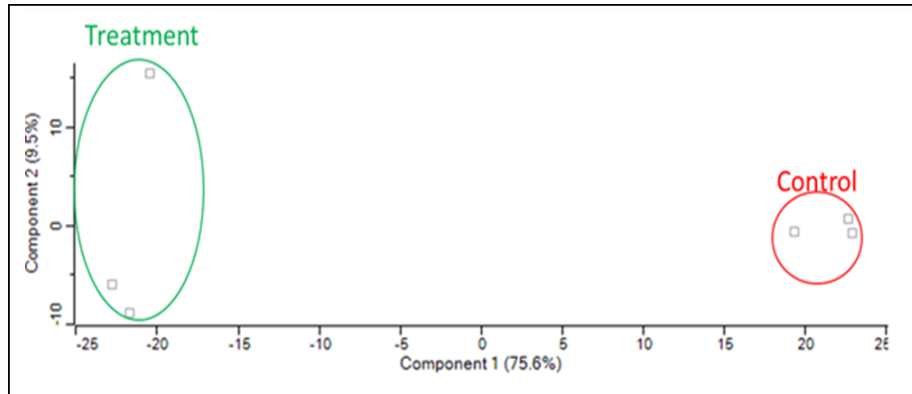


**Figure 3.15:** Shotgun proteomics of responses of *C. albicans* to atorvastatin (12  $\mu\text{g/ml}$ ) after 24 h at 30 °C. Principal component analysis of control and atorvastatin treated *C. albicans* for 24 h showing a clear distinction between control and treatment.

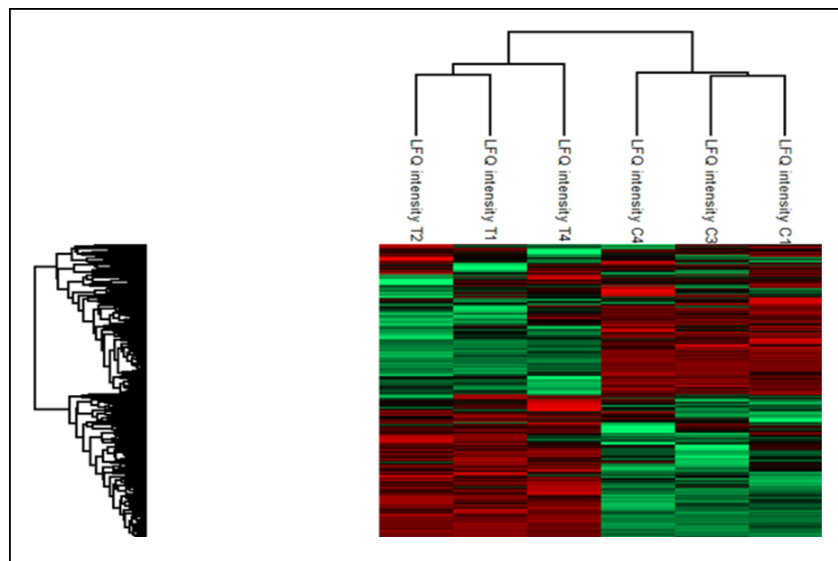


**Figure 3.16:** Shotgun proteomics of responses of *C. albicans* to atorvastatin (12  $\mu\text{g/ml}$ ) after 24 h at 30 °C. Two-way unsupervised hierarchical clustering of the median protein expression values of all statistically significant differentially abundant proteins from *C. albicans* control (C1, C3, C4) and atorvastatin treated (T1, T2, T4) *C. albicans*.

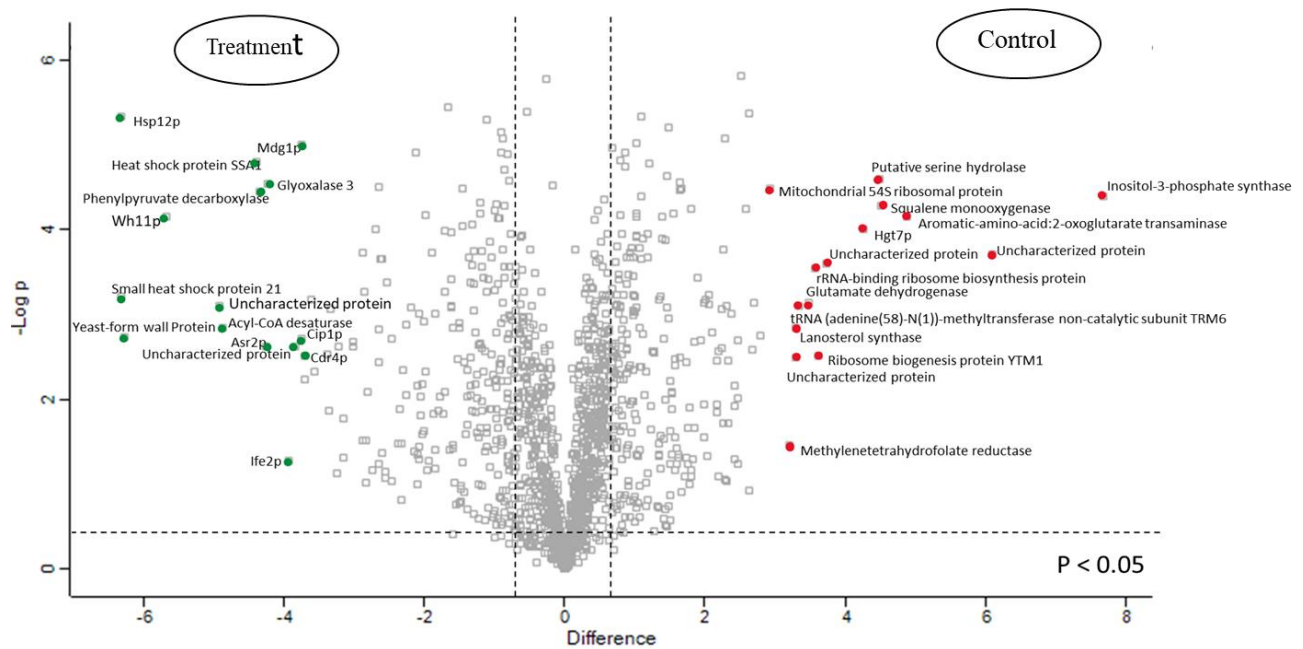


**Figure 3.17:** Shotgun proteomics of responses of *C. albicans* to atorvastatin (12  $\mu\text{g}/\text{ml}$ ) after 24 h at 30 °C. Volcano plot showing the distribution of quantified proteins according to p value ( $-\log_{10}$  p-value) and fold change ( $\log_2$  mean LFQ intensity difference). Proteins above the horizontal line are considered statistically significant (p value  $< 0.05$ ) and those to the right and left of the vertical lines indicate relative fold changes  $\pm 1.5$ .



The volcano plot (Fig 3.18) shows the relative increase in abundance of proteins involved in ergosterol biosynthesis in atorvastatin-treated cells compared to non-treated cells, these included squalene monooxygenase ERG1 (4.52 fold), lanosterol synthase (3.30 fold), 3-keto-steroid reductase (2.78 fold), lanosterol 14-alpha demethylase (2.57 fold), acetyl-CoA C-acetyltransferase (2.23 fold) and more proteins listed in Table 3.3. The genomes (KEGG) analysis of proteins that showed altered abundance in atorvastatin-treated cells revealed seven proteins that showed increased abundance in the fungal steroid pathway (Fig. 3.19). This suggests that the cell may be attempting to increase ergosterol biosynthesis or redirect biosynthesis following the inhibition of the action of the fungal 3-hydroxy-3-methylglutaryl-CoA reductase. The results were confirmed by STRING analysis (Fig. 3.20).

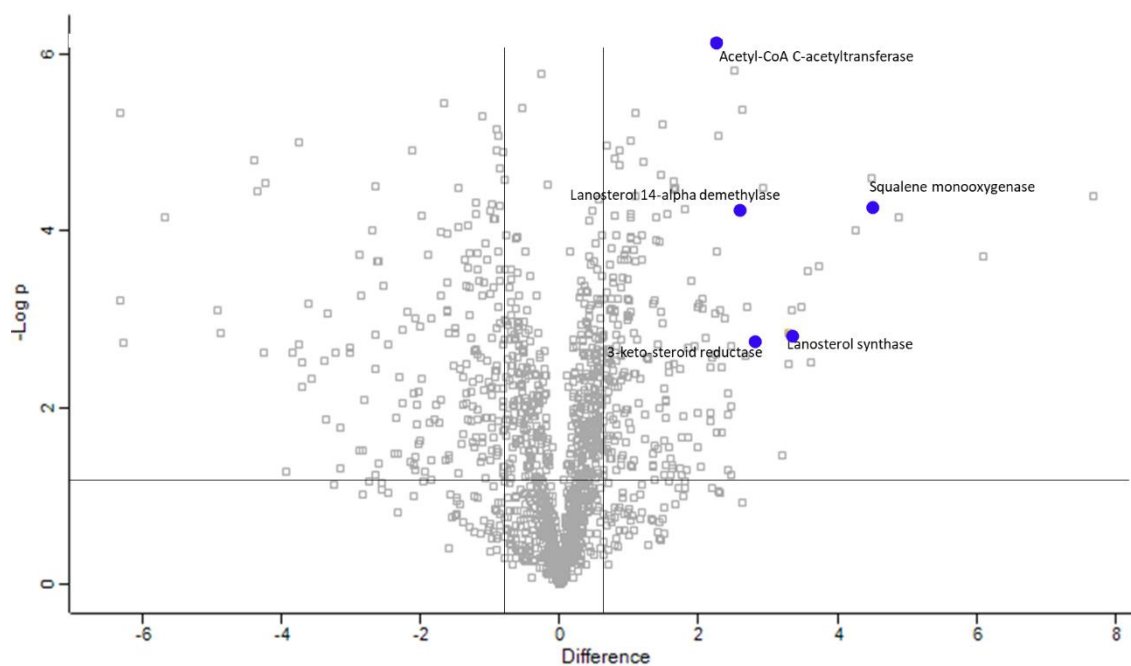


**Figure 3.18:** Volcano plot showing the distribution of quantified ergosterol biosynthesis related proteins (blue) according to p value ( $-\log_{10}$  p-value) and fold change ( $\log_2$  mean LFQ intensity difference). Proteins above the horizontal line are considered statistically significant (p value < 0.05) and those to the right and left of the vertical lines indicate relative fold changes  $\pm 1.5$ .

**Table 3.3:** List of identified ergosterol related proteins, using label-free proteomics leaking from the *C. albicans* when the culture was exposed atorvastatin (12 µg/ml).

No.	Protein name	Accession no.	Fold change
1	Squalene monooxygenase ERG1	Q92206	4.52
2	Lanosterol synthase ERG7	Q04782	3.3
3	3-keto-steroid reductase ERG27	Q5A888	2.78
4	Lanosterol 14-alpha demethylase ERG11	P10613	2.57
5	Acetyl-CoA C-acetyltransferase ERG10	A0A1D8PH52	2.23

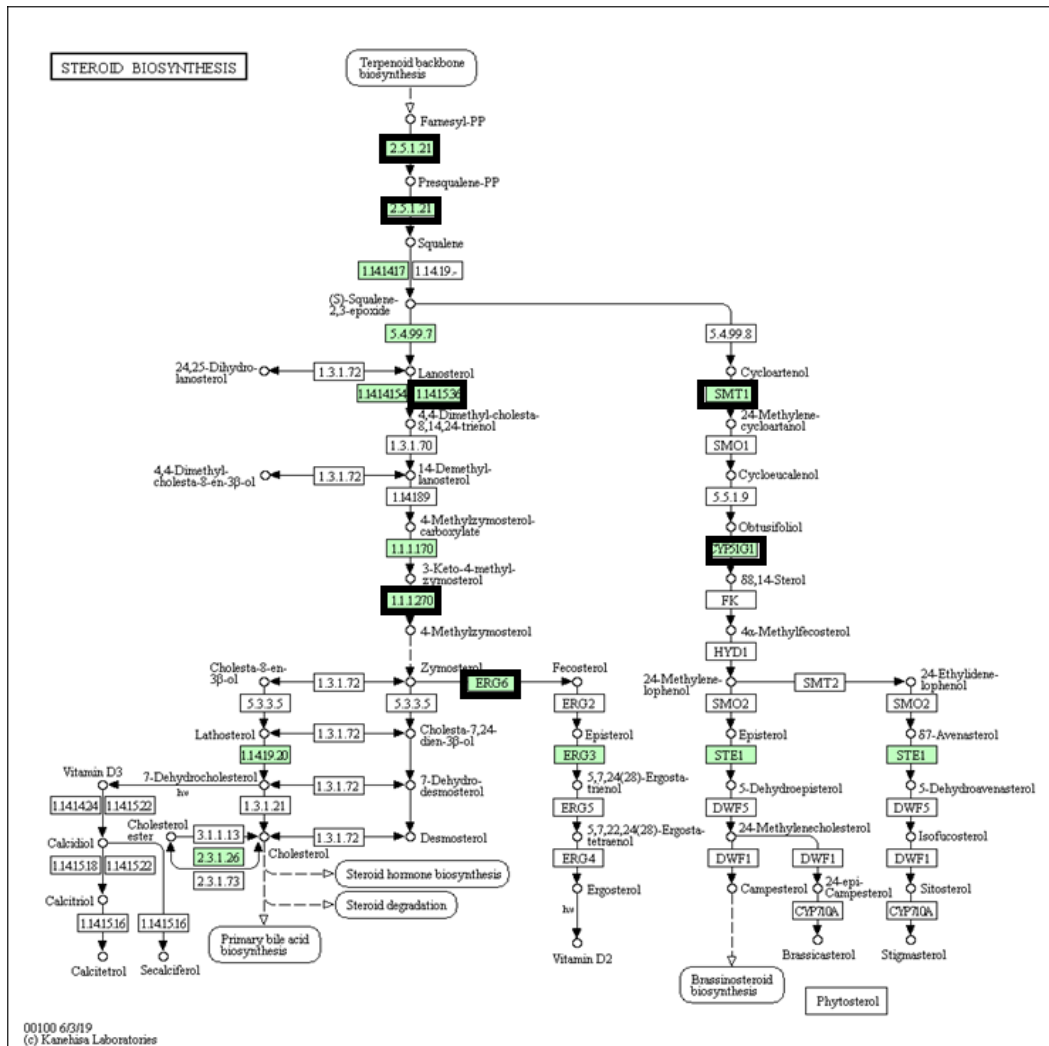


**Figure 3.19:** KEGG analysis of proteins changed in abundance in the steroid biosynthesis pathway in *C. albicans*. Proteins which are colored black are differentially abundant in *C. albicans* treated with atorvastatin (12 µg/ml).

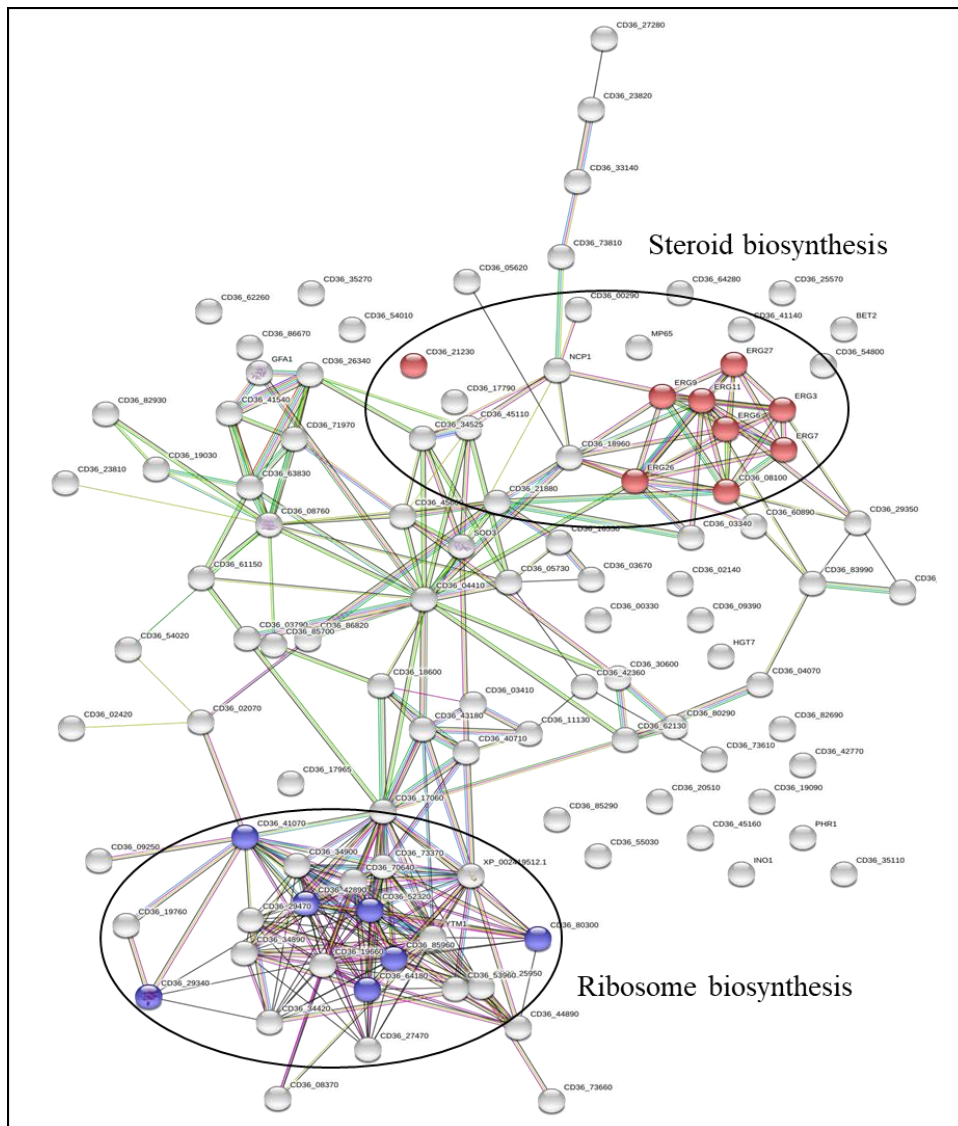


**Figure 3.20:** Interaction network analysis of up regulated proteins in atorvastatin (12  $\mu\text{g/ml}$ ) treated *C. albicans*. Protein interaction information was obtained from the STRING database using gene lists extracted for statistically significant differentially abundant (SSDA) proteins of increased abundance in treated *C. albicans*. Statistically enriched KEGG and Gene Ontology (GO) terms were examined to identify pathways and processes enriched within each set of proteins.

**Table 3.4:** Relative fold changes of proteins increased in abundance of atorvastatin (12 µg/ml) treated *C. albicans* and the number of matched peptides, sequence coverage, and overall intensity. Only proteins that had more than two matched peptides and were found to be differentially expressed at a level greater than  $\pm 1.5$ -fold were considered to be in significantly variable abundances between control and treated.

<b>N0.</b>	<b>Protein name</b>	<b>Unique peptides</b>	<b>Sequence coverage [%]</b>	<b>Mean LFQ intensity</b>	<b>Fold change</b>
1	Inositol-3-phosphate synthase	31	75	3.66E+09	7.69
2	Uncharacterized protein	8	57.5	7.98E+08	6.10
3	Aromatic-amino-acid:2-oxoglutarate transaminase	16	48.2	5.38E+08	4.88
4	Squalene monooxygenase	25	64.3	1.12E+10	4.52
5	Putative serine hydrolase	12	51.9	3.58E+08	4.50
6	Hgt7p	9	20.1	3.73E+08	4.25
7	Uncharacterized protein	17	35.3	4.02E+08	3.74
8	Ribosome biogenesis protein YTM1	12	39.5	1.74E+08	3.62
9	rRNA-binding ribosome biosynthesis protein	10	24.8	1.68E+08	3.56
10	Glutamate dehydrogenase	33	81.4	1.91E+10	3.48
11	tRNA (adenine(58)-N(1))-methyltransferase non-catalytic subunit TRM6	10	32.7	1.22E+08	3.35
12	Uncharacterized protein	10	24.7	1.56E+08	3.31
13	ERG7_CANAL Lanosterol synthase	11	19.2	1.46E+08	3.30
14	Methylenetetrahydrofolate reductase	18	38.1	3.46E+08	3.20
15	Mitochondrial 54S ribosomal protein YmL24/YmL14	8	42.3	1.81E+08	2.92
16	3-keto-steroid reductase	9	25.4	3.12E+08	2.79
17	Carbamoyl-phosphate synthase arginine-specific small chain	7	24	1.62E+08	2.71
18	Protein RMD9, mitochondrial	8	17.9	1.6E+08	2.67
19	Bifunctional urea carboxylase/allophanate hydrolase	15	12.7	1.2E+08	2.63
20	Lanosterol 14-alpha demethylase	42	62.9	8.57E+09	2.58
21	Extracellular glycosidase CRH11	5	15	1.26E+08	2.51
22	Predicted GPI-anchored protein 45	5	13.2	1.01E+08	2.46
23	rRNA-binding ribosome biosynthesis protein	4	20.6	1.32E+08	2.46
24	Uncharacterized protein	15	44.2	2.06E+08	2.44
25	Nucleolar GTP-binding protein 2	9	21.2	1.14E+08	2.43

<b>N0.</b>	<b>Protein name</b>	<b>Unique peptides</b>	<b>Sequence coverage [%]</b>	<b>Mean LFQ intensity</b>	<b>Fold change</b>
26	Putative tRNA acetyltransferase	10	46.6	1.24E+08	2.37
27	Uncharacterized protein	3	49.4	1.88E+08	2.34
28	Kinase	6	33.4	1.17E+08	2.33
29	Exopolyphosphatase	11	39.2	1.28E+08	2.32
30	Glutamine--fructose-6-phosphate aminotransferase [isomerizing]	39	65.2	7.28E+09	2.29
31	Arginine biosynthesis bifunctional protein ArgJ, mitochondrial	9	41	2.13E+08	2.27
32	Tyrosine protein phosphatase	8	12.3	8.53E+07	2.26
33	54S ribosomal protein L51, mitochondrial	6	48.6	1.05E+08	2.24
34	Hmx1p	4	14.8	1.29E+08	2.24
35	Acetyl-CoA C-acetyltransferase	26	76.6	2.60E+10	2.24
36	Uncharacterized protein	6	18.8	9.83E+07	2.18
37	Pex7p	6	25.8	9.34E+07	2.17
38	Utp8p	11	24.7	1.10E+08	2.17
39	Mitochondrial 54S ribosomal protein YmL27	4	28.6	9.18E+07	2.17
40	Mitochondrial 37S ribosomal protein MRPS17	8	26.4	1.41E+08	2.10
41	Survival factor 1	19	63.6	1.69E+09	2.06
42	Sphingolipid homeostasis protein	4	34.7	9.53E+07	2.06
43	Phosphoglycerate mutase	7	32.6	7.29E+07	2.03
44	Glycerol-3-phosphate dehydrogenase [NAD(+)]	21	80.1	1.92E+09	2.01
45	Meiotic recombination directing protein	16	36.5	6.06E+08	1.99
46	ATP synthase complex assembly protein	6	16.9	9.24E+07	1.98
47	Uncharacterized protein	5	43.2	1.33E+08	1.98
48	Ubiquinone biosynthesis monooxygenase COQ6, mitochondrial	17	37.1	1.28E+09	1.95
49	Nucleolar GTP-binding protein 1	19	38.3	4.55E+08	1.90
50	Crd2p	6	73.7	1.65E+08	1.85
51	Rab geranylgeranyltransferase	4	16.7	8.75E+07	1.84
52	Uncharacterized protein	4	36	1.49E+08	1.84
53	NADPH--cytochrome P450 reductase	39	70.9	4.29E+09	1.80
54	Protoporphyrinogen oxidase	8	26.2	1.24E+08	1.79
55	Q59KQ1_CANAL Glycerol kinase	15	35.3	3.38E+08	1.75

<b>N0.</b>	<b>Protein name</b>	<b>Unique peptides</b>	<b>Sequence coverage [%]</b>	<b>Mean LFQ intensity</b>	<b>Fold change</b>
56	Succinate dehydrogenase [ubiquinone] cytochrome b small subunit	3	26.6	1.05E+08	1.75
57	Ribosome biogenesis protein NSA2	4	19.9	8.61E+07	1.74
58	Nucleotidase	10	38.7	2.64E+08	1.66
59	Phosphopantothenate--cysteine ligase	20	78.7	1.90E+09	1.65
60	Bifunctional acetylglutamate kinase/N-acetyl-gamma-glutamyl-phosphate reductase	29	44.2	9.10E+08	1.65
61	Delta 8-(E)-sphingolipid desaturase	8	20.7	3.14E+08	1.65
62	Uncharacterized protein	3	18.8	8.48E+07	1.63
63	Uncharacterized protein	11	21	1.59E+08	1.62
64	Pre-rRNA-processing protein RIX1	4	8.8	6.51E+07	1.60
65	O-acyltransferase	4	10.5	1.05E+08	1.57
66	Tyrosine--tRNA ligase	8	23.8	9.65E+07	1.57
67	WD repeat-containing protein JIP5	4	14.2	6.62E+07	1.57
68	NADH-cytochrome b5 reductase 1	15	66	2.78E+09	1.55
69	tRNA (guanine(26)-N(2))-dimethyltransferase	9	21.8	2.26E+08	1.53
70	5-3 exoribonuclease 2	9	14	5.20E+07	1.53
71	Zcf39p OS=Candida albicans	5	10.6	7.82E+07	1.53
72	ATP-dependent rRNA helicase RRP3	8	21.2	1.55E+08	1.53
73	Glycerol-1-phosphatase	10	57.9	1.90E+09	1.51
74	tRNA (adenine(58)-N(1))-methyltransferase catalytic subunit TRM61	7	26.9	1.05E+08	1.50



**Table 3.5:** Relative fold changes of proteins decreased in abundance of atorvastatin (12  $\mu$ g/ml) treated *C. albicans* and the number of matched peptides, sequence coverage, and overall intensity. Only proteins that had more than two matched peptides and were found to be differentially expressed at a level greater than  $\pm 1.5$ -fold were considered to be in significantly variable abundances between control and treated.

<b>N0.</b>	<b>Protein name</b>	<b>Unique peptides</b>	<b>Sequence coverage [%]</b>	<b>Mean LFQ intensity</b>	<b>Fold change</b>
1	Hsp12p	11	75.6	2.83E+01	-6.33
2	Small heat shock protein 21	9	49.2	2.62E+01	-6.33
3	Yeast-form wall Protein 1	1	3.2	2.76E+01	-6.27
4	Wh11p	6	78.5	2.54E+01	-5.68
5	Uncharacterized protein	25	35.2	2.46E+01	-4.93
6	Acyl-CoA desaturase	24	51.2	2.55E+01	-4.88
7	Heat shock protein SSA1	49	34.3	2.98E+01	-4.40
8	Phenylpyruvate decarboxylase	15	35.5	2.52E+01	-4.35
9	Asr2p	12	47.7	2.50E+01	-4.25
10	Glyoxalase 3	21	75.4	2.90E+01	-4.22
11	Uncharacterized protein	7	64.5	2.51E+01	-3.85
12	Mdg1p	17	38.5	2.65E+01	-3.75
13	Cip1p	12	56.2	2.57E+01	-3.74
14	Cdr4p	24	21.3	2.45E+01	-3.71
15	dehydrogenase 1	12	54.9	2.45E+01	-3.69
16	Uncharacterized protein	3	29.4	2.42E+01	-3.62
17	Cytochrome c oxidase subunit VII	1	11	2.49E+01	-3.57
18	Uncharacterized protein	11	38.7	2.54E+01	-3.39
19	mRNA-binding translational activator	5	49.1	2.49E+01	-3.36
20	Csp37p	14	54.5	2.67E+01	-3.35
21	Phm7p	14	25.8	2.45E+01	-3.22
22	Uncharacterized protein	6	22.4	2.59E+01	-3.16
23	Uncharacterized protein	4	64.5	2.63E+01	-3.16
24	Pst2p	7	70.1	2.44E+01	-3.01
25	Proline dehydrogenase	11	37.6	2.45E+01	-3.01

<b>N0.</b>	<b>Protein name</b>	<b>Unique peptides</b>	<b>Sequence coverage [%]</b>	<b>Mean LFQ intensity</b>	<b>Fold change</b>
26	Tricalbin	17	23.1	2.49E+01	-2.88
27	Arginase	8	31.5	2.44E+01	-2.87
28	Pleiotropic ABC efflux transporter of multiple drugs CDR1	16	16.1	2.43E+01	-2.85
29	Glycogenin glucosyltransferase	12	23.9	2.51E+01	-2.82
30	Uncharacterized protein	19	21.2	2.51E+01	-2.80
31	mRNA stability protein	7	61.2	2.39E+01	-2.69
32	l-pyrroline-5-carboxylate dehydrogenase	22	47.9	2.68E+01	-2.65
33	Pst1p	3	32.8	2.43E+01	-2.64
34	Uncharacterized protein	8	40	2.36E+01	-2.64
35	Uncharacterized protein	7	73	2.43E+01	-2.62
36	Glycerol-3-phosphate dehydrogenase	16	32.5	2.45E+01	-2.61
37	ysophospholipase	9	19.1	2.44E+01	-2.60
38	Uncharacterized protein	14	92.6	2.86E+01	-2.53
39	Hgt2p	4	7.9	2.45E+01	-2.46
40	Phosphorelay intermediate protein YPD1	6	37	2.36E+01	-2.38
41	Putative mannosyltransferase	17	45	2.54E+01	-2.36
42	Phosphoenolpyruvate carboxykinase	42	82.6	3.15E+01	-2.33
43	Uncharacterized protein	5	52.7	2.41E+01	-2.29
44	Uncharacterized protein	8	34.3	2.41E+01	-2.26
45	Uncharacterized protein	6	21	2.35E+01	-2.26
46	Uncharacterized protein	6	42.1	2.36E+01	-2.19
47	Ahp2p	5	57.3	2.48E+01	-2.15
48	Ifr2p	13	45.5	2.85E+01	-2.12
49	Serine/threonine/tyrosine protein kinase	5	16.7	2.37E+01	-2.11
50	Uncharacterized protein	10	45.4	2.45E+01	-2.09
51	Vtc4p	14	24.3	2.47E+01	-2.08
52	Uncharacterized protein	9	32	2.38E+01	-2.07
53	Uncharacterized protein	12	55.3	2.50E+01	-2.06
54	Glutathione peroxidase	5	33.1	2.35E+01	-2.06
55	Dihydroorotate dehydrogenase (quinone), mitochondrial	16	54.1	2.68E+01	-2.03

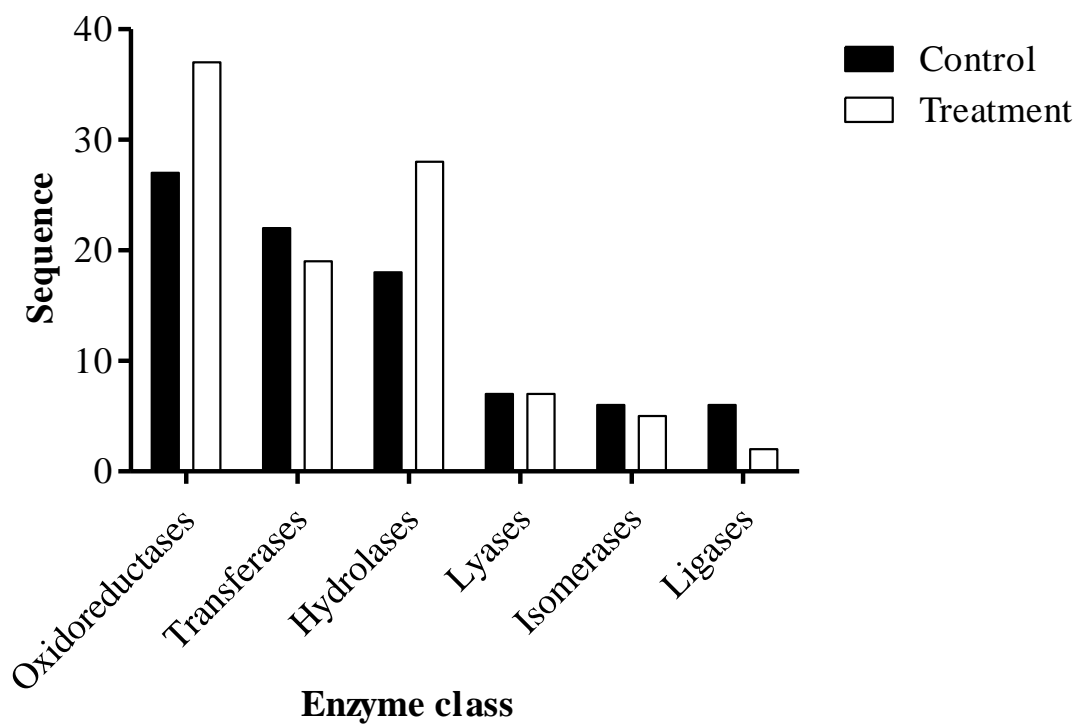
<b>N0.</b>	<b>Protein name</b>	<b>Unique peptides</b>	<b>Sequence coverage [%]</b>	<b>Mean LFQ intensity</b>	<b>Fold change</b>
56	hydrolase	12	43.5	2.59E+01	-2.03
57	Monothiol glutaredoxin	5	29.7	2.43E+01	-2.01
58	Ebp1p	28	78.4	2.88E+01	-2.00
59	Hgt1p	9	16.3	2.65E+01	-1.98
60	Uncharacterized protein	19	69.1	2.83E+01	-1.98
61	Trehalose 6-phosphate synthase/phosphatase complex subunit	32	48.6	2.70E+01	-1.90
62	Uncharacterized protein	4	38	2.37E+01	-1.88
63	Uncharacterized protein	5	12.3	2.37E+01	-1.85
64	Ifg3p	4	20.7	2.31E+01	-1.85
65	Uncharacterized protein	7	38.3	2.41E+01	-1.79
66	Vacuolar protein-sorting protein BRO1	8	12.3	2.39E+01	-1.78
67	,3-beta-glucanosyltransferase PGA4	8	25.9	2.41E+01	-1.72
68	Medium-chain fatty acid ethyl ester synthase/esterase	6	25.6	2.34E+01	-1.71
69	Uncharacterized protein	27	38.4	2.67E+01	-1.70
70	Putative NADPH-dependent methylglyoxal reductase GRP2	32	85.6	3.11E+01	-1.70
71	Uncharacterized protein	18	74.7	2.92E+01	-1.67
72	Uncharacterized protein	10	48.5	2.44E+01	-1.64
73	Malate synthase	42	76.6	2.88E+01	-1.63
74	Glycine cleavage system P protein	31	52.8	2.78E+01	-1.62
75	Putative phosphotransferase	28	63.2	2.71E+01	-1.61
76	4a-hydroxytetrahydrobiopterin dehydratase	8	88.6	2.64E+01	-1.61
77	Uncharacterized protein	7	14.3	2.36E+01	-1.60
78	Uncharacterized protein	2	10.5	2.33E+01	-1.58
79	Uncharacterized protein	6	61	2.46E+01	-1.58
80	Xylulokinase	15	47.2	2.60E+01	-1.52
81	Cytochrome c peroxidase, mitochondrial	20	66.4	2.90E+01	-1.51
82	Uncharacterized protein	8	16.3	2.38E+01	-1.51

Blast2GO annotation software was used to group proteins based on conserved GO terms in order to identify processes and pathways potentially associated with atorvastatin effect. GO terms were categorized by enzyme classes (EC), biological processes (BP), molecular function (MF) and

cellular components (CC). The enzyme classes that altered in abundance of *C. albicans* treated with atorvastatin (12 µg/ml) were; oxidoreductases, transferases, hydrolases, lyases, isomerases and ligases (Fig. 3.21). The enzyme class that shows the highest increase in abundance in *C. albicans* exposed to atorvastatin was oxidoreductases enzymes class followed by hydrolase class. The increases in BP in atorvastatin *C. albicans* treatment included proteins labelled as single-organism cellular process (69 - 81), single-organism cellular process (74 - 93), filamentous growth (18 - 20), response to stress (22 - 44), response to chemicals (23-31), cellular response to stimulus (33 - 46), catabolic process (15 - 27) and establishment of localization (19 - 32) (Fig. 3.22). The significant changes were observed.

The increases in MF in *C. albicans* treatment included proteins labelled in small molecule binding (36 proteins in control – 39 proteins in treated *C. albicans*), ion binding (54 - 60), ion binding carbohydrate derivative binding (25 - 30), hydrolase activity (27 - 33) and oxidoreductase activity (35 - 47) (Fig. 5.23). Changes were observed.

The increase in CC in *C. albicans* treatment included proteins labelled intracellular organelle (100 proteins in control – 72 proteins in treated *C. albicans*), ribonucleoprotein complex (27 - 0), membrane-bounded organelle (93 - 65), non-membrane-bounded organelle (34 - 18), intracellular organelle part (54 - 0), catalytic complex (20 - 0) and cell periphery (25 - 40). The decrease in MF in *C. albicans* treatment included proteins labelled intracellular (128 - 101), intracellular part (126 - 99), intracellular organelle (100 - 72), membrane-bounded organelle (93 - 65) and catalytic complex (20 - 0) (Fig. 3.24). The significant changes were observed.



---

**Figure 3.21:** Bar chart showing changes to number of proteins involved in various enzyme classes at level 3 ontology. Proteins were assigned groups based on involvement in enzyme classes for control and atorvastatin treated. Closed bar: control, open bar: treated.

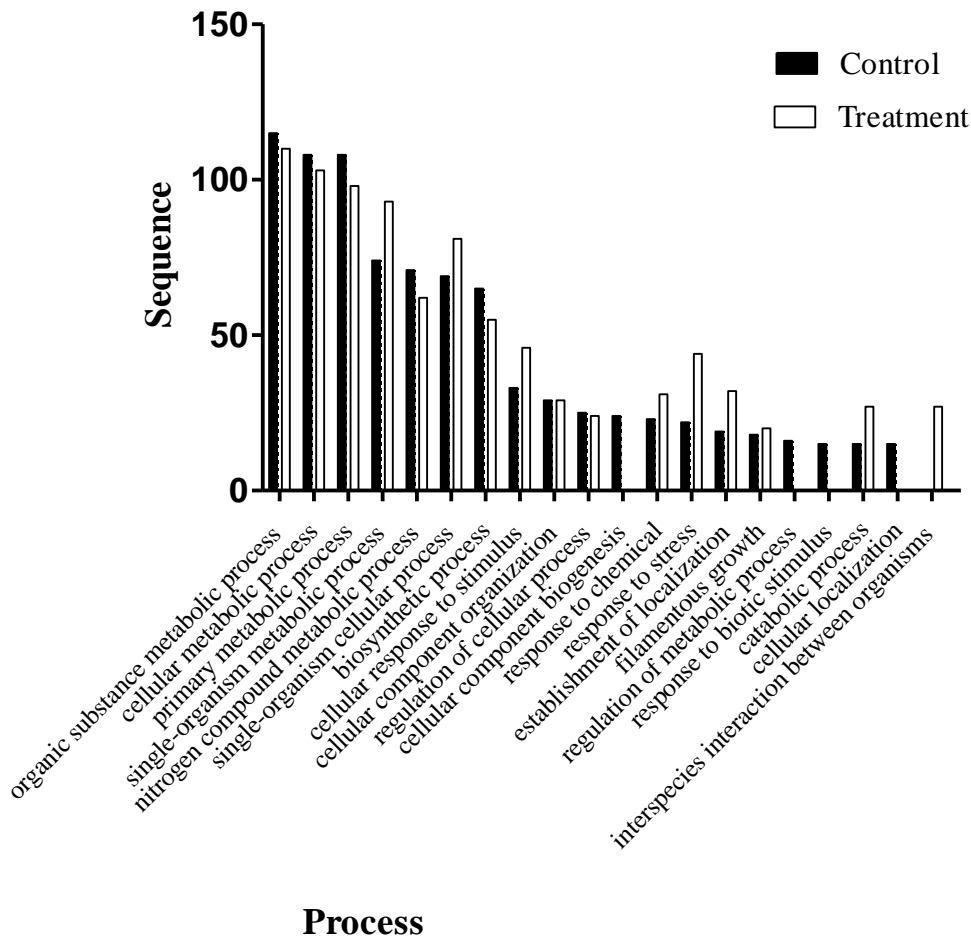


**Figure 3.22:** Bar chart showing changes to number of proteins involved in various biological processes at level 3 ontology. Proteins were assigned groups based on involvement in biological processes for control and atorvastatin treated. Closed bar: control, open bar: treated.

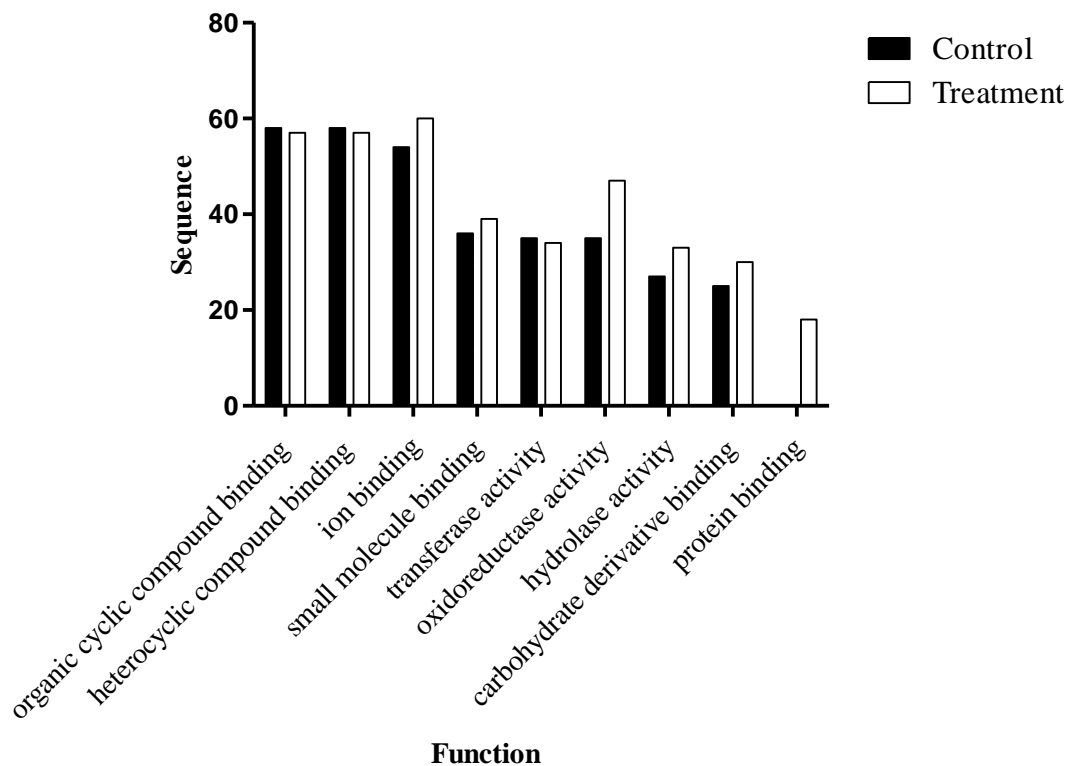


**Figure 3.23:** Bar chart showing changes to number of proteins given various molecular functions at level 3 ontology. Proteins were assigned groups based on involvement in molecular function for control and atorvastatin (12  $\mu\text{g/ml}$ ) treated *C. albicans*. Closed bar: control, open bar: treated.

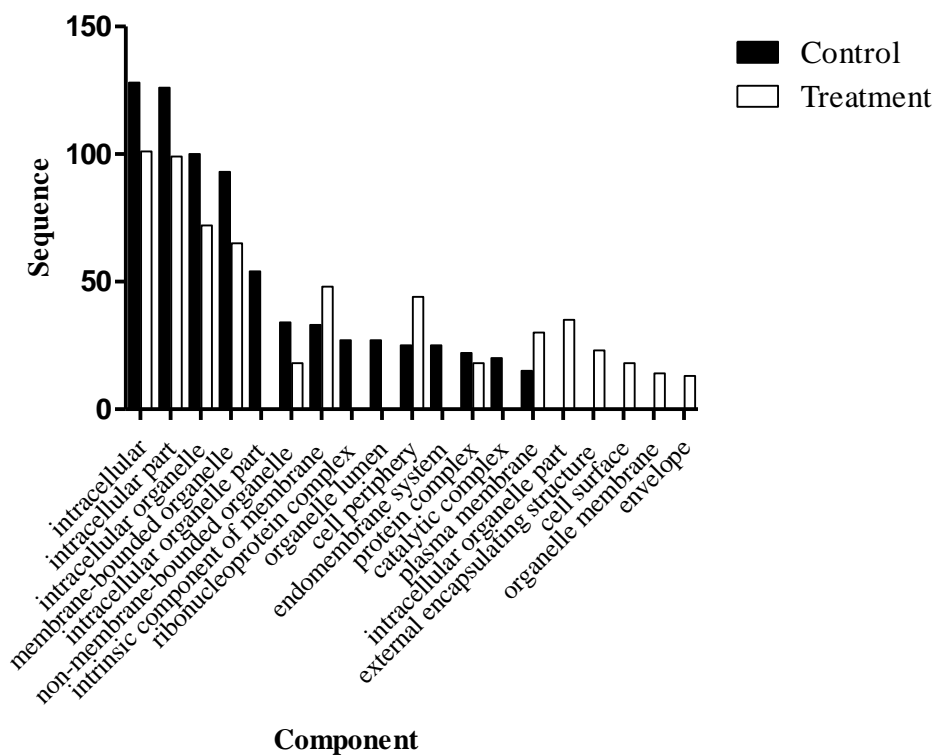


**Figure 3.24:** Bar chart showing changes to number of proteins in various cellular components at level 3 ontology. Proteins were assigned groups based on involvement in cellular components in the total proteome for control and treated. Closed bar: control, open bar: treated.



### 3.14 Discussion

Statins are used to reduce the cholesterol level in the body by inhibiting the action of HMG-Co A (3-hydroxy-3-methylglutaryl-CoA) reductase (Manzoni and Rollini, 2002). Cholesterol in mammals and ergosterol in fungi have a similar structure and biosynthetic pathways consequently both pathways are sensitive to the same inhibitory effects of statins (Stancu and Sima, 2001). Patients on statin therapy display less fungal infections therefore prompting the suggestion that statins may have potential applications as anti-fungal agents *in vivo* (Sun and Singh, 2009) (Galgóczy, 2011). This raises the possibility that statins, in addition to being used to control cholesterol levels, may also be used in the control of fungal infections either as sole therapies or in combination with existing antifungal therapies (Galgóczy, 2011). For example, statins could be useful in the treatment of fungal pathogens showing resistance to conventional antifungal agents (e.g. azoles). The work presented here evaluated the interaction of atorvastatin with *C. albicans* and demonstrated the *in vivo* activity of the statin against *C. albicans* infection in *G. mellonella* larvae.

The information presented in Macreadie *et al.* (2006), suggests that statins inhibit the growth of *C. albicans*. This was concluded as *C. albicans* cultures grown in the presence of statin showed reduced growth. A second study, Wikhe *et al.*, (2007), showed that *C. albicans* that had been treated with statin also had inhibited growth through a reduction in ergosterol level. Both of these results are based on the growth of *C. albicans* in solid media that had been treated with statin. None the less, both studies show that statin interrupts the production of ergosterol by interacting with its precursor farnesyl diphosphate (Macreadie *et al.*, 2006a). The results presented in this research correlate with the results of both previous studies. The determination of susceptibility of *C. albicans* to a serial dilution of atorvastatin (200 µg/ml) stock solution showed that atorvastatin

does inhibit the growth of *C. albicans*. On the other hand, the combination of atorvastatin (12 µg/ml) and the serial dilution of amphotericin B (6.25 µg/ml), caspofungin (3.75 µg/ml), miconazole (250 µg/ml) or DMSO (25 µg/ml) stock solutions showed that no clear different effect except with amphotericin B where it has slightly antagonist effect.

Exposure of *C. albicans* to atorvastatin reduced growth and also caused a small reduction in viability. Ergosterol plays a key role in maintaining the integrity and permeability of the fungal cell membrane and reduced levels of ergosterol could indicate a more porous membrane (Macreadie *et al.*, 2006b; Song *et al.*, 2016). Statin exposure did lead to an increase in the release of amino acid and proteins from cells indicating increased permeability.

The release of protein from *C. albicans* following exposure to atorvastatin could indicate a general increase in cell permeability thus suggesting the need for the cell to counteract the elevated permeability of the cell. In one and two-dimensional analysis the changes in the abundance of proteins following exposure of *C. albicans* to 12 µg/ml atorvastatin indicated the increased expression of a number of proteins associated with the oxidative stress response including band1 (Hsp72), spot and band 2 (Hsp SSA2). Protein related to cell wall, spot 2 enolase protein (1.4 fold) cell wall organization or biogenesis and filamentous growth (Reyna-Beltrán *et al.*, 2018), and spot 5 alcohol dehydrogenase 1 (10.7) cell wall organization or biogenesis filamentous growth and pathogenesis (Dagley *et al.*, 2011). However, exposure of *C. albicans* control and atorvastatin treatment to lysing enzyme (*Trichoderma*) showed no significant changes in wall degradation. this indicated that no significant effect of atorvastatin on the cell wall.

In addition, exposure of *C. albicans* to atorvastatin increased the activity of catalase enzyme. The activation of *C. albicans* oxidative stress response genes and enzymes following exposure to atorvastatin is evidence of the generation of oxidative stress within this medically important yeast.

Atorvastatin treated cells displayed elevated levels of chitin, were larger than untreated cells and demonstrated incomplete cell division. Interestingly proteomic analysis revealed glutamine-fructose-6-phosphate aminotransferase (+2.29-fold), an enzyme which plays a role in chitin synthesis and hyphal growth, was increased in abundance in atorvastatin treated cells. Adherence to host cells is an important virulence factor of *C. albicans* (Pendrak and Klotz, 1995) and is mediated by a variety of specific and non-specific mechanisms. The dominant adherence mechanism is mediated by cell wall bound adhesins which attach to host cell receptors and anchor the cell in hostile environments to form a focal point for tissue invasion. Exposure of *C. albicans* to atorvastatin lead to a reduction in the adherence ability of cells possibly as a consequence of the altered cell wall composition as indicated by the increased calcofluor staining. Proteomic analysis revealed decreased abundance of yeast form wall protein (-6.26-fold) which plays a role in adherence and promoting dispersal and in Wh11p (-5.68fold) – a protein involved in biofilm formation and pathogenesis.

A number of proteins involved in the ability of the cell to respond to stress were reduced in abundance. Heat shock proteins such as Hsp12p (-6.33-fold), small heat shock protein 21 (-6.33-fold) and heat shock protein SSA1 (-4.40 fold) were reduced in abundance and these play roles in the pathogenicity of the yeast and in its ability to respond to oxidative and osmotic stress. Reduced abundance of these protein may have an impact on the cell's ability to grow and proliferate *in vivo*. Protein such as Cip1p (-3.73-fold), Pst2p (-3.01-fold), pleiotropic ABC efflux transporter (-2.85-fold) were also reduced in abundance and all play a role in the cell's response to oxidative stress (Brown *et al.*, 2010).

Proteomic analysis revealed an increase in the abundance of proteins involved in ergosterol biosynthesis in atorvastatin-treated cells. In particular squalene monooxygenase (+4.52-fold),

lanosterol synthase (+3.30-fold), keto-steroid reductase (+2.78-fold) and lanosterol 14-alpha demethylase (+2.57-fold) were all increased in abundance. Atorvastatin treated cells displayed a reduced ergosterol content and perhaps the cells responded to statin exposure by attempting to increase its biosynthesis. Statins inhibit the synthesis of important isoprenoids, e.g. farnesyl pyrophosphate and geranylgeranyl pyrophosphate, which are important lipid attachments for the  $\gamma$  subunit of heterotrimeric G-proteins (Pella *et al.*, 2005), guanosine triphosphate binding protein Ras, and Ras-like proteins (Rho, Rab, Rac, Ral, or Rap) (Ghittoni *et al.*, 2005; Liao, 2008; Pella *et al.*, 2005). Moreover, statins act as inhibitors of some G-protein actions and Ras or Ras-like signalling, which affect several important bioprocesses (Cordle *et al.*, 2005).

Larvae of *G. mellonella* can be employed to assess the virulence of fungal pathogens (Brennan *et al.*, 2002b; Fuchs and Mylonakis, 2006) and for determining the *in vivo* activity of antifungal agents (Kavanagh and Sheehan, 2018; Maurer *et al.*, 2015). Their use offers the possibility of quickly establishing the *in vivo* toxicity and efficacy of antimicrobial agents without the need to resort to the use of mammals in initial screening studies. In the work presented here atorvastatin was shown to be non-toxic to larvae and to be able to protect larvae following infection with *C. albicans*. The doses used in larvae of 50 and 100  $\mu\text{g/ml}$  are equivalent to 4.55 and 9.09 mg/kg, respectively. Interestingly, atorvastatin had a negative effect on survival of mice infected with *C. albicans* and followed up with atorvastatin (40 mg/kg) and this was due to decreased INF-gamma and IL-4 levels in response to *C. albicans* while the LD<sub>50</sub> for atorvastatin is 5000 mg/kg in mice (Rahal *et al.*, 2015). However, other work has demonstrated that pravastatin enhanced survival and a decreased fungal burden in C3H/HeN mice infected with *C. albicans* and the potential benefits of statins in the clinic against *Candida* have been described (Cuervo *et al.*, 2013; Forrest *et al.*, 2010; Spanakis *et al.*, 2010; Tashiro *et al.*, 2012). The proteomic results indicated

reduced abundance of proteins associated with virulence and stress response (e.g. Hsp12p, ABC efflux transporter) in *C. albicans* and this may have made the cells more susceptible to killing by the larval immune response.

The results presented here indicate that atorvastatin has a profound effect on *C. albicans* and reduced its ability to grow and increases its susceptibility to killing in the *G. mellonella* larval model system. While the anti-microbial activity of statins is well established this work demonstrates how they interact with the fungal proteome to induce their effects and highlight their ability to retard proliferation *in vivo*. The continuing problems associated with existing antifungal therapies (e.g. toxicity, drug resistance) offer the possibility of employing an active, non-toxic therapy such as atorvastatin to supplement existing therapies (Galgóczy, 2011; Nyilasi *et al.*, 2010).

## **Chapter 4**

### **Analysis of impact of Atorvastatin on the virulence of *A. fumigatus***

## 4.1 Introduction

*Aspergillus* is a species of fungus that lives in soil, plant matter, and household dust. The most pathogenic and the primary causative agent of *Aspergillus* related infections is *A. fumigatus* (Morgan *et al.*, 2005). *A. fumigatus* is a serious cause of disease in immunocompromised patients or in those with pulmonary malfunction. *A. fumigatus* is widely distributed in the environment and produces large numbers of small conidia which are inhaled on a daily basis (O’Gorman, 2011). In a healthy individual, the immune system eliminates them from the body without a problem. However, it is a serious cause of disease in immunocompromised patients or in patients with pulmonary disease like cystic fibrosis (CF) and asthma, conidia can quickly germinate and grow in the lung (Dagenais and Keller, 2009). The fungus can cause three types of disease; Saprophytic infection involves the growth of the fungus in the lung and is seen in asthmatic and CF patients. Allergic bronchopulmonary aspergillosis occurs when the body reacts to toxins and allergens secreted by the fungus as it grows in the thick mucus secretion found in the CF or asthmatic lung. Invasive aspergillosis occurs in severely immunocompromised patients and involves the fungus growing through viable tissue and disseminating to other sites in the body (Kousha *et al.*, 2011). Invasive aspergillosis can have a mortality rate of 80 – 90% and is difficult to diagnose and treat (Latgé, 1999). *A. fumigatus* displays a number of characteristics that facilitate its growth and persistence in the lung. The fungus is thermotolerant and can survive temperature up to 45°C (Maheshwari *et al.*, 2000). It can produce a wide range of enzymes which may facilitate the degradation of tissue and toxins which may play a role in suppressing the local immune response (Sales-Campos *et al.*, 2013). In addition, it can withstand the immune response (Chotirmall *et al.*, 2014). Treatment of aspergillosis involves the use of a range of antifungal drugs. The triazole voriconazole is highly effective against *A. fumigatus* and recommended as first-line treatment

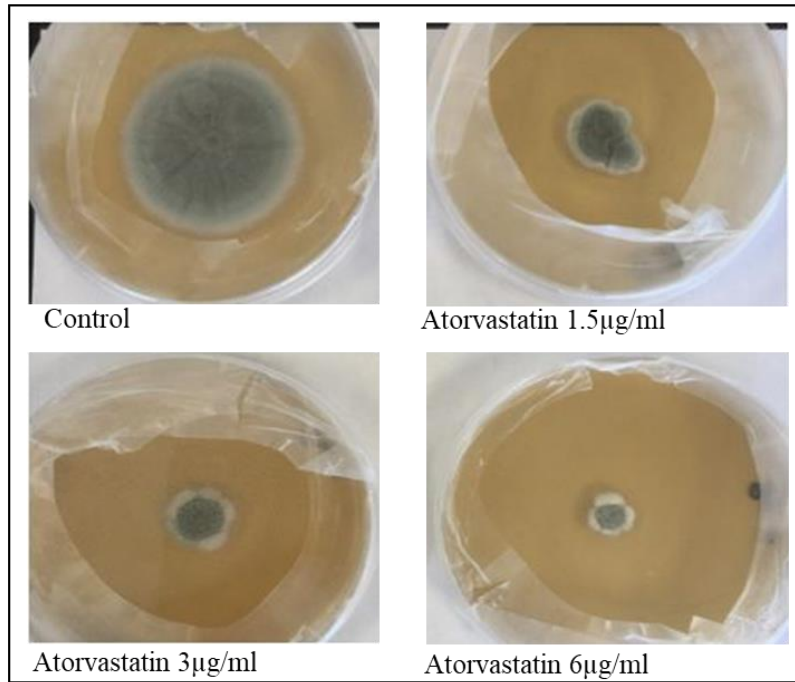
(Geißel *et al.*, 2018). Amphotericin B has been widely used for the treatment of invasive aspergillosis and, due to its inherent toxicity, is now usually administered in a liposomal formulation (Pound *et al.*, 2011). Echinocandins, such as caspofungin, show good efficacy against aspergillosis and have the advantages of being well tolerated *in vivo* (Morris and Villmann, 2006). Statins are widely used for the control of cholesterol and display strong antifungal properties (Stancu and Sima, 2001). They inhibit the action of 3-hydroxy-3-methylglutaryl-CoA (HMG-CoA) reductase and thus block cholesterol biosynthesis (Bonetti *et al.*, 2003). Consequently, fungal cells exposed to statins show reduced ergosterol content (Macreadie *et al.*, 2006a; Wikhe *et al.*, 2007). It has been reported that patients on high doses of statins show fewer fungal infections prompting the suggestion that statins may represent a well-tolerated antifungal therapy that could be used alone or in combination with conventional therapies for the treatment of recalcitrant infections. The aim of the work presented here was to characterize the response of *A. fumigatus* to statin exposure with a view to determining its potential as a novel antifungal therapy.

#### **4.2 Analysis of atorvastatin effect on growth of *A. fumigatus* on solid medium**

In this experiment the growth of *A. fumigatus* in presence of atorvastatin (1.5, 3 and 6 µg/ml) at 37 °C was assessed. Growth of *A. fumigatus* was examined at different time points (48, 72 and 96 h) by measuring surface area on the solid (malt extract agar) medium. In medium supplemented with atorvastatin we observed less growth surface area compared with control after 48 h (Fig. 4.1A). The surface area was decreased with increased atorvastatin concentration (Fig. 4.1B) this indicated that the atorvastatin inhibited the growth of *A. fumigatus*.



(A)



(B)

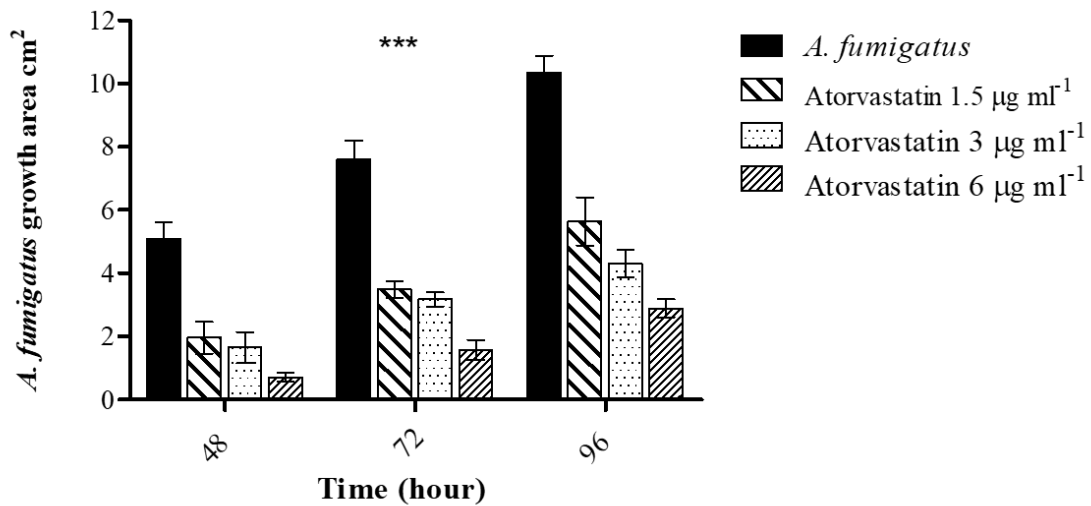


**Figure 4.1:** Growth surface area of *A. fumigatus* on Malt agar plate supplemented with different concentrations of atorvastatin (1.5, 3 and 6 µg/ml) incubated at (A). A bar chart of growth area per square centimeter of *A. fumigatus* vs time (48, 72 and 96 h) (B) (\*\*\*,  $p < 0.001$ ).

### 4.3 Susceptibility assay

#### 4.3.1 Susceptibility of *A. fumigatus* to atorvastatin

Exposure of *A. fumigatus* conidia (initial density  $10^4$ /ml) to atorvastatin for 48 h at 37 °C resulted in reduced growth. An atorvastatin dose of 6.25  $\mu\text{g/ml}$  inhibited growth by  $86.4 \pm 2.7\%$  ( $p < 0.0001$ ) while doses of 3.12 and 1.56  $\mu\text{g/ml}$  reduced growth by  $83 \pm 2$  and  $47.6 \pm 4.7\%$  ( $p < 0.002$ ) respectively at the same timepoint (Fig 4.2).

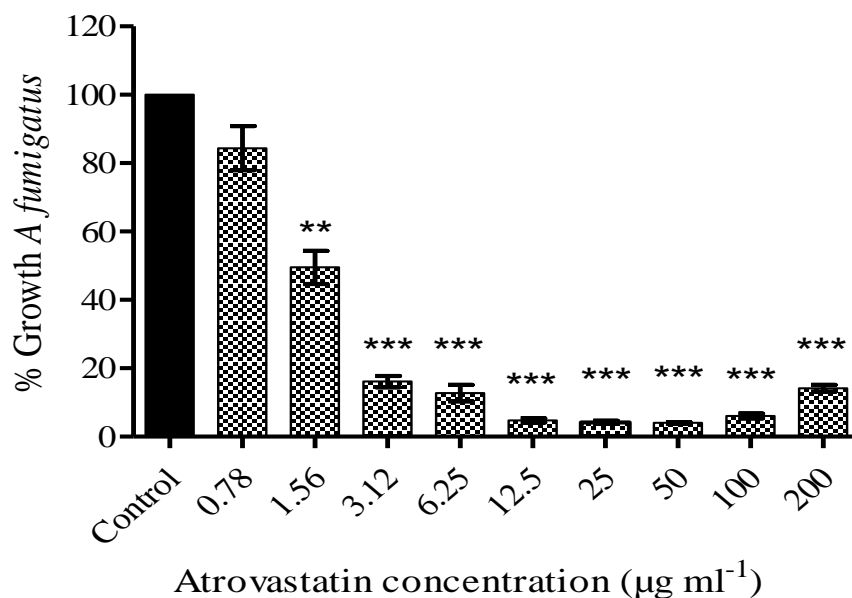


**Figure 4.2:** Effect of atorvastatin on growth of *A. fumigatus*. *A. fumigatus* (initial concentration  $10^6$ /ml) was exposed to atorvastatin SAB culture medium. Growth (%) was calculated by comparing atorvastatin treated *A. fumigatus* to control cells after 48 h growth (\*\*;  $p < 0.01$  \*\*\*;  $p < 0.001$ ).

#### 4.3.2 Susceptibility of *A. fumigatus* to a combination of antifungal drugs and atorvastatin

Susceptibility assays were carried out on *A. fumigatus* to test the sensitivity of the fungus to amphotericin B (6.25 µg/ml), caspofungin (3.75µg/ml), miconazole (250µg/ml) or DMSO (25%) stock solutions (Fig 4.3 A, B, C and D) both singly and in combination with, atorvastatin (3µg/ml) in accordance with the protocol set out in method (2.5). The results showed a significant decrease in the percentage growth of *A. fumigatus* when the atorvastatin was combined with amphotericin B and DMSO ( $P>0.05$  and  $P<0.01$ ) respectively increased *A. fumigatus* growth in combination of atorvastatin and miconazole and no significant changes when combined with caspofungin.

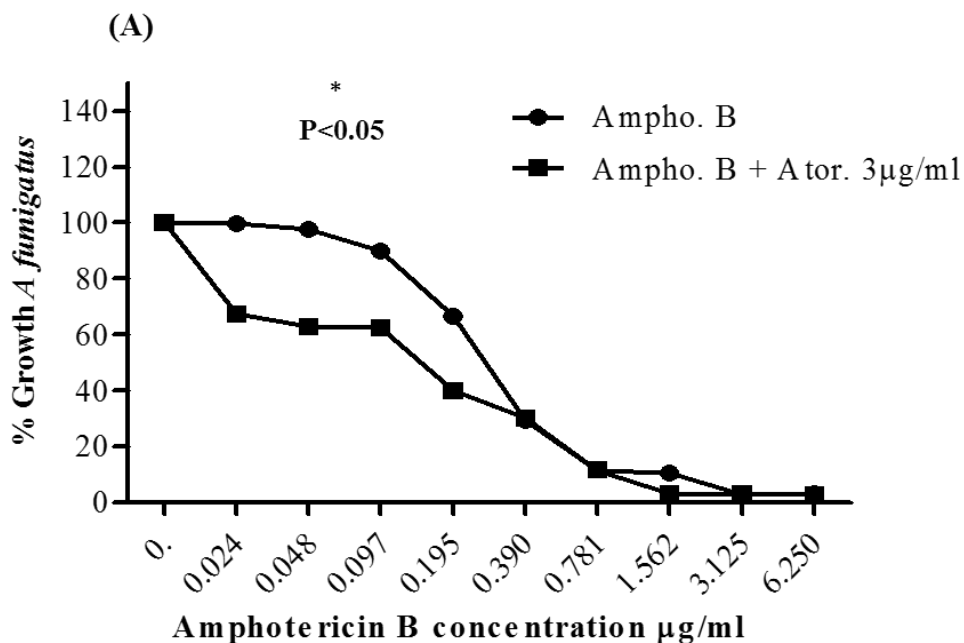


**Figure 4.3A:** The percentage growth of *A. fumigatus* exposed to a serial dilution of Amphotericin B (6.25 µg/ml) stock solution in presence atorvastatin (3 µg/ml).

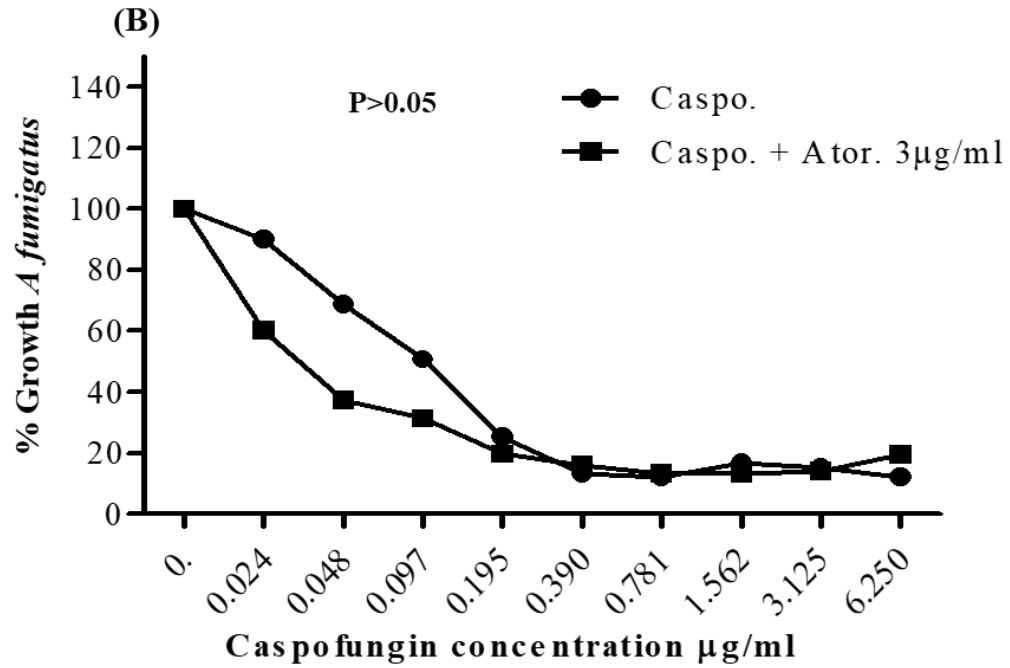


**Figure 4.3B:** The percentage growth of *A. fumigatus* exposed to a serial dilution of caspofungin (3.75 µg/ml) stock solution and in presence atorvastatin (3 µg/ml).

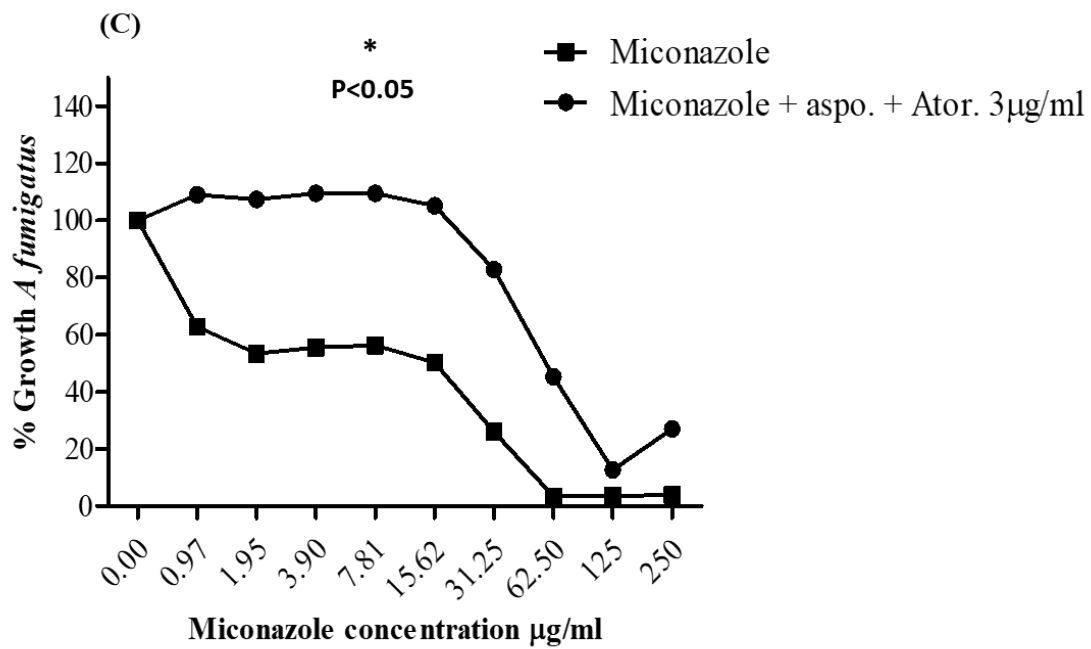


**Figure 4.3C:** The percentage growth of *A. fumigatus* exposed to a serial dilution of miconazole (250 µg/ml) stock solution and in presence atorvastatin (3 µg/ml).

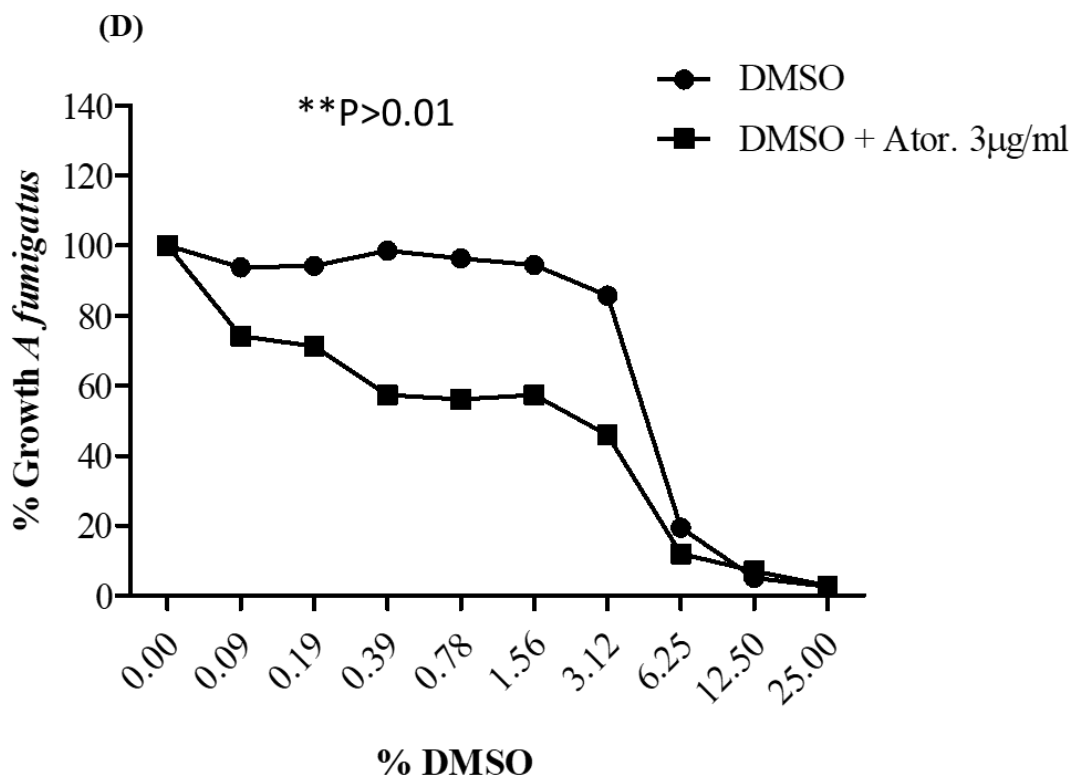
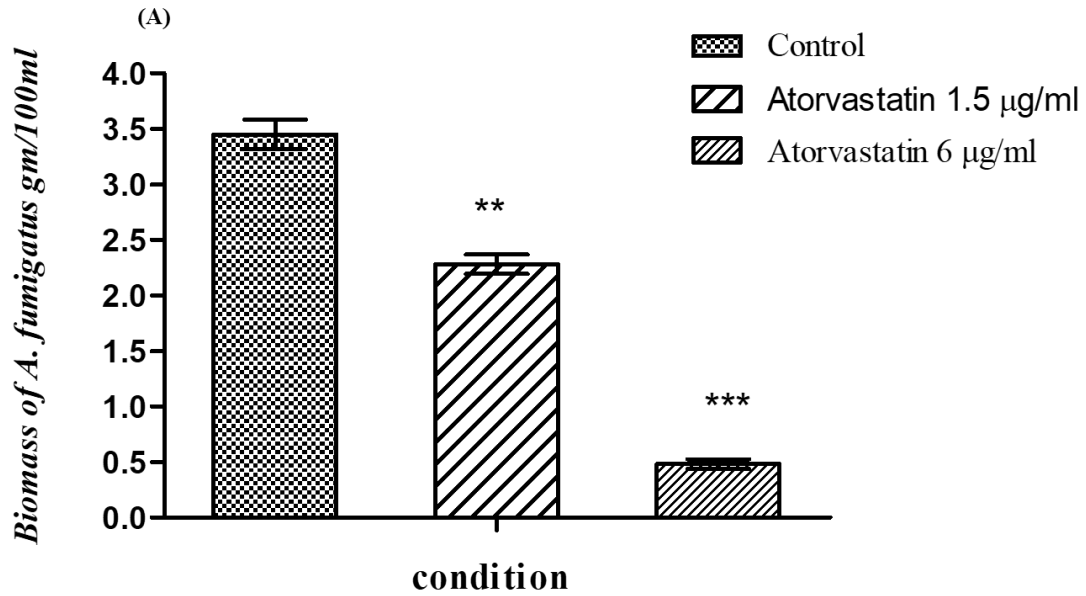


**Figure 4.3D:** The percentage growth of *A. fumigatus* exposed to a serial dilution of DMSO (25 %) stock solution and in presence atorvastatin (3 µg/ml).

#### 4.4 Effect of atorvastatin with amphotericin B on biomass of *A. fumigatus*

Exposure of cultures of *A. fumigatus* to atorvastatin lead to a significant inhibition of a biomass accumulation at 72 h. Cultures were pre-grown for 24 h and then supplemented with atorvastatin at the concentrations stated for a further 48 h. Biomass was reduced from  $3.45 \pm 0.13$  g/100 ml in control to  $2.28 \pm 0.08$  gr/100 ml ( $p = 0.0018$ ) at a concentration of (1.5 µg/ml) and at a concentration of (6 µg/ml) biomass decreased to  $0.488 \pm 0.04$ g/100 ml ( $p < 0.0001$ ) (Fig 4.4 A and B).



(B)

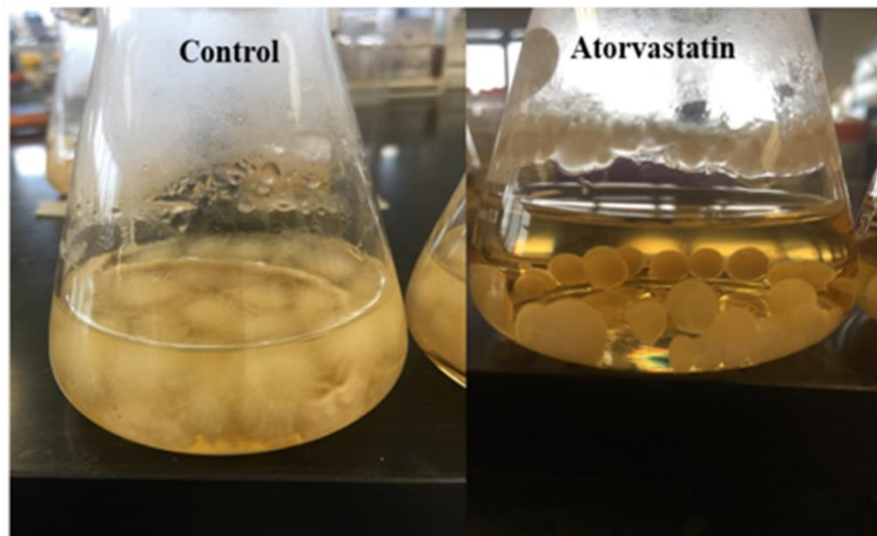


**Figure 4.4A and B:** The biomass of *A. fumigatus* exposed to atorvastatin (1.5 and 6 µg/ml). *A. fumigatus* was grown in SAB culture medium at 37°C. Biomass was calculated by comparing atorvastatin treated *A. fumigatus* to control cells after 72 h growth (\*\*;  $p < 0.01$  \*\*\*;  $p < 0.01$ ). Morphological difference of *A. fumigatus* cultures that supplemented with atorvastatin (3 µg/ml) (B).

#### 4.5 Fluorescence microscopy

Staining cells with calcofluor following exposure to atorvastatin (3  $\mu\text{g/ml}$ ) for 24 h displayed an increase in hyphal condensation and shows thinner hyphae in atorvastatin treatment than in control sample (Fig 4.5).

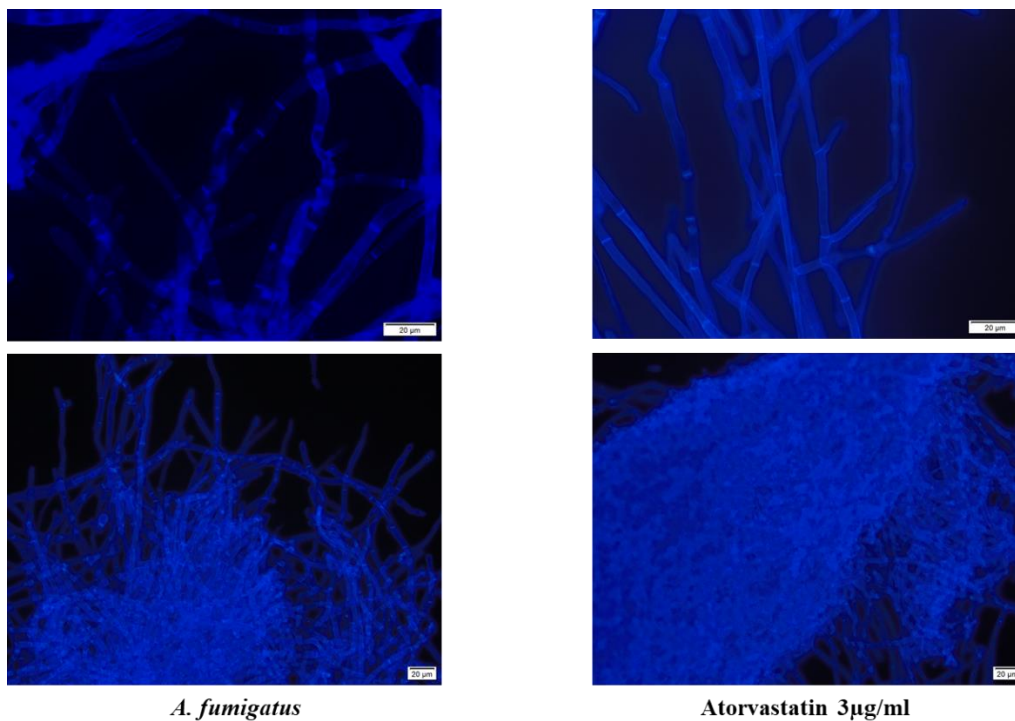


**Figure 4.5:** Calcofluor staining of *A. fumigatus* following exposure to atorvastatin. (Magnification x 400). *A. fumigatus* cells were exposed to atorvastatin (3  $\mu\text{g/ml}$ ) for 24 hr., stained with Calcofluor white and visualized with an Olympus BX51 fluorescence microscope.



#### 4.6 Ergosterol extraction and quantification

Exposure of *A. fumigatus* to atorvastatin (3 µg/ml) for 72 h lead to a reduction in the ergosterol content of cells (control =  $0.044 \pm 0.004$  mg/ml and atorvastatin =  $0.003 \pm 0.0006$  (p = 0.008) (Fig 4.6).

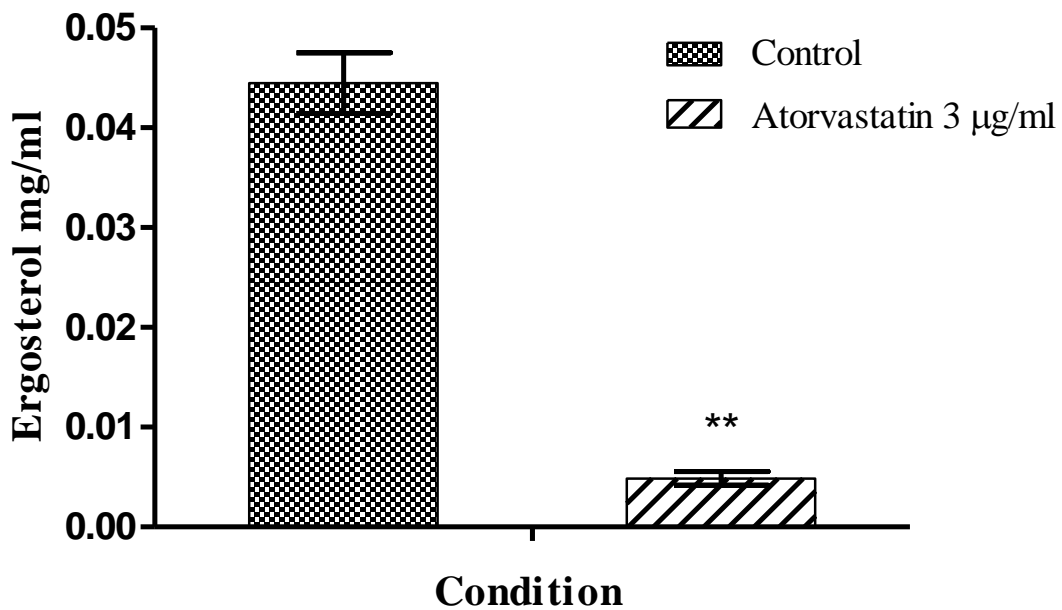


**Figure 4.6:** Atorvastatin (3 µg/ml) exposure reduced the ergosterol content of *A. fumigatus*. Ergosterol quantification was performed using a Gas Chromatograph with a flame ionization detector and a chrompack capillary column. Ergosterol standards were used to calibrate the instrument. Ergosterol content was expressed in terms of mg/ml (\*\*; p < 0.01).

## **4.7 Atorvastatin induces leakage from *A. fumigatus***

The effect of atorvastatin on membrane permeability was assessed by quantifying amino acid and protein release from cells.

### **4.7.1 Determination of Amino acid Leakage**

Exposure of cells to atorvastatin (3  $\mu\text{g/ml}$ ) for 4 or 6 h lead to an increase in amino acid release from cells (Fig 4.7). At 4 h amino acid release from control cells was  $0.14 \pm 0.0035 \mu\text{g/ml}$  but from the 3  $\mu\text{g/ml}$  atorvastatin treatment it was  $0.5 \pm 0.0037 \mu\text{g/ml}$ . At 6 h exposure the amino acid release from control cells was  $0.4 \pm 0.004 \mu\text{g/ml}$  and  $1.08 \pm 0.04 \mu\text{g/ml}$  ( $p < 0.003$ ) in the treatment 3  $\mu\text{g/ml}$ .

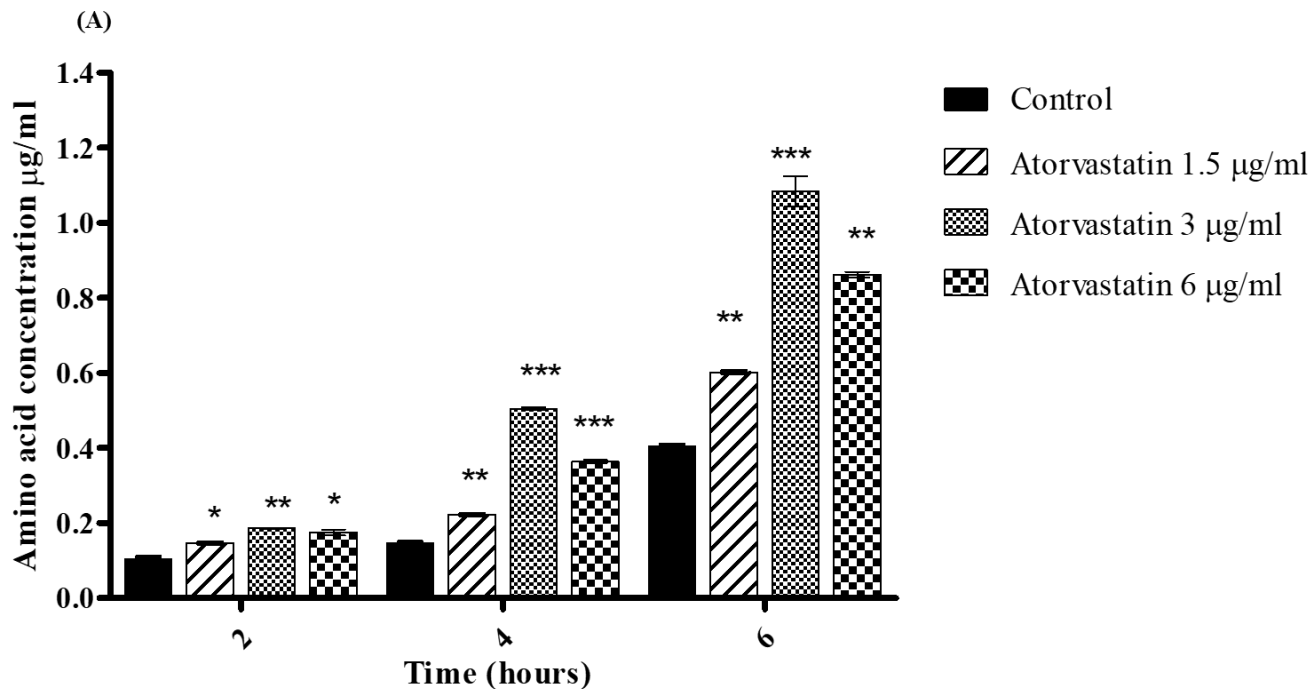


**Figure 4.7:** Effect of atorvastatin on release of amino acids from *A. fumigatus*. The effect of atorvastatin (3 µg/ml) on *A. fumigatus* amino acid release was determined by ninhydrin colorimetric assay. Atorvastatin treatment resulted in increased amino acid release relative to control cells (\*;  $p < 0.05$ , \*\*;  $p < 0.01$  \*\*\*;  $p < 0.001$ ).

#### 4.7.2 Assessment of protein release

Exposure of *A. fumigatus* to atorvastatin also lead to increased protein leakage (Fig 4.8). Exposure to atorvastatin for 4 h lead to protein concentration of  $107.6 \pm 5.2$  µg/ml in treatment (3 µg/ml) compared to  $85.6 \pm 6$  µg/ml in control and after 6 h in control the protein release was  $106.8 \pm 3.1$  µg/ml compared to  $150.5 \pm 3.6$  µg/ml in treatment (3 µg/ml) ( $p < 0.02$ ).

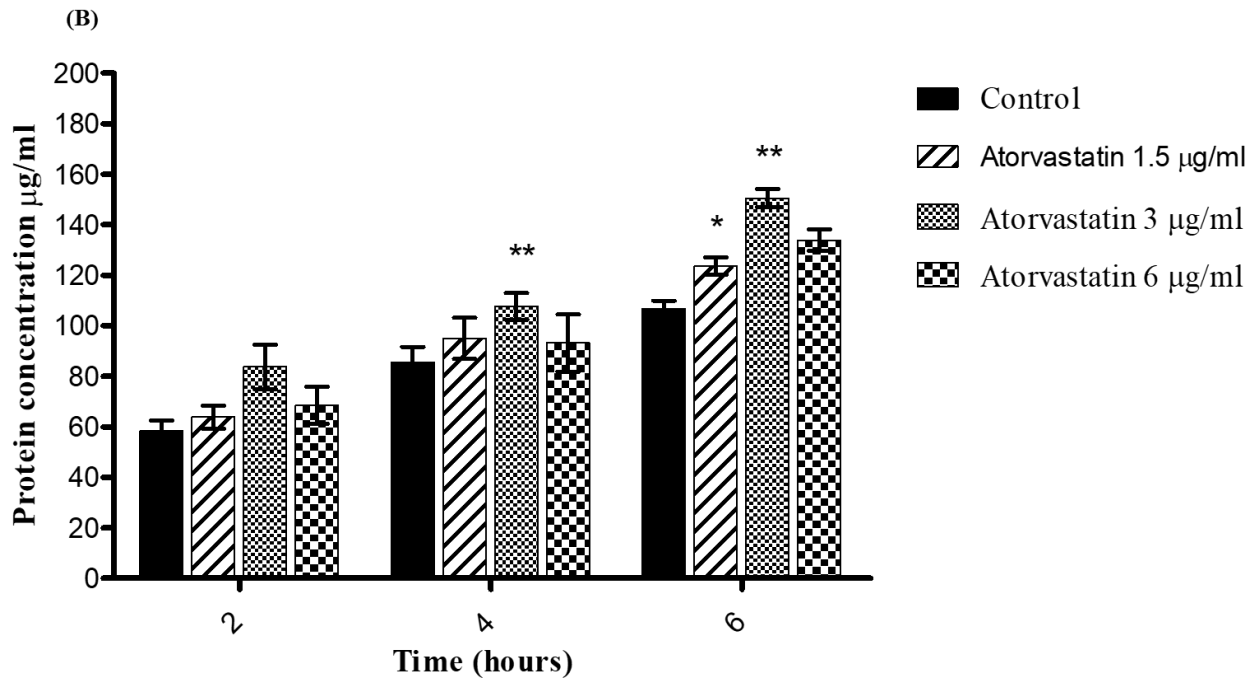
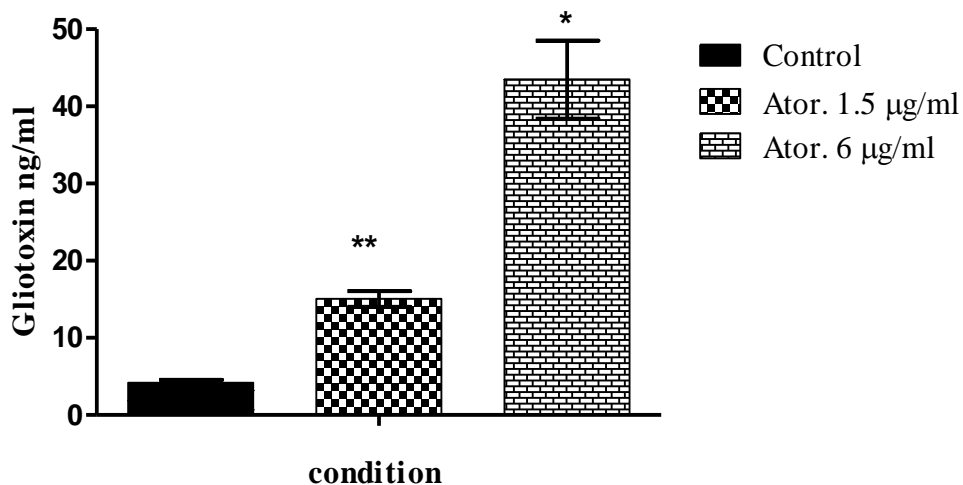


**Figure 4.8:** Effect of atorvastatin on release of protein from *A. fumigatus*. The effect of atorvastatin (3 µg/ml) on *A. fumigatus* protein release was determined by Bradford protein assay. Atorvastatin treatment resulted in increased protein release relative to control cells (\*;  $p < 0.05$ , \*\*;  $p < 0.01$ ).

#### 4.8 Effect of atorvastatin and atorvastatin in combination with amphotericin B on Gliotoxin release of *A. fumigatus*

Atorvastatin exposure induced an increase in the release of gliotoxin from *A. fumigatus* cultures (Fig 4.9). After 72 h growth at 37 °C gliotoxin was  $14.04 \pm 1.01$  ng/ml at an atorvastatin concentration of 1.5 µg/ml compared to control which was  $4.2 \pm 0.6$  ng/ml ( $p = 0.005$ ) and at an atorvastatin concentration of 6 µg/ml the gliotoxin concentrations  $47.22 \pm 5.06$  ng/ml ( $p = 0.01$ ). When *A. fumigatus* was exposed to atorvastatin in combination with amphotericin B (3 µg/ml and (0.4 µg/ml respectively) the gliotoxin release was increased (Fig 4.10). After 72 h growth gliotoxin

release increased to  $29.06 \pm 0.9$  ng/ml compared to control which was  $10 \pm 1$  ng/ml ( $p = 0.005$ ) and in atorvastatin concentration of  $3 \mu\text{g/ml}$  the gliotoxin concentration was  $33.10 \pm 4.9$  ng/ml under the same conditions ( $p = 0.04$ ).



---

**Figure 4.9:** Atorvastatin ( $3 \mu\text{g/ml}$ ) exposure increased the gliotoxin release from *A. fumigatus*. Gliotoxin quantification was performed using a HPLC. The gliotoxin standards were used to calibrate the instrument. Gliotoxin content was expressed in terms of ng/ml (\*;  $p < 0.01$ \*\*;  $p < 0.01$ ).

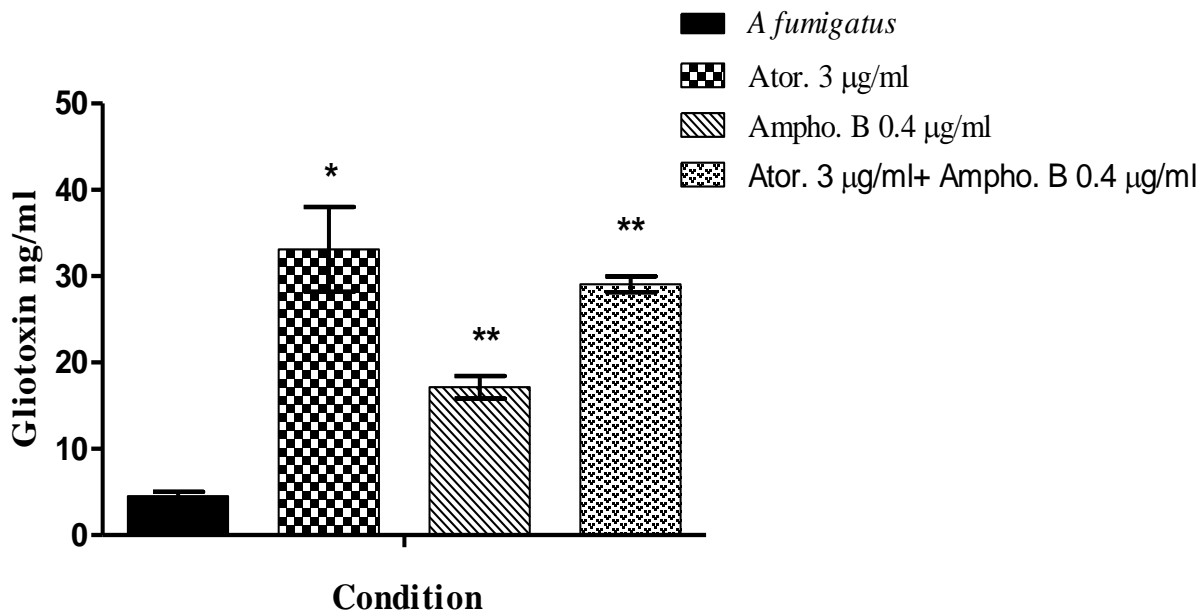


**Figure 4.10:** Atorvastatin and atorvastatin in combination with amphotericin B exposure increased the gliotoxin release from *A. fumigatus*. Gliotoxin quantification was performed using a HPLC. The gliotoxin standards were used to calibrate the instrument. Gliotoxin content was expressed in terms of ng/ml (\*;  $p < 0.01$ ; \*\*,  $p < 0.01$ ).

#### 4.9 Label-free proteomic analysis of response of *A. fumigatus* to atorvastatin

Proteomic analysis of *A. fumigatus* cultures exposed to atorvastatin (3 µg/ml) revealed 25915 peptides representing 1360 proteins and 128 proteins which represented by 2596 peptide were determined in different abundance with fold change of  $> 1.5$  of which 83 were increased in abundance and 45 were decreased in abundance. These proteins were subsequently used to statistically analyse the total differentially expressed group after imputation of the zero values as described and were then included in statistical analysis after data imputation. A principal component analysis (PCA) (Fig. 4.11) was performed on all filtered proteins and clearly distinguished the control and atorvastatin treated *A. fumigatus* samples. The heat maps also show

major differences in the relative abundance of proteins in the control and atorvastatin treated cells (Fig. 4.12). The volcano plot shows the relative distribution of these proteins (Fig. 4.13). Of the proteins increased in abundance (Table 4.1) the most notable were: socyanide synthase A (+ 8.52 fold), glutathione S-transferase family protein (+ 8.43 fold), kynureninase 2 (4.48 fold), and nonribosomal peptide synthetase fmpE (+3.06 fold). And proteins decrease in abundance (Table 4.2) the main peptides decreased were O-methyltransferase (-3.68 fold), aflatoxin B1(-2.86 fold), allergen Asp f 15 (-2.45 fold) and GNAT family acetyltransferase, (-2.25 fold). The results were confirmed by STRING analysis (Fig. 4.14).

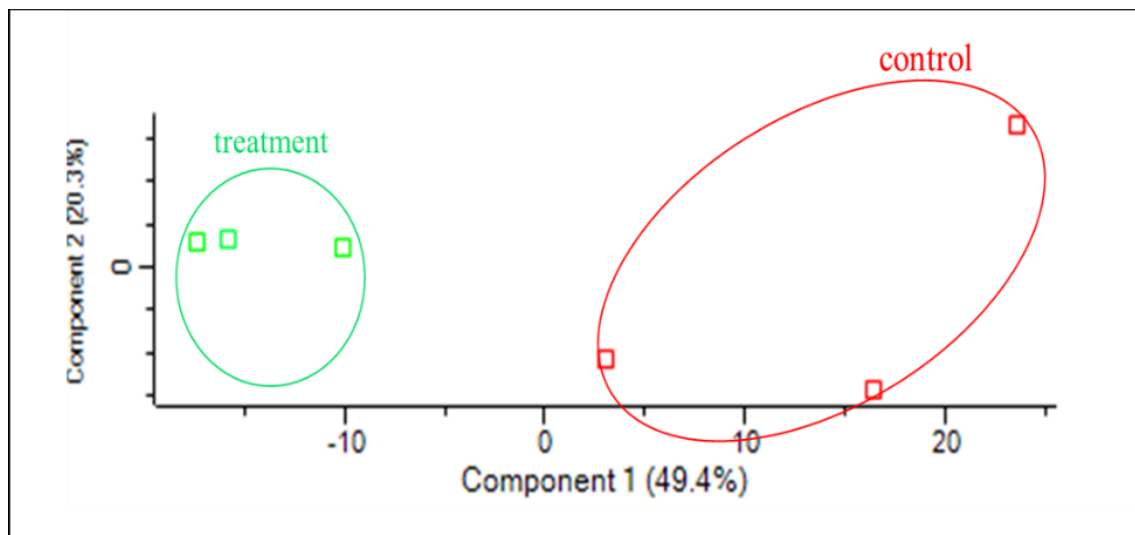


**Figure 4.11:** Principal component analysis of control and atorvastatin treated *A. fumigatus* for 24 h showing a clear distinction between control and treatment.

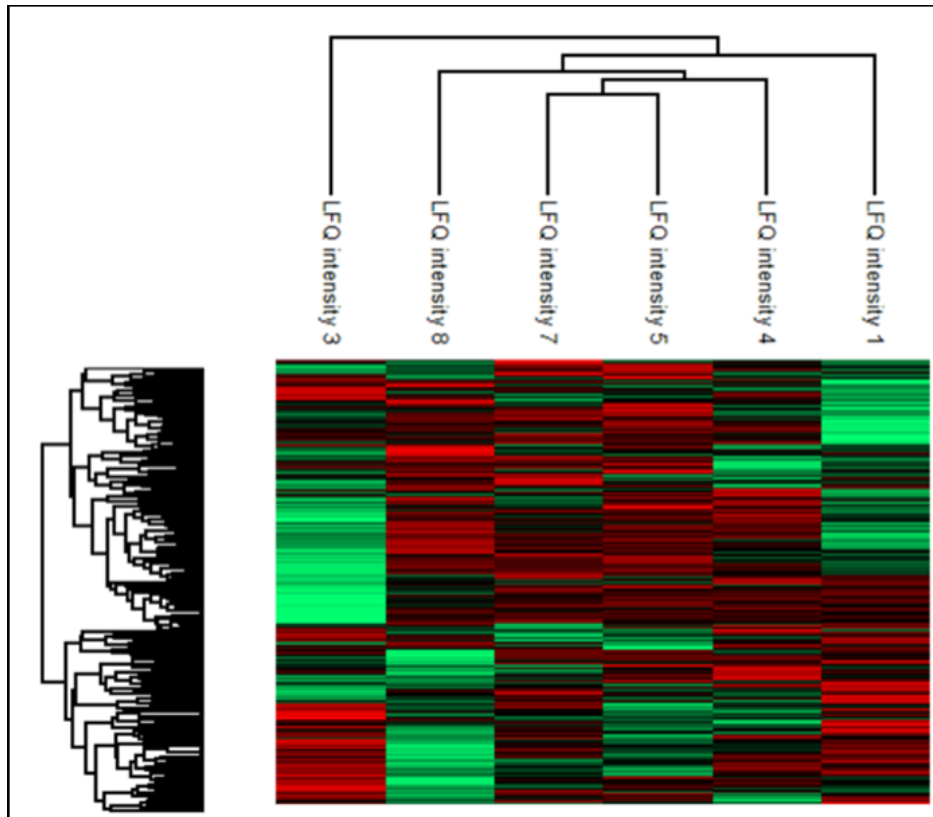


**Figure 4.12:** Two-way unsupervised hierarchical clustering (B) of the median protein expression values of all statistically significant differentially abundant proteins from *A. fumigatus* control (C1, C3, C4) and atorvastatin treated (T5, T7, T8) *A. fumigatus*.



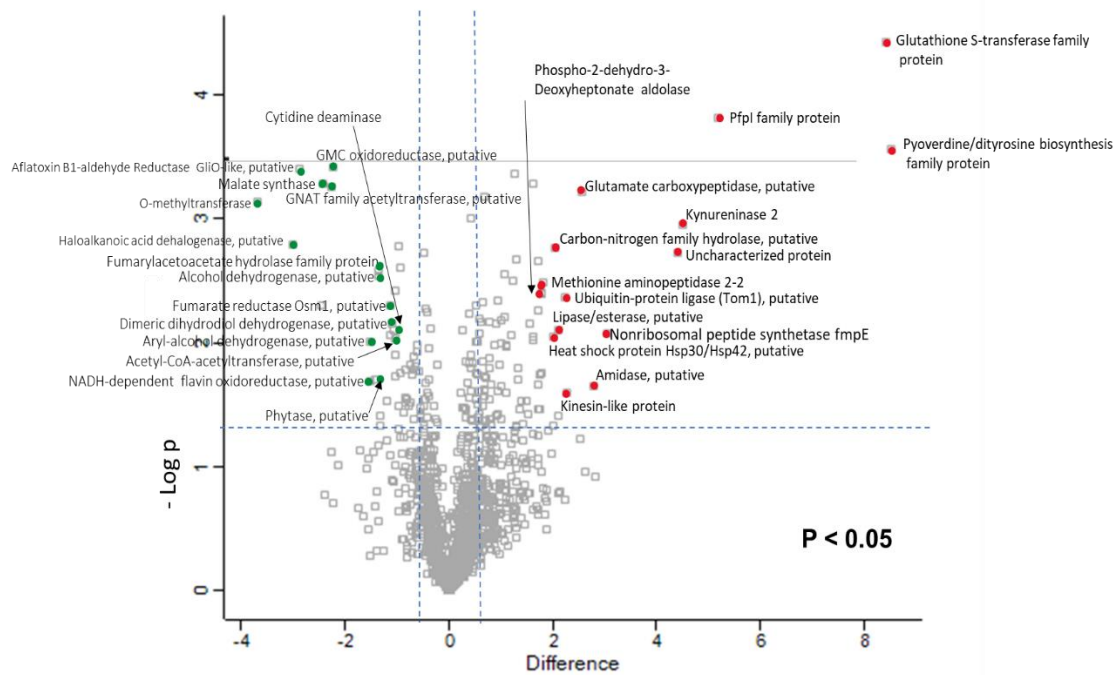


**Figure 4.13:** Volcano plot showing the distribution of quantified proteins according to p value ( $-\log_{10}$  p-value) and fold change ( $\log_2$  mean LFQ intensity difference). Proteins above the horizontal line are considered statistically significant (p value < 0.05) and those to the right and left of the vertical lines indicate relative fold changes  $\pm 1.5$ .

**Table 4.1:** Relative fold changes of proteins increased in abundance in atorvastatin (3 µg/ml) treated *A. fumigatus* and the number of matched peptides, sequence coverage, and overall intensity. Only proteins that had more than two matched peptides and were found to be differentially expressed at a level greater than +1.5-fold were considered to be in significantly variable abundances between control and treated.

N0.	Protein name	Unique peptides	Sequence coverage [%]	Mean LFQ intensity	Fold change
1	Pyoverdine/dityrosine biosynthesis family protein	68	82.7	3.54E+10	8.52
2	Glutathione S-transferase family protein	23	84.8	2.27E+10	8.43
3	ThiJ/PfpI family protein	19	79.2	3.78E+09	5.18
4	Kynureninase	25	76.3	2.34E+09	4.49
5	Uncharacterized protein	26	37.1	1.23E+09	4.41
6	Nonribosomal peptide synthetase fmpE	26	27.3	7.36E+08	3.06
7	Amidase, putative	15	33.1	1.52E+09	2.78
8	Glutamate carboxypeptidase, putative	10	25.6	3.98E+08	2.56
9	Kinesin-like protein	20	50.3	9.62E+08	2.28
10	Ubiquitin-protein ligase (Tom1), putative	46	17.8	7.80E+08	2.24
11	Lipase/esterase, putative	9	48.2	3.66E+08	2.12
12	Polyketide synthase, putative	55	35.7	3.48E+09	2.11
13	Carbon-nitrogen family hydrolase, putative	16	74.5	3.51E+09	2.05
14	Heat shock protein Hsp30/Hsp42, putative	6	38.3	1.51E+09	2.02
15	Phosphatidylinositol transporter, putative	15	54.1	1.16E+09	2.00
16	Methionine aminopeptidase	23	54.9	1.80E+09	1.83
17	Phospho-2-dehydro-3-deoxyheptonate aldolase	12	52.3	3.83E+08	1.80
18	IMP-specific 5'-nucleotidase	12	34.7	4.61E+08	1.80
19	Mitochondrial pyruvate carrier	5	54.4	4.17E+08	1.79
20	U6 small nuclear ribonucleoprotein (Lsm3), putative	3	74.7	5.87E+08	1.77
21	HAD superfamily hydrolase, putative	5	30.2	4.88E+08	1.76
22	ABC multidrug transporter Mdr1	25	26.2	7.22E+08	1.74
23	Amino acid oxidase fmpA	43	73	7.09E+09	1.74
24	Trehalase	21	39.2	7.25E+08	1.73
25	5-demethoxyubiquinone hydroxylase, mitochondrial	6	33.9	2.60E+08	1.73
26	Transcriptional activator	7	28	5.01E+08	1.63
27	Alcohol dehydrogenase, putative	35	80.9	3.35E+10	1.62
28	1,3-beta-glucanosyltransferase Bgt1	8	32.8	5.06E+08	1.61
29	Psi-producing oxygenase A	67	67.6	8.87E+09	1.55
30	Uncharacterized protein	9	30.1	3.67E+08	1.54

**Table 4.2:** Relative fold changes of proteins decreased in abundance in atorvastatin (3 µg/ml) treated *A. fumigatus* and the number of matched peptides, sequence coverage, and overall intensity. Only proteins that had more than two matched peptides and were found to be differentially expressed at a level greater than -1.5-fold were considered to be in significantly variable abundances between control and treated.

<b>N0.</b>	<b>Protein name</b>	<b>Unique peptides</b>	<b>Sequence coverage [%]</b>	<b>Mean LFQ intensity</b>	<b>Fold change</b>
1	O-methyltransferase	15	55.6	1.03E+09	-3.69
2	Haloalkanoic acid dehalogenase, putative	15	92.4	2.39E+09	-3.00
3	Aflatoxin B1-aldehyde reductase GliO-like, putative	13	52.9	4.44E+08	-2.86
4	Allergen Asp f 15	5	40.1	1.07E+09	-2.46
5	Malate synthase	33	59	3.68E+09	-2.41
6	GNAT family acetyltransferase, putative	24	88.3	2.63E+09	-2.26
7	GMC oxidoreductase, putative	26	50.5	3.32E+09	-2.23
8	alcohol dehydrogenase, putative	21	58.1	2.16E+09	-1.53
9	NADH-dependent flavin oxidoreductase, putative	9	38.9	6.52E+08	-1.51

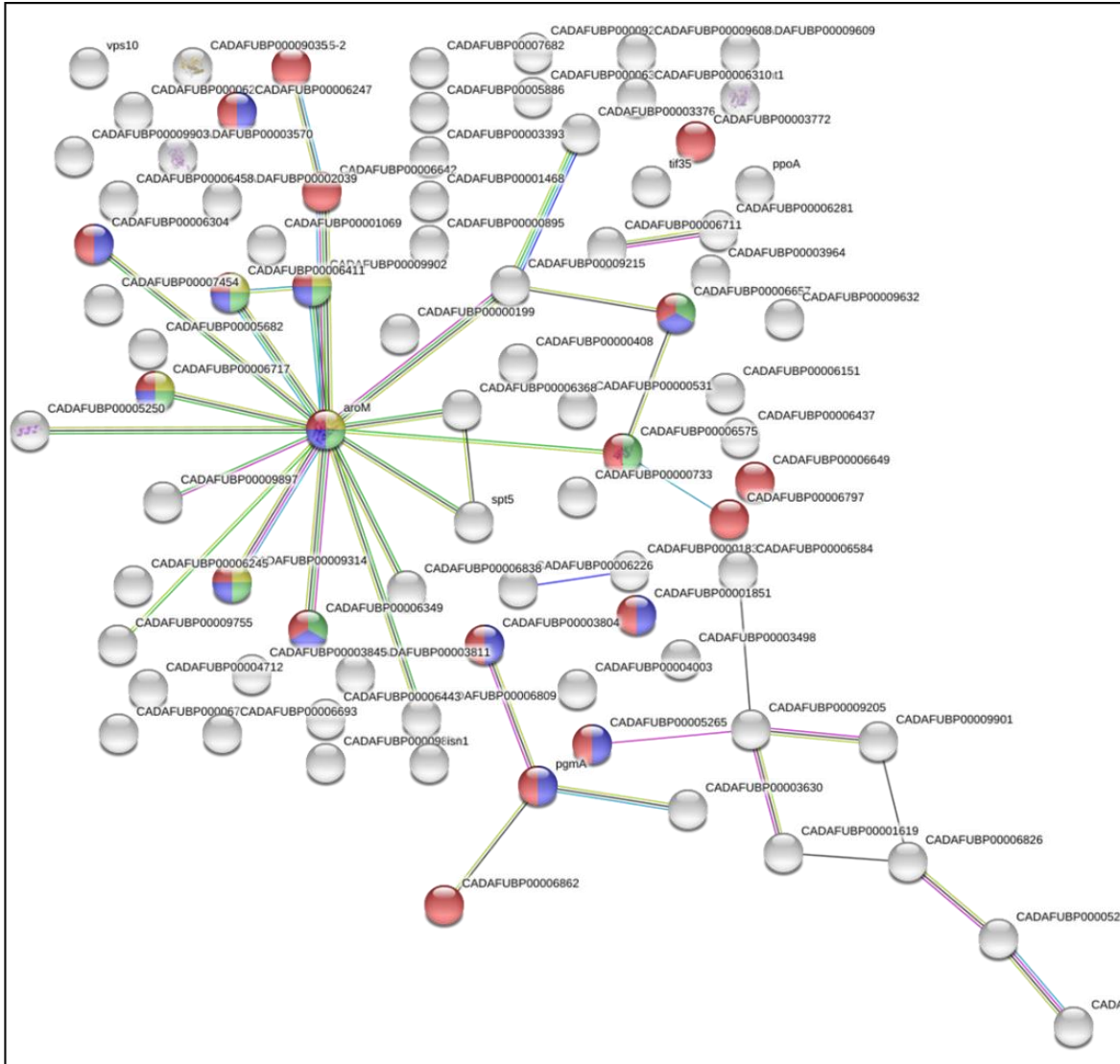


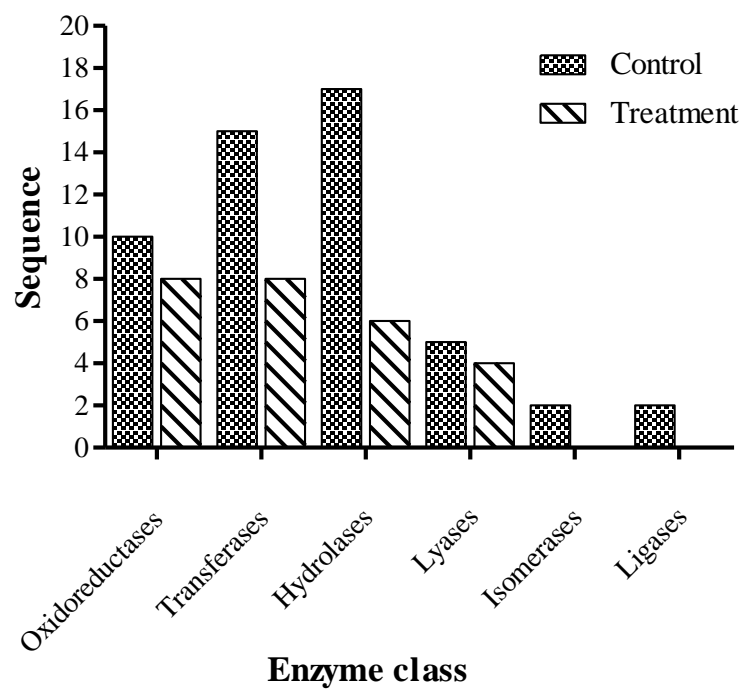
**Figure 4.14:** Interaction network analysis of up regulated proteins in atorvastatin (3 $\mu$ g/ml) treated *A. fumigatus*. Protein interaction information was obtained from the STRING database using gene lists extracted for statistically significant differentially abundant (SSDA) proteins of increased abundance in treated *A. fumigatus*. Statistically enriched KEGG and Gene Ontology (GO) terms were examined to identify pathways and processes enriched within each set of proteins.

Blast2GO annotation software was used to group proteins based on conserved GO terms in order to identify processes and pathways potentially associated with atorvastatin effect. GO terms were categorized by enzyme classes (EC), biological processes (BP), molecular function (MF) and cellular components (CC).

The enzyme classes that altered in abundance of *A. fumigatus* treated with atorvastatin (3 µg/ml) were; oxidoreductases, transferases, hydrolases, lyases, isomerases and ligases (Fig. 4.15). The enzyme class that shows the highest decrease in abundance in *A. fumigatus* exposed to atorvastatin was lyase enzymes class followed by hydrolase enzymes.

In the BP, the most changed process in atorvastatin *A. fumigatus* treatment included proteins labelled as cellular metabolic process (45 proteins in control – 21 proteins in treated *A. fumigatus*), primary metabolic process (45 – 16), nitrogen compound metabolic process (39 - 17), biosynthesis process (28 - 10) and small molecule metabolic process (21 - 13) (Fig. 4.16). The results showed a significant change of biological process. The changes in MF in *A. fumigatus* treatment included proteins labelled in ion binding (32 proteins in control – 20 proteins in treated *A. fumigatus*), small molecule binding (22 - 14), drug binding (18 - 5), hydrolase activity (26-8) and transferase activity (26 -16) (Fig. 4.17). Changes were observed in abundance of molecular function.

The changes in CC in *A. fumigatus* treatment included proteins labelled intracellular part (47 proteins in control – 17 proteins in treated *A. fumigatus*), intracellular organelle (26 - 10), ribonucleoprotein complex (7 - 2), membrane-bounded organelle (93-65), membrane-bounded organelle (22 - 8) and intracellular organelle part (17-5) (Fig. 4.18). The results displayed a difference in protein abundance according to cell component.




---

**Figure 4.15:** Bar chart showing changes to number of proteins involved in enzyme classes at level 3 ontology. Proteins were assigned groups based on involvement in biological processes for control and atorvastatin treated. Open bar: control, closed bar: treated.

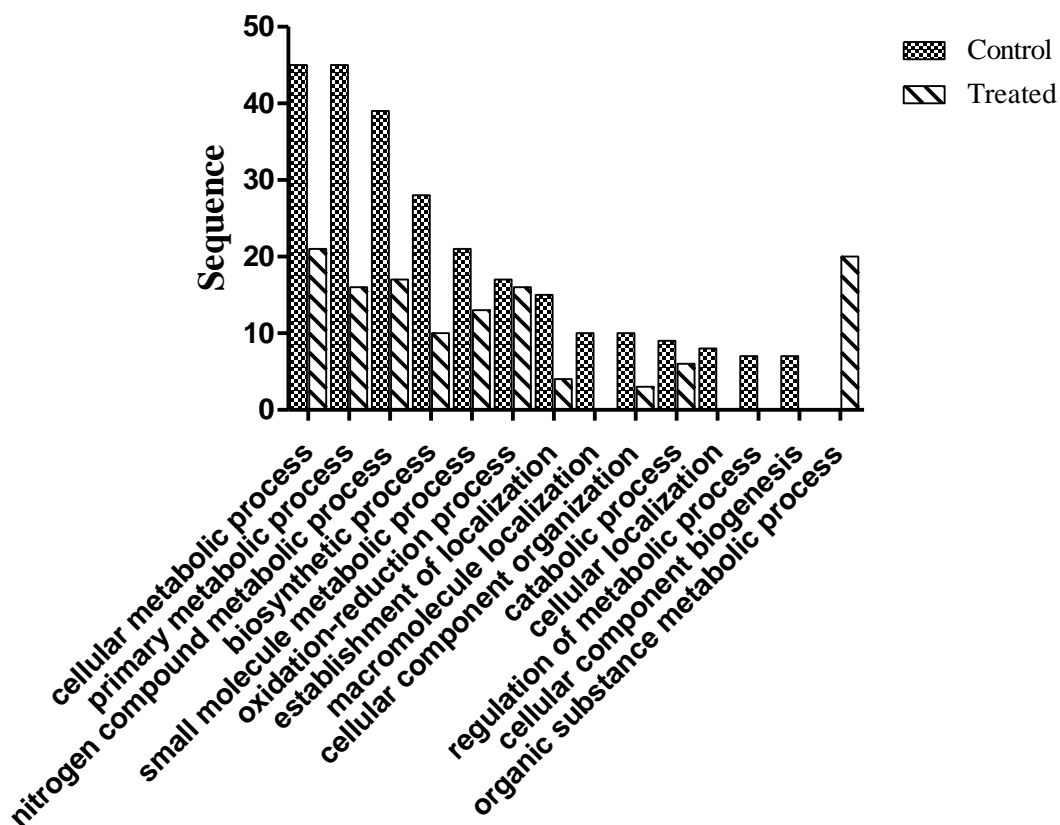


**Figure 4.16:** Bar chart showing changes to number of proteins involved in various biological processes at level 3 ontology. Proteins were assigned groups based on involvement in biological processes for control and atorvastatin treated. Open bar: control, closed bar: treated.

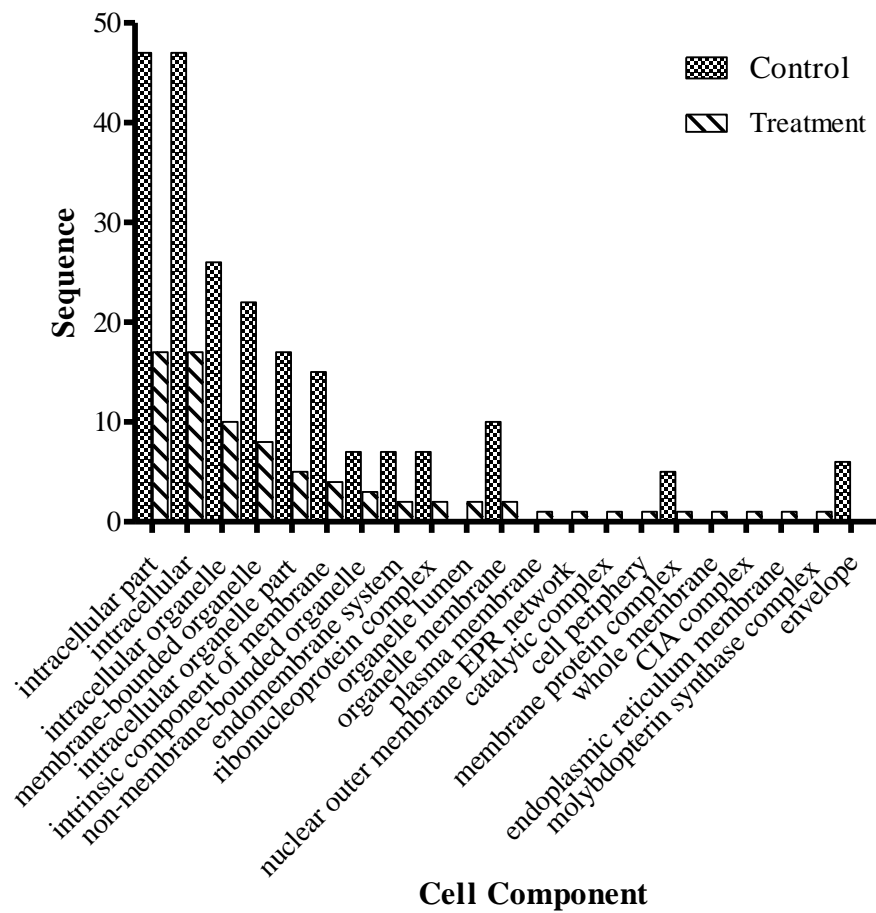


**Figure 4.17:** Bar chart showing changes to number of proteins in various cellular components at level 3 ontology. Proteins were assigned groups based on involvement in cellular components in the total proteome for control and treated.



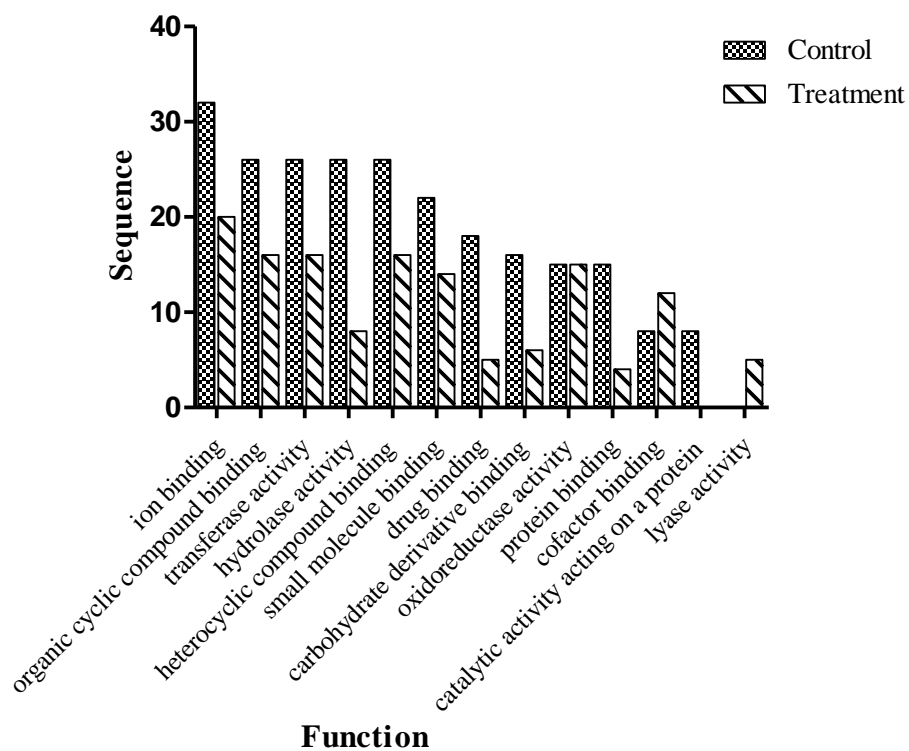


**Figure 4.18:** Bar chart showing changes to number of proteins given various molecular functions at level 3 ontology. Proteins were assigned groups based on involvement in molecular function for control and atorvastatin (3 $\mu$ g/ml) treated *A. fumigatus*. Open bar: control, closed bar: treated.

#### 4.10 Effect of statin on *Galleria* infected with *A. fumigatus*

Atorvastatin (9.09mg/kg) treatment of *G mellonella* larvae infected with *A fumigatus* showed a significant increase in survival of the larvae (Fig. 4.19). After 2 h, infected larvae displayed an increase in survival by 43.3 %  $\pm$  3.3 and after 4 h to 36.6 %  $\pm$  6.6 compared to non-treated sample 3.3 %  $\pm$  3.3.

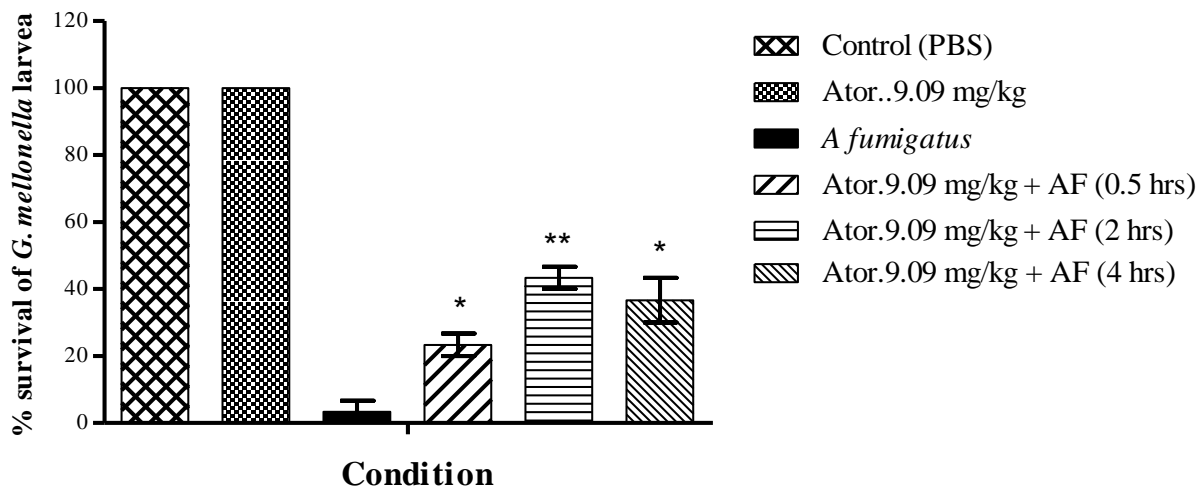


**Figure 4.19:** Effect of atorvastatin on viability of *G. mellonella* larvae infected with *A fumigatus*. Larvae administered a dose of with atorvastatin (9.09 mg/kg) displayed no decrease in survival. Larvae were inoculated with *A fumigatus* ( $1 \times 10^6$ /larva) and followed up 30 mins, 2 h, or 4 h later with atorvastatin (9.09 mg/kg). Atorvastatin treatment enhanced larval survival relative to non-treated larvae.

#### 4.11 Discussion

Statins, 3-hydroxymethyl-3-methylglutaryl coenzyme A (HMG-CoA) reductase inhibitors, belong to a group of drugs that are able to inhibit a key enzyme in the cholesterol biosynthesis (Kotyla, 2010) (Corsini *et al.*, 1998). Sterols are constituents of the cellular membranes that are essential for their normal structure and function (de Souza and Rodrigues, 2009). Cholesterol in mammals and ergosterol in fungi have similar structure and biosynthetic pathways consequently both pathways are sensitive to the same inhibitory effects of statins (Camélia Stancu and Sima, 2001). Patients on statin therapy display less fungal infections thereby encourage the suggestion that statins may have potential effects as anti-fungal agents *in vivo* (Sun and Singh, 2009) (Galgóczy, 2011). Statins exhibit antifungal properties *in vitro*, but the concentrations used in these experiments are dramatically high, and also statins have effects on fungal physiology beyond direct growth inhibition (Bergman and Björkhem-Bergman, 2013). This raises the possibility that statins, in addition to being used to control cholesterol levels, may also be used in the control of fungal infections either as sole therapies or in combination with existing antifungal therapies (Galgóczy, 2011). They also have synergistic interactions with antimicrobial agents (Sun and Singh, 2011). The information presented in Qiao *et al.*, (2007), suggests that statins do inhibit the growth of *A. fumigatus*. This was concluded as *A. fumigatus* cultures grown in the presence of statin showed reduced growth. A second study, (Macreadie *et al.*, 2006a), showed that *A. fumigatus* that had been treated with statin also had inhibited growth through a reduction in ergosterol level. Both of these results are based on the growth of *A. fumigatus* in solid media that had been treated with statin. None the less, both studies show that statin interrupts the production of ergosterol by interacting with its precursor farnesyl diphosphate (Macreadie *et al.*, 2006). The results of this study correlate with the results of both previous studies.

The work presented here evaluated the interaction of atorvastatin with *A. fumigatus* and demonstrated the *in vivo* activity of the statin against *A. fumigatus* infection in *G. mellonella* larvae. The determination of susceptibility of *A. fumigatus* to a serial dilution of atorvastatin (200 µg/ml) stock solution showed that atorvastatin does inhibit the growth of *A. fumigatus*. However, the combination of atorvastatin (3 µg/ml) and the serial dilution of amphotericin B (6.25 µg/ml), caspofungin (3.75 µg/ml), miconazole (250 µg/ml) or DMSO (µg/ml) stock solutions showed a significant decrease in the percentage growth of *A. fumigatus* when the atorvastatin combined with amphotericin B and DMSO  $P > 0.05$  and  $P < 0.01$  respectively, increase in *A. fumigatus* growth in combined of atorvastatin and miconazole and in terms of caspofungin no significant changes. These results indicated that the atorvastatin has a synergistic effect in combination with amphotericin B against *A. fumigatus*. Sterol analysis conducted during this project showed that atorvastatin does inhibit the amount of ergosterol produced. Results present a reduction in the amount of ergosterol produced from *A. fumigatus* that were treated with atorvastatin (3 µg/ml) at 72 h in liquid cultures compared to nontreated culture. This would support Macreadie *et al.*, (2006), in suggesting that statin does inhibit ergosterol synthesis in *A. fumigatus*, and therefore the growth. Statins reduce cholesterol biosynthesis *in vivo* (Matilde Manzoni and Rollini, 2002). Exposure of *A. fumigatus* to atorvastatin reduced fungal growth and induced increased membrane permeability as evidenced by increased release of protein and amino acids. Maximum amino acid and protein leakage occurred in the 3 µg/mL treatment at 6 h and this concentration may be optimal for this effect. Analysis of the fungal biomass produced from liquid cultures of *A. fumigatus* treated with atorvastatin showed that the biomass decreased in response to increase in the atorvastatin concentration, this indicates that the *A. fumigatus* are sensitive to atorvastatin. In addition, staining cells with calcofluor following exposure to atorvastatin (3 µg/ml) for 24 h showed an increase in

hyphal condensation and shows thinner hyphae in atorvastatin treatment than in the control sample. This indicates that the cells under stress and started to protect themselves by changing the biological process to withstand the environment changes.

Cultures treated with atorvastatin also released elevated levels of gliotoxin, which also has been observed in *A. fumigatus* exposed to amphotericin B and may indicate an oxidative stress response (Reeves *et al.*, 2004). *A. fumigatus* under stress, produces more gliotoxin than if it was not under stress (Belkacemi *et al.*, 1999). Depletion of the intracellular gliotoxin concentration may increase the biosynthesis of the toxin to recover the lost gliotoxin in order to restore the redox balance within the cell. (Schrettl *et al.* 2010). This phenomenon of gliotoxin leakage has the potential to contribute to elevated levels of pulmonary damage and immunosuppression (Tsunawaki *et al.*, 2004). It is possible that administration of atorvastatin to patients may lead to eventual fungal cell death but that before this is achieved internal gliotoxin would be released from cells and the cells could have the opportunity to commence synthesizing more toxins to recover that which is lost into the surrounding tissue. Previous work that examined the response of *A. fumigatus* to amphotericin B illustrated the ability of cells to recover from antifungal therapy even though they appeared incapable of replicating in culture thus highlighting the possibility of continued cell survival in the presence of fungicidal concentrations of drug (Liao *et al.*, 1999). An analysis of gliotoxin in *A. fumigatus* control and atorvastatin (6 µg/ml) treatment would give an idea of the atorvastatin increased stress in the cells. The results display that the sample treated with 1.5 and 6 µg/ml of atorvastatin for 72 h produced more gliotoxin in the treated samples compared to the control sample. Exposure *A. fumigatus* to atorvastatin in combination with amphotericin B (0.4µg/ml) under the same conditions, results in less gliotoxin release in the case of atorvastatin and more gliotoxin release in case of exposure only to amphotericin B. The result illustrates that

*A. fumigatus* appears to overcome the presence of atorvastatin and is capable of produce gliotoxin and also the results indicate that *A. fumigatus* cells more sensitive to gliotoxin release in the case of atorvastatin treatment. Proteomic analysis revealed an increased abundance of a range of proteins involved in dealing with oxidative stress, including pyoverdine/dityrosine biosynthesis (+8.52-fold), 5 demethoxyubiquinone hydroxylase, mitochondrial (+1.74-fold) and alcohol dehydrogenase (+1.61fold). In *Saccharomyces cerevisiae*, dityrosine is a major component of the spore wall surface and plays a role in the resistance of ascospores to environmental stress (Neiman, 2005). Furthermore, the glutathione Stransferase family protein is increased in abundance (+8.43-fold), and this protein functions to detoxify xenobiotics. The fumipyrrole biosynthetic (*fmpE*) protein was also increased in abundance (+3.06-fold). Deletion of *fmpE* in *A. fumigatus* resulted in reduced growth and sporulation of the mutant strains but virulence was not altered as compared to the WT strain in a murine infection model (Macheleidt *et al.*, 2015). A range of heat shock proteins, such as Hsp30/Hsp42 (+2.02-fold), also increased in abundance in response to atorvastatin. Heat shock proteins play an important role in adaptation of the fungal cell to environmental and chemical stresses (Tamayo *et al.*, 2013). *A. fumigatus* heat shock proteins are also immune-dominant and elicit strong humoral immune responses (Kumar *et al.*, 1993). Proteomic analysis also revealed the reduced abundance of a number of peptides associated with virulence, including aflatoxin B1 (-2.86-fold) and allergen Asp f 15 (-2.45-fold). Asp f 15 is cell-wall associated and its decreased abundance could be due to an altered cell-wall composition as a result of an altered membrane composition. Statins inhibit the growth of *A. fumigatus* and supplementation of media with ergosterol or cholesterol blocked the growth-inhibiting effect of atorvastatin, thus indicating the specificity of statins for the mevalonate synthesis pathway (Macreadie *et al.*, 2006a). However, another study found that statins were fungistatic against *A.*

*fumigatus*, but the MICs were greater than the clinically achievable concentrations (Qiao *et al.*, 2007). Furthermore, a variety of *Candida* strains that were resistant to fluconazole and nystatin were all sensitive to atorvastatin (Esfahani *et al.*, 2019). Atorvastatin combined with fluconazole improved cryptococcosis caused by *Cryptococcus gattii* and mice treated with atorvastatin had increased survival and better clinical outcomes; this was mediated via modifications in the capsule and cell membrane in the presence of a statin that induced cell death within phagocytes (de Queiroz Ribeiro *et al.*, 2017).

Larvae of *G. mellonella* can be employed to assess the virulence of fungal pathogens (Brennan *et al.*, 2002, Fuchs and Mylonakis, 2006) and for determining the *in vivo* activity of antifungal agents (Kavanagh and Sheehan, 2018; Maurer *et al.*, 2015). Their use displays the chance of quickly establishing the *in vivo* toxicity and effectiveness of antimicrobial agents without the need to resort to the use of mammals in initial screening research. In the work presented here atorvastatin was shown to be non-toxic to larvae and to be able to protect larvae following infection with *A. fumigatus*. The doses used in larvae was 9.09 mg/kg. The results presented here indicate that atorvastatin has a profound effect on *A. fumigatus* and reduced its ability to grow and increases its susceptibility to killing in the *G. mellonella* larval model system. While the anti-microbial activity of statins is well established this work demonstrates how they interact with the fungal proteome to induce their effects and highlight their ability to retard proliferation *in vivo*. The continuing problems associated with existing antifungal therapies (e.g. toxicity, drug resistance) offer the possibility of employing an active, non-toxic therapy such as atorvastatin to supplement existing therapies (Galgóczy, 2011; Nyilasi *et al.*, 2010a).

## **Chapter 5**

### **Analysis of the effect of Atorvastatin**

#### **on *Galleria mellonella* larvae**



## 5.1 Introduction

*Galleria mellonella*, the greater wax moth or honeycomb moth, is a moth of the family *Pyralidae* (Park *et al.*, 2017). The moth is spread throughout the world, including Asia, Europe and North America (Park *et al.*, 2017). The size of the *G. mellonella* larvae (range between 1.5 - 2.5 cm) enables an easy means of inoculation with specific amounts of drug or pathogen via the pro-leg (Fig. 2.6) making *G. mellonella* more amenable to drug pharmacodynamics studies (Kavanagh and Fallon, 2010). Wax moth (*G. mellonella*) larvae are economic, survive at 37°C and require no specialist equipment, they are considered as a viable alternative to other models of infection (Kay *et al.*, 2019). Their economic importance has led to a number of investigations on their biology, molecular biology, ecology, physiology, and behavior. Wax moth larvae are widely used as model organisms for research in insect physiology and human pathogens (Browne and Kavanagh, 2013). In *G. mellonella*, antimicrobial effects and pathogen virulence testing can be analysed by using a number of parameters including the degree of melanisation in response to a pathogen, larval death, quantification of fungal load, changes in haemocyte densities and changes in antimicrobial peptide expression (Bergin *et al.*, 2003). *G. mellonella* are able to be used *in vivo* as models as they have a high throughput (Cotter *et al.*, 2000) and can be incubated between 30 - 37°C enabling possible temperature-dependent virulence factors to be studied (Mowlds and Kavanagh, 2008). It is also possible to evaluate phagocytic cell function and immune responses to set the virulence of pathogens (Cotter *et al.*, 2000). This initial concept in the study of fungal virulence was developed further by Brennan *et al.*, (2002) with the discovery of a direct correlation between the virulence of *C. albicans* mutants in BalbC mice and *G. mellonella* larvae. *G. mellonella* larvae were used to assess the virulence of *C. albicans* and to investigate the virulence of pathogenic and non-pathogenic yeast species (Cotter *et al.*, 2000). Slater *et al.*, (2011)

demonstrated a strong correlation between the virulence of *A. fumigatus* mutants in larvae and mice. Fallon *et al.*, (2011) and Renwick *et al.*, (2007) established the actions of immunosuppressive molecules such as gliotoxin and fumagillin released from the fungus *A. fumigatus* on phagocytic functions. The immune system of *G. mellonella* shows functional and structural similarities to the innate immune response of mammals (Mylonakis *et al.*, 2005) (Browne and Kavanagh, 2013) (Binder *et al.*, 2016) and (Kay *et al.*, 2019). *G. mellonella* larvae have also been utilized for assessing the *in vivo* activity of amphotericin B, flucytosine and fluconazole following challenge with *C. neoformans* (Mylonakis *et al.*, 2005) and to evaluate the antifungal properties of novel silver-based compounds (Rowan *et al.*, 2009). Maguire *et al.*, (2016) established that *G. mellonella* larvae may be used as a model to assess the relative toxicity of food preservatives. Administration of silver nitrate (Rowan *et al.*, 2009), glucan (Mowlds *et al.*, 2010) or caspofungin (Kelly and Kavanagh, 2011) to *G. mellonella* larvae induces a nonspecific immune response which operates in parallel with the antifungal activity of the introduced agent. Caffeine is metabolized in a similar way in *G. mellonella* larvae to that in mammals and results in a variety of behavioral and developmental alterations (Maguire *et al.*, 2017). Clearly the use of *G. mellonella* is a highly advantageous approach in the study and research of microbial pathogenesis and chemotherapy however the characterization of alterations to the immunological profile of larvae is warranted in order to fully utilize this model. This chapter studied the effect of atorvastatin on *G. mellonella* larvae and analysed the proteomic responses to atorvastatin exposure.

### **5.1.1 Melanisation**

The melanisation reaction is a common response to parasite entry in invertebrate animals, especially arthropods, is due to the activity of an oxidoreductase, phenoloxidase. Prophenoloxidase shows similar sequence regions to vertebrate complement proteins C3 and C4 (Söderhäll and Cerenius, 1998). The prophenoloxidase activating system in a non-self-recognition system that leads to the deposition of melanin on microbial surfaces. The recognition of foreign material such as lipopolysaccharides by pathogen recognition receptors activates the phenoloxidase cascade. Monophenyl L-dopa oxygen oxidoreductase, also known as phenoloxidase, is an enzyme that catalyses the oxidization of phenols to quinones. These quinones are then polymerized non-enzymatically to melanin (Söderhäll and Cerenius, 1998).

### **5.1.2. Haemocytes**

Haemocytes are found freely in the haemolymph or adhering to internal organs like the fat body or the digestive tract of the insect and can be rapidly mobilised upon breach of the cuticle or entry of a pathogen. In order for phagocytic cells to engulf and kill pathogens, haemocytes must first recognize invading pathogens and this pathogen recognition mechanism shows further similarities in both insects and mammals (Kavanagh and Reeves, 2004). Phagocytosis in insects is known to be lectin mediated and is similar to what occurs in human neutrophil (Kavanagh and Reeves, 2004). The insect haemocyte shows structural and functional similarities to the mammalian neutrophil in that both can phagocytose and neutralize engulfed pathogens through the generation of superoxide and the secretion of lytic enzymes in the process known as degranulation (Renwick *et al.*, 2007, Browne *et al.*, 2013).

## 5.2 Effect of atorvastatin on *C. albicans* infected *G. mellonella*

The effect of atorvastatin on *C. albicans* infected *G. mellonella* is presented (Fig.5.1 A and B). At 24 h the average survival of larvae in negative control group was 100% and in case of atorvastatin treated group was  $67.83 \pm 0.16$  % compared to positive control which was  $19.5 \pm 0.5$  %. After 48 h the average survival of larvae of the negative control group was  $95.8 \pm 0.089$  and in case of atorvastatin treated group was  $46.83 \pm 0.16$  compared to positive control which was  $3.07 \pm 0.3$  % at the same time. The results displayed that the atorvastatin decreased ability of *C. albicans* to kill *G. mellonella* larvae (Fig 5.1 A).

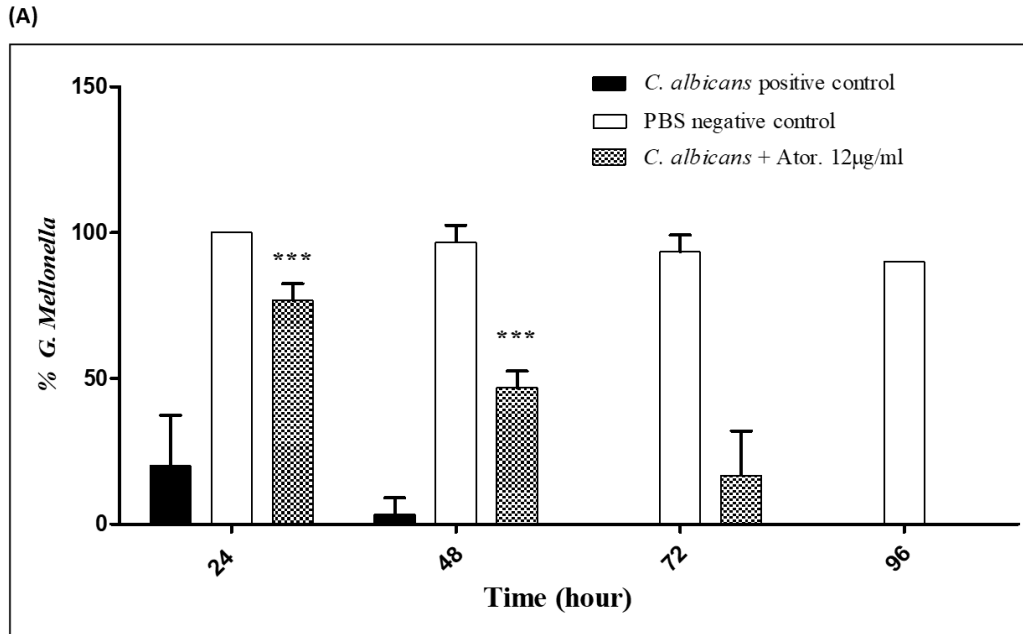


**Figure 5.1A:** Effect of atorvastatin on viability of *G. mellonella* larvae infected with *C. albicans*. Viability was monitored over 96 h. Larvae injected with atorvastatin (12 µg/ml) treated *C. albicans* culture displayed decrease in ability to kill *G. mellonella* larvae. Atorvastatin treatment enhanced larval survival relative to non-treated larvae. (\*\*\*,  $p < 0.0001$ ).

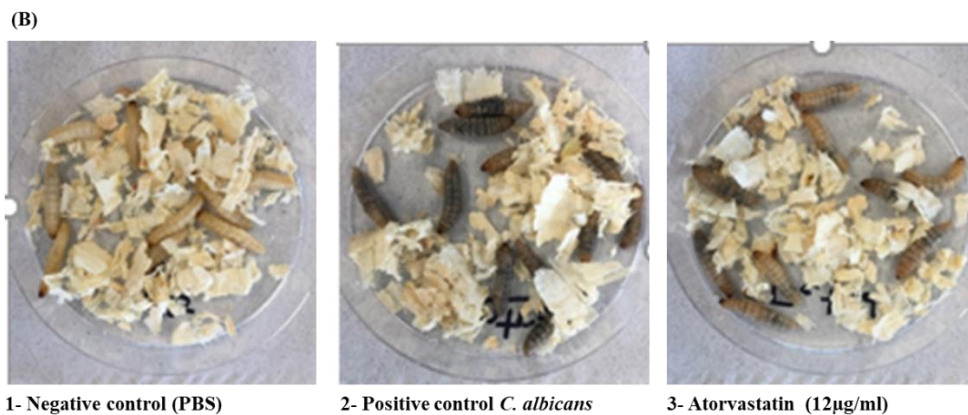


**Figure 5.1B:** Effect atorvastatin on *G. mellonella* larvae infected with *C. albicans* and extent of melanisation over 48 h. Group 1 (10 larvae) negative control were injected with 20µl PBS, group (10 larvae) positive control were injected with 20µl *C. albicans* cells ( $1 \times 10^6$ ) and group 3 (10 larvae) were injected with *C. albicans* cells ( $1 \times 10^6$ ) and atorvastatin (12 µg/ml).

### **5.3 Quantification of atorvastatin of injected *G. mellonella* larvae by using HPLC**

Atorvastatin concentration in larvae was determined by reversed phase-HPLC (Agilent 1200 Series). Atorvastatin extract (20  $\mu$ l) was injected onto a C18 Hewlett Packard column. The results showed that the quantity of atorvastatin was decreased. The two groups of larvae that are administered atorvastatin (5 and 10 mg/ml), the atorvastatin concentration after 6 h became 0.205 and 0.279 mg/ml respectively compared to the samples of zero time which were 2.76 and 5.86 mg/ml respectively (Fig. 5.2). The results demonstrated that a significant interaction between treatment and time, due to the possible metabolism of atorvastatin by *G. mellonella* larvae.

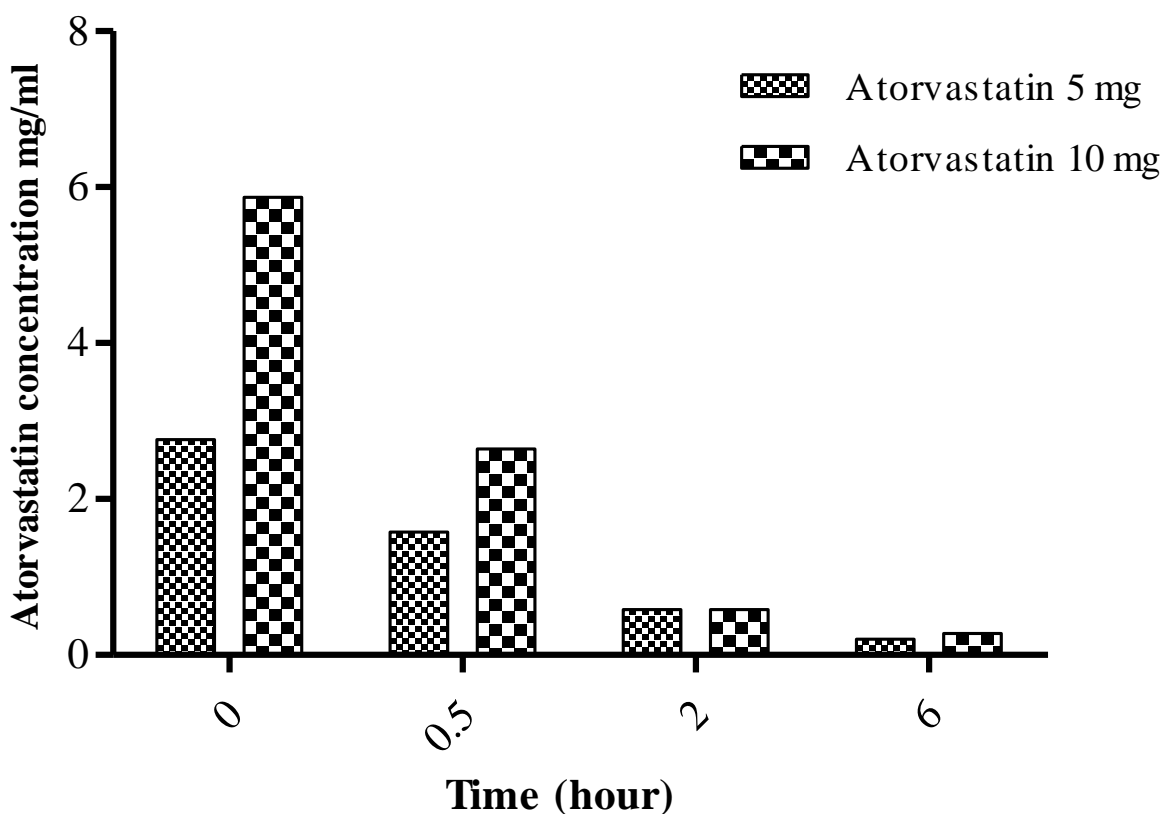


**Figure 5.2:** *G. mellonella* inoculated by intra-hemocoel injection with atorvastatin (5 and 10 mg/ml). Atorvastatin quantification was performed using a HPLC. The standards atorvastatin was used to calibrate the instrument. (\*\*\*:  $P < 0.001$ ).

#### 5.4 Determination of fungal load in *G. mellonella* larvae

Larvae were inoculated by intra-hemocoel injection with  $5 \times 10^5$  yeast cells of control and treated culture and incubated at  $30^\circ\text{C}$  as described in chapter two. At different time point (1, 2, 3,4 and 24 h), 3 larvae were homogenized using a pestle and mortar in 3 ml of sterile PBS. This was serially diluted with PBS, and 100  $\mu\text{l}$  aliquots of the resulting dilutions were plated on YEPD plates containing erythromycin and incubated at  $30^\circ\text{C}$ . After incubation of 48 h the results (Fig. 5.3)

showed that the decrease in the cell density of atorvastatin treatment sample compared to the control sample. The yeast cell density in infected larvae at 1h was  $5.6 \times 10^4 \pm 3.1 \times 10^3/\text{ml}$  compared to the control growth which was  $6.4 \times 10^4 \pm 2.8 \times 10^3/\text{ml}$ . By 24 h was  $6.2 \times 10^5 \pm 2.4 \times 10^4/\text{ml}$  relative to control  $7.8 \times 10^5 \pm 3.5 \times 10^4/\text{ml}$ . The result indicated that the atorvastatin inhibits growth of *C. albicans*.

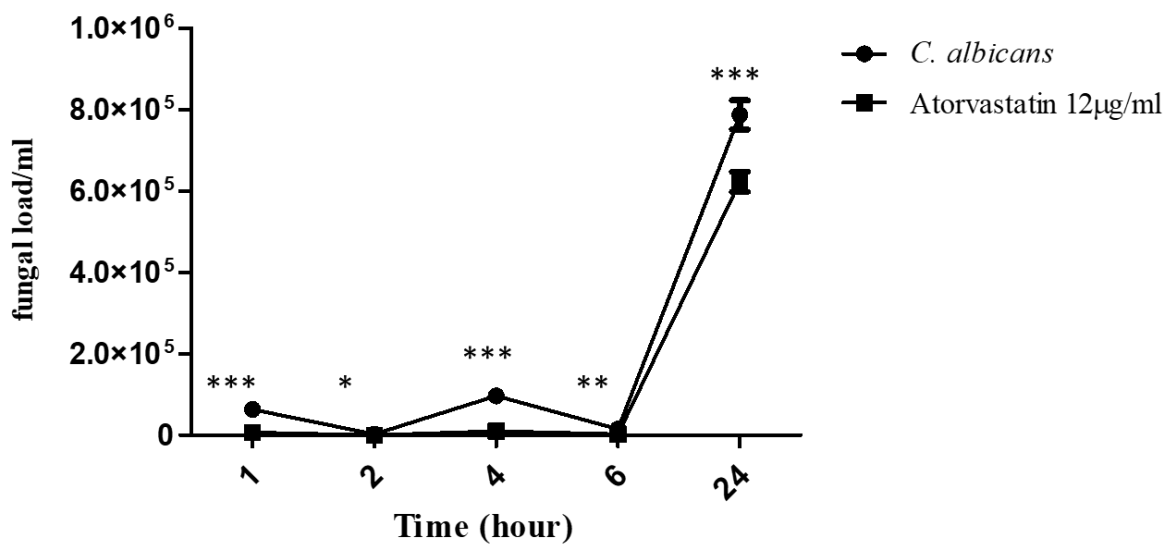


**Figure 5.3:** Determination of fungal load in *G. mellonella* larvae. Survival of larvae and fluctuations in fungal cell density in *C. albicans* infected larvae. All values are the mean  $\pm$  SE of three independent replicates. (\*\*\*,  $p < 0.001$ ).

### 5.5 Determination of haemocyte density

Larvae were inoculated by intra-hemocoel injection with different concentration of atorvastatin (25, 50, 100, and 200 µg/ml) and were incubated at 30 °C for 24 h. The results demonstrated no significant changes in haemocyte density following administration of atorvastatin (25 and 100



$\mu\text{g/ml}$ ). At atorvastatin (50 and 200  $\mu\text{g/ml}$ ) the haemocyte number was  $83 \pm 3.6 \times 10^5$  and  $86.3 \pm 5.5 \times 10^5$  respectively compared to control  $62.6 \pm 4.3 \times 10^5$  (Fig. 5.4). The results showed a small increase in number of haemocytes compared to the control.

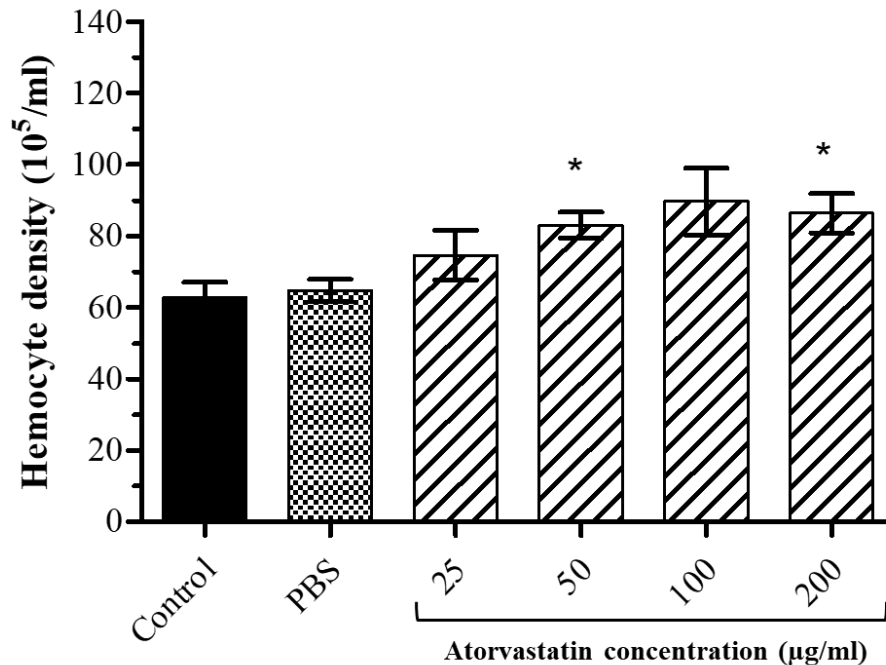


**Figure 5.4:** The effect of atorvastatin on hemocytes densities of *G. mellonella* larvae. Larvae were inoculated by intra-hemocoel injection with different concentration of atorvastatin (25, 50, 100, and 200  $\mu\text{g/ml}$ ) and were incubated at  $30^\circ\text{C}$  for 24 h. Changes in haemocyte density in response to Atorvastatin. (\*;  $p < 0.05$ )

### 5.6 Determination of response of atorvastatin treated *C. albicans* cell to haemocytes.

*C. albicans* cells were grown in the presence of atorvastatin ( $12\mu\text{g/ml}$ ) for 24 h. Hemocytes were extracted from larvae and incubated at a density of  $1 \times 10^5/\text{ml}$  at  $30^\circ\text{C}$  in PBS in a thermally

controlled stirring chamber. Cell free hemolymph opsonized *C. albicans* ( $2 \times 10^5$  cells) was added and killing was measured as described previously by diluting and plating yeast cell suspensions onto YEPD agar plates. Plates were incubated, and the resulting number of colonies enumerated. Results (Fig. 5.5) displayed that the significant increase in percent *C. albicans* viability of atorvastatin treatment relative to non-treatment. After 20 min the percentage of viability increased from  $53.83 \pm 5.199$  % of *C. albicans* control sample to  $76.70 \pm 5.205$  % of treated sample ( $p < 0.05$ ). And at 60 min increased to  $55.74 \pm 6.356$  % compared to control which was  $32.85 \pm 2.891$  was ( $p < 0.05$ ).

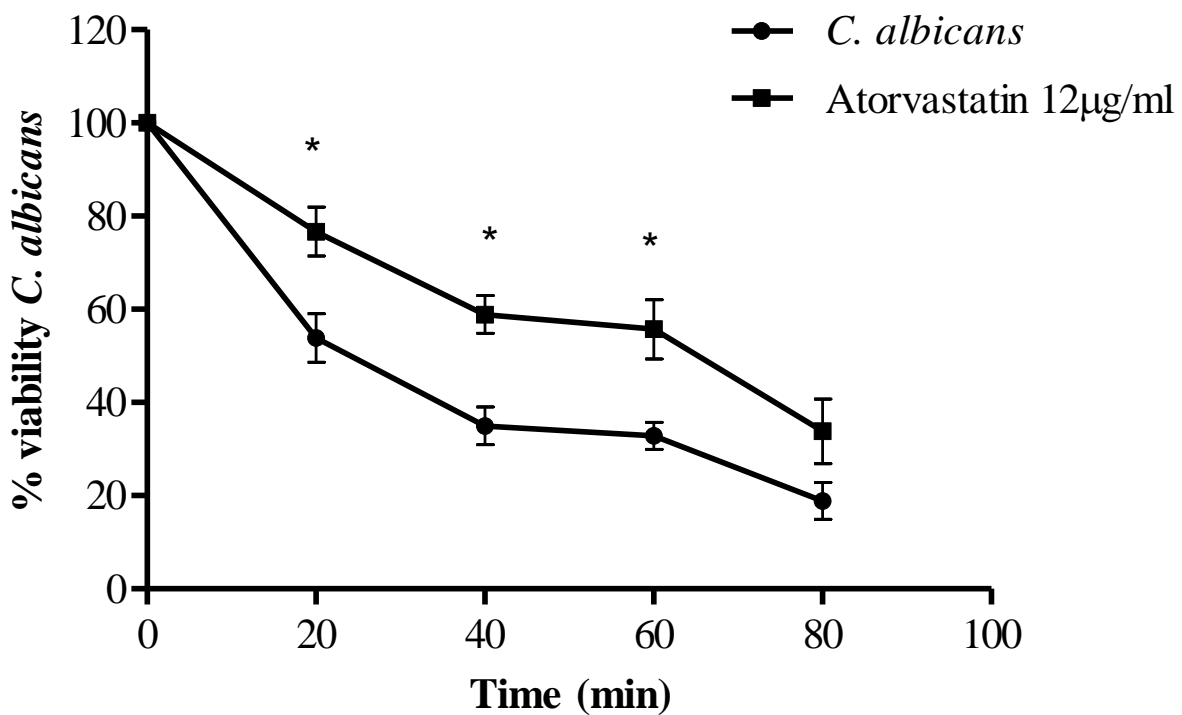


**Figure 5.5:** Response of atorvastatin (12µg/ml) treated *C. albicans* cell to hemocytes at different time points (0, 20, 40, 60 and 80 minutes). Results displayed that the percent of colony count were decreased by time. (\*:  $p < 0.05$ ).

## **5.7 Label-free Proteomic analysis of response of *G. mellonella* to atorvastatin**

### **5.7.1 Administration of atorvastatin to *G. mellonella* larvae by intra haemocoel injection**

Proteomic analysis of atorvastatin injected *G. mellonella* larvae revealed 1601 peptides representing 112 proteins and only one protein was determined in different abundance with fold change of  $> 1.5$  of which, this protein was increased in abundance. The peptides were subsequently used to statistically analyse the total differentially expressed group after imputation of the zero values as described and were then included in statistical analysis after data imputation. A principal component analysis (PCA) (Fig. 5.6) was performed on all filtered proteins and clearly distinguished the control and atorvastatin treated *G. mellonella* larvae samples. The heat maps also show major differences in the relative abundance of proteins in the control and atorvastatin treated cells (Fig. 5.7). The volcano plot shows the relative distribution of these proteins (Fig. 5.8). The only protein increased in abundance (Table 5.1) was apolipoporphins (+ 5.66-fold).

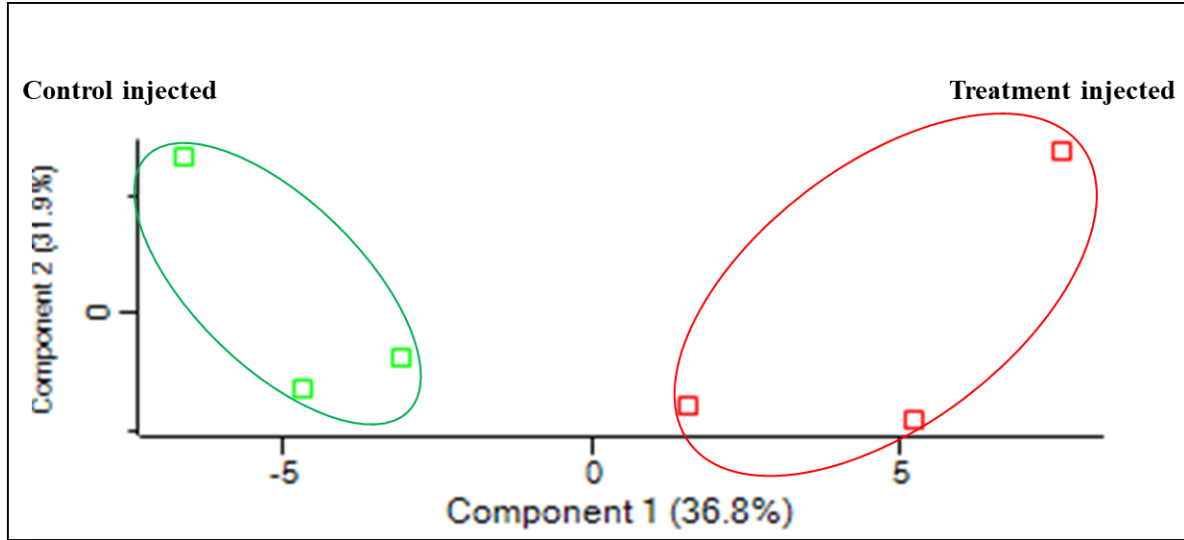


**Figure 5.6:** Principal component analysis of control *G. mellonella* larvae and intra haemocoel atorvastatin injected *G. mellonella* larvae for 24 h showing a clear distinction between control and treatment.

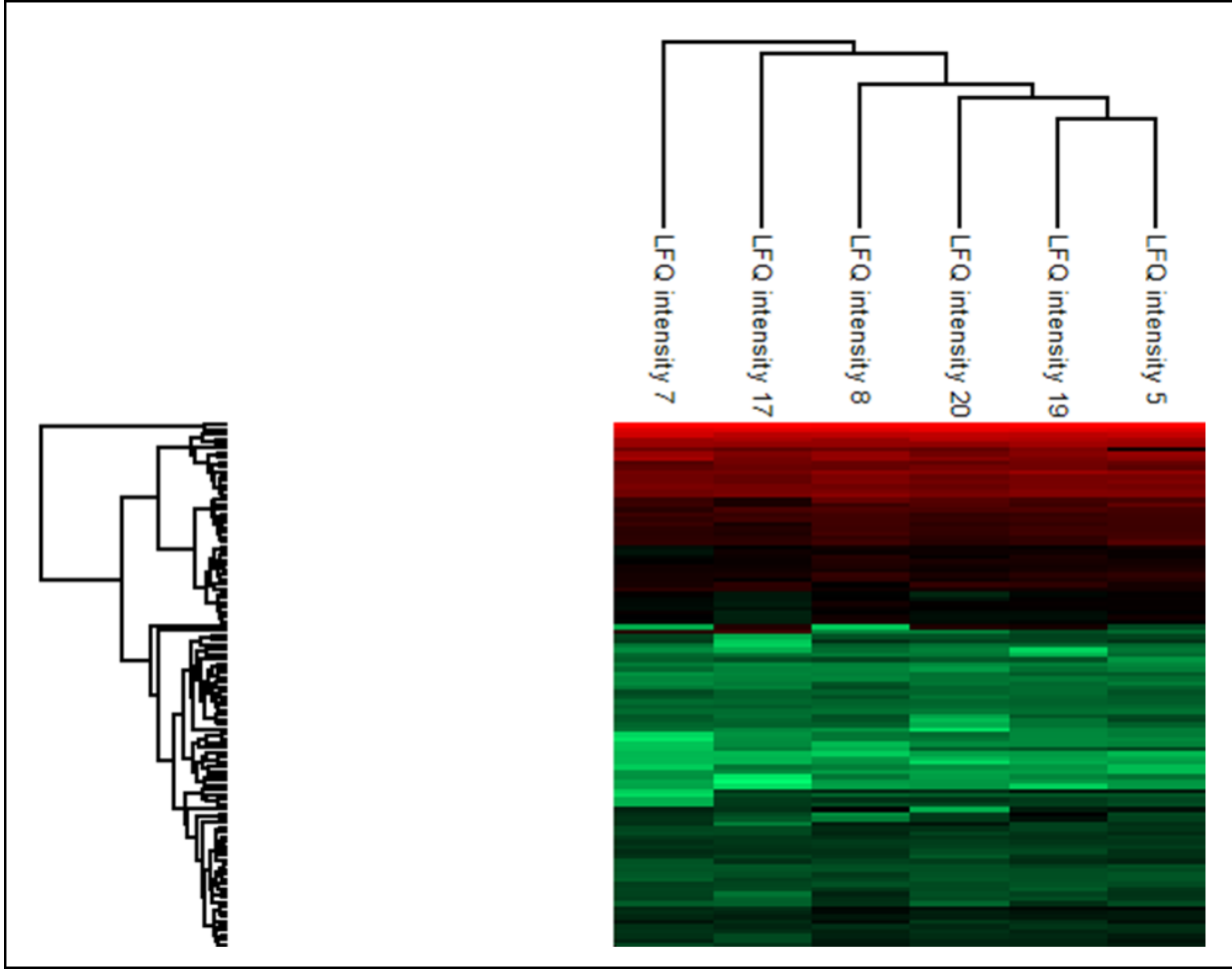


**Figure 5.7:** Two-way unsupervised hierarchical clustering of the median protein expression values of all statistically significant differentially abundant proteins from *G. mellonella* control (5, 7 and 8) and intra haemocoel atorvastatin injected *G. mellonella* larvae (17, 18 and 20).

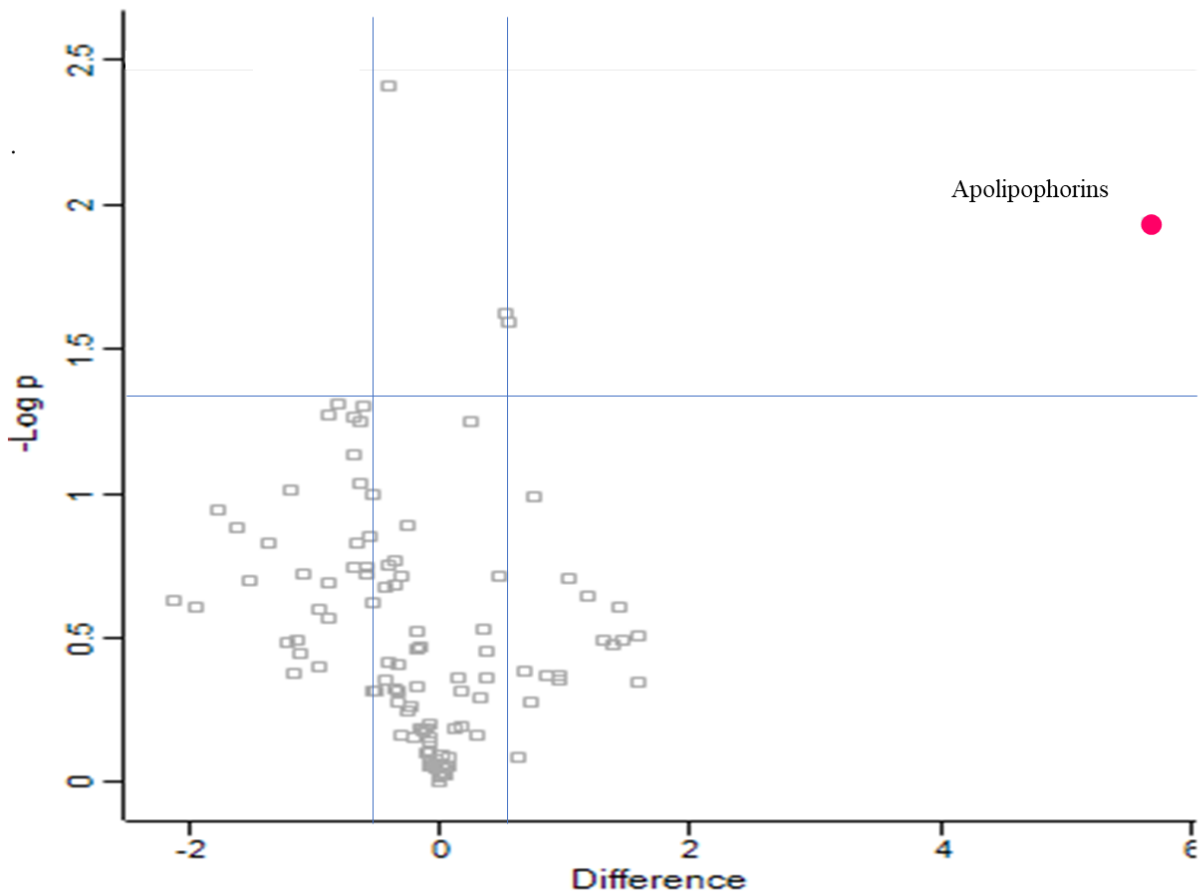


**Figure 5.8:** Volcano plot showing the distribution of quantified proteins according to p value ( $-\log_{10}$  p-value) and fold change ( $\log_2$  mean LFQ intensity difference). Proteins above the horizontal line are considered statistically significant (p value  $< 0.05$ ) and those to the right and left of the vertical lines indicate relative fold changes  $\pm 1.3$ .

**Table 5.1:** Relative fold changes of proteins increased in abundance of intra haemocoel atorvastatin injected *G. mellonella* larvae and the number of matched peptides, sequence coverage, and overall intensity. Proteins had more than two matched peptides and were found to be differentially expressed at a level greater than  $\pm 1.5$ -fold were considered to be in significantly variable abundances between control and treated larvae.

<b>N0</b>	<b>Protein name</b>	<b>Unique peptides</b>	<b>Sequence coverage [%]</b>	<b>Mean LFQ intensity</b>	<b>Fold change</b>
1	Apolipoporphins	3	22.1	3.57E+10	5.66

### 5.7.2 Administration of atorvastatin to *G. mellonella* larvae by force feeding

Proteomic analysis of atorvastatin force feeding *G. mellonella* larvae revealed 1785 peptides representing 132 proteins and 21 proteins were determined in different abundance with fold change of  $> 1.5$  of which 1 were increased in abundance and 20 were decreased in abundance. These proteins were subsequently used to statistically analyse the total differentially expressed group after imputation of the zero values as described and were then included in statistical analysis after data imputation. A principal component analysis (PCA) (Fig. 5.9) was performed on all filtered proteins and clearly distinguished the control and atorvastatin treated *G. mellonella* larvae samples. The heat maps also show major differences in the relative abundance of proteins in the control and atorvastatin treated cells (Fig. 5.10). The volcano plot shows the relative distribution of these proteins (Fig. 11). The only one protein increased in abundance (Table 5.2) was Hexamerin storage protein PinSP1 (+ 2.9-fold). And proteins decrease in abundance (Table 5.3) the main peptides decreased were Diazepam binding inhibitor-like protein (- 3.8-fold), Cecropin-D-like peptide (- 3.54-fold) and Carboxylesterase (- 3.1-fold).

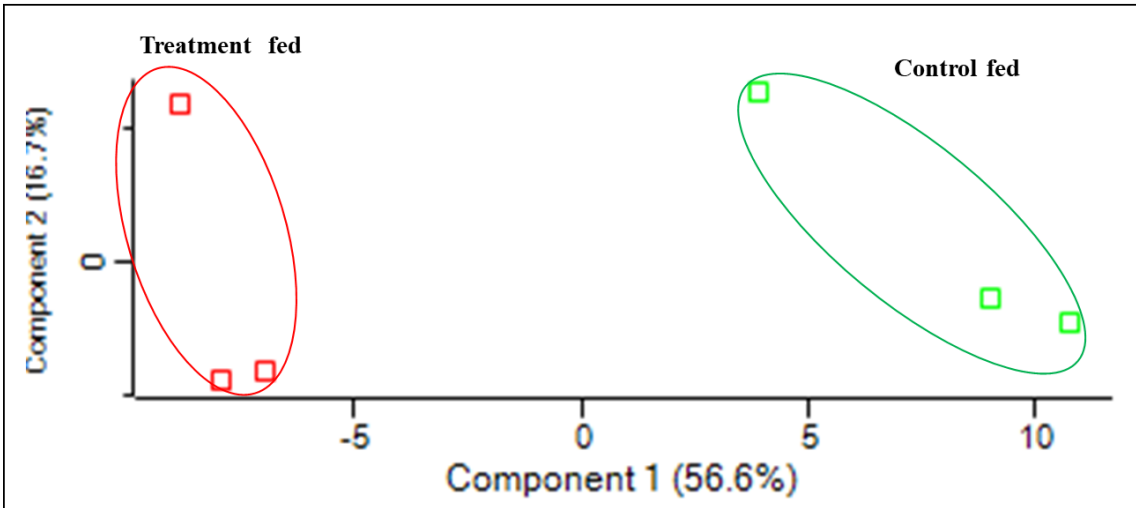


**Figure 5.9:** Principal component analysis of control *G. mellonella* larvae and atorvastatin force fed *G. mellonella* larvae for 24 h showing a clear distinction between control and treatment.



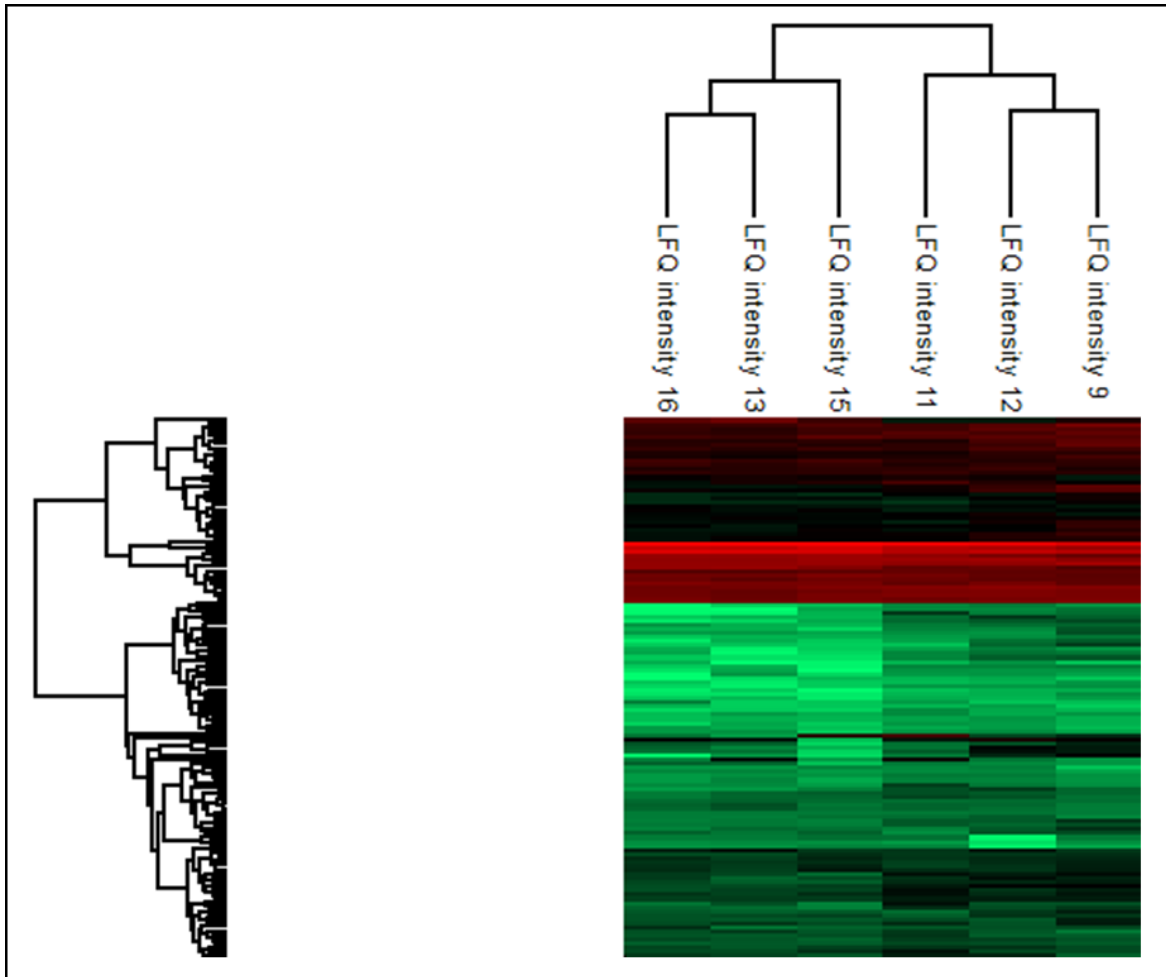


**Figure 5.10:** Two-way unsupervised hierarchical clustering of the median protein expression values of all statistically significant differentially abundant proteins from *G. mellonella* control (9, 11 and 12) and atorvastatin force fed *G. mellonella* larvae (13, 15 and 16).

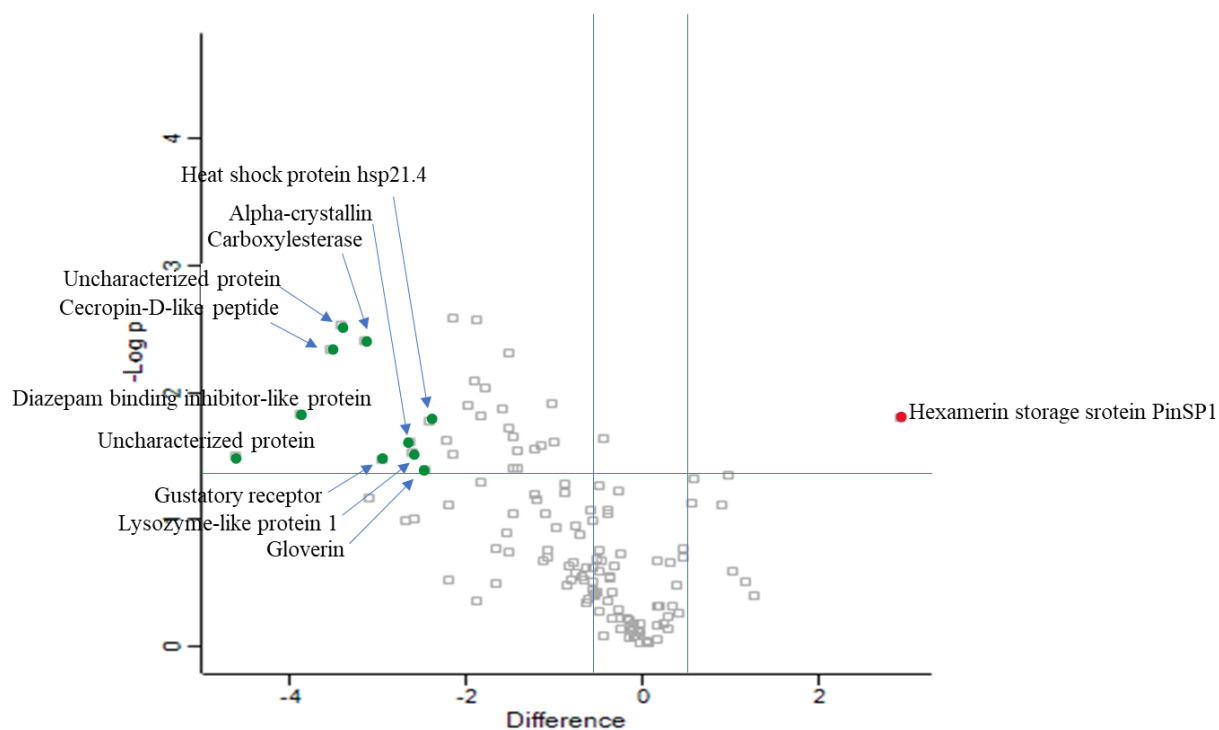


**Figure 5.11:** Volcano plot showing the distribution of quantified proteins according to p value ( $-\log_{10}$  p-value) and fold change ( $\log_2$  mean LFQ intensity difference). Proteins above the horizontal line are considered statistically significant (p value < 0.05) and those to the right and left of the vertical lines indicate relative fold changes  $\pm 1.3$ .

**Table 5.2:** Relative fold changes of proteins increased in abundance of atorvastatin force fed *G. mellonella* larvae and the number of matched peptides, sequence coverage, and overall intensity. Proteins had more than two matched peptides and were found to be differentially expressed at a level greater than  $\pm 1.5$ -fold were considered to be in significantly variable abundances between control and treated larvae.

N0.	Protein name	Unique peptides	Sequence coverage [%]	Mean LFQ intensity	Fold change
1	Hexamerin storage protein PinSP1	76	78.7	2.0326E+11	2.90

**Table 5.3:** Relative fold changes of proteins increased in abundance of atorvastatin force fed *G. mellonella* larvae and the number of matched peptides, sequence coverage, and overall intensity. Proteins had more than two matched peptides and were found to be differentially expressed at a level greater than  $\pm 1.5$ -fold were considered to be in significantly variable abundances between control and treated larvae.

<b>N0.</b>	<b>Protein name</b>	<b>Unique peptides</b>	<b>Sequence coverage [%]</b>	<b>Mean LFQ intensity</b>	<b>Fold change</b>
1	Uncharacterized protein	12	34.8	8.03E+09	-4.60
2	Diazepam binding inhibitor-like protein	3	25.9	3.46E+09	-3.89
3	Cecropin-D-like peptide	2	14.5	2.28E+09	-3.54
4	Uncharacterized protein	7	31.8	2.43E+09	-3.42
5	Carboxylesterase	13	57	3.75E+09	-3.14
6	Gustatory receptor	4	26.4	1.94E+09	-2.95
7	Alpha-crystallin	11	40.4	2.91E+09	-2.64
8	Lysozyme-like protein 1	9	18.9	1.45E+09	-2.63
9	Gloverin	2	28.8	1.20E+09	-2.47
10	Heat shock protein hsp21.4	5	15	1.21E+09	-2.43
11	Yellow-d	12	26.9	1.94E+09	-2.24
12	Inducible serine protease inhibitor 2	3	9.8	6.27E+10	-2.15
13	Beta-1,3-glucan recognition protein	21	45.5	3.87E+09	-1.99
14	Hdd1-like protein	5	56.9	4.23E+08	-1.90
15	Apolipoporphins	2	26.6	1.87E+10	-1.87
16	Beta-galactosidase	23	35.1	1.43E+10	-1.83
17	Similar to CG10638-PA	17	37.4	2.91E+09	-1.79
18	Odorant-binding protein	7	18.2	7.48E+09	-1.59
19	Peptidoglycan recognition protein	11	56	1.28E+10	-1.53
20	Protease inhibitor 1	3	21.2	4.73E+09	-1.52

## 5.8 Discussion

Statins are the main therapeutic agents used to decrease high serum cholesterol levels and are among the most widely prescribed drugs currently in the world (Macreadie *et al.*, 2006a). The sterol in plants and eukaryotic microorganisms is ergosterol (Macreadie *et al.*, 2006c). The statins might be expected that statins or their derivatives could also be used to inhibit the growth of fungal pathogens through inhibition of ergosterol synthesis. Statins have *in vitro* activities against several human pathogenic fungi, including *Candida spp.*, *Cryptococcus neoformans*, and *Zygomycetes* (Chamilos *et al.*, 2006). Wax moth (*G. mellonella*) larvae are widely used as model organisms for researches in insect physiology and human with pathogens (Browne and Kavanagh, 2013). In *G. mellonella*, antimicrobial effects and pathogen virulence testing of agents can be analysed by using a number of parameters including the degree of melanisation in response to a pathogen, larval death, quantification of fungal load, changes in haemocyte densities and changes in antimicrobial peptide expression (Bergin *et al.*, 2003).

The results presented here show that the atorvastatin decreased in the ability of *C. albicans* to kill *G. mellonella* larvae relative to non-treated. Presence of atorvastatin increased the survival of *G. mellonella* larvae by 50 % comparable to non-treated and this indicates that atorvastatin has *in vivo* effect to inhibit the *C. albicans* infected *G. mellonella* larvae. HPLC analysis of atorvastatin administrated *G. mellonella* larvae displayed a considerable interaction between atorvastatin concentration and time of extraction, there was a reduction in atorvastatin concentration by increase the time. This reduction due to the possibility of atorvastatin metabolism by *G. mellonella* larvae. In this study atorvastatin (5 and 10 mg/ml) were used, and atorvastatin extracted for detection at (zero, 0.5, 2 and 6 h) post-administration of atorvastatin, and the HPLC analysis at these two concentrations showed a significant decrease in atorvastatin concentration ( $p < 0.001$ ).

this indicates that the atorvastatin metabolized in *G. mellonella* larvae in a similar manner to that in mammals. In the fungal load of *C. albicans* in *G. mellonella* larvae experiment there was a slow rate of growth of treated larvae. Results showed that the decrease in the *C. albicans* cell density of atorvastatin treatment sample compared to the control sample ( $P < 0.001$ ). This indicate that the atorvastatin inhibits growth of *C. albicans in vivo*. In order to characterize the changes in the hemocyte population in larvae, larvae were administered a different concentrations of atorvastatin which produced a rise in hemocyte density at atorvastatin concentration of (50 ug/ml and 200 ug/ml), this elevation of hemocyte possibly due to the release of sessile hemocytes normally attached to the fat body and inner surface of the hemocoel of larvae (Bergin *et al.*, 2003) (Sheehan and Kavanagh, 2018). In addition, the of response of atorvastatin treated *C. albicans* cell to hemocytes displayed that the significant increase in percent *C. albicans* viability of atorvastatin treatment relative to nontreatment samples. Shotgun proteomics was employed to analyse the response of *G. mellonella* larvae to atorvastatin. Atorvastatin administration was done by intra haemocoel injection and by force feeding. In the proteomic analysis of intra-haemocoel injection of atorvastatin showed that only one protein has a different in abundance by more than 1.5-fold. This protein was apolipoporphins which increase in abundance by (5.22-fold). This protein is major component of lipophorin, which mediates transport for various types of lipids in hemolymph acts by forming lipoprotein particles that bind lipoproteins and lipids (Sundermeyer *et al.*, 1996). Proteomic analysis of *G. mellonella* administered the atorvastatin by force feeding displayed 21 proteins were different in abundance by more than 1.5-fold. Only one protein that increase in abundance this protein was Hexamerin storage protein PinSP1(2.9-fold). In insects, tope kind of proteins are storage proteins or hexamerins accumulate to serve as sources of amino acids during metamorphosis and reproduction (Zhu *et al.*, 2002).

A number of immune related proteins were decreased in abundance in larvae administered atorvastatin including Cecropin-D-like peptide (-3.54 fold), which is an innate immune response protein, killing of cells of other organism and antibacterial activity (Mak *et al.*, 2001), and Lysozyme-like protein 1 (- 2.63 fold) has immune response and antimicrobial activity (Gandhe *et al.*, 2007). Proteins related to stress like Heat shock protein hsp21.4 (-2.42-fold). And also, some of decreased protein related to fungal cell wall such as Beta-1,3-glucan recognition protein (-1.99-fold) which has strong specific affinity for  $\beta$ -1,3-glucan, a component of the fungal cell wall. Its interaction with initiates the activation of the prophenoloxidase cascade, which is an important defense system in invertebrates of many species (Ochiai and Ashida, 2000).

Proteomic analysis revealed only two proteins that increase and 20 protein that decreases in abundance in both ways of atorvastatin administration (intra-haemocoel injection and by force-feeding) by 1.5-fold or more. Changes in proteomic analysis of *G. mellonella* larvae implies that no significant stress effect of atorvastatin. This possibly indicates that the atorvastatin is nontoxic on the *G. mellonella* larvae.

## **Chapter 6**

### **General Discussion**

## General discussion

Fungal pathogens of humans cause harmful infections and thus, are considered to be hidden killers (Brown *et al.*, 2012). Fungi can cause diverse diseases in humans which range from superficial skin infections to life-threatening diseases causing damage to internal organs. Invasive infections caused by fungi could be life-threatening especially for patients who are diagnosed with autoimmune disorder (Jain *et al.*, 2010).

Statins are the main therapeutic agents used to decrease high serum cholesterol levels and are among the most widely prescribed drugs currently on the market (Macreadie *et al.*, 2006). They inhibit (HMG-CoA) reductase enzyme (Qiu *et al.*, 1991). HMG-CoA is an enzyme that catalyses the conversion of HGM-CoA to mevalonate, which leads to the production of farnesyl diphosphate which is the precursor for the production of cholesterol in humans or ergosterol in plants and eukaryotic microorganisms (Macreadie *et al.*, 2006). If the statin-binding site of fungal HMG-CoA reductase is like that of human HMG-CoA reductase, it might be expected that statins or their derivatives could also be used to inhibit the growth of fungal pathogens through inhibition of ergosterol synthesis. It could, therefore, be supposed that if statins could inhibit cholesterol, they could inhibit the production of ergosterol (Macreadie *et al.*, 2006).

*G. mellonella* larvae have been considered as a viable alternative to other models of infection since they are cheap and require no specialist equipment (Kay *et al.*, 2019). *G. mellonella* larvae were used to assess the virulence of *C. albicans* and to investigate the virulence of pathogenic and non-pathogenic yeast species (Cotter *et al.*, 2000). *G. mellonella* has several innate immune similarities to mammals they lack many defined organ systems preventing the full study of fungal dissemination and antifungal therapy which is possible in mammals (Kavanagh and Fallon, 2010).



*G. mellonella* larvae have also been utilised for assessing the *in vivo* activity of amphotericin B, flucytosine and fluconazole following challenge with *C. neoformans* (Mylonakis *et al.*, 2005).

The aim of this study was to determine the antifungal activity of atorvastatin and its effect on *C. albicans* and *A. fumigatus* by using *G. mellonella* larva as a model of infection and also to analyze the impact of atorvastatin on *G. mellonella* larvae.

**The main results from Chapter 3** showed that the atorvastatin reduced growth and also caused a small reduction in viability. However, the combination of atorvastatin, amphotericin B, caspofungin and, miconazole showed that no clear different effect. Ergosterol plays a key role in maintaining the integrity and permeability of the fungal cell membrane and reduced levels of ergosterol could indicate a more porous membrane (Macreadie *et al.*, 2006b; Song *et al.*, 2016). Statin exposure did lead to an increase in the release of amino acid and proteins from cells indicating increased permeability. The release of protein from *C. albicans* following exposure to atorvastatin could indicate a general increase in cell permeability thus suggesting the need for the cell to counteract the elevated permeability of the cell. Atorvastatin lead to a reduction in the adherence ability of cells possibly as a consequence of the altered cell wall composition as indicated by the increased calcofluor staining. Proteomic analysis revealed decreased abundance of yeast form wall protein which plays a role in adherence and promoting dispersal and in Wh11p protein a protein involved in biofilm formation and pathogenesis. In addition, atorvastatin increased the activity of catalase enzyme. Activation of *C. albicans* oxidative stress response genes and enzymes following exposure to atorvastatin is evidence of the generation of oxidative stress. Several proteins involved in the ability of the cell to respond to stress were reduced in abundance such as Hsp12p and small heat shock protein which play roles in the pathogenicity of the yeast and in its ability to respond to oxidative and osmotic stress. Reduced abundance of these protein may

have an impact on the cell's ability to grow and proliferate *in vivo*. Proteins such as Cip1p, Pst2p and pleiotropic ABC efflux transporter were also reduced in abundance and all play a role in the cell's response to oxidative stress (Brown *et al.*, 2010). The proteomic analysis also revealed an increase in the abundance of some proteins involved in ergosterol biosynthesis in treated cells. In particular squalene monooxygenase and lanosterol synthase, were increased in abundance. Atorvastatin treated cells displayed a reduced ergosterol content and perhaps the cells responded to statin exposure by attempting to increase its biosynthesis. Statins inhibit the synthesis of important isoprenoids, e.g. farnesyl pyrophosphate and geranylgeranyl pyrophosphate, which are important lipid attachments for the  $\gamma$  subunit of heterotrimeric G-proteins (Pella *et al.*, 2005), guanosine triphosphate binding protein Ras, and Ras-like proteins (Rho, Rab, Rac, Ral, or Rap) (Ghittoni *et al.*, 2005; Liao, 2008; Pella *et al.*, 2005). Moreover, statins act as inhibitors of some G-protein actions and Ras or Ras-like signaling, which affect several important bioprocesses (Cordle *et al.*, 2005).

Larvae of *G. mellonella* can be employed to assess the virulence of fungal pathogens (Brennan *et al.*, 2002; Fuchs and Mylonakis, 2006) and for determining the *in vivo* activity of antifungal agents (Kavanagh and Sheehan, 2018; Maurer *et al.*, 2015). Their use offers the possibility of quickly establishing the *in vivo* toxicity and efficacy of antimicrobial agents without the need to resort to the use of mammals in initial screening studies. In the work presented here atorvastatin was shown to be non-toxic to larvae and to be able to protect larvae following infection with *C. albicans*. The doses used in larvae of 50 and 100  $\mu\text{g/ml}$  are equivalent to 4.55 and 9.09  $\text{mg/kg}$ , respectively. The results also displayed that atorvastatin has a profound effect on *C. albicans* and reduced its ability to grow and increases its susceptibility to killing in the *G. mellonella* larval model system. While the anti-microbial activity of statins is well established this work demonstrates how they

interact with the fungal proteome to induce their effects and highlight their ability to retard proliferation *in vivo*.

**The experiments in Chapter 4** showed that exposure of *A. fumigatus* to atorvastatin resulted in a reduction in growth and rescued viability as measure in *G. mellonella* larvae. These results indicated that the atorvastatin has a synergistic effect in combination with amphotericin B against *A. fumigatus*. And in terms of miconazole and caspofungin no significant changes. Sterol analysis conducted during this project showed that atorvastatin does inhibit the amount of ergosterol produced. This would support Macreadie *et al.*, (2006), in suggesting that statin does inhibit ergosterol synthesis in *A. fumigatus*, and therefore the growth. Atorvastatin increased membrane permeability of *A. fumigatus* as evidenced by increased release of protein and amino acids.

Cultures treated with atorvastatin also released elevated levels of gliotoxin, which also has been observed in *A. fumigatus* exposed to amphotericin B and may indicate an oxidative stress response (Reeves *et al.*, 2004). *A. fumigatus* under stress, produces more gliotoxin than if it was not under stress (Belkacemi *et al.*, 1999). Depletion of the intracellular gliotoxin concentration may increase the biosynthesis of the toxin to recover the lost gliotoxin in order to restore the redox balance within the cell (Schrettl *et al.* 2010).

The results displayed that the sample treated with atorvastatin produced more gliotoxin in the treated samples compared to the control sample. The result illustrated that *A. fumigatus* appears to overcome the presence of atorvastatin and is capable of produce gliotoxin, and the results indicate that *A. fumigatus* cells are more sensitive to gliotoxin release in the case of atorvastatin treatment.

Proteomic analysis revealed an increased abundance of a range of proteins involved in dealing with oxidative stress, including pyoverdine/dityrosine biosynthesis 5 demethoxyubiquinone

hydroxylase, mitochondrial and alcohol dehydrogenase. In *Saccharomyces cerevisiae*, dityrosine is a major component of the spore wall surface and plays a role in the resistance of ascospores to environmental stress (Neiman, 2005). Furthermore, the glutathione S-transferase family protein is increased in abundance, and this protein functions to detoxify xenobiotics. The fumipyrrole biosynthetic (fmpE) protein was also increased in abundance. Deletion of fmpE in *A. fumigatus* resulted in reduced growth and sporulation of the mutant strains but virulence was not altered as compared to the WT strain in a murine infection model (Macheleidt *et al.*, 2015). A range of heat shock proteins, such as Hsp30/Hsp42, also increased in abundance in response to atorvastatin. Heat shock proteins play an important role in adaptation of the fungal cell to environmental and chemical stresses (Tamayo *et al.*, 2013). Proteomic analysis also revealed the reduced abundance of a number of peptides associated with virulence, including aflatoxin B1 and allergen Asp f 15. Asp f 15 is cell-wall associated and its decreased abundance could be due to an altered cell-wall composition as a result of an altered membrane composition. Statins inhibit the growth of *A. fumigatus* and supplementation of media with ergosterol or cholesterol blocked the growth-inhibiting effect of atorvastatin, thus indicating the specificity of statins for the mevalonate synthesis pathway (Macreadie *et al.*, 2006a). However, another study found that statins were fungistatic against *A. fumigatus*, but the MICs were greater than the clinically achievable concentrations (Qiao *et al.*, 2007). Furthermore, a range of *Candida* strains that were resistant to fluconazole and nystatin were all sensitive to atorvastatin (Esfahani *et al.*, 2019). Atorvastatin combined with fluconazole improved cryptococcosis caused by *Cryptococcus gattii* and mice treated with atorvastatin had increased survival and better clinical outcomes; this was mediated via modifications in the capsule and cell membrane in the presence of a statin that induced cell death within phagocytes (de Queiroz Ribeiro *et al.*, 2017).

As discussed before use of *G. mellonella* displays the chance of quickly establishing the *in vivo* toxicity and effectiveness of antimicrobial agents. In this study atorvastatin was shown to be non-toxic to larvae and to be able to protect larvae following infection with *A. fumigatus*. The doses used in larvae was 9.09 mg/kg. The results presented here indicate that atorvastatin has a profound effect on *A. fumigatus* and reduced its ability to grow and increases its susceptibility to killing in the *G. mellonella* larval model system. While the anti-microbial activity of statins is well established this work demonstrates how they interact with the fungal proteome to induce their effects and highlight their ability to retard proliferation *in vivo*. The continuing problems associated with existing antifungal therapies (e.g. toxicity, drug resistance) offer the possibility of employing an active, non-toxic therapy such as atorvastatin to supplement existing therapies (Galgóczy, 2011, Nyilasi *et al.*, 2010a).

**The results of chapter 5** showed that the atorvastatin decreased in the ability of *C. albicans* to kill *G. mellonella* larvae relative to the control. The presence of atorvastatin increased the survival of *G. mellonella* larvae by 50 % compared to non-treated and this indicates that atorvastatin has *in vivo* effect to inhibit the *C. albicans* infected *G. mellonella* larvae. HPLC analysis of atorvastatin administrated *G. mellonella* larvae displayed a considerable interaction between atorvastatin concentration and time of extraction, there was a reduction in atorvastatin concentration over time. This reduction may be due to the possibility of atorvastatin metabolism by *G. mellonella* larvae. This result indicates that the atorvastatin metabolized in *G. mellonella* larvae in a similar manner to that in mammals. In the fungal load of *C. albicans* in *G. mellonella* larvae experiment there was a slow rate of growth of yeast cells in treated larvae. Results showed that the decrease in the *C. albicans* cell density of atorvastatin treatment sample compared to the control sample ( $P < 0.001$ ). This indicate that the atorvastatin inhibits growth of *C. albicans in vivo*. In order to characterize

the changes in the hemocyte population in larvae, larvae were administered a different concentrations of atorvastatin which produced a rise in hemocyte density at atorvastatin concentration of (50 ug/ml and 200 ug/ml), this elevation of hemocyte possibly due to the release of sessile hemocytes normally attached to the fat body and inner surface of the hemocoel of larvae (Bergin *et al.*, 2003) (Sheehan and Kavanagh, 2018). Shotgun proteomics was employed to analyse the response of *G. mellonella* larvae to atorvastatin. Atorvastatin administration was done by intra haemocoel injection and by force feeding. Proteomic analysis revealed only two proteins that increased and 20 protein that decreased in abundance in both ways of atorvastatin administration (intra-haemocoel injection and by force-feeding) by 1.5-fold or more. Changes in proteomic analysis of *G. mellonella* larvae imply that there was no significant stress effect of atorvastatin. This possibly indicates that the atorvastatin may be nontoxic on the *G. mellonella* larvae.

**In conclusion,** the results presented in this thesis indicate that atorvastatin is non-toxic and capable of inhibiting the growth and virulence of *C. albicans* and *A. fumigatus*. While statins are widely used to control cholesterol this work and that of others (Nyilasi *et al.*, 2010, Cabral *et al.*, 2013) indicates they may be used alone or in conjunction with conventional antifungal agents to control fungal pathogen *in vivo* and may represent a novel, non-toxic antifungal therapy with a distinct mode of action.

## **Chapter 7**

## **References**

## References

- Abidalla, M., 2018. Morphogenesis of early embryonic development in the greater wax moth, *Galleria mellonella* (Lepidoptera: Pyralidae). *Journal of Entomology* 15, 1–12.
- Aldardeer, N.F., Albar, H., Al-Attas, M., Eldali, A., Qutub, M., Hassaniien, A., Alraddadi, B., 2020. Antifungal resistance in patients with Candidaemia: a retrospective cohort study. *BMC infectious diseases* 20, 1–7.
- Alexander, B.D., Johnson, M.D., Pfeiffer, C.D., Jiménez-Ortigosa, C., Catania, J., Booker, R., Castanheira, M., Messer, S.A., Perlin, D.S., Pfaller, M.A., 2013. Increasing echinocandin resistance in *Candida glabrata*: clinical failure correlates with presence of FKS mutations and elevated minimum inhibitory concentrations. *Clinical infectious diseases* 56, 1724–1732.
- Aljofan, M., Sganga, M.L., Lo, M.K., Rootes, C.L., Porotto, M., Meyer, A.G., Saubern, S., Moscona, A., Mungall, B.A., 2009. Antiviral activity of gliotoxin, gentian violet and brilliant green against Nipah and Hendra virus *in vitro*. *Virology journal* 6, 187.
- Barnes, P.D., Marr, K.A., 2007. Risks, diagnosis and outcomes of invasive fungal infections in haematopoietic stem cell transplant recipients. *British journal of haematology* 139, 519–531.
- Belkacemi, L., Barton, R.C., Hopwood, V., Evans, E.G.V., 1999. Determination of optimum growth conditions for gliotoxin production by *Aspergillus fumigatus* and development of a novel method for gliotoxin detection. *Medical mycology* 37, 227–233.



- Ben-Ami, R., 2011. Innate immunity against moulds: lessons learned from invertebrate models. *Immunological investigations* 40, 676–691.
- Ben-Ami, R., Lewis, R.E., Kontoyiannis, D.P., 2010. Enemy of the (immunosuppressed) state: an update on the pathogenesis of *Aspergillus fumigatus* infection. *British journal of haematology* 150, 406–417.
- Bergin, D., Brennan, M., Kavanagh, K., 2003. Fluctuations in haemocyte density and microbial load may be used as indicators of fungal pathogenicity in larvae of *Galleria mellonella*. *Microbes and infection* 5, 1389–1395.
- Bergin, D., Reeves, E.P., Renwick, J., Wientjes, F.B., Kavanagh, K., 2005. Superoxide production in *Galleria mellonella* hemocytes: identification of proteins homologous to the NADPH oxidase complex of human neutrophils. *Infection and immunity* 73, 4161–4170.
- Bergman, P.W., Björkhem-Bergman, L., 2013. Is there a role for statins in fungal infections? *Expert review of anti-infective therapy* 11, 1391–1400.
- Binder, U., Maurer, E., Lass-Flörl, C., 2016. *Galleria mellonella*: An invertebrate model to study pathogenicity in correctly defined fungal species. *Fungal biology* 120, 288–295.
- Blatzer, M., Latge, J.-P., 2017. Metal-homeostasis in the pathobiology of the opportunistic human fungal pathogen *Aspergillus fumigatus*. *Current opinion in microbiology* 40, 152–159.
- Blyth, C.C., Palasanthiran, P., O'Brien, T.A., 2007. Antifungal therapy in children with invasive fungal infections: a systematic review. *Pediatrics* 119, 772–784.
- Boddy, L., 2016. Interactions with humans and other animals, in: *The Fungi*. Elsevier, pp. 293–336.

- Bodey, G.P., Vartivarian, S., 1989. Aspergillosis. *European Journal of Clinical Microbiology and infectious diseases* 8, 413–437.
- Bonetti, P.O., Lerman, L.O., Napoli, C., Lerman, A., 2003. Statin effects beyond lipid lowering—are they clinically relevant? *European heart journal* 24, 225–248.
- Bongomin, F., Gago, S., Oladele, R., Denning, D., 2017. Global and multi-national prevalence of fungal diseases—estimate precision. *Journal of fungi* 3, 57.
- Brennan, M., Thomas, D.Y., Whiteway, M., Kavanagh, K., 2002. Correlation between virulence of *Candida albicans* mutants in mice and *Galleria mellonella* larvae. *FEMS Immunology & Medical Microbiology* 34, 153–157.
- Brilhante, R.S.N., Caetano, E.P., Oliveira, J.S. de, Castelo-Branco, D. de S.C., Souza, E.R.Y., Alencar, L.P. de, Cordeiro, R. de A., Bandeira, T. de J.P.G., Sidrim, J.J.C., Rocha, M.F.G., 2015. Simvastatin inhibits planktonic cells and biofilms of *Candida* and *Cryptococcus* species. *Brazilian Journal of Infectious Diseases* 19, 459–465.
- Brown, A.J.P., Leach, M.D., Nicholls, S., 2010. The relevance of heat shock regulation in fungal pathogens of humans. *Virulence* 1, 330–332. <https://doi.org/10.4161/viru.1.4.12364>
- Brown, G.D., Denning, D.W., Gow, N.A., Levitz, S.M., Netea, M.G., White, T.C., 2012. Hidden killers: human fungal infections. *Science translational medicine* 4, 165rv13–165rv13.
- Browne, N., Heelan, M., Kavanagh, K., 2013. An analysis of the structural and functional similarities of insect hemocytes and mammalian phagocytes. *Virulence* 4, 597–603.
- Browne, N., Kavanagh, K., 2013. Developing the potential of using *Galleria mellonella* larvae as models for studying brain infection by *Listeria monocytogenes*. *Virulence* 4, 271–272.

- Bruder Nascimento, A.C.M. de O., dos Reis, T.F., de Castro, P.A., Hori, J.I., Bom, V.L.P., de Assis, L.J., Ramalho, L.N.Z., Rocha, M.C., Malavazi, I., Brown, N.A., 2016. Mitogen activated protein kinases SakAHOG1 and MpkC collaborate for *Aspergillus fumigatus* virulence. *Molecular microbiology* 100, 841–859.
- Brunke, S., Mogavero, S., Kasper, L., Hube, B., 2016. Virulence factors in fungal pathogens of man. *Current opinion in microbiology* 32, 89–95.
- Cabral, M.E., Figueroa, L.I., Fariña, J.I., 2013. Synergistic antifungal activity of statin–azole associations as witnessed by *Saccharomyces cerevisiae*-and *Candida utilis*-bioassays and ergosterol quantification. *Revista iberoamericana de micología* 30, 31–38.
- Calderone, R.A., Fonzi, W.A., 2001. Virulence factors of *Candida albicans*. *Trends in microbiology* 9, 327–335.
- Cassone, A., 2015. Vulvovaginal *Candida albicans* infections: pathogenesis, immunity and vaccine prospects. *BJOG: An International Journal of Obstetrics & Gynaecology* 122, 785–794.
- Cavalieri, D., Di Paola, M., Rizzetto, L., Tocci, N., De Filippo, C., Lionetti, P., Ardizzoni, A., Colombari, B., Paulone, S., Gut, I.G., 2018. Genomic and phenotypic variation in morphogenetic networks of two *Candida albicans* isolates subtends their different pathogenic potential. *Frontiers in immunology* 8, 1997.
- Chamilos, G., Lewis, R.E., Kontoyiannis, D.P., 2006. Lovastatin has significant activity against zygomycetes and interacts synergistically with voriconazole. *Antimicrobial agents and chemotherapy* 50, 96–103.

- Chandra, J., Kuhn, D.M., Mukherjee, P.K., Hoyer, L.L., McCormick, T., Ghannoum, M.A., 2001. Biofilm formation by the fungal pathogen *Candida albicans*: development, architecture, and drug resistance. *Journal of bacteriology* 183, 5385–5394.
- Charoenpornsook, K., Kavisarasai, P., 2006. Mycotoxins in animal feed stuffs of Thailand. *KMITL Science and Technology Journal* 6, 25–28.
- Chotirmall, S.H., Mirkovic, B., Lavelle, G.M., McElvaney, N.G., 2014. Immuno-evasive *Aspergillus* virulence factors. *Mycopathologia* 178, 363–370.
- Cirillo, V.P., Harsch, M., Lampen, J.O., 1964. Action of the polyene antibiotics filipin, nystatin and N-acetylcandidin on the yeast cell membrane. *Microbiology* 35, 249–259.
- Cordle, A., Koenigsnecht-Talboo, J., Wilkinson, B., Limpert, A., Landreth, G., 2005. Mechanisms of statin-mediated inhibition of small G-protein function. *Journal of Biological Chemistry* 280, 34202–34209. <https://doi.org/10.1074/jbc.M505268200>
- Corey, K.E., Cohen, D.E., 2015. Lipid and lipoprotein metabolism in liver disease, in: Endotext [Internet]. MDText. com, Inc.
- Cornely, O.A., Lass-Flörl, C., Lagrou, K., Arsic-Arsenijevic, V., Hoenigl, M., 2017. Improving outcome of fungal diseases—guiding experts and patients towards excellence. *Mycoses* 60, 420–425.
- Corsini, A., Pazzucconi, F., Arnaboldi, L., Pfister, P., Fumagalli, R., Paoletti, R., Sirtori, C.R., 1998. Direct effects of statins on the vascular wall. *Journal of cardiovascular pharmacology* 31, 773–778.

- Côté, R.G., Griss, J., Dianes, J.A., Wang, R., Wright, J.C., van den Toorn, H.W.P., van Breukelen, B., Heck, A.J.R., Hulstaert, N., Martens, L., Reisinger, F., Csordas, A., Ovelleiro, D., Perez-Rivevol, Y., Barsnes, H., Hermjakob, H., Vizcaíno, J.A., 2012. The Proteomics identification (PRIDE) Converter 2 Framework: An Improved Suite of Tools to Facilitate Data Submission to the PRIDE Database and the Proteome Xchange Consortium. *Molecular & Cellular Proteomics: MCP* 11, 1682–1689. <https://doi.org/10.1074/mcp.O112.021543>
- Cotter, G., Doyle, S., Kavanagh, K., 2000. Development of an insect model for the *in vivo* pathogenicity testing of yeasts. *FEMS Immunology & Medical Microbiology* 27, 163–169.
- Cuervo, G., Garcia-Vidal, C., Nucci, M., Puchades, F., Fernández-Ruiz, M., Mykietiuk, A., Manzur, A., Gudiol, C., Pemán, J., Viasus, D., Ayats, J., Carratalà, J., 2013. Effect of Statin Use on Outcomes of Adults with Candidemia. *PLoS ONE*. <https://doi.org/10.1371/journal.pone.0077317>
- da Silva Dantas, A., Lee, K.K., Raziunaite, I., Schaefer, K., Wagener, J., Yadav, B., Gow, N.A., 2016. Cell biology of *Candida albicans*–host interactions. *Current opinion in microbiology* 34, 111–118.
- Dagenais, T.R., Keller, N.P., 2009. Pathogenesis of *Aspergillus fumigatus* in invasive aspergillosis. *Clinical microbiology reviews* 22, 447–465.
- Dagley, M.J., Gentle, I.E., Beilharz, T.H., Pettolino, F.A., Djordjevic, J.T., Lo, T.L., Uwamahoro, N., Rupasinghe, T., Tull, D.L., McConville, M., 2011. Cell wall integrity is linked to mitochondria and phospholipid homeostasis in *Candida albicans* through the activity of the post-transcriptional regulator Ccr4-Pop2. *Molecular microbiology* 79, 968–989.
- Davis, D., 2003. Adaptation to environmental pH in *Candida albicans* and its relation to pathogenesis. *Current genetics* 44, 1–7.

- Davis, D.A., 2009. How human pathogenic fungi sense and adapt to pH: the link to virulence. *Current opinion in microbiology* 12, 365–370.
- de Melo, W., Scorzoni, L., Rossi, S.A., Costa-Orlandi, C.B., Yonashiro, M., 2017. Update on Fungal Disease: From Establish Infection to Clinical Manifestation. *J Biotechnol Biomater* 7, 2.
- de Queiroz Ribeiro, N., Costa, M.C., Magalhães, T.F.F., Carneiro, H.C.S., Oliveira, L.V., Fontes, A.C.L., Santos, J.R.A., Ferreira, G.F., de Sousa Araujo, G.R., Alves, V., 2017. Atorvastatin as a promising anticryptococcal agent. *International journal of antimicrobial agents* 49, 695–702.
- de Souza, W., Rodrigues, J.C.F., 2009. Sterol biosynthesis pathway as target for anti-trypanosomatid drugs. *Interdisciplinary perspectives on infectious diseases* 2009.
- Denning, D.W., 2003. Echinocandin antifungal drugs. *The Lancet* 362, 1142–1151.
- Denning, D.W., Anderson, M.J., Turner, G., Latgé, J.-P., Bennett, J.W., 2002. Sequencing the *Aspergillus fumigatus* genome. *The Lancet Infectious Diseases* 2, 251–253.
- Dhar, M.K., Koul, A., Kaul, S., 2013. Farnesyl pyrophosphate synthase: a key enzyme in isoprenoid biosynthetic pathway and potential molecular target for drug development. *New biotechnology* 30, 114–123.
- Diaz-Guerra, T.M., Mellado, E., Cuenca-Estrella, M., Rodriguez-Tudela, J.L., 2003. A point mutation in the 14 $\alpha$ -sterol demethylase gene *cyp51A* contributes to itraconazole resistance in *Aspergillus fumigatus*. *Antimicrobial Agents and Chemotherapy* 47, 1120–1124.

- Dobesh, P.P., Klepser, D.G., McGuire, T.R., Morgan, C.W., Olsen, K.M., 2009. Reduction in mortality associated with statin therapy in patients with severe sepsis. *Pharmacotherapy* 29, 621–630. <https://doi.org/10.1592/phco.29.6.621>
- Donnino, M.W., Cocchi, M.N., Howell, M., Clardy, P., Talmor, D., Cataldo, L., Chase, M., Al-Marshad, A., Ngo, L., Shapiro, N.I., 2009. Statin therapy is associated with decreased mortality in patients with infection. *Academic Emergency Medicine* 16, 230–234. <https://doi.org/10.1111/j.1553-2712.2009.00350.x>
- Esfahani, A.N., Golestannejad, Z., Khozeimeh, F., Dehghan, P., Maheronnaghsh, M., Zarei, Z., 2019. Antifungal effect of Atorvastatin against *Candida* species in comparison to Fluconazole and Nystatin. *Medicine and pharmacy report* 92, 368.
- Fjårvik, E., Zotchev, S.B., 2005. Biosynthesis of the polyene macrolide antibiotic nystatin in *Streptomyces noursei*. *Applied microbiology and biotechnology* 67, 436–443.
- Forrest, G.N., Kopack, A.M., Perencevich, E.N., 2010. Statins in Candidemia: Clinical outcomes from a matched cohort study. *BMC Infectious Diseases*. <https://doi.org/10.1186/1471-2334-10-152>
- Frisvad, J.C., Larsen, T.O., 2016. Extralites of *Aspergillus fumigatus* and other pathogenic species in *Aspergillus* section *Fumigati*. *Frontiers in Microbiology* 6, 1485.
- Fuchs, B.B., Mylonakis, E., 2006. Using non-mammalian hosts to study fungal virulence and host defense. *Current Opinion in Microbiology* 9, 346–351. <https://doi.org/10.1016/j.mib.2006.06.004>
- Galgóczy, L., 2011. Statins as antifungal agents. *World Journal of Clinical Infectious Diseases* 1, 4. <https://doi.org/10.5495/wjcid.v1.i1.4>

- Gandhe, A.S., Janardhan, G., Nagaraju, J., 2007. Immune upregulation of novel antibacterial proteins from silkmoths (Lepidoptera) that resemble lysozymes but lack muramidase activity. *Insect biochemistry and molecular biology* 37, 655–666.
- Geißel, B., Loiko, V., Klugherz, I., Zhu, Z., Wagener, N., Kurzai, O., van den Hondel, C.A., Wagener, J., 2018. Azole-induced cell wall carbohydrate patches kill *Aspergillus fumigatus*. *Nature communications* 9, 3098.
- Ghannoum, M.A., Rice, L.B., 1999. Antifungal agents: mode of action, mechanisms of resistance, and correlation of these mechanisms with bacterial resistance. *Clinical microbiology reviews* 12, 501–517.
- Ghittoni, R., Patrussi, L., Pirozzi, K., Pellegrini, M., Lazzerini, P.E., Capecchi, P.L., Pasini, F.L., Baldari, C.T., 2005. Simvastatin inhibits T-cell activation by selectively impairing the function of Ras superfamily GTPases. *The FASEB Journal* 19, 605–607. <https://doi.org/10.1096/fj.04-2702fje>
- Ghorbel, D., Hadrich, I., Neji, S., Trabelsi, H., Belaaj, H., Sellami, H., Cheikhrouhou, F., Makni, F., Ayadi, A., 2019. Detection of virulence factors and antifungal susceptibility of human and avian *Aspergillus flavus* isolates. *Journal de Mycologie Médicale* 100900.
- Gray, K.C., Palacios, D.S., Dailey, I., Endo, M.M., Uno, B.E., Wilcock, B.C., Burke, M.D., 2012. Amphotericin primarily kills yeast by simply binding ergosterol. *Proceedings of the National Academy of Sciences* 109, 2234–2239.
- Green, C.B., Cheng, G., Chandra, J., Mukherjee, P., Ghannoum, M.A., Hoyer, L.L., 2004. RT-PCR detection of *Candida albicans* ALS gene expression in the reconstituted human



- epithelium (RHE) model of oral candidiasis and in model biofilms. *Microbiology* 150, 267–275.
- Gustin, M.C., Albertyn, J., Alexander, M., Davenport, K., 1998. MAP Kinase Pathways in the Yeast *Saccharomyces cerevisiae*. *Microbiol. Mol. Biol. Rev.* 62, 1264–1300.
- Hamamoto, H., Kurokawa, K., Kaito, C., Kamura, K., Razanajatovo, I.M., Kusuhara, H., Santa, T., Sekimizu, K., 2004. Quantitative evaluation of the therapeutic effects of antibiotics using silkworms infected with human pathogenic microorganisms. *Antimicrobial agents and chemotherapy* 48, 774–779.
- Harriott, M.M., Lilly, E.A., Rodriguez, T.E., Fidel Jr, P.L., Noverr, M.C., 2010. *Candida albicans* forms biofilms on the vaginal mucosa. *Microbiology* 156, 3635.
- Hawser, S.P., Douglas, L.J., 1994. Biofilm formation by *Candida* species on the surface of catheter materials *in vitro*. *Infection and immunity* 62, 915–921.
- Hof, H., Kupfahl, C., 2009. Gliotoxin in *Aspergillus fumigatus*: an example that mycotoxins are potential virulence factors. *Mycotoxin research* 25, 123.
- Höfs, S., Mogavero, S., Hube, B., 2016. Interaction of *Candida albicans* with host cells: virulence factors, host defense, escape strategies, and the microbiota. *Journal of Microbiology* 54, 149–169.
- Hornsey, M., Wareham, D.W., 2011. *In vivo* efficacy of glycopeptide-colistin combination therapies in a *Galleria mellonella* model of *Acinetobacter baumannii* infection. *Antimicrobial agents and chemotherapy* 55, 3534–3537.

- Istvan, E.S., 2002. Structural mechanism for statin inhibition of 3-hydroxy-3-methylglutaryl coenzyme A reductase. *American heart journal* 144, S27–S32.
- Jain, A., Jain, S., Rawat, S., 2010. Emerging fungal infections among children: A review on its clinical manifestations, diagnosis, and prevention. *Journal of Pharmacy And Bioallied Sciences* 2, 314.
- Johnson, A., Pérez, J.C., Kumamoto, C.A., Johnson, A.D., 2013. *Candida albicans* Commensalism and Pathogenicity Are Intertwined Traits Directed by a Tightly Knit Transcriptional Regulatory Circuit.
- Kaur, S., Singh, S., 2014. Biofilm formation by *Aspergillus fumigatus*. *Medical mycology* 52, 2–9.
- Kavanagh, K., Fallon, J.P., 2010. *Galleria mellonella* larvae as models for studying fungal virulence. *Fungal Biology Reviews* 24, 79–83.
- Kavanagh, K., Reeves, E.P., 2004. Exploiting the potential of insects for *in vivo* pathogenicity testing of microbial pathogens. *FEMS microbiology reviews* 28, 101–112.
- Kavanagh, K., Sheehan, G., 2018. The Use of *Galleria mellonella* Larvae to Identify Novel Antimicrobial Agents against Fungal Species of Medical Interest. *Journal of Fungi* 4, 113. <https://doi.org/10.3390/jof4030113>
- Kay, S., Edwards, J., Brown, J., Dixon, R., 2019. *Galleria mellonella* Infection Model Identifies Both High and Low Lethality of *Clostridium perfringens* Toxigenic Strains and Their Response to Antimicrobials. *Frontiers in microbiology* 10.

- Kelly, J., Kavanagh, K., 2011. Caspofungin primes the immune response of the larvae of *Galleria mellonella* and induces a non-specific antimicrobial response. *Journal of medical microbiology* 60, 189–196.
- Kemp, M.W., Massey, R.C., 2007. The use of insect models to study human pathogens. *Drug Discovery Today: Disease Models* 4, 105–110.
- Kim, J., Sudbery, P., 2011. *Candida albicans*, a major human fungal pathogen. *The Journal of Microbiology* 49, 171.
- Kolotila, M.P., Diamond, R.D., 1990. Effects of neutrophils and *in vitro* oxidants on survival and phenotypic switching of *Candida albicans* WO-1. *Infection and immunity* 58, 1174–1179.
- Kotyla, P., 2010. The role of 3-hydroxy-3-methylglutaryl coenzyme a reductase inhibitors (statins) in modern rheumatology. *Therapeutic advances in musculoskeletal disease* 2, 257–269.
- Kousha, M., Tadi, R., Soubani, A.O., 2011. Pulmonary aspergillosis: a clinical review. *European Respiratory Review* 20, 156–174.
- Kriaa, A., Bourgin, M., Potiron, A., Mkaouar, H., Jablaoui, A., Gérard, P., Maguin, E., Rhimi, M., 2019. Microbial impact on cholesterol and bile acid metabolism: current status and future prospects. *Journal of lipid research* 60, 323–332.
- Kruger, P.S., 2006. Statins: the next anti-endotoxin. *Critical care and resuscitation: journal of the Australasian Academy of Critical Care Medicine*.
- Kullberg, B.J., Arendrup, M.C., 2015. Invasive candidiasis. *New England Journal of Medicine* 373, 1445–1456.

- Kumar, A., Reddy, L.V., Sochanik, A., Kurup, V.P., 1993. Isolation and characterization of a recombinant heat shock protein of *Aspergillus fumigatus*. *Journal of allergy and clinical immunology* 91, 1024–1030.
- Kvaal, C., Lachke, S.A., Srikantha, T., Daniels, K., McCoy, J., Soll, D.R., 1999. Misexpression of the opaque-phase-specific gene PEP1 (SAP1) in the white phase of *Candida albicans* confers increased virulence in a mouse model of cutaneous infection. *Infection and immunity* 67, 6652–6662.
- Kwon-Chung, K.J., Sugui, J.A., 2013. *Aspergillus fumigatus*—what makes the species a ubiquitous human fungal pathogen? *PLoS pathogens* 9, e1003743.
- Kwon-Chung, K.J., Sugui, J.A., 2009. What do we know about the role of gliotoxin in the pathobiology of *Aspergillus fumigatus*? *Medical mycology* 47, S97–S103.
- Latgé, J.-P., 2001. The pathobiology of *Aspergillus fumigatus*. *Trends in microbiology* 9, 382–389.
- Latgé, J.-P., 1999. *Aspergillus fumigatus* and aspergillosis. *Clinical microbiology reviews* 12, 310–350.
- Lemaitre, B., Hoffmann, J., 2007. The host defense of *Drosophila melanogaster*. *Annu. Rev. Immunol.* 25, 697–743.
- Lemaitre, B., Nicolas, E., Michaut, L., Reichhart, J.-M., Hoffmann, J.A., 1996. The dorsoventral regulatory gene cassette spätzle/Toll/cactus controls the potent antifungal response in *Drosophila* adults. *Cell* 86, 973–983.

- Lengeler, K.B., Davidson, R.C., D'souza, C., Harashima, T., Shen, W.-C., Wang, P., Pan, X., Waugh, M., Heitman, J., 2000. Signal transduction cascades regulating fungal development and virulence. *Microbiol. Mol. Biol. Rev.* 64, 746–785.
- Liao, J.K., 2008. Isoprenoids as mediators of the biological effects of statins. *Journal of Clinical Investigation* 110, 285–288. <https://doi.org/10.1172/jci16421>
- Liao, R.S., Rennie, R.P., Talbot, J.A., 1999. Assessment of the effect of amphotericin B on the vitality of *Candida albicans*. *Antimicrobial agents and chemotherapy* 43, 1034–1041.
- Liew, W.-P.-P., Mohd-Redzwan, S., 2018. Mycotoxin: its impact on gut health and microbiota. *Frontiers in cellular and infection microbiology* 8, 60.
- London, R., Orozco, B.S., Mylonakis, E., 2006. The pursuit of cryptococcal pathogenesis: heterologous hosts and the study of cryptococcal host–pathogen interactions. *FEMS yeast research* 6, 567–573.
- Lorenz, M.C., Bender, J.A., Fink, G.R., 2004. Transcriptional response of *Candida albicans* upon internalization by macrophages. *Eukaryotic cell* 3, 1076–1087.
- Macheleidt, J., Scherlach, K., Neuwirth, T., Schmidt-Heck, W., Straßburger, M., Spraker, J., Baccile, J.A., Schroeder, F.C., Keller, N.P., Hertweck, C., 2015. Transcriptome analysis of cyclic AMP-dependent protein kinase A–regulated genes reveals the production of the novel natural compound fumipyrrole by *Aspergillus fumigatus*. *Molecular microbiology* 96, 148–162.
- Maciejak, A., Leszczynska, A., Warchol, I., Gora, M., Kaminska, J., Plochocka, D., Wysocka-Kapcinska, M., Tulacz, D., Siedlecka, J., Swiezewska, E., 2013. The effects of statins on

- the mevalonic acid pathway in recombinant yeast strains expressing human HMG-CoA reductase. *BMC biotechnology* 13, 68.
- Macreadie, I.G., Johnson, G., Schlosser, T., Macreadie, P.I., 2006a. Growth inhibition of *Candida* species and *Aspergillus fumigatus* by statins. *FEMS microbiology letters* 262, 9–13.
- Macreadie, I.G., Johnson, G., Schlosser, T., Macreadie, P.I., 2006b. Growth inhibition of *Candida* species and *Aspergillus fumigatus* by statins. *FEMS Microbiology Letters* 262, 9–13. <https://doi.org/10.1111/j.1574-6968.2006.00370.x>
- Macreadie, I.G., Johnson, G., Schlosser, T., Macreadie, P.I., 2006c. Growth inhibition of *Candida* species and *Aspergillus fumigatus* by statins. *FEMS microbiology letters* 262, 9–13.
- Maguire, R., Duggan, O., Kavanagh, K., 2016. Evaluation of *Galleria mellonella* larvae as an *in vivo* model for assessing the relative toxicity of food preservative agents. *Cell biology and toxicology* 32, 209–216.
- Maguire, R., Kunc, M., Hyrsl, P., Kavanagh, K., 2017. Caffeine administration alters the behaviour and development of *Galleria mellonella* larvae. *Neurotoxicology and teratology* 64, 37–44.
- Maheshwari, R., Bharadwaj, G., Bhat, M.K., 2000. Thermophilic fungi: their physiology and enzymes. *Microbiol. Mol. Biol. Rev.* 64, 461–488.
- Mak, P., Chmiel, D., Gacek, G.J., 2001. Antibacterial peptides of the moth *Galleria mellonella*. *Acta Biochimica Polonica* 48, 1191–1195.

- Manzoni, M., Rollini, M., 2002. Biosynthesis and biotechnological production of statins by filamentous fungi and application of these cholesterol-lowering drugs. *Applied microbiology and biotechnology* 58, 555–564.
- Manzoni, Matilde, Rollini, M., 2002. Biosynthesis and biotechnological production of statins by filamentous fungi and application of these cholesterol-lowering drugs. *Applied Microbiology and Biotechnology*. <https://doi.org/10.1007/s00253-002-0932-9>
- Maurer, E., Browne, N., Surlis, C., Jukic, E., Moser, P., Kavanagh, K., Binder, U., 2015. *Galleria mellonella* as a host model to study *Aspergillus terreus* virulence and amphotericin B resistance. *Virulence* 6(6), 1–8. <https://doi.org/10.1080/21505594.2015.1045183>
- Mayer, François L., Wilson, D., Hube, B., 2013. *Candida albicans* pathogenicity mechanisms. *Virulence* 4, 119–128.
- Mayer, F.L., Wilson, D., Jacobsen, I.D., Miramón, P., Gro\s se, K., Hube, B., 2012. The novel *Candida albicans* transporter Dur31 Is a multi-stage pathogenicity factor. *PLoS pathogens* 8, e1002592.
- Maza, P.K., Bonfim-Melo, A., Padovan, A.C., Mortara, R.A., Orikaza, C.M., Ramos, L.M.D., Moura, T.R., Soriani, F.M., Almeida, R.S., Suzuki, E., 2017. *Candida albicans*: The Ability to Invade Epithelial Cells and Survive under Oxidative Stress Is Unlinked to Hyphal Length. *Frontiers in microbiology* 8, 1235.
- McDougall, J.K., 1969. Antiviral action of gliotoxin. *Archives of Virology* 27, 255–267.
- Morgan, Juliette, Meltzer, M.I., Plikaytis, B.D., Sofair, A.N., Huie-White, S., Wilcox, S., Harrison, L.H., Seaberg, E.C., Hajjeh, R.A., Teutsch, S.M., 2005. Excess mortality, hospital stay,

- and cost due to candidemia: a case-control study using data from population-based candidemia surveillance. *Infection Control & Hospital Epidemiology* 26, 540–547.
- Morgan, J., Wannemuehler, K.A., Marr, K.A., Hadley, S., Kontoyiannis, D.P., Walsh, T.J., Fridkin, S.K., Pappas, P.G., Warnock, D.W., 2005. Incidence of invasive aspergillosis following hematopoietic stem cell and solid organ transplantation: interim results of a prospective multicenter surveillance program. *Medical mycology* 43, S49–S58.
- Morris, M.I., Villmann, M., 2006. Echinocandins in the management of invasive fungal infections, part 1. *American Journal of Health-System Pharmacy* 63, 1693–1703.
- Mowlds, P., Coates, C., Renwick, J., Kavanagh, K., 2010. Dose-dependent cellular and humoral responses in *Galleria mellonella* larvae following  $\beta$ -glucan inoculation. *Microbes and infection* 12, 146–153.
- Mowlds, P., Kavanagh, K., 2008. Effect of pre-incubation temperature on susceptibility of *Galleria mellonella* larvae to infection by *Candida albicans*. *Mycopathologia* 165, 5–12.
- Mukherjee, P.K., Chandra, J., Kuhn, D.M., Ghannoum, M.A., 2003. Mechanism of fluconazole resistance in *Candida albicans* biofilms: phase-specific role of efflux pumps and membrane sterols. *Infection and immunity* 71, 4333–4340.
- Murciano, C., Moyes, D.L., Runglall, M., Tobouti, P., Islam, A., Hoyer, L.L., Naglik, J.R., 2012. Evaluation of the role of *Candida albicans* agglutinin-like sequence (Als) proteins in human oral epithelial cell interactions. *PLoS One* 7.
- Murphy, A.R., Kavanagh, K.A., 2001. Adherence of clinical isolates of *Saccharomyces cerevisiae* to buccal epithelial cells. *Medical mycology* 39, 123–127.



- Mylonakis, E., Moreno, R., El Khoury, J.B., Idnurm, A., Heitman, J., Calderwood, S.B., Ausubel, F.M., Diener, A., 2005. *Galleria mellonella* as a model system to study *Cryptococcus neoformans* pathogenesis. *Infection and immunity* 73, 3842–3850.
- Naglik, J.R., Challacombe, S.J., Hube, B., 2003. *Candida albicans* secreted aspartyl proteinases in virulence and pathogenesis. *Microbiol. Mol. Biol. Rev.* 67, 400–428.
- Navarro-Garcia, F., Eisman, B., Roman, E., Nombela, C., Pla, J., 2001. Signal transduction pathways and cell-wall construction in *Candida albicans*. *Medical mycology* 39, 87–100.
- Neiman, A.M., 2005. Ascospore formation in the yeast *Saccharomyces cerevisiae*. *Microbiol. Mol. Biol. Rev.* 69, 565–584.
- Netea, M.G., Warris, A., Van der Meer, J.W., Fenton, M.J., Verver-Janssen, T.J., Jacobs, L.E., Andresen, T., Verweij, P.E., Kullberg, B.J., 2003. *Aspergillus fumigatus* evades immune recognition during germination through loss of toll-like receptor-4-mediated signal transduction. *The Journal of infectious diseases* 188, 320–326.
- Nguyen, V.-T., Lee, J., Qian, Z.-J., Li, Y.-X., Kim, K.-N., Heo, S.-J., Jeon, Y.-J., Park, W., Choi, I.-W., Je, J.-Y., 2014. Gliotoxin isolated from marine fungus *Aspergillus* sp. induces apoptosis of human cervical cancer and chondrosarcoma cells. *Marine drugs* 12, 69–87.
- Nyilasi, I., Kocsubé, S., Krizsán, K., Galgóczy, L., Pesti, M., Papp, T., Vágvölgyi, C., 2010. *In vitro* synergistic interactions of the effects of various statins and azoles against some clinically important fungi. *FEMS Microbiology Letters* 307, 175–184.

- Ochiai, M., Ashida, M., 2000. A pattern-recognition protein for  $\beta$ -1, 3-glucan the binding domain and the cDNA cloning of  $\beta$ -1, 3-glucan recognition protein from the silkworm, *Bombyx mori*. *Journal of Biological Chemistry* 275, 4995–5002.
- Odds, F.C., Brown, A.J., Gow, N.A., 2003. Antifungal agents: mechanisms of action. *Trends in microbiology* 11, 272–279.
- O’Gorman, C.M., 2011. Airborne *Aspergillus fumigatus* conidia: a risk factor for aspergillosis. *Fungal biology reviews* 25, 151–157.
- Orciuolo, E., Stanzani, M., Canestraro, M., Galimberti, S., Carulli, G., Lewis, R., Petrini, M., Komanduri, K.V., 2007. Effects of *Aspergillus fumigatus* gliotoxin and methylprednisolone on human neutrophils: implications for the pathogenesis of invasive aspergillosis. *Journal of Leukocyte Biology* 82, 839–848.
- Ostrowsky, B., Greenko, J., Adams, E., Quinn, M., O’Brien, B., Chaturvedi, V., Berkow, E., Vallabhaneni, S., Forsberg, K., Chaturvedi, S., 2020. *Candida auris* isolates resistant to three classes of antifungal medications—New York, 2019. *Morbidity and Mortality Weekly Report* 69, 6.
- Pahl, H.L., Krauss, B., Schulze-Osthoff, K., Decker, T., Traenckner, E.B., Vogt, M., Myers, C., Parks, T., Warring, P., Mühlbacher, A., 1996. The immunosuppressive fungal metabolite gliotoxin specifically inhibits transcription factor NF-kappaB. *Journal of Experimental Medicine* 183, 1829–1840.
- Pardo, J., Urban, C., Galvez, E.M., Ekert, P.G., Müller, U., Kwon-Chung, J., Lobigs, M., Müllbacher, A., Wallich, R., Borner, C., 2006. The mitochondrial protein Bak is pivotal for gliotoxin-induced apoptosis and a critical host factor of *Aspergillus fumigatus* virulence in mice. *J Cell Biol* 174, 509–519.

- Park, Y.-J., Park, C.E., Hong, S.-J., Jung, B.K., Ibal, J.C., Park, G.-S., Shin, J.-H., 2017. The complete mitochondrial genome sequence of the greater wax moth *Galleria mellonella* (Insecta, Lepidoptera, Pyralidae): sequence and phylogenetic analysis comparison based on whole mitogenome. *Mitochondrial DNA Part B* 2, 714–715.
- Paulussen, C., Hallsworth, J.E., Álvarez-Pérez, S., Nierman, W.C., Hamill, P.G., Blain, D., Rediers, H., Lievens, B., 2017. Ecology of aspergillosis: insights into the pathogenic potency of *Aspergillus fumigatus* and some other *Aspergillus* species. *Microbial biotechnology* 10, 296–322.
- Pella, D., Rybar, R., Mechirova, V., 2005. Pleiotropic effects of statins. *Acta Cardiologica Sinica*.
- Pendrak, M.L., Klotz, S.A., 1995. Adherence of *Candida albicans* to host cells. *FEMS Microbiology Letters*. [https://doi.org/10.1016/0378-1097\(95\)00167-4](https://doi.org/10.1016/0378-1097(95)00167-4)
- Pfaller, M.A., Diekema, D.J., 2007. Epidemiology of invasive candidiasis: a persistent public health problem. *Clinical microbiology reviews* 20, 133–163.
- Pfaller, M.A., Diekema, D.J., 2004. Rare and emerging opportunistic fungal pathogens: concern for resistance beyond *Candida albicans* and *Aspergillus fumigatus*. *Journal of clinical microbiology* 42, 4419–4431.
- Phan, Q.T., Myers, C.L., Fu, Y., Sheppard, D.C., Yeaman, M.R., Welch, W.H., Ibrahim, A.S., Edwards Jr, J.E., Filler, S.G., 2007. Als3 is a *Candida albicans* invasin that binds to cadherins and induces endocytosis by host cells. *PLoS biology* 5.
- Pound, M.W., Townsend, M.L., Dimondi, V., Wilson, D., Drew, R.H., 2011. Overview of treatment options for invasive fungal infections. *Medical mycology* 49, 561–580.

- Qiao, J., Kontoyiannis, D.P., Wan, Z., Li, R., Liu, W., 2007. Antifungal activity of statins against *Aspergillus* species. *Medical mycology* 45, 589–593.
- Rahal, E.A., Constantin, W.N., Zeidan, N., Abdelnoor, A.M., 2015. Atorvastatin reduces the survival of *Candida albicans*-infected BALB/c mice. *Frontiers in Microbiology*. <https://doi.org/10.3389/fmicb.2015.01474>
- Raksha, G.S., Urhekar, A.D., 2017. Virulence Factors Detection in *Aspergillus* Isolates from Clinical and Environmental Samples. *Journal of clinical and diagnostic research: JCDR* 11, DC13.
- Ramage, G., Martínez, J.P., López-Ribot, J.L., 2006. *Candida* biofilms on implanted biomaterials: a clinically significant problem. *FEMS yeast research* 6, 979–986.
- Reeves, E.P., Murphy, T., Daly, P., Kavanagh, K., 2004. Amphotericin B enhances the synthesis and release of the immunosuppressive agent gliotoxin from the pulmonary pathogen *Aspergillus fumigatus*. *Journal of medical microbiology* 53, 1–7.
- Renwick, J., Reeves, E.P., Wientjes, F.B., Kavanagh, K., 2007. Translocation of proteins homologous to human neutrophil p47phox and p67phox to the cell membrane in activated hemocytes of *Galleria mellonella*. *Developmental & Comparative Immunology* 31, 347–359.
- Reyna-Beltrán, E., Iranzo, M., Calderón-González, K.G., Mondragón-Flores, R., Labra-Barrios, M.L., Mormeneo, S., Luna-Arias, J.P., 2018. The *Candida albicans* ENO1 gene encodes a transglutaminase involved in growth, cell division, morphogenesis, and osmotic protection. *Journal of Biological Chemistry* 293, 4304–4323.

- Ribeiro, F.C., de Barros, P.P., Rossoni, R.D., Junqueira, J.C., Jorge, A.O.C., 2017. *Lactobacillus rhamnosus* inhibits *Candida albicans* virulence factors *in vitro* and modulates immune system in *Galleria mellonella*. *Journal of applied microbiology* 122, 201–211.
- Richardson, M.D., 2005. Changing patterns and trends in systemic fungal infections. *Journal of Antimicrobial Chemotherapy* 56, i5–i11.
- Richardson, M.D., 1991. Opportunistic and pathogenic fungi. *Journal of Antimicrobial Chemotherapy* 28, 1–11.
- Romani, L., 2004. Immunity to fungal infections. *Nature Reviews Immunology* 4, 11–24.
- Rowan, R., Moran, C., McCann, M., Kavanagh, K., 2009. Use of *Galleria mellonella* larvae to evaluate the *in vivo* anti-fungal activity of [Ag 2 (mal)(phen) 3]. *Biometals* 22, 461.
- Sales-Campos, H., Tonani, L., Cardoso, C.R.B., Kress, M.R.V.Z., 2013. The immune interplay between the host and the pathogen in *Aspergillus fumigatus* lung infection. *BioMed research international* 2013.
- Sandin, R.L., Rogers, A.L., Beneke, E.S., Fernandez, M.I., 1987. Influence of mucosal cell origin on the *in vitro* adherence of *Candida albicans*: are mucosal cells from different sources equivalent? *Mycopathologia* 98, 111–119.
- Saville, S.P., Lazzell, A.L., Monteagudo, C., Lopez-Ribot, J.L., 2003. Engineered control of cell morphology *in vivo* reveals distinct roles for yeast and filamentous forms of *Candida albicans* during infection. *Eukaryotic cell* 2, 1053–1060.
- Schrettl M, Carberry S, Kavanagh K, *et al.* (2010). - Google Scholar [WWW Document], n.d.  
URL

- Scorzoni, L., de Paula e Silva, A.C., Marcos, C.M., Assato, P.A., de Melo, W.C., de Oliveira, H.C., Costa-Orlandi, C.B., Mendes-Giannini, M.J., Fusco-Almeida, A.M., 2017. Antifungal therapy: new advances in the understanding and treatment of mycosis. *Frontiers in microbiology* 8, 36.
- Seidler, M.J., Salvenmoser, S., Müller, F.-M.C., 2008. *Aspergillus fumigatus* forms biofilms with reduced antifungal drug susceptibility on bronchial epithelial cells. *Antimicrobial agents and chemotherapy* 52, 4130–4136.
- Sellam, A., Chaillot, J., Mallick, J., Tebbji, F., Albert, J.R., Cook, M.A., Tyers, M., 2019. The p38/HOG stress-activated protein kinase network couple's growth to division in *Candida albicans*. *PLoS genetics* 15, e1008052.
- Sheehan, G., Kavanagh, K., 2018. Analysis of the early cellular and humoral responses of *Galleria mellonella* larvae to infection by *Candida albicans*. *Virulence* 9, 163–172.
- Slater, J.L., Gregson, L., Denning, D.W., Warn, P.A., 2011. Pathogenicity of *Aspergillus fumigatus* mutants assessed in *Galleria mellonella* matches that in mice. *Medical mycology* 49, S107–S113.
- Söderhäll, K., Cerenius, L., 1998. Role of the prophenoloxidase-activating system in invertebrate immunity. *Current opinion in immunology* 10, 23–28.
- Song, J., Zhai, P., Zhang, Y., Zhang, C., Sang, H., Han, G., Keller, N.P., Lu, L., 2016. The *Aspergillus fumigatus* damage resistance protein family coordinately regulates ergosterol biosynthesis and azole susceptibility. *mBio* 7. <https://doi.org/10.1128/mBio.01919-15>

- Spanakis, E.K., Kourkoumpetis, T.K., Livanis, G., Peleg, A.Y., Mylonakis, E., 2010. Statin therapy and decreased incidence of positive *Candida* cultures among patients with type 2 diabetes mellitus undergoing gastrointestinal surgery. *Mayo Clinic Proceedings* 85, 1073–1079. <https://doi.org/10.4065/mcp.2010.0447>
- Spettel, K., Barousch, W., Makristathis, A., Zeller, I., Nehr, M., Selitsch, B., Lackner, M., Rath, P.-M., Steinmann, J., Willinger, B., 2019. Analysis of antifungal resistance genes in *Candida albicans* and *Candida glabrata* using next generation sequencing. *PloS one* 14.
- Staab, J.F., Bradway, S.D., Fidel, P.L., Sundstrom, P., 1999. Adhesive and mammalian transglutaminase substrate properties of *Candida albicans* Hwp1. *Science* 283, 1535–1538.
- Stancu, Camelia, Sima, A., 2001. Statins: mechanism of action and effects. *Journal of cellular and molecular medicine* 5, 378–387.
- Stancu, Camelia, Sima, A., 2001. Statins: Mechanism of action and effects. *Journal of Cellular and Molecular Medicine* 5, 378–387. <https://doi.org/10.1111/j.1582-4934.2001.tb00172.x>
- Sugui, J.A., Kwon-Chung, K.J., Juvvadi, P.R., Latgé, J.-P., Steinbach, W.J., 2015. *Aspergillus fumigatus* and related species. *Cold Spring Harbor perspectives in medicine* 5, a019786.
- Sun, H., Singh, N., 2009. Antimicrobial and Immunomodulatory Attributes of Statins: Relevance in Solid-Organ Transplant Recipients. *Clinical Infectious Diseases* 48, 745–755.
- Sun, H.-Y., Singh, N., 2011. Potential role of statins for the management of immune reconstitution syndrome. *Medical hypotheses* 76, 307–310.

- Sundermeyer, K., Hendricks, J.K., Prasad, S.V., Wells, M.A., 1996. The precursor protein of the structural apolipoproteins of lipophorin: cDNA and deduced amino acid sequence. *Insect biochemistry and molecular biology* 26, 735–738.
- Tamayo, D., Muñoz, J.F., Torres, I., Almeida, A.J., Restrepo, A., McEwen, J.G., Hernández, O., 2013. Involvement of the 90 kDa heat shock protein during adaptation of *Paracoccidioides brasiliensis* to different environmental conditions. *Fungal genetics and biology* 51, 34–41.
- Tashiro, M., Kimura, S., Tateda, K., Saga, T., Ohno, A., Ishii, Y., Izumikawa, K., Tashiro, T., Kohno, S., Yamaguchi, K., 2012. Pravastatin inhibits farnesol production in *Candida albicans* and improves survival in a mouse model of systemic candidiasis. *Medical Mycology*. <https://doi.org/10.3109/13693786.2011.610037>
- Toyotome, T., Yamaguchi, M., Iwasaki, A., Watanabe, A., Taguchi, H., Qin, L., Watanabe, H., Kamei, K., 2012. Fetuin A, a serum component, promotes growth and biofilm formation by *Aspergillus fumigatus*. *International Journal of Medical Microbiology* 302, 108–116.
- Tracy, M., Okorie, C., Foley, E., Moss, R., 2016. Allergic bronchopulmonary aspergillosis. *Journal of fungi* 2, 17.
- Trown, P.W., Bilello, J.A., 1972. Mechanism of action of gliotoxin: elimination of activity by sulfhydryl compounds. *Antimicrobial agents and chemotherapy* 2, 261–266.
- Tsunawaki, S., Yoshida, L.S., Nishida, S., Kobayashi, T., Shimoyama, T., 2004. Fungal metabolite gliotoxin inhibits assembly of the human respiratory burst NADPH oxidase. *Infection and immunity* 72, 3373–3382.
- Utz, J.P., 1980. Chemotherapy for the systemic mycoses: the prelude to ketoconazole. *Reviews of infectious diseases* 2, 625–632.



- Vargas, K.G., Joly, S., 2002. Carriage frequency, intensity of carriage, and strains of oral yeast species vary in the progression to oral candidiasis in human immunodeficiency virus-positive individuals. *Journal of clinical microbiology* 40, 341–350.
- Vaughan, C.J., Gotto, A.M., Basson, C.T., 2000. The evolving role of statins in the management of atherosclerosis. *Journal of the American College of Cardiology* 35, 1–10.
- 2
- Vila, T., Romo, J.A., Pierce, C.G., McHardy, S.F., Saville, S.P., Lopez-Ribot, J.L., 2017. Targeting *Candida albicans* filamentation for antifungal drug development. *Virulence* 8, 150–158.
- Weitz-Schmidt, G., 2002. Statins as anti-inflammatory agents. *Trends in Pharmacological Sciences*. [https://doi.org/10.1016/S0165-6147\(02\)02077-1](https://doi.org/10.1016/S0165-6147(02)02077-1)
- Westermeyer, C., Macreadie, I.G., 2007. Simvastatin reduces ergosterol levels, inhibits growth and causes loss of mtDNA in *Candida glabrata*. *FEMS Yeast Research* 7, 436–441. <https://doi.org/10.1111/j.1567-1364.2006.00194.x>
- Wikhe, K., Westermeyer, C., Macreadie, I.G., 2007. Biological consequences of statins in *Candida* species and possible implications for human health. *Biochemical Society Transactions* 35, 1529–1532.
- Wisplinghoff, H., Bischoff, T., Tallent, S.M., Seifert, H., Wenzel, R.P., Edmond, M.B., 2004. Nosocomial bloodstream infections in US hospitals: analysis of 24,179 cases from a prospective nationwide surveillance study. *Clinical infectious diseases* 39, 309–317.
- Wong, S.S., Samaranayake, L.P., Seneviratne, C.J., 2014. In pursuit of the ideal antifungal agent for *Candida* infections: high-throughput screening of small molecules. *Drug Discovery Today* 19, 1721–1730.

- Woo, P.C., Lau, S.K., Lau, C.C., Tung, E.T., Au-Yeung, R.K., Cai, J.-P., Chong, K.T., Sze, K.H., Kao, R.Y., Hao, Q., 2017. Mp1p homologues as virulence factors in *Aspergillus fumigatus*. *Medical mycology* 56, 350–360.
- YeSudhaSon, B.L., MohanraM, K., 2015. *Candida tropicalis* as a predominant isolate from clinical specimens and its antifungal susceptibility pattern in a tertiary care hospital in Southern India. *Journal of clinical and diagnostic research: JCDR* 9, DC14.
- Zain, M.E., 2011. Impact of mycotoxins on humans and animals. *Journal of Saudi Chemical Society* 15, 129–144.
- Zhu, W., Smith, J.W., Huang, C.-M., 2009. Mass spectrometry-based label-free quantitative proteomics. *BioMed Research International* 2010.
- Zhu, Y.C., Muthukrishnan, S., Kramer, K.J., 2002. cDNA sequences and mRNA levels of two hexamerin storage proteins PinSP1 and PinSP2 from the *Indianmeal* moth, *Plodia interpunctella*. *Insect biochemistry and molecular biology* 32, 525–536.